APPLICATION OF FRICTION STIR WELDING IN CIVIL ENGINEERING

Teză destinată obţinerii
titlului ştiinţific de doctor inginer
la
Universitatea "Politehnica" din Timişoara
în domeniul INGINERIA CIVILĂ
de către

Ing. Gabor Florentina Ramona

Conducător ştiinţific: prof.univ.dr.ing.Radu Băncilă (UP Timişoara)
Referenţi ştiinţifici: dr. ing. Jorge dos Santos (GKSS – Hamburg)
prof.univ.dr. ing. Dorin Dehelean (ISIM Timişoara)
prof.univ.dr.ing. Dan Dubină (UP Timişoara)

Ziua susţinerii tezei: 29.01.2010

Seriile Teze de doctorat ale UPT sunt:

1. Automatică
2. Chimie
3. Energetică
4. Ingineria Chimică
5. Inginerie Civilă
6. Inginerie Electrică
7. Inginerie Electronică şi Telecomunicaţii
8. Inginerie Industrială
9. Inginerie Mecanică
10. Ştiinţa Calculatoarelor
11. Ştiinţa şi Ingineria Materialelor

Universitatea „Politehnica” din Timişoara a iniţiat seriile de mai sus în scopul diseminării expertizei, cunoştinţelor şi rezultatelor cercetărilor întreprinse în cadrul şcolii doctorale a universităţii. Seriile conţin, potrivit H.B.Ex.S Nr. 14 / 14.07.2006, tezele de doctorat susţinute în universitate începând cu 1 octombrie 2006.

România, 300159 Timişoara, Bd. Republicii 9,
tel. 0256 403823, fax. 0256 403221
e-mail: editura@edipol.upt.ro

Forword

This Phd thesis has been realized during my activity in the Faculty of Civil Engineering at the Steel Constructions Department from Technical University „Politehnica" of Timişoara. The the trainings accomplished at the Technical University from Munich, the experimental tests realized at the Research Center GKSS Hamburg (Germany) and all my research activity during the development of this Phd have been integrant part of some national and international research projects.

This thesis refers to everyone who is interested in the use of aluminium alloys in the field of civil engineering and especially in the domain of road bridges, but also to that one who is interested about the new welding procedure for the aluminium alloys – Friction Stir Welding.

I would like to thank to my coordinator professor Mr. prof.dr.ing. Radu Băncilă for the support and confidence that I always had, beginning with my first steps in my scientific carrier.

I would like to give my thanks to prof. dr. ing. Dorin Dehelean for the collaboration possibilities during the development time of the CEEX contract No. 66, together with the team leaded by him, from the National R&D Institute for Welding and Material Testing (ISIM Timişoara), for the possibility to participate to the development of this new welding procedure.

I would like to thank very specially to dr. ing. Jorge dos Santos for the big opportunity to realize an important part of the weldings and the experimental tests to one of the most important research center in this domain from Europe – GKSS Forschungszentrum, but also for the possibility to learn directly how this kind of weld seams are realized.

I would like to thank Mr. prof. Dr. Ing. Dan Dubină for accepting to be one of my thesis referents and for the help, during the steps of my formation as a researcher.

Many thanks for the extraordinary working team from GKSS Forschungszentrum – Arne Roos, Volker Leiser, Luciano Bergmann, Matthias Beyer – for the un-conditioning help during my training in Geesthacht. I cannot forget the cooperation with the wonderful team from ISIM Timişoara – Mr. Ing. Radu Cojocaru, Ms. Ing. Lia Boţilă, ing. Cristian Ciucă – thank you for your cooperation and help.

Thank you to my dear colleagues from the Steel Construction Department for your help and support and the good word

And last, but not least, my big thanks to my family and friends for their un-conditioning support.

Timişoara, ianuarie 2010 ing. Gabor Florentina Ramona

Gabor, Florentina - Ramona

Application of Friction Stir Welding in Civil Engineering

Aplicaţii ale procedeului de sudare prin frecare cu element active rotator în domeniul construcţiilor

Teze de doctorat ale UPT, Seria 5, Nr. 52, Editura Politehnica, 2010, 184 pagini, 130 figuri, 38 tabele.

ISSN: 1842-581X

ISBN: 978-606-554-048-4

Cuvinte cheie:
Aluminium, alloys, wrought alloy, casting alloy, chemical composition, copper, manganese, silicon, magnesium, zinc, lithium, temper, age hardening alloy, duralumin, extrusion, cold rolling, hot rolling, strength, corrosion, weldability, solid profile, semi-hollow profile, hollow profile, application, marine industry, transport industry, civil engineering industry, tensile properties, ductility, thermal working condition, hardness, fatigue resistance, thermal conductivity, naval architecture, ship, superstructure, tanker, ferries, catamaran, off-shore platform, cost advantages, inter-metallic corrosion, joining methods, heat affected zone, air transport, railway transport, lightweight, durable, damage tolerant, aircraft, fuselage skin, façade panels, roofing, surface appearance, history, aluminium bridges, light unit weight, high toughness, initial costs, modulus of elasticity, thermal stresses, railroad aluminium bridge, pedestrian bridge, deck slab element, movable bridges, telescopic bridge, design, friction stir welding, welding tool, tool shoulder, pin, advancing side, retracting side.

Rezumat:
This thesis brings in discussion two actual subjects: the use of aluminium alloys in civil engineering and the new welding procedure – Friction Stir Welding. The two subjects are parallel presented in the first five chapters and brought together in chapter six, where the superstructure for an emergency bridge is designed and calculated, according to Eurocode 9.

CONTENT

Forward		3
Content		5
List of figures		8
List of tables		12
Summary		13
Rezumat		15
1.	Introduction	18
2.	State of the art of aluminium	20
2.1.	Aluminium – short history	20
2.1.1.	History and production of aluminium	20
2.1.2.	Alloys and tempers	21
2.1.3	Aluminium product forms	25
2.2.	Applications of aluminium	26
2.2.1	History of aluminium in marine industry	28
2.2.2	Present situation of aluminium in marine industry	29
2.2.3.	Transport Industry	33
2.2.4.	Civil engineering	37
2.3.	History of aluminium in bridge construction	38
2.4.	Present situation of aluminium in bridge construction	42
2.5.	Conclusions	50
3.	Friction Stir Welding (FSW)	54
3.1.	Process description	54
3.1.1.	The process parameters	58
3.1.2.	Forces	59
3.1.3.	Temperature	60
3.1.4.	Tools	64
3.1.5.	Relation between base material and FSW	67
3.1.6.	Properties	68
3.1.7.	Residual stress	69
3.1.8.	Hardness	69
3.1.9.	Mechanical properties	70
3.1.10.	Conclusions regarding FSW	73
3.2.	Process advantages for aluminium and in bridge construction	75
3.2.1	The advantages of the process for the aluminium and its alloys	75
3.2.2.	The advantages of the process for bridge construction	76
3.3.	Present situation regarding FS welds evaluation in international standards	78
4.	Aluminium design and fatigue	79
4.1.	Aluminium design according to British Standard	79
4.1. 1	Introduction	79
4.1. 2.	Limit state design and limiting stresses	81
4.2.	Aluminium design according to Eurocode	86
4.2.1	The Design Analysis Process	89
4.2.1. 1.	Introduction	89

4.2.1. 2.	Methods of Verification	90
4.2.1. 3	The Load and Resistance Design Factor Method	91
4.2.1. 4.	Method of Allowable Stresses	92
4.2. 2.	Loads and Load Factors	92
4.2.2 1.	Introduction	92
4.2.2 2.	Classification of Loads	93
4.2.2 3.	Characteristic Loads, Normal Loads and Long-Term Loads	94
4.2.2 4.	Load Combinations, Design Value of the Load	95
4.2.2 5.	Loads on Buildings, Bridges and Hydraulic Structures	97
4.2. 3.	Resistance and Resistance Factors	98
4.2.3. 1.	Assumptions Concerning Strength Properties	98
4.2.3. 2.	Models of analysis	99
4.2. 4.	Design Criteria	100
4.2.4. 1.	The load and resistance factor method	100
4.2.4. 2.	Method of allowable stresses	100
4.2. 5.	Aluminium Alloys as a Structural Material	101
4.3.	Design of members	102
4.3. 1.	Geometrical imperfections	104
4.3.1. 1.	Initial curvature	104
4.3.1. 2.	Deviation of cross sectional dimensions	105
4.3.1. 3.	Initial buckles	105
4.3.1. 4.	Residual stress in extruded profiles	106
4.3.1. 5.	Bauschinger effect	106
4.3.1. 6.	Heat affected zones	107
4.3.1. 7.	Influence of heat-affected zones	107
4.3.1. 8.	Stress-strain relationship	109
4.3.1. 9.	The Ramberg-Osgood law	109
4.3.2.	Basic values of strength	109
4.3.3.	Local buckling	111
4.3.4.	Bending moment	113
4.3.5.	Axial forces	117
4.3.6.	Shear forces	119
5.	Experimental procedure	121
5.1.	Methodology	121
5.2.	Base materials (6082-T6 and 5083-H111)	122
5.2.1.	Aluminium alloy 6082 – $AlSi_1MgMn$	122
5.2.2.	Aluminium alloy 5083 – $AlMg_{4,5}Mn_{0,7}$	123
5.3.	FSW process	123
5.3.1.	Machines	123
5.3.2.	Tools	125
5.4.	Initial parameters matrix	126
5.5.	Temperature measurements	128
5.6.	Force measurements	130
5.7.	Mechanical Characterisation. Bending tests	132
5.8.	Macrostructures	135
5.9.	Hardness measurements	137
5.10.	Tensile Test	138
5.11.	Results and discussions of the preliminary welds	141
5.12.	Parameters for the fatigue welded samples	143

5.13.	Fatigue tests	146
5.14.	Conclusions	150
6.	Case study - design of an aluminium bridge superstructure	151
6.1.	Structure general description	154
6.2.	Loads on the structure	155
6.2.1.	Permanent loads	156
6.2.2.	Variable loads	156
6.2.3.	Load combinations	157
6.2.4.	Buckling evaluation	157
6.3.	Structure analysis	160
6.3.1.	Limit states and design situation	160
6.3.2.	Ultimate limit state	161
6.3.3.	Serviceability limit state	167
6.4.	Conclusions	169
7.	Conclusions and contributions	170
7.1.	Conclusion	170
7.2.	Contributions	171
	References	173
8.	Annex	178

LIST OF FIGURES

Fig. 2.1. Bayer method to obtain aluminium
Fig. 2.2. Schema of the aluminium production
Fig.2.3. Synopsis of the principal aluminium alloys
Fig. 2.4. The three basic types of the extruded cross-sections
Fig. 2.5. a) The effect of the alloying elements on tensile strength, hardness and ductility; b) The effect of the alloying elements on fatigue strength and corrosion resistance
Fig. 2.6. Catamaran realized from aluminium extrusions
Fig. 2.7. Possible qquality problems in fusion welds
Fig. 2.8. Offshore aluminium hemodule
Fig. 2.9. Hitachi train – Japan
Fig. 2.10. Applications of aluminium alloys for aircraft
Fig. 2.11. Possible alloys for an aircraft
Fig. 2.12. Aluminium façade
Fig. 2.13. Aluminium sheet used for roofing
Fig. 2.14. Arvida bridge (Quebec, Canada)
Fig. 2.15. Telescopi aluminium gangway for ocean terminal
Fig. 2.16. Lyon Groslee bridge (France)
Fig. 2.17. The Forsmo river aluminium road bridge
Fig. 2.18. Bridge in Lüneburg (Germany)
Fig. 2.19. Aluminium trough bridge – Selzbach
Fig. 2.20. The Corbin bridge in Huntingdon
Fig. 2.21. Transversal section of an aluminium deck slab element
Fig. 2.22. Welded elements of an aluminium bridge deck panel
Fig. 2.23. Telescopic bridge
Fig. 2.24. The German military bridge: erection phase
Fig. 2.25. Riekerhaven bridge (Amsterdam)
Fig. 2.26. Function schema of a movable bridge: a. Not open; b. Open
Fig. 2.27. Extension design
Fig. 2.28. Bridge over Amsterdam-Rhine canal
Fig. 2.29. General corrosion behaviour of Al and steel – a factor of maintenance costs
Fig. 3.1. Schematic of the friction stir welding process
Fig. 3.2. The welding process steps
Fig. 3.3. Zone distribution in the weld cross-section
Fig. 3.4. Orientations relative to the tool rotation and the welding direction
Fig. 3.5. A schema of the parameters influence to the mechanical properties
Fig. 3.6. Repreentation of the coordinates system adopted in FSW
Fig. 3.7. The real heat propagation by the FSW
Fig. 3.8. Effect of depth on peak temperature as a function of distance from the weld center line for a 6061 T6 FSW weld made at 400 rpm and 120 mm/min traverse speed
Fig. 3.9. Microstructure of thermo-mechanically affected zone in FSW 7075 alloy
Fig. 3.10. Schematic presentation of a FSW Tool
Fig. 3.11. Combinations of tools
Fig. 3.12. Twin-stir prototype head assembly

Fig. 3.13. Twin-stir variants. a) parallel side-by-side transverse to the welding direction. b) Tandem in-line with the welding direction. c) Staggered to ensure tethe edges of the weld regions partially overlap
Fig. 3.14. Simultaneous double-sided frictin stir welding with contra-rotating tools
Fig. 3.15. Typical hardness curve accros the weld of FSW 6063-T5 alloy
Fig. 3.16. Tensile properties of base material, as-welded, aged weld and SHAT weld of 6063-T5 alloy
Fig. 3.17. S-N curve of base material, FSW weld, laser and MIG weld for 6005-T5 alloy
Fig. 3.18. The fatigue life of MIG-pulse and TIG, in comparison with FS welds
Fig. 3.19. S-N fatigue data of the welded specimens: (a) MIG welded and (b) FS welded
Fig. 3.20. MIG welded Al6082-T6 and FS welded Al6082-T6
Fig.4.1. Static strength: (a) elastic design (S1=material strength, S2=allowable stress, S3=stress arising at nominal working load); (b) limit state design
Fig. 4.2. Elastic (Δ_{el}) and plastic (Δ_{pl}) components of deflection at nominal working load
Fig. 4.3. Limit states
Fig. 4.4. Schematic description of the design analysis process
Fig. 4.5. Frequency diagram illustrating shematically the method of partial coefficients
Fig. 4.6. Variation of load with time
Fig.4.7. Stress-strain diagram for steel (St52) and aluminium alloy (AA6082-T6)
Fig. 4.8. The stress and strain for beams made of St52 and AA 6082-T6
Fig. 4.9. Comparison between buckling behavior of an idealized Euler bar and of a real bar with imperfections
Fig. 4.10. Definition of initial curvature and eccentricity
Fig. 4.11. Tolerated divergence from flatness of web and flanges
Fig. 4.12. The extent of heat affected zones
Fig. 4.13. Width of heat affected zone (b_{haz})
Fig. 4.14. Principle relationship between mean stress σ_m and compression ε for different slenderness β
Fig. 4.15. Principle relationships between compression u and axial load N
Fig. 4.16. Moment-strain curves
Fig. 4.17. Stress-strain curves for compression flange in different cross section class
Fig.4.18. Effective section of a welded hollow section
Fig.4.19. Stress in gross and net section
Fig. 4.20. Compressive force on a column
Fig. 4.21. a) Pure shear state of stress; b) Ideal tension field
Fig. 5.1. Experimental procedure flow chart
Fig. 5.2. Tricept 805 Robot
Fig. 5.3. Guttering machine
Fig. 5.4. Tool for weld A to G
Fig. 5.5. Tool for welds H to W
Fig. 5.6. Thermocouples positions: a) in plates; b) in backing bar
Fig. 5.7. Temperature measurements for FS welded 5083-H111 alloy
Fig. 5.8. Temperature measurements for FS welded 6082-T651 alloy

Fig. 5.9. Forces measured during joining with butt joint the 6 mm thickness plates for C sample (AA 5083-H111, 600 RPM, 200mm/min)
Fig. 5.10. Forces measured during joining with butt joint the 6 mm thickness plates for E sample (AA 5083-H111, 800 RPM, 267mm/min)
Fig. 5.11. Forces measured during joining with butt joint the 6 mm thickness plates for K sample (AA 5083-H111, 600 RPM, 100mm/min)
Fig. 5.12. Forces measured during joining with butt joint the 6 mm thickness plates for L sample (AA 6082-T651, 1200 RPM, 180mm/min)
Fig. 5.13. Forces measured during joining with butt joint the 6 mm thickness plates for M sample (AA 6082-T651, 1200 RPM, 300mm/min)
Fig. 5.14. Bending specimens for 5083-H111 joint root (up) and joint surface (down). Surface rupture
Fig. 5.15. Bending specimens joint for 5083-H111 root (up) and joint surface (down). Surface rupture
Fig. 5.16. Bending specimens' joint for 5083-H111 root (up) and joint surface (down). Surface rupture
Fig.5.17. Bending specimens for 6082-T651 joint root (up) and joint surface (down)
Fig. 5.18. Bending specimens for 6082-T651 joint root (up) and joint surface (down). Surface rupture
Fig. 5.19. OM Micrographs for 5083-H111 welded samples
Fig. 5.20. OM Macrographs for 6082-T651 welded samples
Fig. 5.21. Specimens for hardness measurements
Fig. 5.22. Dimensions of the FSW tensile test specimens
Fig. 5.23. Comparison weld-BM for 5083-H111 alloy
Fig. 5.24. Comparison weld-BM for 6082-T651 alloy
Fig. 5.25. Hardness measurements for 5083-H111, welded with FSW
Fig. 5.26. Hardness measurements for 6082-T651, welded with FSW
Fig. 5.27. Test results CEALS07
Fig. 5.28. Tests results CEALS08
Fig. 5.29. Tests results CEALS10
Fig. 5.30. Hardness measurements CEALS07, CEALS08, CEALS10
Fig. 5.31. Experimental flow chart – step 3
Fig. 5.32. Fatigue samples dimensions
Fig. 5.33. Fatigue testing machine
Fig. 5.34. Comparison between predicted fatigue strength curve logΔσ-logN- CEALS07 FS welded plate and the test results
Fig. 5.35. a) AA6082-T6 FS welded fatigue tested specimen, fracture location; b) AA6082-T6 FS welded specimen, fracture surface
Fig. 6.1. Longitudinal (top) and transverse (bottom) cross-section of the bridge
Fig. 6.2. a. Aluminum deck on steel girders; b. Connection of aluminum deck to steel girder
Fig. 6.3. Bridge structure
Fig. 6.4. Cross-sections. a. Main girder; b. Extruded profile
Fig. 6.5. Variable load A 30
Fig. 6.6. Deck profile elements
Fig. 6.7. Main girder elements
Fig. 6.8. Maximum bending moment – main girder
Fig. 6.9. Bending moment on the main girder under the permanent and movable loads
Fig. 6.10. Maximum bending moment – deck section

Fig. 6.11. Shear forces on the main girder
Fig. 6.12. Shear forces on the deck section
Fig. 6.13. Vertical deflections to be considered
Fig. 6.14. Maximum deformation of the main girder, under loadings
Fig. 6.15. Maximum deformation of the deck girder, under loadings
Fig. 8.1. Main window of Sofistik structural desktop
Fig. 8.2. Mash definition
Fig. 8.3. Load definition – permanent load
Fig. 8.4. Load definition – payload 1 – mode 1 A30 truck position
Fig. 8.5. Load definition – payload 2 – mode 2 A30 truck position
Fig. 8.6. Load definition – payload 3 – mode 3 A30 truck position
Fig. 8.7. Load combination
Fig. 8.8. Usage grade of the deck element under the considered load combination
Fig. 8.9. Frequenz eigenvalue
Fig. 8.10. Structure deformation under the consideren load combination

LIST OF TABLES

Table 2.1. Mechanical properties of aluminium extrusions (minimum values)
Table 2.2. Main mechanical properties for fuselage skin
Table 2.3. Aluminium bridges constructed in Europe
Table 3.1. Mechanical properties of base materials
Table 3.2. FSW process parameters used to fabricate the joints
Table 3.3. Friction stir weld joint efficiency for various aluminium alloys
Table 4.1. Suggested γ-values for checking the limit state of static strength
Table 4.2. Design values of the loads
Table 4.3. Partial factors
Table 4.4. Ψ factors for buildings
Table 4.5. Combinations of dominant action
Table 4.6. Strength ($R_{p0,2}$) and modulus of elasticity (E) for some materials
Table 4.7. Factors for steel and aluminium alloy
Table 4.8. HAZ softening factor (ρ_{HAZ})
Table 4.9. Minimum characteristic values of yield strength f_0, ultimate strength f_a and strength f_{haz} in the heat-affected zone for some wrought aluminium alloys
Table 4.10. Design values of yield strength $f_{0,d}$, ultimate strength $f_{a,d}$ and strength $f_{haz,d}$ in the heat-affected zone for some wrought aluminium alloys
Table 4.11. Slenderness parameters
Table 4.12. Reduction factor ρ_v for shear buckling
Table 5.1. Typical chemical composition for aluminium alloy 6082
Table 5.2. Typical chemical composition for aluminium alloy 5083
Table 5.3. The parameters for 5083-H111 alloy
Table 5.4. The parameters for 6082-T651 alloy
Table 5.5. Investigated elements
Table 5.6. Base material resistance – AA 5083-H111 alloy
Table 5.7. Base material resistance – AA 6082-T6 alloy
Table 5.8. Welded samples performances – 5083-H111
Table 5.9. Performance of the welded samples – 6082-T651
Table 5.10. Final welding parameters
Table 5.11. Standardized $\Delta\sigma_c$ values (N/mm^2)
Table 5.12. Average results of fatigue life for FS welded specimens – CEALS08 series
Table 5.13. Average results of fatigue life for FS welded specimens – CEALS10 series
Table 6.1. Mechanical properties of alloys employed in the structure
Table 6.2. Design values of material
Table 6.3. Permanent loads
Table 6.4. Partial safety factors for applied loads
Table 6.5. Partial safety material factors
Table 6.6. Slenderness factor calculation
Table 6.7. Values of shape factor α

SUMMARY

The increasing use of aluminium alloys in the field of civil engineering, not only in aeronautics, automotive, railways and shipbuilding sectors, creates the need for research on the more efficient and reliable welding processes. In order to allow the industry to use new manufacturing techniques as Friction Stir Welding, research on the mechanical behaviour of joints manufactured using such new procedure should be performed.

The aim of this thesis is to provide contributions to fundamental knowledge for aluminium alloys as a structural material and an introduction of the "young" welding process – friction stir welding - FSW. The aluminium alloys are well known and have been used starting with the period between the two World Wars, especially in United States of America. In Europe aluminium alloys are more used in North Europe, but also in Germany and France.

The joining technologies for aluminium require more attention, especially the welding procedures. Taking into account the properties reduction, classical welding of aluminium alloys does not represent the best choice for joining. Also other joining technologies for aluminium alloys need more attention that similar joining techniques for steels.

In present time, the need of fast solutions in case of construction, but also the maintenance reduced costs, indicate the aluminium alloys to be used on a larger scale. In order to help the industries using the aluminium alloys, in 1991 - the new joining technology - Friction Stir Welding has been discovered. This procedure has been practically invented for aluminium alloys, where it has been used for the first time. Nowadays this young technique is also applied for joining high strength steels.

Despite the widespread interest of the possibilities offered by Friction Stir Welding, general data concerning its mechanical behaviour are still scarce. This technique leads to a type of weld seam structure which is close to the initial surface structure, offering benefits from the point of view of costs, but also from the damage tolerance behaviour. In present only the costs and the complexity of the welding devices limits the application of this procedure.

This thesis wants to underline the vast possibilities offered to the industries by the large number of existing aluminium alloys (AA). The aim is also to introduce in Romania Friction Stir Welding in Civil Engineering.

The thesis is divided in 7 Chapters and comprises 154 pages.

In **chapter 1** a general presentation of the discussed items is given.

Chapter **2** presents the history of aluminium, the main types of alloys, the use of this material in marine industry, in transport industries (aeronautics, automotives, train constructions) and in civil engineering. Also a short history of aluminium bridges all over the world is presented. This chapter offers also a today situation of aluminium alloys as a structural material for bridges, in particular in Europe. The chapter concluded with the importance of a better understanding of aluminium alloys and the necessity of more educational and informative materials about how to use structural aluminium alloys.

Chapter 3 describes the very new, especially for Romania, welding procedure – Friction Stir Welding. Here there have been presented the principal

welding process steps, like the input and the process parameters, the characteristics of this joining procedure and the main types of welding tools. A brief overlook of the joint properties is also presented, the advantages of the process in comparison with the "usual" welding procedure for aluminium alloys is underlined.

In order to offer educational material for the designers, **Chapter 4** develops the design methods according to the main standards for the aluminium alloys from Europe. In this direction a detailed overview of Eurocode 9 – is given with comments.

The experimental program is the subject of the **Chapter 5**. The technology of preliminary welds and their evaluation is described; also the welding samples for the fatigue analysis are presented and tested.

Chapter 6 presents a case study regarding the design of an aluminium bridge with the deck welded with FSW. The main aim of this structure is to be used as an "emergency bridge" in case of natural disasters.

The conclusions and personal contributions are presented in **Chapter 7**.

The main contributions are:

- at the beginning of the thesis a briefly presentation of the aluminium production and the present method for aluminium alloys production is given;
- state of the art about the applications of aluminium and its alloys in different interest fields as marine industry, transport industry and especially in civil engineering;
- short history and the development of different conceptions in aluminium bridges;
- detailed description of Friction Stir Welding technology;
- practical application of the new Friction Stir Welding procedure, realizing the first welded elements together with National R&D Institute for Welding and Material Testing (ISIM) Timisoara;
- over 50 tests specimens were realized and tested;
- for two the most used alloys in civil engineering the optimum welding parameters were established;
- the complex characteristic of the friction stir welds in order to optimize the procedure were studied;
- experimental fatigue tests on friction stir welded elements were also performed;
- the initiation of a program for the design of emergency bridges with short spans, entirely realized from aluminium alloys, with low costs, light weight and short erection time;
- large possibilities for the application of Friction Stir Welding in Civil Engineering are opened.

The results of this work have been partially valorized through a number of publications. The experimental program has been integrated in the research contract CEEX 66.

REZUMAT

Utilizarea pe scară tot mai largă a aliajelor de aluminiu, nu numai în aeronautică, automobile, căi ferate şi sectoarele de construcţii navale, dar şi în domeniul ingineriei civile, creează nevoia de cercetare în domeniul proceselor de sudare mai eficiente şi mai fiabile. În scopul de a permite industriei folosirea tehnicilor de fabricaţie noi, cum este şi sudarea prin frecare cu element activ rotitor, sunt necesare a fi efectuate programe de cercetare asupra caracterizărilor îmbinărilor efectuate cu ajutorul unor astfel de proceduri noi.

Scopul acestei teze este de a oferi contribuţii la cunoştinţe fundamentale pentru aliajele de aluminiu ca materiale structurale şi o iniţiere în tainele procesului de sudare considerat încă "tânăr" – sudarea prin frecare cu element activ rotitor – FSW (Friction Stir Welding). Aliaje de aluminiu sunt bine cunoscute şi au fost utilizate începând cu perioada dintre cele două războaie mondiale, în special în Statele Unite ale Americii. În Europa aliajele de aluminiu sunt folosite cu precădere în Europa de Nord, dar şi în Germania şi Franţa.

Tehnologiile de îmbinare pentru aluminiu necesită mai multă atenţie, în special procedeele de sudare. Ţinând seama de reducerea proprietăţilor, sudarea în cazul aliajelor de aluminiu nu reprezintă cea mai bună alegere pentru realizarea îmbinărilor. De asemenea, şi celălalte tehnologii de îmbinare pentru aliaje de aluminiu au nevoie de o mai mare atenţie la realizare, comparativ cu tehnici similare de îmbinare pentru oţeluri.

În prezent, nevoia de soluţii rapide în caz de construcţie, dar şi costurile de întreţinere reduse, recomandă aliajele de aluminiu pentru a fi utilizate pe o scară mai mare. În scopul de a ajuta industriile ce folosesc aliaje de aluminiu, în 1991 a fost descoperită o nouă tehnologie de îmbinare – sudarea prin frecare cu element activ rotitor. Această procedură a fost practic inventată pentru aliajele de aluminium, materiale la care această procedură şi-a întâlnit primele aplicaţii În zilele noastre această tehnică este, de asemenea, aplicată şi pentru îmbinarea oţelurilor de înaltă rezistenţă, având perspective largi de dezvoltare în viitor.

În ciuda interesului pe scară largă a posibilităţilor oferite de sudarea prin frecare cu element activ rotitor, date generale privind comportamentul mecanic al îmbinărilor sunt încă extrem de reduse. Această tehnică produce o structură a suprafeţei îmbinate ce este aproape similară cu suprafaţa iniţială a elementelor îmbinate, acest fapt oferind avantaje din punctul de vedere al costurilor de prelucrare, dar şi din punctul de vedere al comportamentului toleranţelor la defecte. În prezent doar costurile şi complexitatea dispozitivelor de sudare limitează aplicabilitatea acestei proceduri.

Această teză vrea să sublinieze posibilităţile vaste oferite industriilor de numărul mare de aliaje de aluminiu existente. Scopul este de a introduce, de asemenea, în România sudarea prin frecare cu element activ rotitor în domeniul Ingineriei Civile.

Teza este împărţit în 7 capitole şi cuprinde 154 pagini.

În **capitolul 1**- se face o prezentare generală a problemelor abordate şi discutate.

Capitolul 2 prezintă istoria aluminiului, principalele tipuri de aliaje, utilizarea acestui material în industria marină, în industria transporturilor (aeronautică, autovehicule rutiere, construcţii de vagoane) şi în domeniul construcţiilor. De asemenea este prezentat un scurt istoric al poduri de aluminiu în toată lumea. Acest capitol oferă, de asemenea, o situaţie actuală a aliajelor de aluminiu ca material structural pentru poduri, în special în Europa. Capitol se încheie cu sublinierea importanţei unei mai bune înţelegeri a aliajelor de aluminiu şi necesitatea mai multor materiale informative si educative cu privire la modul de utilizare a aliajelor de aluminiu structurale.

Capitolul 3 descrie noul procedeu de sudare, în special pentru România, sudarea prin frecare cu element activ rotitor. Aici au fost prezentate etapele principale de sudare, parametrii introduşi şi cei din timpul procesului de sudare, caracteristicile acestei proceduri de îmbinare şi principalele tipuri de unelte de sudare. Este făcută o scurtă trecere în revistă a proprietăţilor îmbinării; de asemenea sunt prezentate avantajele procesului, în comparaţie cu "procedurile uzuale de sudare" pentru aliajele de aluminiu.

În scopul de a oferi materiale educaţionale pentru proiectanţi, **capitolul 4** trece în revistă metodele de proiectare în conformitate cu principalele standarde pentru aliajele de aluminiu utilizate curent în Europa. În acest sens este făcută o prezentare detaliată a Eurocodului 9 - cu comentarii.

Programul experimental constitue obiectul **capitolului 5**. Este descrisă tehnologia de realizare a îmbinărilor preliminare, dar şi modul de evaluare şi testare a acestor îmbinări; de asemenea sunt prezentate şi încercările la oboseală a probelor sudate cu aceasta tehnologie.

Capitolul 6 prezintă un studiu de caz privind proiectarea unui pod din aluminiu cu platelajul realizat cu ajutorul sudurii prin frecare cu element activ rotitor. Scopul principal al acestei structuri este de a fi folosit ca un „pod de urgenţă" (emergency bridges) utilizabil în caz de catastrofe naturale.

Concluziile şi contribuţiile personale sunt prezentate în **capitolul 7**.
Principalele contribuţii sunt:

- la începutul tezei este realizată o prezentare pe scurt a producţiei de aluminiu şi metoda actuală de producţie a aliajelor de aluminiu;
- stadiul actual cu privire la aplicabilitatea aluminiului şi a aliajelor sale în diferite domenii de interes precum industria marină, industria de transport şi în special în domeniul construcţiilor civile;
- scurt istoric privind alcătuirea şi dezvoltarea la poduri din aluminiu;
- descrierea detaliată a sudării prin frecare cu element activ rotitor;
- aplicarea în practică a tehnologiei de sudare prin frecare cu element activ rotitor, realizând primele elemente sudate, împreună cu Institutul Naţional de Cercetare-Dezvoltare în Sudură şi Încercări de Materiale (ISIM) Timişoara;
- au fost realizate peste 50 de exemplare de suduri care au fost şi testate;
- pentru două dintre aliajele cele mai utilizate în construcţiile civile au fost studiaţi parametrii optimi de sudare;
- au fost efectuate caracterizări complexe ale îmbinării în scopul de a optimiza procedura;
- au fost realizate teste experimentale de oboseală la elementele sudate prin frecare cu element activ rotitor;
- iniţierea unui program pentru proiectarea unor poduri utilizabile în cazuri de urgenţă cu deschideri mici, realizate în întregime din aliaje de aluminiu, cu costuri scăzute, greutate şi mentenanţă reduse şi cu timp scurt de punere în operă.

Rezultatele tezei au fost parţial valorificate prin publicarea câtorva articole în reviste de specialitate şi în volumele unor seminarii şi conferinţe din domeniu. Programul experimental a fost integrat în contractul de cercetare CEEX 66.

1. INTRODUCTION

Aluminium has been produced first time to am industrial scale in 1892, using the Bayer method. Since than this method has been developed and today an important number of aluminium alloys are known. The characteristic of these alloys are given by the alloying elements and the thermal treatments.

The use of aluminium alloys in structural applications has grown considerably in the past few decades. In transportation, the **low density** of aluminium, resulting in a high **strength-to-weight ratio**, makes it a favourable material for aircraft, high speed trains and ferries. In building and civil engineering, low density is sometimes the determining factor in the choice of aluminium; e.g. movable bridges, helicopter decks on offshore platforms, etc. However, other favorable properties such as **corrosion resistance**, **easy shaping** of profiles by extrusion, and **aesthetics** are often more important.

All structural materials have different properties and technical characteristics, and consequently differ in their suitability for a given application. For some obvious cost reasons, aluminium will not become an alternative structural material in all cases, even though its use would be technically possible.

In order to evaluate whether aluminium could be the right material in a specific application some decision criteria must be considered:

- Weight reduction
- Maintenance aspects
- Product costs
- Load criteria.

The joining technologies for aluminium require more attention, especially the welding procedures. In order to help the industries using the aluminium alloys, in 1991 - the new joining technology - Friction Stir Welding has been discovered. This procedure has been practically invented for aliminium alloys where it has been used for the first time. What is so unique about FSW is that it is a solid state welding process that does not require the melting of joined sections. FSW is considered to be the most significant development in metal joining in the last two decades and is a ‘‘green’’ technology due to its energy efficiency, environment friendliness, and versatility.

The input parameters that govern, on the first hand, the quality of the weld are the rotational speed (rot/min) ω, the travel speed (mm/min) v and when the process is realized with force input, vertical force (kN) F_z. These input parameters have a very big influence to the process parameters: pin temperature (°C), downwards forging force on the tool shoulder, tool torque, the forces from the weld seam in welding direction and perpendicular on the weld seam, parameters that define the mechanical properties of the welded element. No special preparation is needed for the butt and lap joints of friction stir welding. Two clean metal plates can be easily joined together in the form of butt or lap joints without concern about the surface conditions of the plates.

The FSW joint is created by friction heating with simultaneous severe plastic deformation of the weld zone material. The stirring of the tool minimizes the risk of having excessive local amounts of inclusions, resulting a homogenous and void-free

weld. Since the amount of the heat input is smaller than during fusion welding, heat distortions are reduced and thereby the amount of the residual stresses.

At this moment there are no public standards available for the calculus of strength of such a connection. Until now FSW applications were used on an industrial scale only after an important number of tests. A solution in the direction of realizing a guideline for the calculation of an aluminium structure welded with FSW is to make, for the begin, a classification of the most used alloys on a industrial scale. In case of bridges, the joints have to present a higher resistance, especially to moving loads which may cause the structure failure by assigning of weakest section.

In all modern codes of practice structural safety is established by the application of the partial safety coefficients to the loads (or 'actions') and to the strength (or 'resistance') of components of the structure. The new Eurocodes for the design and execution of buildings and civil engineering structures use a limit state design philosophy defined in Eurocode 1. In this thesis the design rules of these new and modern codes are applied to a case study, realized on a bridge superstructure. The good properties of the FSW weldings are taking into account by introducing the higher resistance to the statically and dynamical loads, identified during the experimental program subjected in this thesis.

2. STATE OF THE ART OF ALUMINIUM

2.1 Aluminium – short history

2.1.1 History and production of aluminium

Aluminium is the second most abundant material in the earth crust and now days it is the most used metal after steel. If measured by volume rather than weight it exceeds now in quality all others non-ferrous metals combined.

The first aluminium small-scale production started in 1855, when Henry Sainte Claire Deville made aluminium by a chemical process. The industrial production began in the late 19th century after the discovery of an electrolytic process in 1886 (made simultaneously but independently by Charles Martin Hall and Paul T. Heroult) and the development in 1892 (by Bayer) of an efficient process to extract alumina from bauxite, which is still used by all aluminium smelters of the world [1].

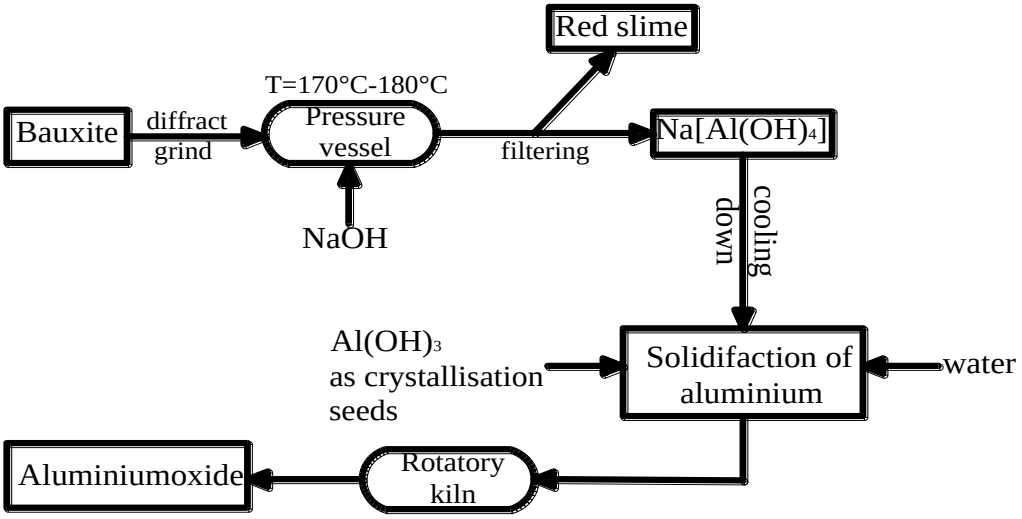

Fig. 2. 1 Bayer method to obtain aluminium

The reason it took so long to produce aluminium was the difficulty of extracting it from its ore. It is strongly combined with oxygen and, unlike iron, cannot be reduced in a reaction with carbon. Between extraction of aluminium from his ore (mainly bauxite) and the processing into finished product several successive operations take place; the production steps can be summarised as in Figure 2.2.

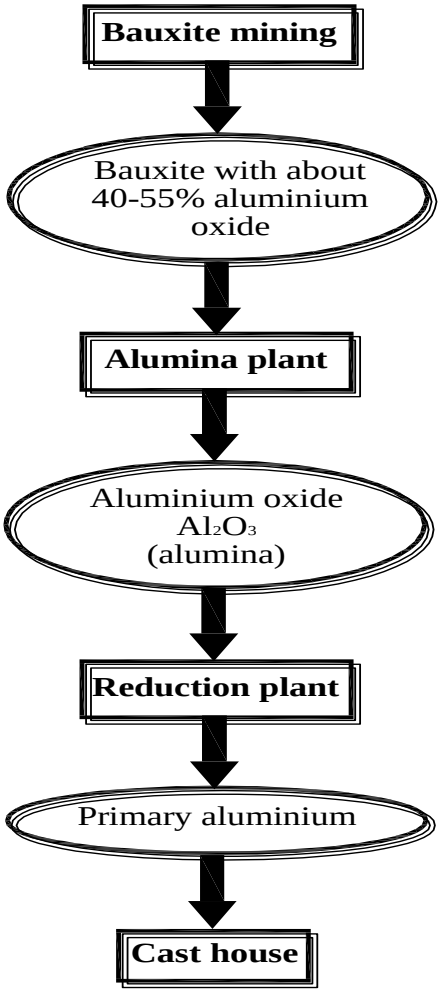

Fig. 2. 2: Schema of the production of aluminium

2.1.2 Alloys and tempers

The principal aluminium alloys are obtained as presented in Figure 2.3.

The most common classification for aluminium alloys is the Aluminium association Alloy & Temper Designation System, recognized by the American National Standards Institute (ANSI); for wrought alloys, four digits identify the material, the first digit is for the alloy group and the second indicates modifications to the original alloy. For the 1xxx group, the last two digits indicate the minimum aluminium percentage; for the 2xxx to 8xxx groups, the last two digits further identify the individual alloy.

Alloying elements added to pure aluminium improve its strength. Commonly used alloying elements are:

- copper (Cu)
- magnesium (Mg)
- zinc (Zn)
- silicon (Si)
- manganese (Mn)

Other alloying elements like bismuth (Bi), boron (B), chromium (Cr), lithium (Li), iron (Fe), lead (Pb), nickel (Ni), titanium (Ti), zirconium (Zr), strontium (Sr) and sodium (Na) are added in small quantities to achieve special metallurgical effects or properties, e.g. grain refining, machinability etc.. Adding lithium (Li) in quantities of 3 to 5% improves the elastic modulus and decreases the density. Structural aluminium-lithium alloys are, however, restricted to aerospace applications, since special care and attention must be paid at the casting, fabrication, use and scrap recycling stages.

The main groups of alloys are as follows:
1xxx: pure aluminium (99,00% or more);
2xxx: the main alloying element is copper (often with magnesium as a secondary addiction);
3xxx: the main alloying is manganese;
4xxx: the main alloying is silicon;
5xxx: the main alloying is magnesium;
6xxx: the main alloying are magnesium and silicon;
7xxx: the main alloying is zinc;
8xxx: the main alloying is lithium;
9xxx: is not used yet and is reserved for a possible use in the future [2].

After the four digits, it is possible to have further information about the temper of the alloy adding the following letters:
F as-fabricated. Applies to as-fabricated products without special control over thermal conditions or strain hardening. For wrought products there are no guaranteed mechanical property limits.
O annealed. Applies to wrought products which are annealed to obtain the lowest strength temper, and to cast products which are annealed to improve ductility and dimensional stability.
H strain hardened. Applies to wrought products which have been cold worked with or without supplementary thermal treatments to produce some reduction in strength. The H is always followed by two or more digits.
W solution heat treated. An unstable temper applicable only to alloys which spontaneously age at room temperature after solution heat treatment.
T thermally treated to produce stable tempers other than F, O, and H. Applies to products which are thermally treated, with or without supplementary strain hardening, to produce stable tempers. The T is always followed by one or more digits.

Subdivisions of basic tempers
The **H-temper -** strain hardened: The first digit indicates the specific combination of basic operations, as follows:
H1 strain hardened only. The number following this designation indicates the degree of strain hardening.
H2 strain hardened and partially annealed. Applies to products that are strain hardened more than the desired final amount and then reduced in strength to the desired level by partial annealing.

H3 strain hardened and stabilized. Applies to products which are strains hardened and whose mechanical properties are stabilized by a low temperature thermal treatment which results in slightly lower tensile strength and improved ductility. This designation is applicable only to those alloys which, unless stabilized, gradually age-soften at room temperature.

The three-digit temper

The following three-digit H temper designation have been assigned for wrought products in all alloys:

H111 Applies to products which are strain hardened less than the amount required for a controlled H11 temper.

H112 Applies to products which acquire some temper from shaping processes not having special control over the amount of strain hardening or thermal treatment, but for which there are mechanical property limits.

The following three-digit temper designations have been assigned for wrought products in alloys containing over a nominal 4% magnesium.

H311 Applies to products which are strain hardened less than the amount required for a controlled H31 temper.

H321 Applies to products which are strain-hardened less than the amount required fro a controlled H32 temper.

H323/H343. Apply to products which are specially fabricated to have acceptable resistance to stress corrosion cracking.

Subdivision of T temper - thermally treated

Numerals 1 through 10 following the T indicate specific sequences of basic treatments. Some of the commonly used designations are:

T4 solution heat treated and naturally aged to a substantially stable condition. Applies to products which are not cold worked after solution heat treatment, or in which the effect of cold work in flattering or straightening may not be recognized as affecting mechanical property limits.

T 5 cooled from an elevated temperature shaping process and then artificially aged. Applies to products which are not cold worked after cooling from an elevated temperature shaping process, or in which the effect of cold work in flattering or straightening may not be recognized in mechanical property limits.

T6 solution heat treated and then artificially aged. Applies to products which are not cold worked after solution heat treatment, or in which the effect of cold work in flattering or straightening may not be recognized in mechanical property limits.

The complete list of temper designations is given in the new European standards EN 515 (1993) [3].

A further distinction is made between **wrought alloys** and **casting alloys**.

Wrought alloys are designed specifically for fabrication by hot and cold forming processes, such as rolling, forging and extrusion. Magnesium and manganese are the principal aloying elements for non-heat treatable, wrought alloys. Magnesium is a very effective solid solution strengthening element, which is added up to 5% by weight. Chemical resistance is improved by adding magnesium, manganese or a combination of magnesium and silicon. If zinc, copper and/or silicon are added in addition to magnesium, very high strength alloys are obtained, which must be subjected to special heat treatments. The machinability is increased by adding lead and bismuth. High temperature strength properties are improved by additions of copper and/or nickel, manganese or iron. It is important to realize that

alloying elements added to achieve improvements of specific properties may well reduce other important properties, eg. ductility, stress corrosion resistance, etc. In order to choose the best alloy for the particular use or working conditions, it is therefore important to be aware of all potentially detrimental working conditions. The choice of an alloy will often be a compromise with respect to best possible over-all performance.

Casting alloys

Casting alloys (or foundry alloys) are exclusively used for the fabrication of cast parts and have favorable characteristics for this process. They exhibit high fluidity in the liquid state and good resistance to hot cracking during solidification. Castability is improved by the addition of silicon (7 to 13% Si). Increasing the silicon content further up to 25% reduces the thermal expansion down to levels of iron and steel. Such high silicon contents assure the dimensional stability upon heating e.g. for pistons in engines.

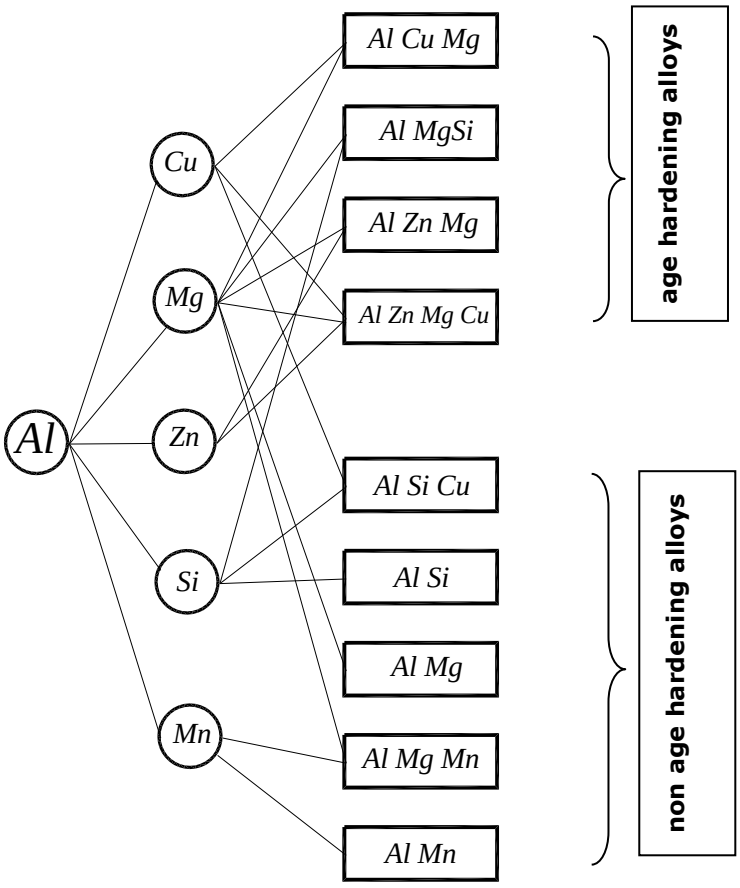

Fig. 2. 3: Synopsis of the principal aluminium alloys [3]

In 1906 Alfred Wilm discovered the firs heat-treatable alloy, named *Duralumin*, later identified as 2017. Almost accidentally, he found that after two

days at room temperature the strength became unusually high. The process is known as *natural ageing* [2].

This discovery was followed by intensive researches and nowadays several heat-treatable alloys are used extensively; they belong to 2xxx, the 6xxx and the 7xxx series.

Commercial aluminium products used in majority of structural applications are selected from 2XXX, 3XXX, 5XXX, 6XXX and 7XXX alloy groups, which offer medium of high strength.

2XXX heat-treatable alloys contain copper, together with other possible elements such as Mg, Mn and Si. The 2XXX-series comprises high-strength products, and is largely confined to aerospace industry.

The relatively low manganese content of 3XXX non-heat treatable alloys makes them half as strong again as pure aluminium, while retaining a very high resistance to corrosion. In construction the main application (in the fully-hard temper) is for profiled sheeting, as used in the cladding of buildings and others structures.

5XXX non-heat treatable alloys represent the major structural use of the non-heat treatable alloys. The magnesium content varies from 1% to 5%, often with manganese added, providing a range of different strengths and ductilities to suit different applications. Corrosion resistance is usually excellent. The 5xxx alloys appear mostly as sheet or plate. This series is little used for extrusions.

The **6XXX** heat-treatable alloys (mainly containing Mg and Si) have the largest tonnage use of the heat treatable alloys. They combine reasonable strength with good corrosion resistance and excellent extrudability. These alloys are readily welded, but with severe local softening in the heat-affected zone (MIG or TIG welding). The stronger type of 6XXX material in the T6 condition is sometimes described as "mild steel" of aluminium, because it is the natural choice for stressed members. In fact it is a weaker material than the mild steel, with a similar proof of yield stress (250 N/mm^2), but a much lower tensile strength (300 N/mm^2) [4].

From these two alloys classes, the most suitable for civil engineering, especially for bridge constructions, are the AA 5083 and the AA 6082.

2.1.3 Aluminium product forms

Extrusions for structural applications
- The extrusion process
- Direct extrusion
- Indirect and hydrostatic extrusion
- Extrusions for structural applications

Sheet and plate for structural applications
- The cold rolling process
- Hot rolling
- Alloys for rolled products

Casting alloys for structural applications

Availability - possibilities and limitations
- Extrusions
- Rolled products

In the extrusion process, a confined billet is forced by pressure to flow through an opening in a steel die forming the section shape of the extrusion. The

shape may be of a simple or intricate form and the cross section may either be solid or hollow. With a suitable die design, aluminium extrusions can be produced in complicated shapes in a single step.

Most commercial extrusion processes are carried out at temperatures in the range of 400° - 500° C using a pre-heated billet. This most frequently used extrusion method is called ”Direct Extrusion”. Other methods in use are the ”Indirect and Hydrostatic Extrusions”. Round billets dominate in use, but sometimes rectangular billets are used to obtain extrusions with large widths.

The most widely used extrusion alloys are the 6000-series (AlMgSi), and the extrusion speed for the 6063 alloy is between 20 and 70 m/min. Material with higher alloy content and/or complicated shape is extruded at a slower speed.

The majority of extrusions are made from the 6000-series alloys (AlMgSi) because of their good overall performance i.e.

- relatively easy to extrude
- medium to high strength in the T6 condition
- good corrosion resistance in marine and industrial environments
- good weldability by all welding methods
- good availability on the market, both as standard and special sections

In Europe, the main alloy used in extrusions for structural applications, is the 6082 (AlMgSi1Mn), and the T6 is the normal used temper.

Three basic profile types (Fig. 2.4) are defined which require different tool design: **solid**, **semi-hollow** and **hollow profiles** [5].

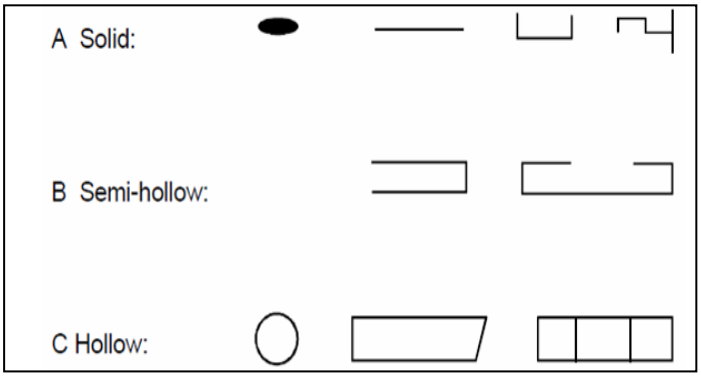

Fig. 2. 4. The Three Basic Types of Extruded Cross Sections

2.2 Applications of aluminium alloys

Aluminium was relatively new when it was first introduced as a structural material. The selection of alloys was limited and the fabrication techniques very primitive compared with the situation today. Despite these facts, structural aluminium applications were successfully introduced into many areas.

In this connection it is most relevant to group the applications into three main fields, and to look at a few examples in:

- the Marine Industry,
- the Transport Industry,
- the Civil Engineering Industry.

It is normal to look to the highest tensile properties, but additional factors must be considered when choosing the optimal alloy and temper. The desired tensile strength should always be matched with requirements for:

- Ductility
- Corrosion behaviour under the actual working conditions
- Weldability
- Fabrication requirements, such as cold forming (bending) etc.
- Thermal working conditions

Some of the high-strength alloys might be sensitive to stress corrosion or intergranular corrosion under certain conditions, others can be difficult to weld. The general corrosion resistance in marine atmospheres may also be different from one alloy to another. Figure 2.5 a and b presents us the effects of alloying elements on tensile strength, hardness, ductility, corrosion resistance and fatigue strength **[6]**.

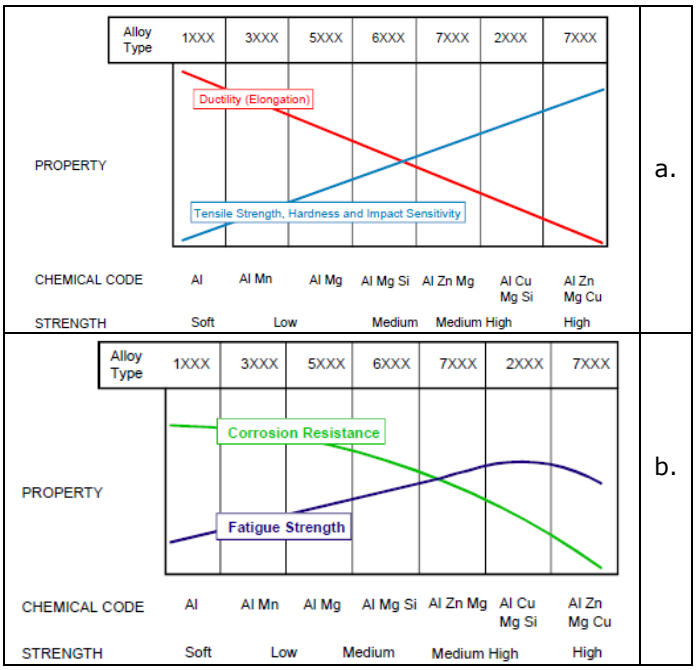

Fig. 2. 5. a) The effect of the alloying elements on tensile strength, hardness and ductility;
b) The effect of the alloying elements on fatigue strength and corrosion resistance

A widely used alloy for structural applications is alloy 5052 ($AlMg_{2,5}$) in tempers from soft (H111) to medium hard as well as in stabilized condition (H32/H34). The tensile properties for this alloy are not the highest possible, but the corrosion resistance in most environments is very good and so is its weldability. There are no special restrictions with respect to bending or thermal working conditions. The availability on the market is very good. Another alloy increasingly used for structural applications is alloy 5083 ($AlMg_{4,5}Mn$). This alloy has higher tensile properties than alloy 5052, but there are restrictions concerning the limits of continuous exposure temperatures (< 65 °C) and also with respect to cold forming requirements in fabrication (e.g. bending). The ready availability is generally

somewhat less than for alloy 5052. Alloy 5083 has an excellent, high general corrosion resistance and very good weldability.

Another important factor to be considered is the dependence of tensile properties on plate thickness for the 5000-series alloys. Alloys 5052 or 5083 are not available in work-hardened tempers beyond thicknesses of 100 mm. If higher strength is needed at larger thicknesses, it is necessary to change to heat treatable alloys such as 6082-T6. It has similar good general corrosion resistance and very good weldability. The stronger 6082 type alloys are used for members where tensile strength and impact resistance as well as stiffness and fatigue are important [7].

2.2.1 History of aluminium in marine industry

While the first steel ship was built in 1859, and only 11 steel ships were built in 1878, aluminium came into use in marine applications interestingly soon after steel. Already during the 1890s aluminium components were added to scores of ships and boats. But the alloys and the fabricating techniques then available were unsatisfactory and aluminium fell into disuse.

The 1922 Washington Disarmament Conference, which limited total naval displacements, again spurred the thinking of naval architects toward aluminium. New aluminium alloys were being developed to meet the strength and corrosion-resisting requirements for marine constructions.

In 1928, the light cruiser U.S.S. Houston was built with deckhouses of the then popular structural alloy Duralumin. This ushered in a new era of warship construction. By 1940, aluminium was used structurally for about 100 U.S. warships. More recently, the U.S.S. Dewey, a guided missile destroyer leader with aluminium superstructure, joined the fleet.

The earliest applications to merchant ships were achieved in 1934 on three Mystic Steamship Company colliers. One of these, a converted freighter, the S.S. Glen White, trimmed badly by the bow. The steel bulkhead between nos. 2 and 3 holds was replaced by an aluminium alloy 6053 bulkhead which corrected the condition and permitted carriage of 65 tons of extra cargo. When inspected 10 years later, there was no indication of corrosion or excessive damage from coal handling. The adjacent steel bulkhead, however, suffered from both.

Further development of alloys continued during the 1930s, a period which saw aluminium used in additional merchant ship structural installations.

The higher-strength aluminium alloy 6061 containing magnesium and silicon as major alloying elements, was under development prior to World War II. In 1944, as a result of wartime experience, it replaced alloy 6053 for structural use, and was quickly adopted for postwar merchant ships.

Aluminium construction received great impetus with the development of high-speed welding techniques and other weldable alloys, particularly the Al-Mg 5000 series. Since the early 1950s the majority of naval and merchant ship aluminium structures have been welded.

As a consequence a total of more than 1000 merchant ships had been built with aluminium superstructures in the beginning of the 1960s.

One of the best known ships with an aluminium superstructure is the S/S United States where the utilization of 2000 tons of aluminium resulted in a total weight saving of 8000 tons for the total vessel.

In addition to commercial ships and warships, aluminium is now used for tankers, fishing vessels, personnel boats, ferries and hydrofoils [8].

2.2.2 Present situation of aluminium in marine industry

Aluminium plate and extrusions are used extensively in the superstructures of ships where the designers wish to increase the above waterline size of the vessel without creating stability problems. In hovercraft and in the various types of surface skimming vessels, such as fast mulithulled catamarans, (Fig. 2. 6), the weight advantage of aluminium has enabled marine architects to obtain more from the available power.

On offshore oil platforms, aluminium has become the established material for helidecks and helideck support structures because of weight and through life maintenance advantages. For the same reasons it has found frequent use in stair towers and telescopic personnel bridges. Aluminium accommodation modules have been installed on the Snorre and on the Statfjord C platforms in the Norwegian sector of the North Sea. These modules have provided a range of benefits. An overall weight saving of the order of 40% compared to steel has been achieved in the case of the Snorre accommodation module. Cost advantages were obtained in the case of Statfjord C as a result of using only 60 tonne maximum load capacity platform crane for erection and assembly purposes.

Fig. 2. 6. The use of large aluminium extrusions gives quality and cost benefits in fast multihulled catamarans.

Market Influences. In world ship building, certain types of vessels are increasing in popularity. The interest in cruise holidays has surged and whereas it was once simply a matter of converting former ocean liners, purpose built vessels

are one of the fastest growing sectors of the industry. New fast ferries which can dramatically shorten journey times are entering service around the world.

The oil industry is seriously affected by the fall in world oil prices. If more marginal fields, for example some of the more difficult North Sea finds, are to be exploited then the costs of oil production hardware will have to be lowered. These market conditioned are pressurising designers, for a variety of technical reasons, to lower effective weight of structures, to cut construction costs and to reduce through life maintenance requirements.

If composite construction is adopted and very high strength fibres are used, fibre reinforced plastics can sometimes be an option to reduce weight, but problems can occur because of high material costs, high moulding costs and difficulties with fire ratings. Often the only feasible way of lowering weight is to adopt or change to aluminium.

Construction costs are very dependant on joining/assembly techniques. If joining can be reduced or made more simple by, for example, using the largest available extrusions or/and, where acceptable, using mechanical joints as opposed to welds, then construction times and hence costs can be lowered. The proven corrosion resistance of unprotected aluminium alloys in marine conditions, for example, the plate alloy AA5083 or the extrusion alloy AA6082, is well documented. This advantage over constructional steel has a considerable influence on through life maintenance costs.

Following the 1988 North Sea Piper Alpha oil and gas platform disaster, which claimed 167 lives, the new approach to safety has meant that accommodation modules are now installed on offshore structures as far away as possible from the more dangerous operations. This frequently means that the weight of the living quarters module is a factor which has a major influence on new build project costs.

Since the first offshore platforms were built, considerable advances have been made in the techniques for recovering ever higher proportions of hydrocarbons from the layered geological structures below the sea bed. These improved techniques have often meant that additional heavy pieces of equipment have had to be installed on the existing offshore facilities. Many of these ageing platforms are approaching their maximum designed topside weight. It is usually much cheaper to replace parts of an existing installation with new light weight modules than to install a completely new structure.

Properties Of Large Extrusions. The mechanical properties of extrusions are influenced by grain size. This in turn is largely determined by recrystalisation characteristics of the alloy, extrusion ratio, extrusion temperature and final heat treatment. The flow of material in the extrusion process causes a directionality of mechanical properties. Transverse proof stress and UTS are 85-90% of the longitudinal values.

One of the main advantages of the aluminium extrusion process is its ability to provide complex hollow shapes. Most hollow profiles are produced from die tooling which forms welds during the extrusion process. Judged by the criteria appropriate for the more familiar fusion welds, there would seem to be no problems with extrusion welds. Composition is constant, there is no filler metal and there is no liquid to solid phase change. Nevertheless, properties across the weld can differ from those of the parent metal because of differences in grain size and variations in the distribution of intermetallic phase particles.

The term extrusion weld covers two types of weld: seam welds formed when two streams of metal flow together in the die, and charge welds formed at the die ports between successive billets. Both types are solid state welds formed under

deformation and pressure. From a correctly designed die it is very difficult to form a low quality seam weld. Quality problems from charge welds are unfortunately far more frequent if correct operating procedures at the press are not followed.

It is most important that the correct length of extruded material is scrapped at the start and end of each billet in order to ensure that the low property material is removed. Proportionally large billets are required for large extrusions to provide a sufficient length of material to allow the potentially defective front and back ends to be removed. This means, particularly for extrusions with high cross-sectional areas, that high extrusion pressures and not just large diameter press containers are essential.

Table 2.1 shows minimum property values for extruded AA6082 T6 material in the longitudinal and transverse directions and includes minimum transverse values taken across extrusion welds. The table also shows values of mechanical properties of AA6082 butt welds for comparison purposes [9].

Table 2. 1. Mechanical properties of aluminium extrusions (minimum values)

Extruded AA6082 T6				
Thickness range (mm)		-5	5-10	10-30
Longitudinal	0.2% Proof stress (MPa)	260	260	260
	UTS (MPa)	310	310	310
	Elongation A5(%)	10	10	10
Transverse no extrusion weld	0.2% Proof stress (MPa)	245	245	235
	UTS (MPa)	290	290	280
	Elongation A5(%)	8	8	6
Transverse with extrusion weld	0.2% Proof stress (MPa)	245	245	230
	UTS (MPa)	290	290	260
	Elongation A5(%)	5	8	3
Butt weld AA6182, filler rod AA5356/5183				
Thickness range (mm)			-15	15-25
0.2% Proof stress (MPa)			115	95
UTS (MPa)			185	165
Elongation A5(%)			3-5	3-5

The longitudinal fatigue strength of AA6082 T6 after 107 cycles at stress ratio(R) = 0, is quoted typically as 130MPa. Fatigue tests made transverse to the extrusion direction give results of approximately 80% of this longitudinal value. Extensive testing of fusion welded flooring sections containing extrusion welds has shown that failures usually occur at the fusion welds or in the heat affected zone on either side of the weld seam.

Fatigue characteristics of samples taken transverse to the extrusion direction containing extrusion welds are similar to transverse values from the base material, always with the proviso that sufficient front end extrusion scrap has been removed to provide satisfactory extrusion weld quality. Large extrusions have better fatigue characteristics than similarly dimensioned assemblies of small extrusions fusion welded together.

Joining Methods. MIG and TIG welding have been in use for many years and have established themselves as reliable techniques when the correct procedures are employed. The various problems which can arise have also been studied in detail. Typical defects are shown in figure 2. The four fusion weld defects represented in the diagram affect different aspects of the mechanical properties on

the base material. Whereas the local heating, over ageing and consequent softening of the heat affected zone on either side of the weld bead lowers proof stress and UTS, the micro and macro porosity and shrinkage defects can act as sites for fatigue initiation and as a result can lower fatigue properties.

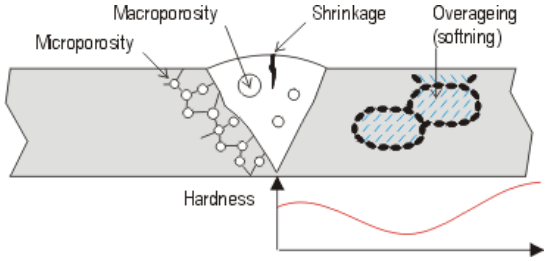

Fig. 2. 7. Possible quality problems in fusion welds

In addition to problems caused by weld flaws, fatigue strength is affected by mechanical factors such as holes, threads and grooves and also by the positioning of flaw free welds. However, extrusion technology can be used to position fusion welds in non critical areas or to enlarge the section close to a weld in order to compensate for the loss in properties caused by the welding process.

The design rules for fatigue of aluminium structures are covered by a number of standards including British code BS8118 Structural use of aluminium and the European code ECCS - paper, Doc 68 European recommendations for aluminium alloy structures fatigue design. Of the two codes the British Standard is in general the more conservative. An efficient quality assurance system is needed to monitor and guarantee both performance of welding equipment and workmanship.

Often the most convenient and technically optimum way of joining two or more aluminium extrusions is to use a specially designed mechanical fixing arrangement. The combination of relatively few welds with a high proportion of mechanical joints has become standard for helidecks. In the latest designs for offshore accommodation modules, the outer skin is a welded structure and selected parts of the interior have been designed to incorporate mechanical joints with sealants between the individual flooring sections.

Fast Catamaran Deck Design. By making use of large extrusion technology simply to reduce the amount of welding, considerable quality and cost benefits can be obtained. Benefits from use of large extrusions in more complex parts of a structure than the deck are more difficult to quantify but nevertheless real. The advantage of being able to free more parts of the design from the potential difficulties created by the need to thoroughly inspect the fusion weld joining two standard extrusions can easily be appreciated.

Offshore Module Design. The Snorre accommodation module was built using more than 20 different profiles, some of which were relatively difficult hollow sections. The welded design needed some 780 tonnes of aluminium making it the largest all aluminium structure ever built. The total finished weight of the Snorre accommodation module was 2100 tonnes. The Statfjord `C' accommodation module was based on the same basic components as were used for Snorre.

It was considered that a design change should make possible a lower weight, lower cost module. The design change has involved reducing and simplifying the number and type of extruded sections and moving to a combination of welded

and mechanical joints to lower construction costs. Since the new design requires relatively few profiles it is intended that these be held in stock to make virtual off

the shelf delivery a possibility. This will make modules available in the very short delivery times, important for the offshore refurbishment market. The primary and secondary beams and ternary decking have been so designed to allow flexibility inside the module so that heavy items can be supported in the structure with relatively little design input [10].

Fig. 2. 8. Offshore Aluminium Helimodule (Helideck, Helihangar, Stairtowers and support structure) – built in 1986

2.2.3. Transport Industry

In this context it is especially worth mentioning

- the air transport,
- the rail transport, and
- the road transport industries.

In air transport the development and use of aluminium alloys is directly linked to the development of that industry. It is clearly documentable that without the availability of aluminium the civil aeroplane industry would still be in its infancy. Although titanium, carbon fibre composites and stainless steel were used for military aircraft 70% of the airframes of civil aircraft is aluminium alloy.

The use of aluminium in rail transport is another success story.

The railway industry took immediate interest in using aluminium when it became available on an industrial scale around the turn of the century. Initially, the interest centered on the light weight and corrosion resistant aluminium as a substitute for brass fittings and wood or steel panelling in a coach structure, which was characterised by a strong, load carrying steel underframe and a largely wooden superstructure.

During the twenties and thirties the design philosophy changed to enhance passenger safety and reduce weight. The approach was to consider underframe and

superstructure as a load bearing entity. Steel panels riveted to a steel framework were used initially followed shortly by aluminium sheet fastened to aluminium extrusions. This "sheet and stringer" or "stretched -skin" design still persists to date for modern steel coaches with the important difference that welding came in to

replace the old-fashioned riveting and that higher strength copper-bearing or stainless steels helped to improve the rust problem and to reduce weight.

A further recognisable change in the design of aluminium railway cars was dictated by economic aspects. The significant increase in labor cost during the seventies spurred the use of larger amounts of extruded sections with integrated functions. Together with the availability of semi-automatic, multiplehead welding equipment, it became possible to fabricate floor, roof and sidewall subassemblies with only a few longitudinal welding passes on extruded shapes running the entire length of the car. By using integrally stiffened extruded side and roof panels the rectification of distorsion, which is inherently necessary in the stitch-welded or spot-welded "sheet and stringer" design, was largely avoided. At the same time, labor-intensive finishing work and the need for filler paste application preparatory to painting was reduced significantly (Fig 2.9).

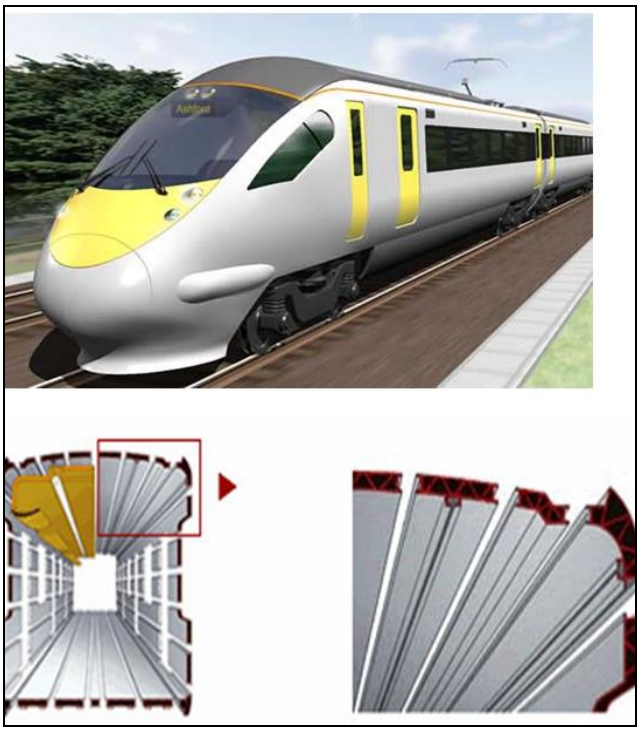

Fig. 2. 9. Hitachi train – Japan

In summary, the full application of the aluminium extrusion technology for the vehicle body design resulted in cost reductions to such an extent that light-weight aluminium coaches were and are being built at equal or lower costs than conventional steel coaches.

In trucks, trailers and tankers aluminium has been used for the past 40 years, the weight advantages resulting in payload increase and for fuel savings which are more obvious than in the automobile [11].

The materials used for aircraft manufacture must meet a demanding set of property requirements. Aircraft structures must be **lightweight, durable and damage tolerant.** Furthermore, these properties must be attained at as **low cost** as possible. High strength aluminium alloys are able to meet the property challenges in a cost effective way and aluminium therefore remains the predominant choice for the construction of civil aircraft, although competition from other materials is increasingly intense.

Applications of aluminium alloys for **aircrafts** (Fig. 2. 10):

- Fuselage skin
- Upper wing skin
- Lower wing skin

First, the materials used for the fuselage skin will be considered. The type of loading (e.g. whether compressive or tensile, static or dynamic) is critical when choosing a material to use. Consider the loading of the aeroplane fuselage: A pressure vessel being inflated and deflated, while being subjected to alternating compression and tensile forces due to bending moments. The fuselage will experience different loads depending on whether the aeroplane is in flight, or on the ground.

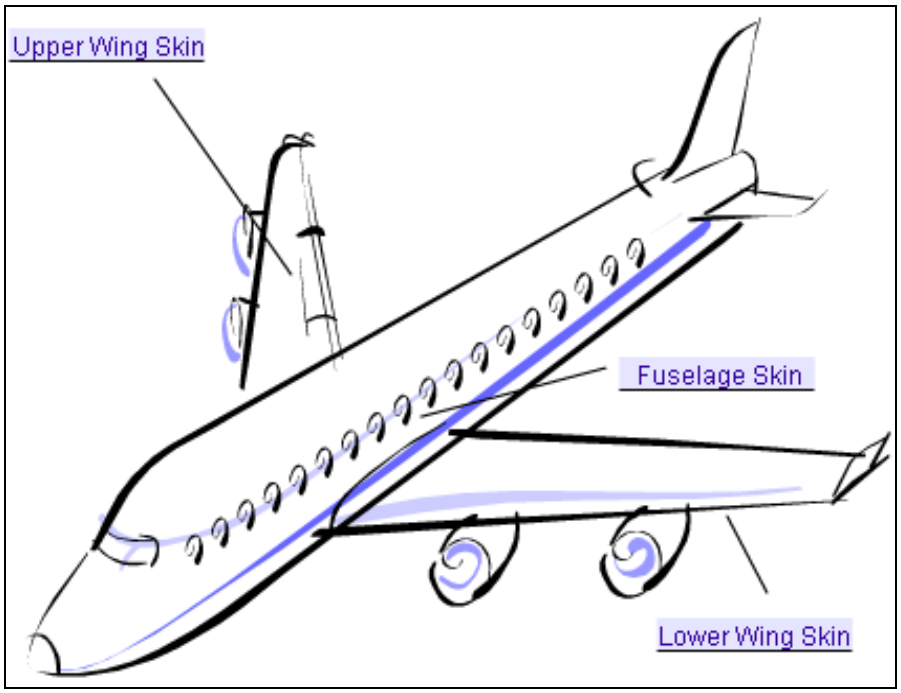

Fig. 2. 10. Applications of aluminium alloys for aircrafts

These loading conditions determine which of the mechanical properties are most critical when selecting a fuselage material (Table 2.2).

Table 2. 2. Main Mechanical properties for fuselage skin

Not Important	Important	Very Important
Strain Hardening Exponent	Compressive strength	Fracture Toughness
Elongation to failure	Tensile Strength	Fatigue Resistance
	Shear Strength	Stiffness
Yes, these properties are not very important for service because they relate to plastic deformation. In service, the material is in the elastic regime and does not deform plastically.	Yes, strength is important. However the lifetime of the fuselage is not limited by its strength and it is not the most critical property.	Yes, these properties are critical for the fuselage. Cyclic loading conditions are experienced, so fatigue resistance and fracture toughness are very important.

The upper and lower wing skins are subject to different loading conditions in flight. This influences the choice of materials in each case:

- The upper wing skins are primarily subjected to compression forces during flight.
- The lower wing skins are primarily subjected to tensile forces during flight.

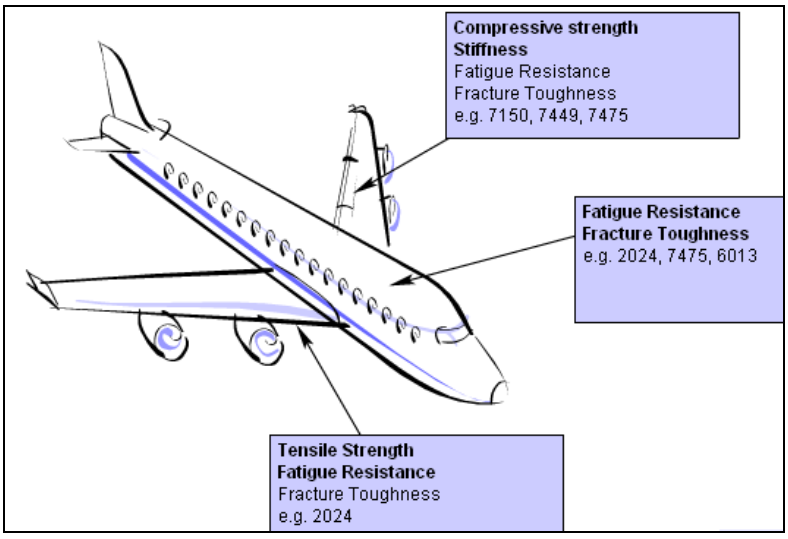

Fig. 2. 11. Possible alloys for an aircraft

A different balance of properties is required for the fuselage, upper wing skin and lower wing skin. To meet these different requirements, different aluminium

alloys are chosen. Using property charts, the best alloy for each application has been identified. This can be summarized as follows (Fig. 2.11).

2.2.4. Civil engineering

Aluminium is used in building and architecture for various reasons:

- Its light weight allows for easier rectification of structures for example façade panels, roofing, doors and windows in architecture, and ladders and platforms as building tools.
- Its good inherent corrosion resistance and methods for protection such as anodising allow for durable outdoor exposure
- Its attractive metallic appearance and the methods for colouring is ideal for decorative design
- These properties in combination with the good strength-to-weight ratio that can be obtained, results in various day to day applications of aluminium, mainly of the 1xxx, 3xxx and 5xxx alloy series for sheet products and 6xxx series for extruded products, in our houses, offices, public buildings and their construction.

Note also that metallic aluminium in "massive" form will not burn. Further, its relatively low melting point (660 °C) means it will "vent" early during a severe fire, releasing heat and thereby saving lives and property. Construction and demolition waste products represent a growing challenge for modern industrial societies.

The depositing or incineration of most types of materials can lead to air, water and soil pollution. This is not the case for aluminium, which even if inadvertently dispersed in the environment does not have harmful side-effects. Therefore, aluminium recycling not only has important economic implications but also contributes to environmental protection. A study has demonstrated that about 95% of aluminium building products are recycled at their end-of-life thanks to the high value of the aluminium scrap.

Aluminium alloys in sheet form are used for a variety of applications on buildings, such as roofing and external cladding. Such applications make use of the material's durability, being hard wearing and resistant to corrosion. The sheet can be used bare, but for many applications a paint coating is applied by the sheet supplier to increase protection from the environment and for aesthetic appearance. For some applications, the sheet surface is anodised to produce a decorative surface finish.

Good surface appearance (Fig. 2. 12, Fig. 2. 13) is obviously a critical requirement of these products, but some strength is generally required for in-service performance as well as formability, for example, to enable the sheet to be shaped into profiled panels for rigidity. Low strength commercial purity alloys such as EN AW-1200 are used for some applications (e.g. flashing), but generally higher strength alloys of the 3xxx series are used.

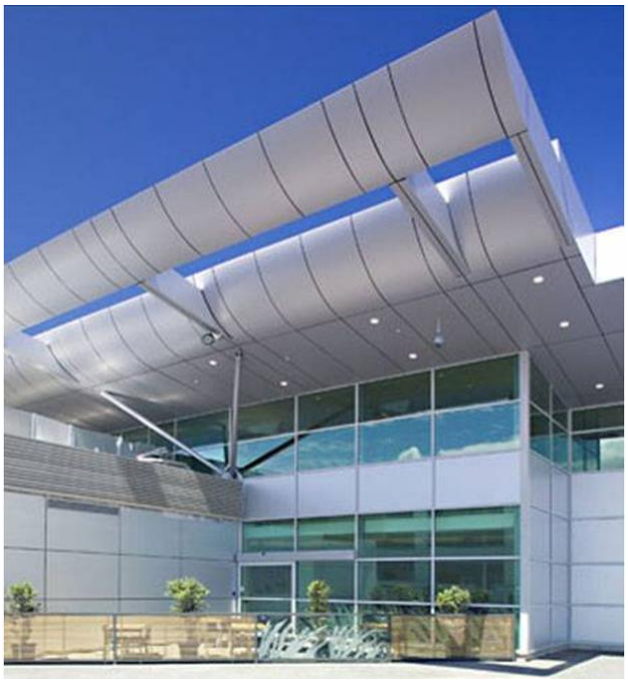

Fig. 2. 12. Aluminium façade

5xxx series alloys are employed where high strength is a particular requirement or where greater corrosion resistance is needed, for example in marine environments. Depending on the product, sheet may be used in the soft-annealed O-temper, where dispersion-hardening and solid solution strengthening alone determine the mechanical properties, or in a range of work-hardened tempers [18].

Fig. 2. 13. Aluminium sheet used for roofing

2.3 History of aluminium in bridge construction

Aluminium is an ideal material to add width without increasing weight to the substructure and decks of load restricted bridges, historic bridges, movable bridges, and bridges with narrow roadways. Because seismic forces are directly proportional to weight, aluminium is also excellent for seismic retrofitting of bridges.

Aluminium alloys have been used in bridge structures for more than 75 years (in 1933 in USA). Since that time aluminium has been used in various ways in hundreds of bridge structures around the world, and most remain in service today, including some for more than 50 years.

While still not considered a standard for bridge structures, aluminium alloys have much to offer for such applications, and continue to be used where their light weight, high strength-to-weight ratio, and excellent corrosions resistance satisfy service requirements and justify the additional initial cost. When considered on a life-cycle coast basic, aluminium bridges components have clear superiority.

As advantages of using the aluminium alloys in bridge construction, the most important are presented:

- light unit weight (only 1/3 that of steel and about 80% of concrete) and strength comparable to typical bridge steels; this conduce to a lighter weight and comparable strength that enable the use of a higher ratio of live load to dead load;
- excellent corrosion resistance, with negligible corrosion even in the presence of rain and road salts; this eliminates the need to paint the aluminium components, except perhaps for aesthetical aspect, resulting in lower maintenance costs;
- high toughness and resistance to low-ductility fracture, even at very low temperatures, and free of any ductile-to-brittle transmission that has sometimes been fatal to older steel bridges;
- excellent fabricability, including ease of extrusion production to complex hollow shapes optimized for structural design; the combination of light weight and ease of fabrication enables the entire aluminium structure or major portions of it to be pre-fabricated, carried to the site, and erected in the flow of traffic and thus less inconvenient to drivers;
- downtime for a bridge receiving an aluminium deck is a fraction of the comparable time needed for concrete.

But, like all things that have advantages, there are also and some limits and borders in using the aluminium alloys in bridge construction:

- the most important of these is the higher initial costs of an aluminium bridge over comparable with steel or concrete;
- another factor limiting the use of aluminium for bridges has been the lack of general knowledge of the properties and the design rules for aluminium in structural applications by many engineers;
- the factors that make the design of aluminium bridges more different from steel structures, such as: aluminium's lower modulus of elasticity 70 GPa (for steel is 210 GPa); the fatigue strength of aluminium is about 1/3 that of steel; aluminium's coefficient of expansion is about twice that of the steel or concrete, so thermal stresses must be considered [12].

Taking a back look, using aluminium in bridge constructions has a history staring in 1933, when the first aluminium deck was used to replace an old steel-

wood deck. This change produced in the first line a big reduction of dead-load and on the other hand, a significantly increase of the live-load-carrying capacity. The alloy was a 2014-T6 (not one of the best choice for corrosion resistance), in rolled plates. The traffic load was: two lanes of motor traffic and two tracks for trolley (ore for every side of the bridge). This structure was in use until 1967, when the structure was improved with an orthotropic deck, to increase the live-load with more and bigger trolleys and trucks. The new deck was realised using the 5456-H321 and 6062-T6 alloys. The new aluminium orthotropic deck was replaced in 1993 with a steel deck, taking in account only the short time costs.

The first railroad aluminium bridge in the USA was erected in 1946. This bridge was constructed by Alcoa, probably with the scope to illustrate the capability of aluminium in bridge construction. For materials were used Alclad 2014-T6 plates for girders, 2117-T4 for rivets.

The first highway aluminium bridge was constructed in Quebec, Canada, in 1950 (Figure 2.14). It is the challenging prototype of a motorway bridge, built according to the Maillart's scheme with a total spam of 150 m, an arch of 87 m of span, and a total weight of 200 000 kg.

Fig. 2. 14. Arvida bridge (Quebec, Canada)

In the period 1958 – 1967 in USA the construction of aluminium bridges known an important increase because of the necessity to realise economical structures and to improve the safety of superhighways by incorporating cloverleaf intersections in them rather than dangerous crossroads. In this case aluminium seemed to be the perfect material, also because of the short time to obtain from bauxite, in comparison to the time to obtain steel (in the 60').

Five bridges were erected in that period. The two of them were conventional built-up I-beam design: a two-lane, four-span welded plate girder bridge near Des Moines and a pair of two-lane, riveted plate girder bridge. In 1958 a two-lane, four-span welded bridge over I-80 in Iowa was erected. The girders were realised from a 5083-H113 welded plate with a concrete deck. This was in service until 1993, because the entirely intersection was re-designed. Laboratory researches were made from the girders: the results of the tensile and the fatigue tests showed, after about 40 years in service, results comparable with the one from the erection time.

The twin Jericho (erected in 1960, two-lanes each) were fabricated of 6061-T6 plate with 2117-T4 riveters, and a concrete deck. The bridge was in service until 1992, when the whole intersection war re-designed [13].

From 1948 there are known the telescopic aluminium gangways for ocean terminals (Fig. 2. 15).

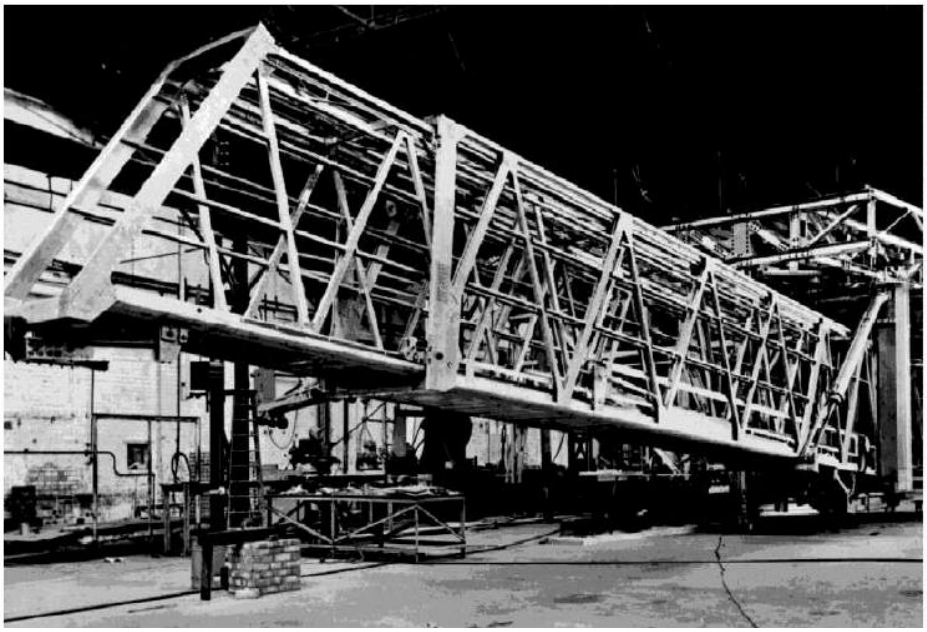

Fig. 2. 15. Telescopic aluminium gangway for ocean terminal

And not only in USA were aluminium bridges erected. Over 50 aluminium bridges have been built in Europe, a number that is increasing yearly.

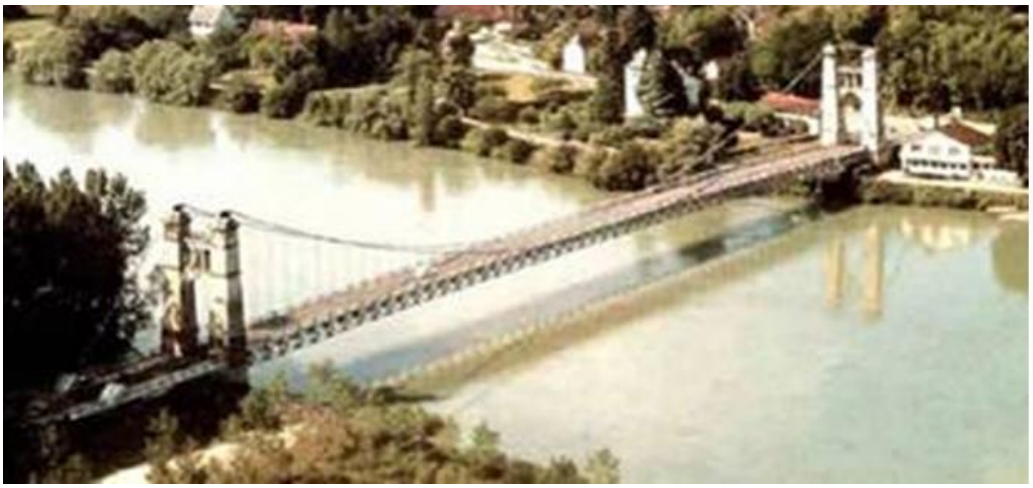

Fig. 2. 16. Lyon Groslee bridge (France)

Since aluminium is lighter than steel and concrete, does not rust or need painting or protective coatings, and lowers maintenance and installation time - hence lowers cost - aluminium has distinct advantages over other materials. A short look to the aluminium bridges erected in early years in Europe is presented in the Table 2.2.

Table 2. 3 Aluminium bridges constructed in Europe [14]

Location	Bridge Type	Destination	Span [m]	Erection year	Type of deck	Alloys Type
Hendon Dock, England	Riveted Double Leaf bascule	highway, rail	37	1948	Alu plate	2014-T6 6151-T6
Tummer River, Scotland	Riveted Truss	pedestrian	21+5 2+21	1950	Alu Sheet	6151-T6
Aberdeen, Scotland	Riveted Double Leaf bascule	highway, rail	30,5	1953	Alu Sheet and wood	2014-T6 6151-T6
Dusseldorf, Germany	Twin weld plate, arched, ribs	pedestrian	55	1953	unknown	unknown
Lunen, Germany	Riveted warren truss	highway	44	1956	Alu shapes	6351-T6
Two bridges in Luzern, Switzerland	Suspension stiffened girder	pedestrian & cattle	20 and 34	1956	timber	5052
Rogerstone, South Wales	Welded W truss, thru girder	pedestrian	18	1957	Corrugated alu sheet	6351-T6
Monmouth-Shire, England	Welded	pedestrian	18	1957	Corrugated alu sheet	6351-T6
Banbury, England	Riveted bascule	highway	3	1959	Corrugated alu sheet	6351-T6
Gloucester, England	Riveted bascule	highway	12	1962	Extruded Alu Shapes	

2.4 Present situation of aluminium in bridge construction

Since 1995 world wide initiatives have been taken in the design of aluminium bridges. In Europe, in particularly in Norway and Sweden, approximately 30 bridges and approximately 80 bridge decks have been built over the last couple of years. This revival of aluminium bridges is mainly due to the market-pull to lightweight and sustainable bridges. A proper design of connections in aluminium bridges is important, because it may simplify the assembly and erection (Fig. 2. 17), which benefits the initial costs of aluminium bridges.

Fig. 2. 17. The Forsmo river aluminium road bridge (courtesy of Hydro Aluminium Structures)

During 1997 and 1998 an international contest has been held for the building of 58 pedestrian and traffic bridges in the planned area of Leidschenveen, near The Hauge, Netherland. In the tradition of Dutch city planning the area is criss-crossed with canals. To accommodate the traffic circulation, a bridge system has been designed for 15 different bridge types, consisting of 45 pedestrian/cycling bridges and 13 traffic bridges [15].

Fig. 2. 18. Lüneburg, Germany

Fig. 2. 19. Aluminium trough bridge - Selzbach

In 1996 in Huntingdon, Pa., occurred a problem: the Corbin suspension bridge that connected the two sides of the city was, as its historical trust designation implied, aging dramatically and posed a potential threat to any heavy vehicles using it. With a posted 7-ton (6.35-metric ton) weight limit, the venerable structure was off-limits to heavy emergency vehicles, which were forced to use a circuitous 24-kilometer detour to avoid the bridge [13].

Desperate to save the bridge, but unable to strengthen its deck using conventional construction materials because of its weak substructure, the city opted to replace the existing superstructure with a lightweight aluminium deck that decreased the bridge's "dead load" and concomitantly increased its bearing or "live load" capacity. The result today is a stronger bridge (Figure 2.20) that literally serves as a lifeline for citizens in need of prompt emergency attention.

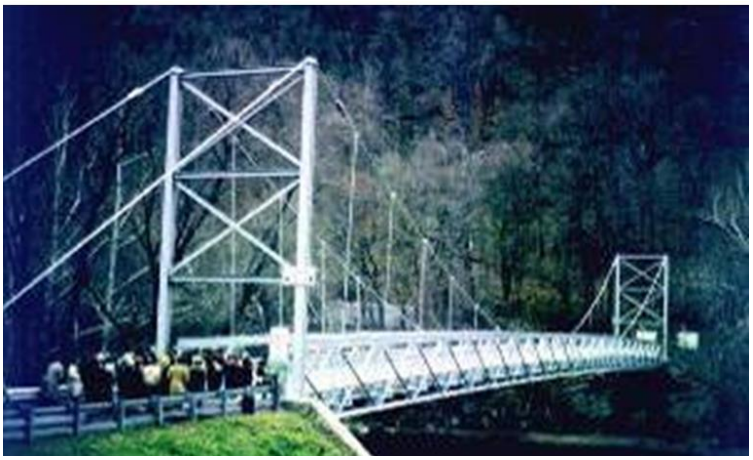

Fig. 2. 20. The Corbin Bridge in Huntingdon, Pa.

Jeffrey M. Dobmeier and his team [13] made, in 1999 a report about analytical and experimental evaluation of an aluminium bridge deck panel. In this report a deck panel realised from aluminium welded extrusions was loaded to failure. The components (Figure. 2.21) were welded together at the top and the bottom flanges.

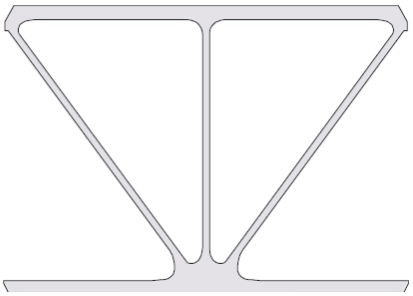

Fig. 2. 21. Transversal section of an aluminium deck slab element

The welds were realised longitudinal (Fig. 2. 21). The deck structure was analyzed experimental and analytical, with the help of finite elements analyse.

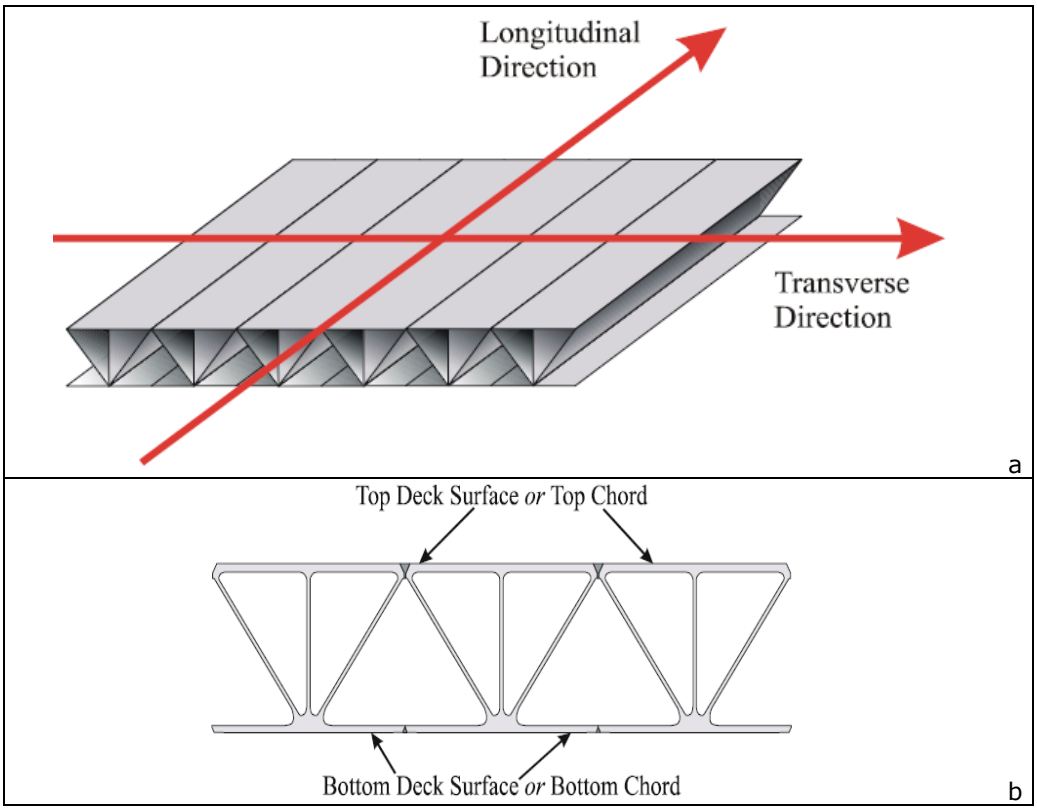

Fig. 2. 22. Welded elements of an aluminium bridge deck panel

Mobility and ease of installation are maintained even for large structural elements, such as link bridges and telescopic bridges (Fig. 2. 23).

Fig. 2. 23. Telescopic bridge

A new important field of application is the one of military bridges in which „lightness" and „corrosion resistance" play a fundamental role. At present, it is possible to reach 40 m of span with prefabricated elements – easy to transport and to erect. The main applications have been developed in Great Britain, Germany and Sweden. In Germany, a military bridge is produced composed of prefabricated units [16] (Fig. 2. 24).

Fig. 2. 24. The German military bridge: erection phase

The above revival of aluminium bridges is due to:

1. A market-pull for lightweight structures in order to
   - increase the live load on a bridge - important with renovation of existing bridges, for example Lyon Groslee Bridge, near Lyon
   - decrease costs for movable bridges and bridges with long spans where dead-weight is the main load;
   - extend existing bridges, by attaching a lightweight structure;
   - simplify assembly and construction;
   - reduce transport costs.
2. A market-pull for sustainable structures to:
   - minimise material consumption;
   - reduce the cost and environmental impacts of the maintenance operations;
3. The availability of a large variety of cross-sectional shapes of extruded aluminium profiles sizing typically up to 600 mm height and up to 400 mm width.
4. The up-to-date knowledge of structural behaviour of aluminium, which has considerably improved in the last decades.
5. The competing costs of aluminium structures. With a proper design initial costs can compete with steel structures while life-time costing analysis usually demonstrates the cost advantage of using aluminium structures due to lower maintenance needs and longer life span.

Although long-span aluminium bridges are interesting because of weight reduction, the number of these bridges is rather small. So, it was decided to concentrate on bridges with typical spans up to 20 m, which are found in large numbers. On the basis of an inventory four application areas were defined in the Netherlands i.e.:

- movable bridges;
- residential area (so-called VINEX) bridges;
- extension of existing bridges; and
- renovation of bridge decks.

Movable bridges

For movable bridges a design study for a non-balanced, hydraulically driven bridge with a span of 18 m and a width of 12 m was carried out. The design of the Riekerhaven bridge (Fig. 2. 25) in Amsterdam was based on the outcome of this study. The design of such a movable bridge is subject of the detailed case study on aluminium bridges.

Fig. 2. 25. Riekerhaven bridge (Amsterdam)

Movable Traffic Bridge Simulation

The 30,000 kg bridge (Fig. 2. 26) should be opened in T seconds by making a 90° turn. To that end, an actuator was designed to exert a horizontal force on the lever a_2, which has an initial inclination of 45° (π/4 radians).

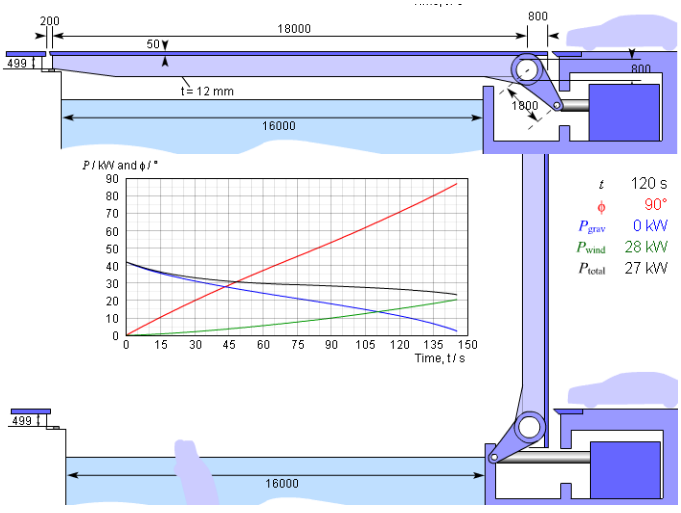

a.

b.

Fig. 2. 26. Function schema of a movable bridge: a. not open; b. open

Assumptions:

- The design weight of the aluminium bridge = 353,160 N (a mass of 30,000 kg and a load factor of 1.2 has been applied)
- A constant velocity of the actuator
- An inclination of the lever arm of 45°

Conclusions

- In the example, the opening time has been taken as 150 seconds. This results in a peak power of 42 kW. From the graph, one may observe that this peak is present at the start of opening and it is zero at complete opening of the bridge.
- As an average a power of 21 kW is estimated which gives an energy consumption of 21×150 = 33000 kWs = 9.17 kW h per opening of the bridge
- During the lifetime of the bridge 500,000 openings have been estimated, so that gives the total energy consumption of 4,585,000 kW h
- For a steel bridge, the gravity force can be estimated two times as high as for aluminium; so for the same opening time for the steel bridge you need double the energy compared to the aluminium bridge.
- In the case of the Groningen movable bridge the two most important requirements were the maximum power demand (3 phase × 80 Amp × 220 V = 52,000 W available) and the time to open the bridge [18].

Extension of existing bridges

The existing, 80 year old steel arc bridge near Maarssen, the Netherlands, (Fig. 2. 27, Fig. 2. 28) with a main span of 120 m, had to be renovated.

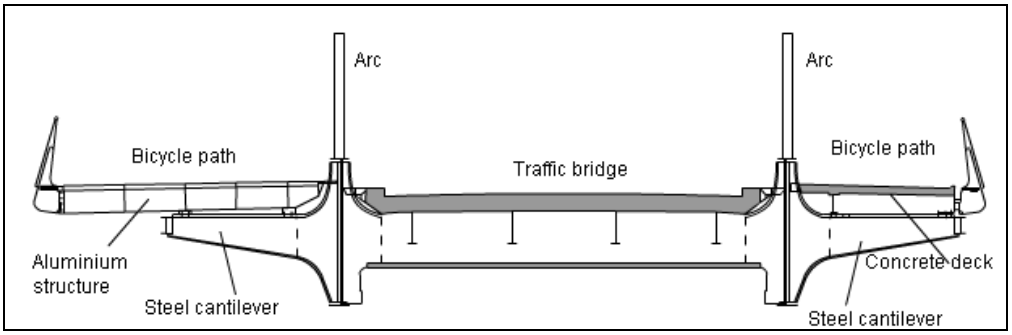

Fig. 2. 27. Extension design

The bridge spans both the Amsterdam-Rhine canal and a railway. It has two traffic lanes and two pedestrian / bicycle lanes, one on each side. One of the renovation aspects was to replace and enlarge the bicycle lanes. The old ones consisted of a concrete deck supported Al Dered by steel cantilevers 8 m apart. As the load-bearing capacity of the cantilevers is limited, a wider bicycle path could not be constructed out of concrete and the maximum width obtained with a steel structure was too small. Applying prefab aluminium panels the width was enlarged from 2.5 to 4.8 m. The length of the panels was 16 m, thus spanning two cantilevers.

Fig. 2. 28. Bridge over Amsterdam-Rhine canal

Renovations of bridge decks use aluminium usually for replacing the hard wooden decks on steel bridges in Europe and North America, most of them built before 1960. These wooden decks need inspection and maintenance, and have to be replaced regularly which causes closure of the bridge. An inventory of existing wooden decks showed that an alternative aluminium system should be composed of panels with a height of 70 mm and a span of 750 mm. The first application in the Netherlands took place in 2003 for the deck of the movable bridge over the Haringvliet locks on the A29 highway. Aluminium panels, 3.5 by 1.5 m, were built up out of welded extrusions. In total an area of 600 m^2 of wooden bridge deck has been replaced. In the meantime, two other bridge decks in the Netherlands and two in Kentucky, USA were also renovated in the same manner [18].

2.5 Conclusions

The present status of aluminium utilization in stressed structures can be summarized as follows:

- Despite the existence of good textbooks and codes of practice, the lack of teaching material is obvious. As a consequence aluminium does not achieve the status of an accepted structural material in engineering education
- A lack of sufficient knowledge - often accompanied by prejudices- leads to decisions against the use of aluminium. Aluminium structures can mainly be found in applications like the rail and road transport industries, speed personnel boats and airplanes where weight saving is at a premium.
- For those applications where traditional building materials like steel and concrete are prevailing, aluminium is facing a stiff competition and sometimes suffering set-backs. The lack of formal education, competence

and obvious commercial interests are probably the major reasons for this situation.

Aluminium has a bright future as a structural material, but only based on following prerequisites:

- A comprehensive upgrading of the materials position at the educational institutions.
- The development of detailed cost studies for the respective potential applications.

An example is the rapid and comprehensive use of aluminium in structural components in the automotive industry. This development takes place as a joint development between strongly motivated commercial interests, i.e. of the aluminium and the automotive. Provided the required development regarding education and commerciality takes place, aluminium has a great potential for making its way into new industries and applications as well as regaining most of the lost positions [17].

The heavy structural use of aluminium was pioneered in 1931 in the USA when a drag-line crane, having a 46 m mainly aluminium boom, started work on the Mississippi embankments. Thirty such booms went into service. Better known is the uprating of the 220 m long Smithfield Street Bridge in Pittsburgh, USA, achieved by redecking it in aluminium (1934). The structural sections for the new deck were produced by hotrolling in steel-mill rolls, large extrusions being then unavailable. Another early application was in a rail-bridge over the Grasse River at Massena, NY, USA, where one of the 26 m plate-girder spans was made in aluminium instead of steel as an experiment (1938). All these early structures were in naturally aged 2xxx-series alloy (duralumin) that would be thought unsuitable by modern ideas. The Smithfield Street deck lasted for 40 years, despite the choice of alloy, after which it was replaced by another aluminium one. This second deck is built of 6xxx series extrusions, using welded construction.

Immediately after the war, steel was scarce and an available alternative was aluminium, which was specified for various structures, such as factory roofs and cranes, despite the extra cost. Much of this market soon disappeared, although aluminium continued to appear in roofs of large span. Today it still appears in some such roofs, typically employing proprietary ‘space-frame’ forms of construction. In bridges, the greatest consumption of aluminium has been in military bridges, which have to be erected and launched in record time. Welded aluminium kits designed for this use are a worthy successor to the famous Bailey, and have consumed thousands of tones. Aluminium also appears in civilian bridges in remote locations, where they are left unpainted. There is a theoretical case for aluminium in bridges of very large span, where self-weight is a major factor, but such a development has yet to appear. A more recent heavy structural development is in the offshore field. Here aluminium is gaining acceptance as a valid material for modules on fixed platforms, where the cost of installation critically depends on weight. Typical examples are helidecks and accommodation modules. The latter may be described as all-aluminium five-storey hotels that are floated out and lifted into place in one piece, complete with cinema. In the late 1940s, some designers followed American earlier practice by specifying 2xxx-series alloy for large structures. In a few cases this was a disastrous choice. For example, a bascule bridge in such material at the docks in Sunderland, UK, failed within a few years, due to corrosion in the severely polluted marine/industrial atmosphere. Another example was British crane jibs designed in the stronger form of 2xxx (superdural), using stress levels that were much too high. These failed by fatigue after a very short life. It was soon realised

that the best alloy for civil engineering structures is usually the stronger type of 6xxx-series material, although the weldable kind of 7xxx is sometimes preferred. A notable example of 7xxx usage is in military bridges [4].

Criteria for Selecting Aluminium

All structural materials have different properties and technical characteristics, and consequently differ in their suitability for a given application. For some obvious cost reasons, aluminium will not become an alternative structural material in all cases, even though its use would be technically possible.

In order to evaluate whether aluminium could be the right material in a specific application some decision criteria must be considered:

- Weight reduction
- Maintenance aspects
- Product costs
- Load criteria

Lightweighting

Since, for all structural applications, aluminium will provide substantial weight saving compared with traditional structural materials such as steel and concrete, all applications where lightweighting has a commercial value are obvious candidates for aluminium utilization. Consequently, in the transport industry where fuel consumption is crucial for the economy of a product, aluminium has a very strong position (aeroplanes, boats, railways) as well as the greatest development potential (automotive).

A very often overseen effect of the lightweighting aspect is the downsizing effect. This can be illustrated by focusing on a cable bridge where a substantial weight saving of the bridge deck structure will also result in the possibility of downsizing towers, cables and fundaments. A total application economy should therefore be introduced in order to find the right solution for any structure.

Maintenance Aspects

Most aluminium alloys require low maintenance because of their good corrosion resistance. Therefore, aluminium is an excellent candidate for all applications where the benefit of freedom from initial protection and maintenance yields a commercial benefit. A general problem in many product developments is still the lack of life-cycle cost evaluations.

A tendency to select the cheapest alternative at the initial cost level could very well result in higher life-cycle costs compared with other, initially more expensive solutions.

There is an increasing experience that life-cycle cost decision criteria will lead to growing utilization of aluminium.

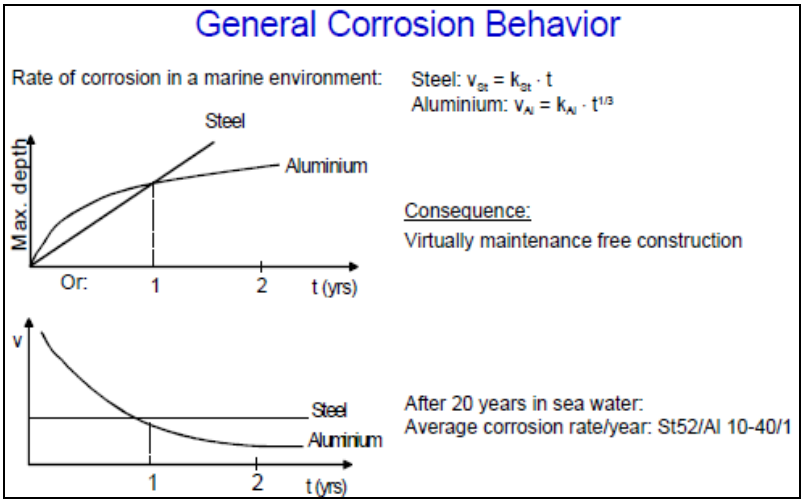

Fig. 2. 29. General corrosion behaviour of Al and Steel – a factor of maintenance costs

Product Costs

Aluminium is a more expensive material (per kg) than most alternative structural materials. However, due to its low weight (resulting in cheap handling) as well as due to modern joining technologies and the possibility of developing functional combinations through utilizing especially shaped extrusions, labor costs become relatively low compared to cheaper alternative materials.

For primary structures (bridges, etc), approximately 63% weight saving is required before product cost equivalence aluminium/steel is achieved. If such a weight saving is not achievable, secondary effects like lightweighting, downsizing and low maintenance costs are needed to evaluate whether aluminium is an optimum material selection or not.

Load criteria

Theoretical weight savings close to 70% compared with steel and 95% compared with concrete are achievable. Consequently, aluminium has the potential of becoming the cheaper alternative already on a product cost level.

Whether such weight savings are achievable or not depends on the load criteria. The higher the dead load/live load ratio, the higher the weight saving which can be expected. Consequently, long span constructions especially with high dead load/live load ratio are obvious candidates for aluminium utilizations [8],[17].

3. FRICTION STIR WELDING (FSW)

3.1 Process description

In 1991 The Welding Institute in England invented and developed a new welding process [19]. Friction stir welding (FSW) is a bending procedure that takes place in solid state which is based on the heating of the materials through friction and plastic deformation realized at the interaction between the non-consumable pin tools which is rotating at surface of the joined elements. The welding shouldered pin tool is introduced in material and with the rotating speed moves across the join (Fig. 3. 1). The shoulder is now in intimate contact with the material surface and the friction between the shoulder and the surface heats the metal and produce a tubular shaft of the material around the pin [20]. The plasticized material is moved behind the tool, realizing a welded joint. The two materials are joined in what would resemble a continuous forging operation. Due to the high frictional forces between the wear resistant tool and the parent material the workpiece temperature rises to a hot forging level (typically in the range of 70-85% of the melting temperature), where re-crystallization is balanced by plastic deformation allowing the material to flow under large plastic deformation leaving a solid phase bond between the two pieces.

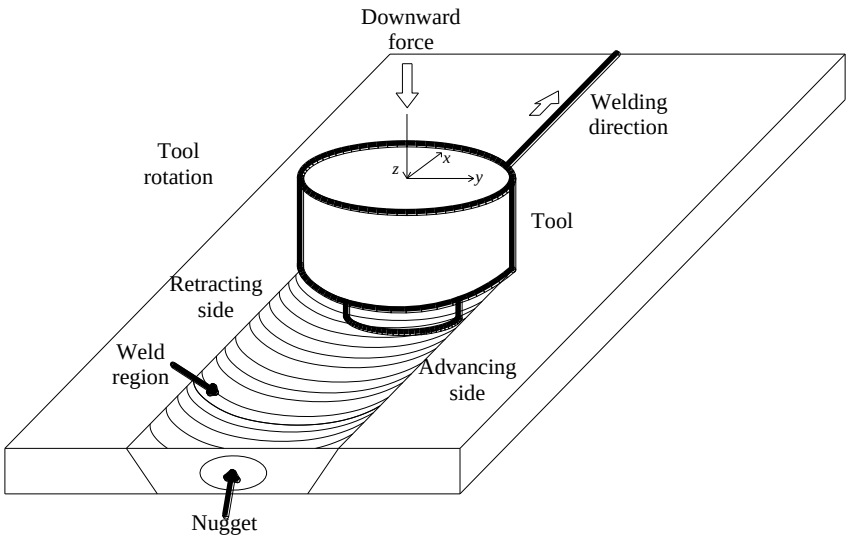

Fig. 3. 1. Schematic of the friction stir welding process

The process can be described in the following principal steps (Fig. 3. 2):

- the tool starts to rotate in the air;

- after that plunged into the material and start to forged; because of the forging between the tool and the material, the material achieved a temperature that permits to the pin of the tool to move „almost melted" material from one side (advancing side) of the weld to the other side (retracting side) and produced the plasticization of the materials and a new re-crystallization;
- the tool moves across of the weld line;
- at the end of the joint the tool will retract and the welding process is over.

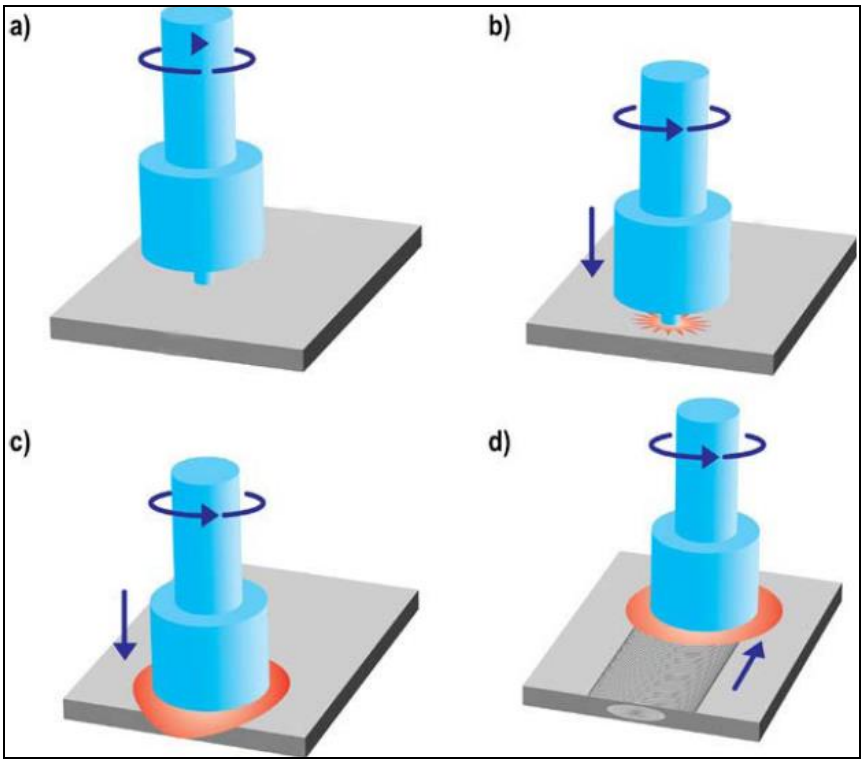

Fig. 3. 2. The steps of the welding process

FSW is considered to be the most significant development in metal joining in a decade and is a ''green'' technology due to its energy efficiency, environment friendliness, and versatility. As compared to the conventional welding methods, FSW consumes considerably less energy. No cover gas or flux is used, thereby making the process environmentally friendly. The joining does not involve any use of filler metal and therefore any aluminum alloy can be joined without concern for the compatibility of composition, which is an issue in fusion welding. When desirable, dissimilar aluminum alloys and composites can be joined with equal ease [21], [22], [23].

FSW involves complex interactions between a variety of simultaneous thermomechanical processes. The interactions affect the heating and cooling rates,

plastic deformation and flow, dynamic recrystallization phenomena and the mechanical integrity of the joint.

During processing, the shoulder contacts the so called crown side and leaves on the surface of the plates typical macro-scale semicircular periodic features: they appear like bands and they are reported to have spacing equal to the increment of pin travel per tool rotation. The cross-section of the weld is divided in more regions that have different properties (Fig. 3. 3) (also in the advancing and the retracting side of the weld are not the identical properties):

- weld nugget
- thermo mechanically affected zone
- heat affected zone
- base material

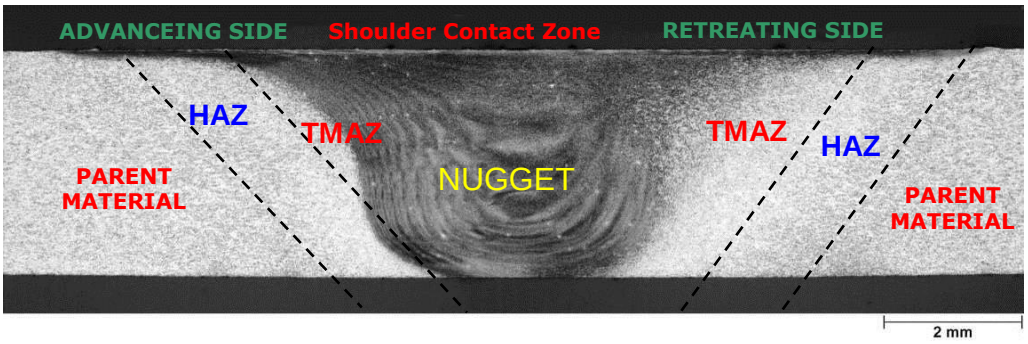

Fig. 3. 3. The zone distribution in the weld cross-section

Intense plastic deformation and frictional heating during FSW/FSP result in generation of are crystallized fine-grained microstructure within stirred zone. This region is usually referred to as nugget zone (or weld nugget) or dynamically recrystallized zone (DXZ). Under some FSW conditions, onion ring structure was observed in the nugget zone. In the interior of the recrystallized grains, usually there is low dislocation density [24], [25]. However, some investigators reported that the small recrystallized grains of the nugget zone contain high density of sub-boundaries [26], subgrains [27] and dislocations [28]. The interface between the recrystallized nugget zone and the parent metal is relatively diffuse on the retreating side of the tool, but quite sharp on the advancing side of the tool [29].

The heat–affected zone (HAZ) is similar to that in conventional welds although the maximum peak temperature is significantly less than the solidus temperature, and the heat–source is rather diffuse. This can lead to somewhat different microstructures when compared with fusion welding processes. The central nugget region containing the "onion ring" appearance is the one which experiences the most severe deformation, and is a consequence of the way in which a threaded tool deposits material from the front to the back of the weld. The thermomechanically affected zone (TMAZ) lies between the HAZ and nugget; the grains of the original microstructure are retained in this region, but often in a deformed state.

Depending on processing parameter, tool geometry, temperature of workpiece, and thermal conductivity of the material, various shapes of nugget zone have been observed. Basically, nugget zone can be classified into two types, basin-shaped nugget that widens near the upper surface and elliptical nugget

Recently, an investigation was conducted on the effect of FSW parameter on the microstructure and properties of cast A356 [30]. The results indicated that lower tool rotation rate of 300–500 rpm resulted in generation of basin-shaped nugget zone, whereas elliptical nugget zone was observed by FSW at higher tool rotation of >700 rpm. This indicates that with same tool geometry, different nugget shapes can be produced by changing processing parameters.

Reynolds [31] investigated the relationship between nugget size and pin size. It was reported that the nugget zone was slightly larger than the pin diameter, except at the bottom of the weld where the pin tapered to a hemispherical termination. Further, it was revealed that as the pin diameter increases, the nugget acquired a more rounded shape with a maximum diameter in the middle of the weld.

Unique to the FSW process is the creation of a transition zone—thermo-mechanically affected zone (TMAZ) between the parent material and the nugget zone [24], [32], [33], as shown in Fig. 3. 3. The TMAZ experiences both temperature and deformation during FSW. The TMAZ is characterized by a highly deformed structure. Furthermore, it was revealed that the grains in the TMAZ usually contain a high density of sub-boundaries [3].

Beyond the TMAZ there is a heat-affected zone (HAZ). This zone experiences a thermal cycle, but does not undergo any plastic deformation (Fig. 3. 3). Mahoney et al. [26] defined the HAZ as a zone experiencing a temperature rise above 250°C for a heat-treatable aluminum alloy. The HAZ retains the same grain structure as the parent material. However, the thermal exposure above 250°C exerts a significant effect on the precipitate structure.

The so called "advancing side" of the weld (Fig. 3. 3) is identified as the side where the translating and the rotating speeds of the tool assume positive values, while on the retracting side of the weld the rotating speed has a negative value in respect to the translating speed.

Fig. 3. 4 describes the position of the advancing side and the retracting side, during the welding tool travel thru the materials [34].

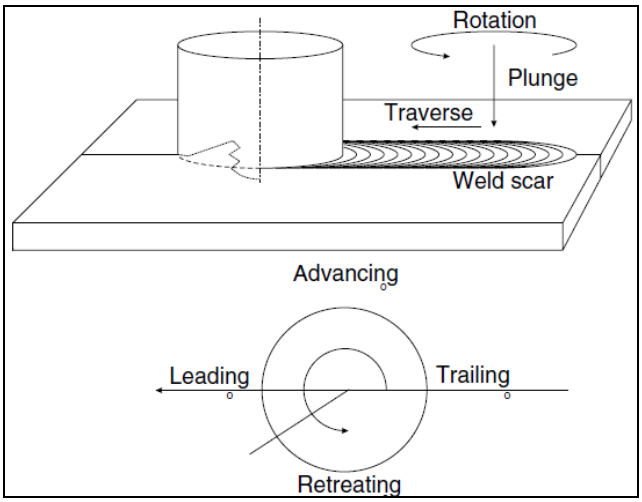

Fig. 3. 4. Orientations relative to the tool rotation and the welding direction

This difference can lead to asymmetry in heat transfer, material flow and the properties of the two sides of the weld; thus, the hardness of particular age–hardened aluminium alloys tends to be lower in the heat–affected zone on the retreating side, which then becomes the location of tensile fracture in cross–weld tests.

3.1.1 The process parameters

The input parameters that govern, on the first hand, the quality of the weld are the rotational speed (rot/min) **ω**, the travel speed (mm/min) **v** and when the process is realized with force input, vertical force (kN) $\mathbf{F_z}$. These input parameters have a very big influence to the process parameters: pin temperature (°C), downwards forging force on the tool shoulder, tool torque, the forces from the weld in welding direction and perpendicular on the weld seam, parameters that define the mechanical properties of the welded element. A schema of influence between the parameters is presented in Fig. 3. 5.

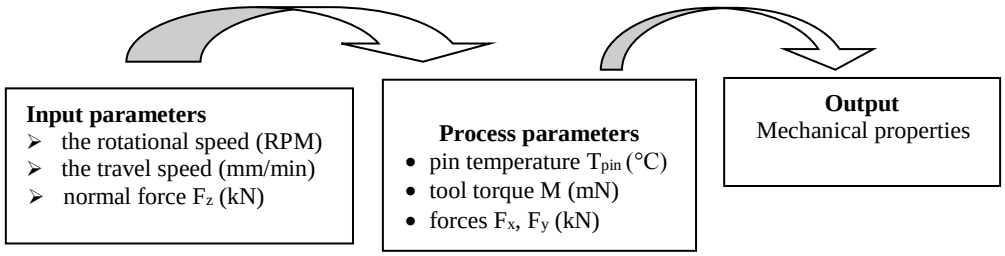

Fig. 3. 5. A schema of the parameters influence to the mechanical properties [35]

The relationship between rotational speed **ω** (RPM) and travel speed **v** (mm/min) results in another weld parameter called weld pitch **λ** (mm/rev), defined to Equation 3.1:

$$\lambda = \frac{v}{\omega} \qquad [mm / rev] \tag{3. 1}$$

The weld pitch can be defined like the distance moved forward along the weld by the tool during one revolution [36].

A small change in the relationship between rotational speed and travel speed, for example, can result in a weld with tunnelling (small volumetric defect along the weld). Furthermore, rotational speed has also a great deal of importance since low rotational speed values cannot transmit the energy necessary for a good material flow in the welded region; and such behaviour could result in weld defects. Therefore it is of extreme importance to identify and understand possible interactions between the welding parameters in order to optimize the performance of the resultant FSW joint.

In addition to the tool rotation rate and traverse speed, another important process parameter is the angle of spindle or tool tilt with respect to the workpiece surface. A suitable tilt of the spindle towards trailing direction ensures that the shoulder of the tool holds the stirred material by threaded pin and move material efficiently from the front to the back of the pin. Further, the insertion depth of pin

into the workpieces (also called target depth) is important for producing sound welds with smooth tool shoulders. The insertion depth of pin is associated with the pin height. When the insertion depth is too shallow, the shoulder of tool does not contact the original workpiece surface. Thus, rotating shoulder cannot move the stirred material efficiently from the front to the back of the pin, resulting in generation of welds with inner channel or surface groove. When the insertion depth is too deep, the shoulder of tool plunges into the workpiece creating excessive flash. In this case, a significantly concave weld is produced, leading to local thinning of the welded plates. It should be noted that the recent development of 'scrolled' tool shoulder allows FSW with 08 tool tilt. Such tools are particularly preferred for curved joints.

Preheating or cooling can also be important for some specific FSW processes. For materials with high melting point such as steel and titanium or high conductivity such as copper, the heat produced by friction and stirring may be not sufficient to soften and plasticizes the material around the rotating tool.

Thus, it is difficult to produce continuous defect-free weld. In these cases, preheating or additional external heating source can help the material flow and increase the process window. On the other hand, materials with lower melting point such as aluminium and magnesium, cooling can be used to reduce extensive growth of recrystallized grains and dissolution of strengthening precipitates in and around the stirred zone [37].

3.1.2 Forces

The welding process is accompanied of forces in all three directions (whether is carried out with position control or with vertical force input).

The coordinates system adopted in FSW is presented in Fig. 3. 6, where the Y-axis represents the forces in the longitudinal direction of the weld; the X-axis is for the forces in the transversal direction of the joint; and the Z-axis represents the downward forces.

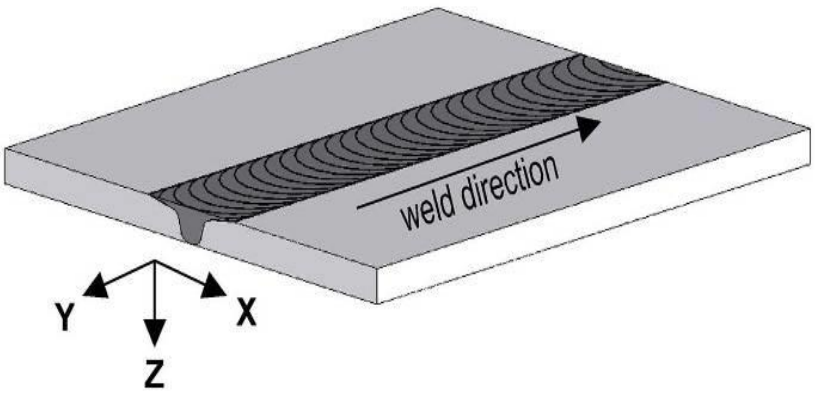

Fig. 3. 6. Representation of the coordinates system adopted in FSW

The downward force (force in the "Z" direction) is the most important to be considered, since it plays an important role in achieving welding full consolidation. The loss of the downward force entails loss in joint and surface texture that may

lead to uncontrollable oscillation of the tool caused by the traverse force (F_y). Such tool oscillation may increase rapidly due to insufficient contact between the shoulder and the workpiece surface. Sometimes the traverse force (F_y) can even change the direction of the tool from the programmed path; thus successful FSW requires the use of force actuators to guarantee constant force required during the process. Other critical variable is the force on the welding tool in the direction of the welding joint (F_x) because if this force increases too much, the tool could be damaged seriously or even break due to bending and torsional stresses. The downward force plays an important role in FSW since it must be kept in an optimized value; if it is higher than the necessary, then the heat generated will melt either the material or the particles in the material just below the tool resulting in poor mechanical properties of the weld and a large flash (hot welds). If the downward force is lower than the optimized value, then the heat generated will not be enough to soften the material, resulting in cold defect welds and even damaging the tool pin and/or shoulder [38].

3.1.3 Temperature

During the FSW process a high temperature (below the melting point) is produced because of the stirring between the tool shoulder and the materials. The distribution of the temperature through the tool and the materials plays a very important role for the appearance of the residual strengths and for the distribution of the tensions in the welded elements. The distribution of the temperature in the tool, welded elements and support table has an important contribution in producing a good weld.

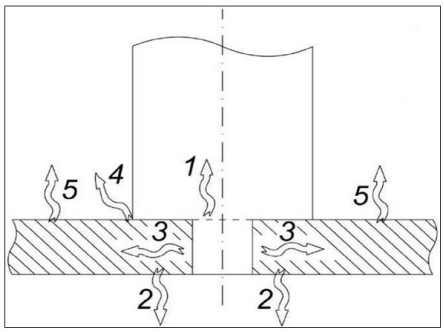

Fig. 3. 7. The real heat propagation by the FSW

In Fig. 3. 7 is presented a schema of heat propagation which results during the FSW process: 1 – heat propagated in welding tool; 2 – heat propagated in welding support table; 3 – heat generated in welded elements; 4 - heat propagated in the environment, near the tool shoulder; 5 – heat dissipation in the environment, from the welded elements [39].

The distribution of the residual stresses is in direct correlation with the temperature during the welding process and the heat input, frictional power. The equation that describes the frictional power, according to Frigaard and Midling [40], is:

$$P_{in} = \frac{4}{3}\pi\mu F_z \omega R \qquad (3.\ 2)$$

where:

P_{in} – the frictional power
μ - the effective friction coefficient
F_z – downwards force on the tool
ω – the rotational speed
R – the radius of the shoulder

From Equation 3.2 it is obvious that the heat input depends both on rotational speed and the shoulder radius, leading to a non-uniform heat generation during welding. These parameters are the main process variables in FSW, since the pressure F_z cannot exceed the actual flow stress of the material at the operating temperature. Varying the weld pitch changes the heat input of the friction energy and some effects in the weld region behaviour can be predicted or controlled. For instance, increasing the travel speed (increase weld pitch) decreases the friction heat input leading to the formation of volumetric defects along the joint. It is possible to observe that keeping constant the heat input and increasing the weld travel speed increases the probability of having defects in the FSW joint since there is no sufficient energy to plastify the material leading to the formation of volumetric defects along the joint.

Starting from the Equation3.2, may be determined the heat input per unit length Q:

$$Q = \frac{\alpha \cdot P_{in}}{v} = \frac{4}{3}\pi^2 \frac{\mu F_z \omega R^3}{v} \qquad (3.3)$$

where:

α – the heat input efficiency; $\alpha = \pi R^2$
v – the welding speed

An attempt was made by Tang et al. [41] to measure the heat input and temperature distribution within friction stir weld by embedding thermocouples in the region to be welded. 6061Al- T6 aluminum plates with a thickness of 6.4 mm were used. They embedded thermocouples in a series of small holes of 0.92 mm diameter at different distances from weld seam drilled into the back surface of the workpiece. Three depths of holes (1.59, 3.18, and 4.76 mm) were used to measure the temperature field at one quarter, one half, and three quarter of the plate thickness. They reported that the thermocouple at the weld center was not destroyed by the pin during welding but did change position slightly due to plastic flow of material ahead of the pin [41]. Fig. 3. 8 shows the variation of the peak temperature with the distance from the weld centerline for various depths below the top surface. Three important observations can be made from this plot.

First, maximum peak temperature was recorded at the weld center and with increasing distance from the weld centerline, the peak temperature decreased. At a tool rotation rate of 400 rpm and a traverse speed of 122 mm/min, a peak temperature of 450°C was observed at the weld center one quarter from top surface. Second, there is a nearly isothermal region 4 mm from the weld centerline. Third, the peak temperature gradient in the thickness direction of the welded joint is very small within the stirred zone and between 25 and 40°C in the region away from the stirred zone. This indicates that the temperature distribution within the stirred zone is relatively uniform. Tang et al. [41] further investigated the effect of weld pressure and tool rotation rate on the temperature field of the weld zone. It was reported that increasing both tool rotation rate and weld pressure resulted in an

increase in the weld temperature. Fig. 3. 9 shows the effect of tool rotation rate on the peak temperature as a function of distance from the weld centerline. Clearly, within the weld zone the peak temperature increased by almost 40°C with increasing tool rotation rate from 300 to 650 rpm, whereas it only increased by 20°C when the tool rotation rate increased from 650 to 1000 rpm, i.e., the rate of temperature increase is lower at higher tool rotation rates. Furthermore, Tang et al. [41] studied the effect of shoulder on the temperature field by using two tools with and without pin. The shoulder dominated the heat generation during FSW.

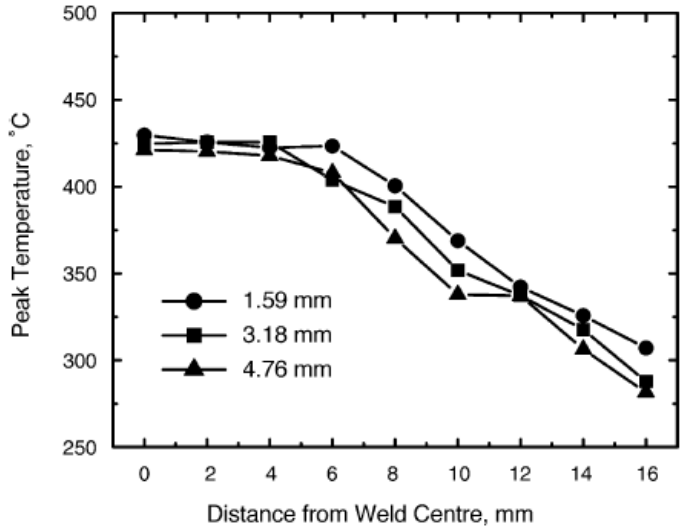

Fig. 3. 8. Effect of depth on peak temperature as a function of distance from weld center line for a 6061 T6 FSW weld made at 400 rpm and 120 mm/min traverse speed [41]

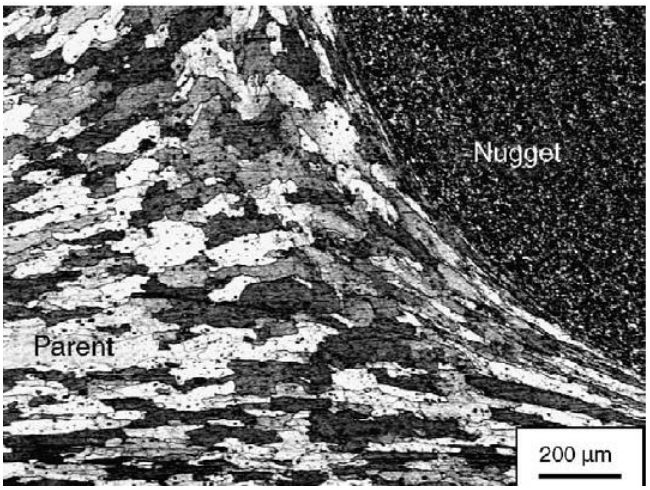

Fig. 3. 9. Microstructure of thermo-mechanically affected zone in FSW 7075 alloy [32]

This was attributed to the fact that the contact area and vertical pressure between the shoulder and workpiece is much larger than those between the pin and workpiece, and the shoulder has higher linear velocity than the pin with smaller radius [41] Additionally, Tang et al. showed that the thermocouples placed at equal distances from the weld seam but on opposite sides of the weld showed no significant differences in the temperature.

Similarly, Kwon et al. [42] Sato et al. [43] and Hashimoto et al. [44]. also measured the temperature rise in the weld zone by embedding thermocouples in the regions adjacent to the rotating pin. Kwon et al. [42] reported that in FSW 1050Al, the peak temperature in the FSP zone increased linearly from 190 to 310 8C with increasing tool rotation rate from 560 to 1840 rpm at a constant tool traverse speed of 155 mm/min. An investigation by Sato et al. [43] indicated that in FSW 6063Al, the peak temperature of FSW thermal cycle increased sharply with increasing tool rotation rate from 800 to 2000 rpm at a constant tool traverse speed of 360 mm/min, and above 2000 rpm, however, it rose gradually with increasing rotation rate from 2000 to 3600 rpm. Peak temperature of >500°C was recorded at a high tool rotation rate of 3600 rpm. A peak temperature >550°C was observed in FSW 5083Al-O at a high ratio of tool rotation rate/traverse speed.

The effect of FSW parameters on temperature was further examined by Arbegast and Hartley [45]. They reported that for a given tool geometry and depth of penetration, the maximum temperature was observed to be a strong function of the rotation rate (ω, rpm) while the rate of heating was a strong function of the traverse speed (v, mm/min). It was also noted that there was a slightly higher temperature on the advancing side of the joint where the tangential velocity vector direction was same as the forward velocity vector. They measured the average maximum temperature on 6.35 mm aluminum plates as a function of the pseudo-"heat index w" $w=\omega^2/v$. It was demonstrated that for several aluminum alloys a general relationship between maximum welding temperature (T,°C) and FSW parameters (v, ω) can be explained by:

$$\frac{T}{T_m} = K\left(\frac{\omega^2}{v \cdot 10^4}\right)^{\alpha} \tag{3.4}$$

where the exponent α was reported to range from 0.04 to 0.06, the constant K is between 0.65 and 0.75, and T_m (°C) is the melting point of the alloy. The maximum temperature observed during FSW of various aluminum alloys is found to be between 0.6 T_m and 0.9T_m, which are within the hot working temperature range for those aluminum alloys. Furthermore, the temperature range is generally within the solution heat-treatment temperature range of precipitation-strengthened aluminum alloys.

In summary, many factors influence the thermal profiles during FSW. From numerous experimental investigations and process modeling, we conclude the following. First, maximum temperature rise within the weld zone is below the melting point of aluminum. Second, tool shoulder dominates heat generation during FSW. Third, maximum temperature increases with increasing tool rotation rate at a constant tool traverse speed and decreases with increasing traverse speed at a constant tool rotation rate. Furthermore, maximum temperature during FSW increases with increasing the ratio of tool rotation rate/traverse speed. Fourth, maximum temperature rise occurs at the top surface of weld zone.

Various theoretical or empirical models proposed so far present different pseudo-heat index. The experimental verification of these models is very limited and attempts to correlate various data sets with models for this review did not show any general trend. The overall picture includes frictional heating and adiabatic heating. The frictional heating depends on the surface velocity and frictional coupling (coefficient of friction). Therefore, the temperature generation should increase from center of the tool shoulder to the edge of the tool shoulder. The pin should also provide some frictional heating and this aspect has been captured in the model of Schmidt et al. [46]. In addition, the adiabatic heating is likely to be maximum at the pin and tool shoulder surface and decrease away from the interface.

Currently, the theoretical models do not integrate all these contributions. Recently, Sharma and Mishra [47] have observed that the nugget area changes with pseudo-heat index. The results indicate that the frictional condition change from 'stick' at lower tool rotation rates to 'stick/slip' at higher tool rotation rates. The implications are very important and needs to be captured in theoretical and computational modeling of heat generation.

3.1.4 Tools

Tool geometry is the most influential aspect of process development. The tool geometry plays a critical role in material flow and in turn governs the traverse rate at which FSW can be conducted. An FSW tool consists of a shoulder and a pin as shown schematically in Fig. 3. **10**. As mentioned earlier, the tool has two primary functions: (a) localized heating, and (b) material flow. In the initial stage of tool plunge, the heating results primarily from the friction between pin and workpiece. Some additional heating results from deformation of material. The tool is plunged till the shoulder touches the workpiece. The friction between the shoulder and workpiece results in the biggest component of heating. From the heating aspect, the relative size of pin and shoulder is important, and the other design features are not critical. The shoulder also provides confinement for the heated volume of material. The second function of the tool is to 'stir' and 'move' the material. The uniformity of microstructure and properties as well as process loads is governed by the tool design. Generally a concave shoulder and threaded cylindrical pins are used.

An important role to produce a weld with very good properties plays the welding tool. The tool geometry combined with proper input parameters, will define most of the properties in the welded joints [48].

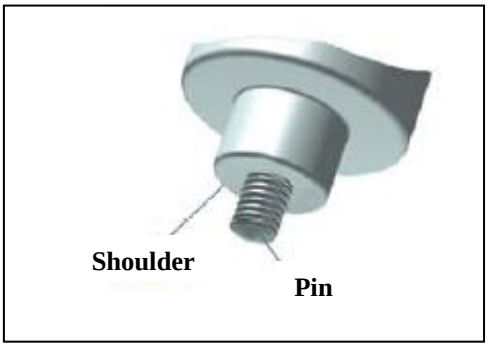

Fig. 3. 10. Schematic presentation of a FSW Tool

The choice of the tool depends on the thickness and material to be joined. The variations of the form of shoulder and tool have some influences to the properties of the weld. The shape of the rotating tool determines the nature of the stirring and heat conduction within the workpiece.

Some from the most used types of tool (shoulders and pins) are presented in

Fig. 3. **11**.

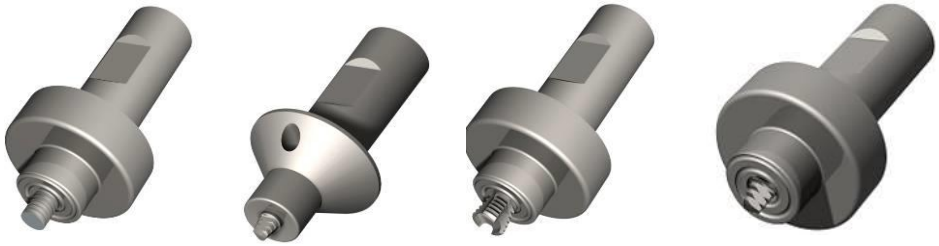

Fig. 3. 11 Combinations of tools

In Fig. 3.11 a. a flat shoulder area with machined spiral flute and a standard threaded pin (thread M6L), flat tip may be observed. Fig. 3.11 b. presents a concave shoulder area with round outer edge and a threaded pin with thread M6L, conical tapered with three milled flats; Fig. 3.11 c. shows a combination between a flat shoulder area with machined spiral flute and a threaded pin (thread M6L) at the socket, conical swelling (10°) with three machined, concave flats (the lower part is machined, to reduce vertical material transport). Fig. 3.11 d. presents a flat shoulder area with machined spiral flute and a threaded pin with thread M6L, conical tapered with three milled flats. The tool presented in

Fig. 3. **11**.c is used especially for overlap welds and in case of plates with thickness up to 10 mm [20].

For better overlap and T – joints, the father of the process, Thomas Wayne developed a new tool at TWI. Twin-stir ™ friction stir welding, as it is known, uses two contra-rotating tools. Their respective reactive process torques practically counter each other, so the parts to be welded require relatively low securing forces.

Fig. 3. 12 Twin-stir prototype head assembly

The Twin-stir™ parallel contra-rotating variant (Fig. 3. 12) enables defects associated with lap welding to be positioned on the 'inside' between the two welds. For low dynamic volume to static volume ratio probes using conventional rotary motion, a possible detrimental feature will be 'plate thinning' on the retreating side. With tool designs and motions designed to minimize plate thinning, so called hooks may be the most significant possible detrimental feature. This feature can be avoided using Twin-stir™ technology.

The Twin-stir™ method may also allow a reduction in welding time for parallel overlap welding. Owing to the additional heat available, increased travel speed or lower rotation process parameters will be possible.

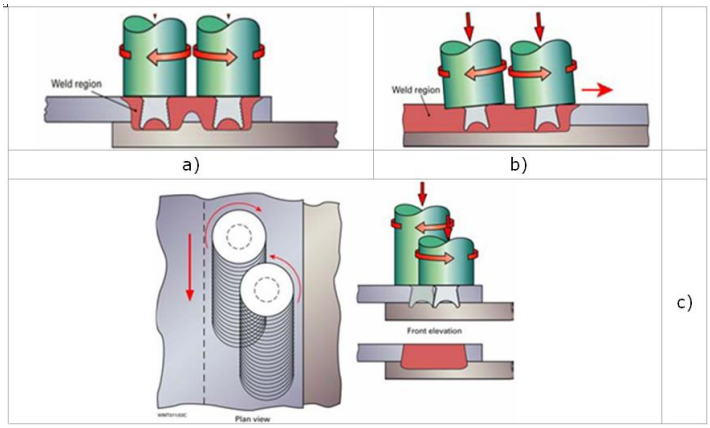

Fig. 3. 13 Twin-stir™ variants. a) Parallel side-by-side transverse to the welding direction. b) Tandem in-line with the welding direction. c) Staggered to ensure the edges of the weld regions partially overlap.

The Twin-stir™ tandem contra-rotating variant (Fig 3.11 b) can be applied to all conventional FSW joints and reduces significantly reactive torque. More importantly, the tandem technique will help improve the weld integrity by disruption and fragmentation of any residual oxide layer remaining within the first weld region by the following tool. Welds have already been produced by conventional rotary FSW, whereby a second weld is made over a previous weld in the reverse direction with no mechanical property loss. The preliminary evidence suggests that further break up and dispersal of oxides is achieved within the weld region.

The Twin-stir™ tandem variant will provide a similar effect during the welding operation. Furthermore, because the tool orientation means that one tool follows the other, the second tool travels through already softened material. This means that the second tool need not be as robust. It is noted that under certain circumstances these tools need not always be used in the contra-rotation mode and their rotational speed can also be varied [49].

The staggered arrangement for Twin-stir™ (Fig 3.11c) means that an exceptionally wide 'common weld region' can be created. Essentially, the tools are positioned with one in front and slightly to the side of the other, so that the second probe partially overlaps the previous weld region. This arrangement will be especially useful for lap welds, as the wide weld region produced will provide greater strength than a single pass weld, given that the detail at the extremes of the weld

region are similar. Residual oxides within the overlapping region of the two welds will be further fragmented, broken up and dispersed. One particularly important advantage of the staggered variant is that the second tool can be set to overlap the previous weld region and eliminate any plate thinning that may have occurred in the first weld. This will be achieved by locating the retreating side of both welds on the 'inside'.

For material processing, the increased amount of material processed will also prove advantageous. In addition, for welding, it would enable much wider gaps and poor fit-up to be tolerated.

With the FSW process also bigger thickness of plate are able to be weld. At this moment tools able to weld plate with a thickness to 50 mm are available. For this kind of welds a double side toot is used (Fig. 3.14).

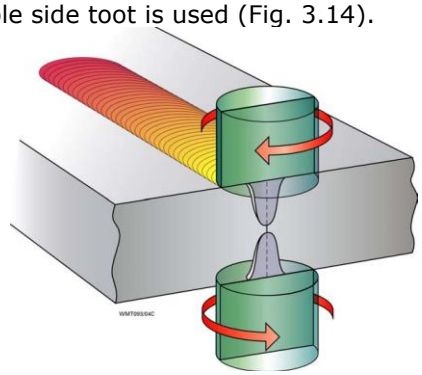

Fig. 3.14 Simultaneous double-sided friction stir welding with contra-rotating tools

The concept involved a pair of tools applied on opposite sides of the workpiece slightly displaced in the direction of travel. The contra-rotating simultaneous double-sided operation with combined weld passes has certain advantages such as a reduction in reactive torque and a more symmetrical weld and heat input through-the-thickness [50]. The probes need not touch together but should be positioned sufficiently close that the softened 'third-body' material around the two probes overlaps near the probe tips to generate a full through-thickness weld [51].

3.1.5 Relation between base material and FSW

The formation of Friction Stir Processing zone is affected by the material flow behaviour under the action of rotating tool. However, the material flow behaviour is predominantly influenced by the material properties such as yield strength, ductility and hardness of the base metal, tool design, and FSW process parameters [52]- [1].

There have been lot of efforts to understand the effect of process parameters on material flow behaviour; microstructure formation and hence mechanical properties of friction stir welded joints. Finding the most effective parameters on properties of friction stir welds as well as realizing their influence on the weld properties has been major topics for researchers [57] - [61].

Balasubramanian [62] carried out an experimental program in order to study the influence of base material to the results of FSW. In this program there have been realized 25 welding joints (5 material x tool rotational speeds). The welding speed (75 mm/min) and axial force (8 kN) were kept constant while varying

the tool rotational speeds. From the macrostructure analysis, it is found that the formation of defect free joints is a function of tool rotational speed and welding speed. Since, FSW is a solid state process and the material under the rotating action of non-consumable tool has to be stirred properly to get good, defect free welds.

The relations established by the author are:

$$\text{Rotational speed } (N) = 204(\text{YS})^{0.31}$$
$$\text{Rotational speed (N)} = 4889(\text{E})^{-0.49}$$
$$\text{Rotational speed } (N) = 48.71(H)^{0.68}$$
$$\text{Welding speed } (S) = 19363(\text{YS})^{-1.02}$$
$$\text{Welding speed}(S) = 0.26(E)^{1.93}$$
$$\text{Welding speed } (S) = 3.06 \times 106(H)^{-2.31}$$

where: YS-yielding stress of base material, H – the hardness of base material, E – elastic modulus of base material.

For a better understanding, the base material properties (Table 3.1) and the welding parameters (Table 3.2) are presented in the next tables:

Table 3. 1. Mechanical properties of base Materials

Material	Yield strength (MPa)	Ultimate tensile strength (MPa)	Elongation (%)	Hardness (VHN)
AA1050	105	115	26	70
AA6061	235	283	22	100
AA2024	340	460	18	115
AA7039	400	460	15	130
AA7075	430	520	10	140

Table 3. 2. FSW process parameters used to fabricate the joints

Alloy	Rotational speed (rpm)	Welding speed (mm/min)
AA1050	700, 800, 900, 1000,1100	
AA6061	900, 1000, 1100, 1200,1300	
AA2024	1000, 1100, 1200, 1300, 1400	22, 45, 75, 100, 135
AA7039	1100, 1200, 1300, 1400, 1500	
AA7075	1300, 1400, 1500, 1600, 1700	

From this investigation, the following important conclusions can be derived:

- The yield strength, ductility and hardness of the aluminium alloys play a major role in deciding weld quality of FSW joints and hence the formation of defect free FSP region.
- The empirical relationships established in this investigation can be effectively used to predict the FSW process parameters to fabricate defect free joints from the known base metal properties of aluminium alloys.

3.1.6 Properties

During fusion welding, complex thermal and mechanical stresses develop in the weld and surrounding region due to the localized application of heat and

accompanying constraint. Following fusion welding, residual stresses commonly approach the yield strength of the base material. It is generally believed that residual stresses are low in friction stir welds due to low temperature solid-state process of FSW. However, compared to more compliant clamps used for fixing the parts in conventional welding processes, the rigid clamping used in FSW exerts a much higher restraint on the welded plates. These restraints impede the contraction of the weld nugget and heat-affected zone during cooling in both longitudinal and transverse directions, thereby resulting in generation of longitudinal and transverse stresses. The existence of high value of residual stress exerts a significant effect on the post weld mechanical properties, particularly the fatigue properties. Therefore, it is of practical importance to investigate the residual stress distribution in the FSW welds [51].

3.1.7 Residual stress

Peel et al. [63] investigated the residual stress distribution on FSW 5083Al using synchrotron X-ray diffraction. Following observations can be made from their investigation. First, while longitudinal residual stress exhibited a ''M''-like distribution across the weld similar to the results of Donne et al. [64] transverse residual stresses exhibited a peak at the weld center. Second, the nugget zone was in tension in both longitudinal and transverse directions. Third, peak tensile residual stress was observed at _10 mm from the weld centerline, a distance corresponding to the edge of the tool shoulder. Fourth, longitudinal residual stress increased with increasing tool traverse speed, whereas transverse residual stresses did not exhibit evident dependence on the traverse speed. Fifth, a mild asymmetry in longitudinal residual stress profile was observed within the nugget zone with the stresses being 10% higher on the advancing side. Sixth, similar to the results of Donne et al. [53], maximum residual stresses in longitudinal direction (40–60 MPa) were higher than those in transverse direction (20–40 MPa).

Clearly, maximum residual stresses observed in various friction stir welds of aluminum alloys were below 100 MPa [63]- [2]. The residual stress magnitudes are significantly lower than those observed in fusion welding, and also significantly lower than yield stress of these aluminum alloys. This results in a significant reduction in the distortion of FSW components and an improvement in mechanical properties.

3.1.8 Hardness

Aluminum alloys are classified into heat-treatable (precipitation-hardenable) alloys and non heat- treatable (solid-solution-hardened) alloys. A number of investigations demonstrated that the change in hardness in the friction stir welds is different for precipitation-hardened and solid-solution- hardened aluminum alloys. FSW creates a softened region around the weld center in a number of precipitation-hardened aluminum alloys [51]. It was suggested that such a softening is caused by coarsening and dissolution of strengthening precipitates during the thermal cycle of the FSW [51]. Sato et al. [26] have examined the hardness profiles associated with the microstructure in an FSW 6063Al-T5. They reported that hardness profile was strongly affected by precipitate distribution rather than grain size in the weld. A typical hardness curve across the weld of FSW 6063Al-T5 is shown in Fig. 3. 15. The average hardness of the solution-treated base material is also included in Fig. 3. 15 for comparison. Clearly, significant softening was produced throughout the weld

zone, compared to the base material in T5 condition. Further, Fig. 3. 15 shows that the lowest hardness does not lie in the center part of the weld zone, but is 10 mm

away from the weld centerline. Sato et al. [26] labeled the hardness curves by BM (the same hardness region as the base material), LOW (the region of lower hardness than base material), MIN (the minimum-hardness region), and SOF (the softened region) (Fig. 3. 15), and examined the microstructure of these four regions.

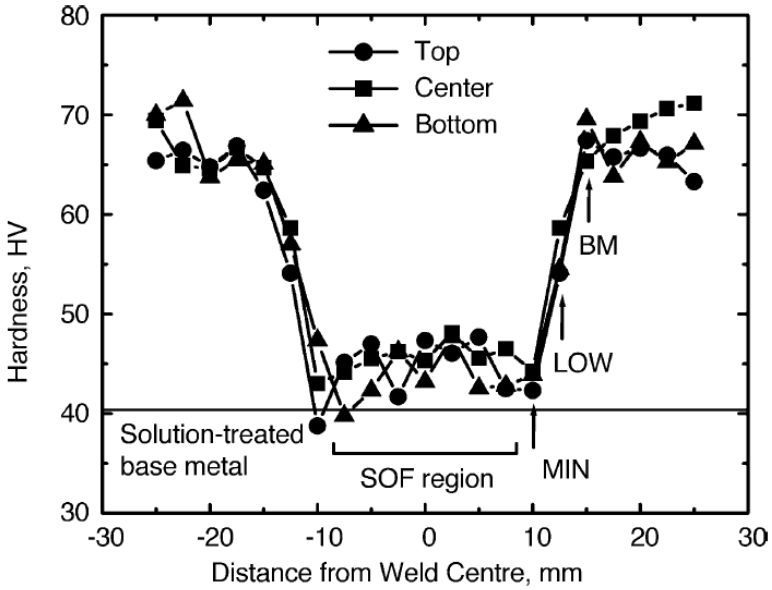

Fig. 3. 15. Typical hardness curve across the weld of FSW 6063-T5 alloy [26]

3.1.9. Mechanical properties

FSW results in significant microstructural evolution within and around the stirred zone, i.e., nugget zone, TMAZ, and HAZ. This leads to substantial change in postweld mechanical properties. In the following sections, typical mechanical properties, such as strength, ductility, fatigue, and fracture toughness are briefly reviewed.

Strength and stability.

Table 3. 3 summarizes the transverse tensile strength of FSW welds and joining efficiency of FSW welds for various aluminum alloys. This table reveals that the joining efficiency of FSW welds ranges from 65 to 96% for heat-treatable aluminum alloys and is 95–119% for non-heat-treatable aluminum alloy 5083Al. The joining efficiency for FSW is significantly higher than that for conventional fusion welding, particularly for heat-treatable aluminum alloys.

Table 3. 3. Friction stir weld joint efficiency for various aluminium alloys [51]

Alloy	Base metal UTS	Friction stir weld UTS	Joint efficiency (%)
AFC458-T8	544.7	362.0	66
2014-T651 (6 mm)	479–483	326–338	68–70
2024-T351 (5 mm)	483–493	410–434	83–90
2219-T87	475.8	310.3	65
2195-T8	593.0	406.8	69
5083-O (6–15 mm)	285–298	271–344	95–119
6061-T6 (5 mm)	319–324	217–252	67–79
7050-T7451 (6.4 mm)	545–558	427–441	77–81
7075-T7351	472.3	455.1	96
7075-T651 (6.4 mm)	622	468	75
6056-T78 (6 mm)	332	247	74
5005-H14 (3 mm)	158	118	75
7020-T6 (5 mm)	385	325	84
6063-T5 (4 mm)	216	155	72
2024-T3 (4 mm)	478	425–441	89–90
7475-T76		465	92
6013-T6 (4 mm)	394–398	295–322	75–81
6013-T4 (4 mm)	320	323	94
2519-T87 (25.4 mm)	480	379	79

Sato et al. [66] investigated the transverse tensile properties of the friction stir weld of 6063-T5 aluminum. In order to reveal the effect of postweld treatment on the weld properties, postweld aging (175°C /12 h) and postweld solution heat treatment and aging (SHTA, 530°C / 1 h + 175°C/12 h) were conducted on the welds. Fig. 3. 16 shows the tensile properties of the base material, the weld, aged weld, and the SHTA weld. Fig. 3. 16 reveals that the strengths and elongation are lowest in the as-welded weld. The aged weld has slightly higher strengths than the base material with concurrently improved ductility. The SHTA increases the strengths of the weld to above those of the base material with almost completely restored ductility.

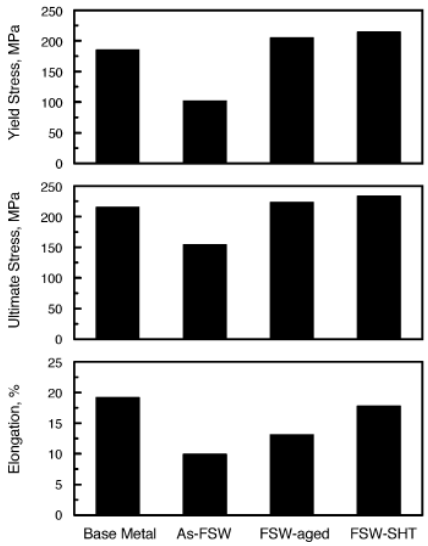

Fig. 3. 16. Tensile properties of base material, as-welded weld, aged weld and SHAT weld of 6063-T5 alloy [66]

Fatigue. For many applications, like aerospace structures, transport vehicles, platforms, and bridge constructions, fatigue properties are critical.

Therefore, it is important to understand the fatigue characteristics of FSW welds due to potentially wide range of engineering applications of FSW technique. This has led to increasing research interest on evaluating the fatigue behavior of FSW welds, including stress–number of cycles to failure (S–N) behavior and fatigue crack propagation (FCP) behavior [51].

In the past few years, several investigations were conducted on the S–N behavior of FSW 6006Al-T5 2024Al-T351, 2024Al-T3, 2024Al-T3, 6013Al-T6, 7475Al-T76, 2219Al-T8751 and 2519Al-T87 [51]. These studies resulted in the following five important observations. First, the fatigue strength of the FSW weld at 10^7 cycles was lower than that of the base metal, i.e., the FSW welds are susceptible to fatigue crack initiation [51]. Further, Bussu and Irving [67] showed that the transverse FSW specimens had lower fatigue strength than the longitudinal FSW specimens. However, the fatigue strength of the FSW weld was higher than that of MIG and laser welds [3], [69]. Typical S–N curves for FSW weld, laser weld, MIG weld, and base metal of 6005Al-T5 are shown in Fig. 3. 17.

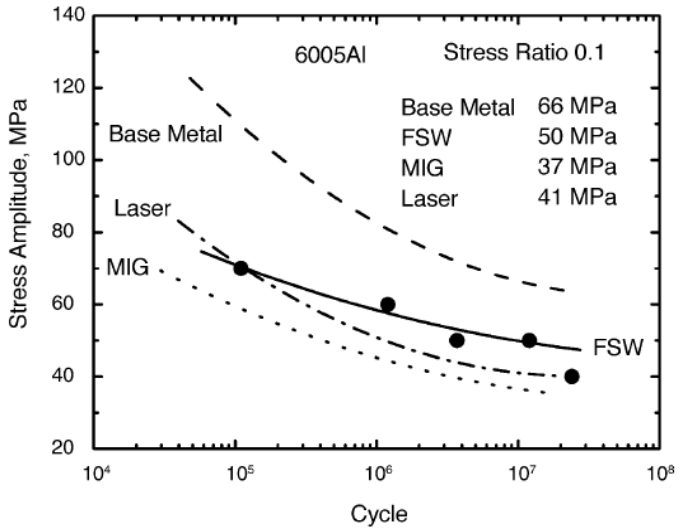

Fig. 3. 17. S-N curves of base material, FSW weld, laser and MIG weld for 6005-T5 alloy [67]

The finer and uniform microstructure after FSW leads to better properties as compared to fusion (laser and MIG) welds. Second, surface quality of the FSW welds exerted a significant effect on the fatigue strength of the welds. Hori et al. [70] reported that the fatigue strength of the FSW weld decreased with increasing tool traverse speed/rotation rate (v/ω) ratio due to the increase of non-welded groove on the root side of the weld. However, when the non-welded groove was skimmed, the fatigue strength of the FSW weld remained unchanged by changing the v/ω ratio. Furthermore, Bussu and Irving [68] reported that skimming 0.5 mm thick layer from both root and top sides removed all the profile irregularities and resulted in fatigue strength, of both transverse and longitudinal FSW specimens, comparable to that of the base metal. Similarly, Magnusson and Källman [71] reported that the removal of 0.1–0.15 mm thick layer from top side by milling can result in a significant improvement in the fatigue strength of FSW welds. These observations suggest that the fatigue life is limited by surface crack nucleation and there are no

inherent defects or internal flaws in successful FSW welds. Third, the effect of FSW parameters on the fatigue strength is complicated and no consistent trend is obtained so far. Hori et al. [70] reported that for a specific v/ω ratio, the fatigue strength of the FSW weld was not affected by the tool traverse speed. However, Biallas et al. [72] observed that for a constant v/ω ratio, the fatigue strength of FSW 2024Al-T3 welds with thickness of 1.6 and 4 mm was considerably enhanced with increasing tool rotation rate and traverse speed. The S–N data of 1.6 mm thick FSW weld made at a high tool rotation rate of 2400 rpm and a traverse speed of 240 mm/min were even within the scatter band of the base metal. Overall, the fatigue results for FSW aluminum alloys are very encouraging.

Fatigue crack propagation behavior. In recent years, several investigations were undertaken to evaluate the effect of FSW on the fatigue crack propagation behavior. Donne et al. [73] investigated the effect of weld imperfections and residual stresses on the fatigue crack propagation (FCP) in FSW 2024Al-T3 and 6013Al-T6 welds using compact tension specimens. Their study revealed following important observations. First, the quality of the FSW welds only exerted limited effects on the da/dN–ΔK curve. Second, at lower loads and lower R-ratio of 0.1, the FCP properties of the FSW welds were superior to that of the base metal for both 2024Al-T3 and 6013Al-T6, where as at higher loads or higher R-ratios of 0.7–0.8, base materials and FSW welds exhibited similar da/dN–ΔK behavior. This was attributed to the presence of compressive residual stresses at the crack tip region in the FSW welds, which decreases the effective stress intensity (ΔK_{eff}) at the crack front. In this case, fatigue crack propagation rates at lower loads and lower R-ratio were apparently reduced due to reduced effective stress intensity. However, at higher loads or higher R-radios, the effect of the compressive residual stress becomes less important and similar base material and FSW da/dN–ΔK curves were achieved. Donne et al. [55] further showed that after subtracting the effect of the residual stress, the da/dN–ΔK_{eff} curves of the base materials and the FSW welds overlapped. Third, specimen geometry exhibited a considerable effect on the FCP behavior of the FSW welds. Donne et al. [73] compared the da/dN–ΔK curves obtained by compact tension specimens and middle cracked tension specimens for both base material and FSW weld at a lower R-ratio of 0.1. While the base material curves overlapped, a large discrepancy was found in the case of the FSW welds. This was attributed to different distribution of the residual stresses in two specimens with different geometries.

Corrosion behaviour. Here should be pointed out that in addition to alloy chemistry, both residual microstructure in FSW welds and corrosion medium exert a significant effect on the corrosion behavior of FSW aluminum alloys.

3.1.10. Conclusions regarding FSW

Tool geometry is very important factor for producing sound welds. However, at the present stage, tool designs are generally proprietary to individual researchers and only limited information is available in open literature. From the open literature, it is known that a cylindrical threaded pin and concave shoulder are widely used welding tool features. Besides, tri-fluted pins such as MX Trifute™ and Flared-Trifute™ have also been developed.

Welding parameters, including tool rotation rate, traverse speed, spindle tilt angle, and target depth, are crucial to produce sound and defect-free weld. As in traditional fusion welding, butt and lap joint designs are the most common joint configurations in friction stir welding. However, no special preparation is needed for

the butt and lap joints of friction stir welding. Two clean metal plates can be easily joined together in the form of butt or lap joints without concern about the surface conditions of the plates.

It is widely accepted that material flow within the weld during FSW is very complex and still poorly understood. It has been suggested by some researchers that FSW can be generally described as an in situ extrusion process and the stirring and mixing of material occurred only at the surface layer of the weld adjacent to the rotating shoulder.

FSW results in significant temperature rise within and around the weld. A temperature rise of 400–500°C has been recorded within the weld for aluminum alloys. Intense plastic deformation and temperature rise result in significant microstructural evolution within the weld, i.e., fine recrystallized grains of 0.1–18 mm, texture, precipitate dissolution and coarsening, and residual stress with a magnitude much lower than that in traditional fusion welding.

Three different microstructural zones have been identified in friction stir weld, i.e., nugget region experiencing intense plastic deformation and high-temperature exposure and characterized by fine and equiaxed recrystallized grains, thermo-mechanically affected region experiencing medium temperature and deformation and characterized by deformed and un-recrystallized grains, and heat-affected region experiencing only temperature and characterized by precipitate coarsening.

Compared to the traditional fusion welding, friction stir welding exhibits a considerable improvement in strength, ductility, fatigue and fracture toughness. Moreover, 80% of yield stress of the base material has been achieved in friction stir welded aluminum alloys with failure usually occurring within the heat-affected region, whereas overmatch has been observed for friction stir welded steel with failure location in the base material. Fatigue life of friction stir welds are lower than that of the base material, but substantially higher than that of laser welds and MIG welds. After removing all the profile irregularities from the weld surfaces, fatigue strengths of FSW specimens were improved to levels comparable to that of the base material. The fracture toughness of friction stir welds is observed to be higher than or equivalent to that of base material. As for corrosion properties of friction stir welds, contradicting observations have been reported. While some studies showed that the pitting and SCC resistances of FSW welds were superior or comparable those of the base material, other reports indicate that FSW welds of some high-strength aluminum alloys were more susceptible to intergranular attack than the base alloys with preferential occurrence of intergranular attack in the HAZ adjacent to the TMAZ.

In addition to aluminum alloys, friction stir welding has been successfully used to join other metallic materials, such as copper, titanium, steel, magnesium, and composites. Because of high melting point and/or low ductility, successful joining of high melting temperature materials by means of FSW was usually limited to a narrow range of FSW parameters. Preheating is beneficial for improving the weld quality as well as increase in the traverse rate for high melting materials such as steel.

Based on the basic principles of FSW, a new generic processing technique for microstructural modification, friction stir processing (FSP) has been developed. FSP has found several applications for microstructural modification in metallic materials, including microstructural refinement for high-strain rate superplasticity, fabrication of surface composite on aluminum substrates, and homogenization of microstructure in nanophase aluminum alloys, metal matrix composites, and cast

Al–Si alloys. Despite considerable interests in the FSW technology in past decade, the basic physical understanding of the process is lacking. Some important aspects, including material flow, tool geometry design, wear of welding tool, microstructural stability, welding of dissimilar alloys and metals, require understanding. However, as pointed out by Prof. Thomas W. Eagar of Massachusetts Institute of Technology, ''New welding technology is often commercialized before a fundamental science emphasizing the underlying physics and chemistry can be developed''. This is quite true with the FSW technology. Although it is only 18 years since FSW technology was invented at The Welding Institute (Cambridge, UK) in 1991 [19], quite a few successful industrial applications of FSW have been demonstrated.

3.2 Process advantages for aluminium and in bridge construction

3.2.1 The advantages of the process for the aluminium and its alloys

The process was first time used to weld aluminium. We can actually say that it was invented for aluminium. From the first begin to weld aluminium elements (plates) with FSW seem to be very proper. FSW has several advantages over commonly used fusion welding techniques. Following from its relatively low process temperature, below the melting point, the method is suited for joining thin or difficult to weld materials. With no melting, the cast microstructure formed during conventional fusion welding is avoided as well as the weld zone shrink from solidification. Furthermore, there is limited risk for porosity in the weld zone, which is common in fusion weld. The FSW joint is created by friction heating with simultaneous severe plastic deformation of the weld zone material. The stirring of the tool minimizes the risk of having excessive local amounts of inclusions, resulting a homogenous and void-free weld. Since the amount of the heat input is smaller than during fusion welding, heat distortions are reduced and thereby the amount of the residual stresses.

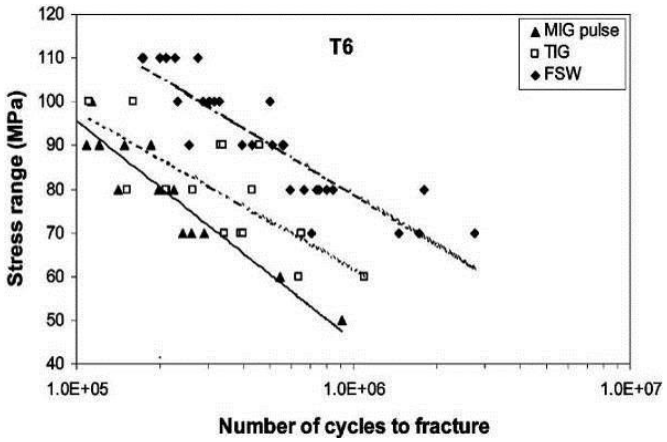

Fig. 3.18 The fatigue life of MIG-pulse and TIG, in comparison with FS welds

In their study, Ericsson and Sandstörm [36] demonstrated that the fatigue life of the FS welds is longer that fusion welds, regardless the welding speed. The results of the SN fatigue tests for each type of weld are presented in Fig. 3.18.

Another report was realized to demonstrate the improvement of the quality of welds realized with FSW, to the AA 6082 and AA 6061 alloys in comparison with MIG fusion weld. In tests of friction stir welded specimens, data show narrow scatters and were fitted using a power equation. For the friction stir welded 6082-T6, it was found that for 65% and 60% of the yield stress the fatigue life is considered infinite. The fatigue life of 5x 10^5 cycles is obtained at a stress range of 105 MPa for AA 6061; the friction stir 6082-T6 specimens were tested at a stress range up to 130 MPa.

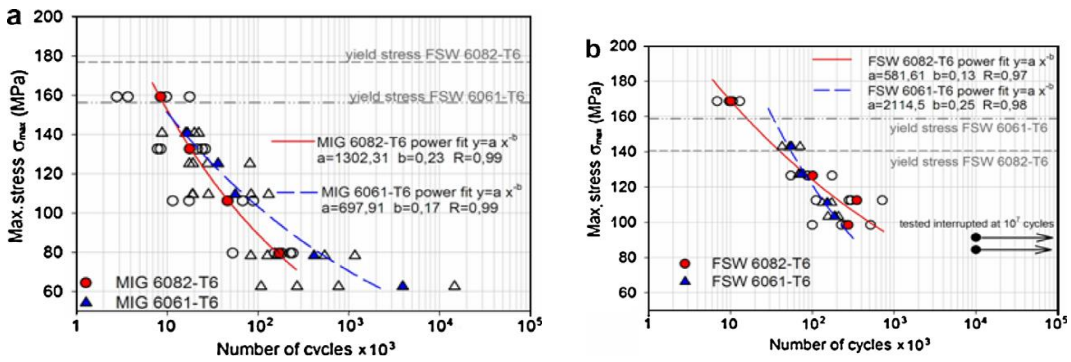

Fig. 3. 19 S–N fatigue data of the welded specimens: (a) MIG welded and (b) FS welded.

The author [74] shows also the improvement of microstructure quality during the FS weld and also the aesthetical aspect of the weld presents an obviously improvement.

It is obviously that the re-crystallization during the FSW is finer that during fusion welds, avoiding the porosity in the welded zone, porosity that may cause defects that lead to a short fatigue life.

These two examples above presented demonstrate that for the alloy 6082, used in structural constructions like airplane fuselage, catamarans body or bridge decks, FSW contributes to the improvement of the weld quality, and with that, the fatigue life of the weld [74].

3.2.2 The process advantages for bridge construction

Even if the process wasn't reported to often in the field of civil engineering, it still represents a challenge also for this domain just like it was using of aluminium in bridge construction. Nowadays, because of the quality demonstrated in time and because of the price drop for aluminium productions, it became a suitable and an economic alternative to the usual bridge materials: structural steel and concrete.

Until now, all the „classical" connection were used to realized the aluminium structures. By that not all the properties of aluminium and its alloys were used 100%. For example, the use of rivets to connect the elements of a bridge increases very much the weight of structure and with that the dead load that is transmitted to the bearing system. On the other hand, the connection of the structural elements of

a bridge with screws may cause another problem – named as galvanic corrosion – appears in the presence of water, on the contact of steel (screw material) and aluminium (elements material). A solution for this problem is to lock the direct contact between screws and elements by using screw coating with a polymer. But this procedure will increase the costs considerably. By using one of the old types of welds (a MIG or a TIG weld connection) it is hard to obtain a good weld seam, without any imperfection that may cause cracks. Also, only some of the aluminium alloys are weldable with MIG or TIG.

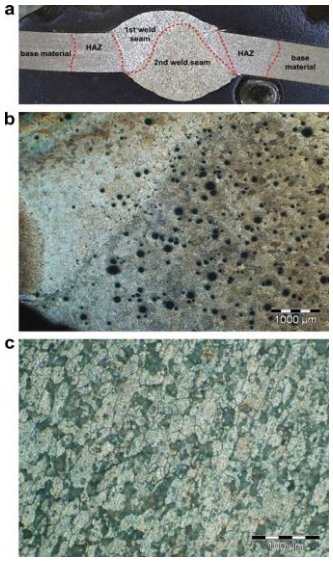

(a) macrostructure of the MIG welded Al6082-T6; (b) microstructure weld, (c) microstructure BM

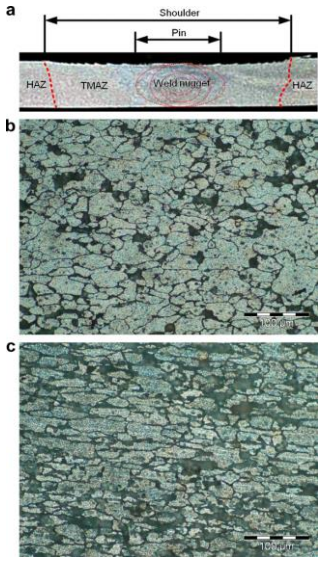

(a) macrostructure of the FS welded Al6082-T6; (b) microstructure weld; (c) microstructure BM

Fig. 3. 20 MIG welded Al6082-T6 and FS welded Al6082-T6

One of the most important quality of the aluminium, and specially the alloys AA 5083 and AA 6082 is the very good behaviour to corrosion. These two alloys were successfully used to realize bodies of ships, catamarans and off shore superstructure (the housing area), welded with FSW. In time it proved to be a good, resistant and proper solution.

Using FS welds to aluminium bridge erection provide us light structures – the dead load is reduced, no additional weight from rivets or screws, with good corrosion behaviour in contact with salt (used against frozen road bed during the winter time), the biggest enemy of the steel bridges. It is generally known that the fusion welding of aluminium alloys is accompanied by the defects like porosity; slag inclusion, solidification cracks etc., and these defects deteriorate the weld quality and joint properties. However, friction stir welded joints are known to be free from these defects since there is no melting takes place during welding and the metals are joined in the solid state itself due to the heat generated by the friction and flow of metal by the stirring action. The erection time is much shorter because of the manufacturing (large bridge elements can be erected in workshop and carry out to the erection place).

Both of these characteristics can be translated in money saving:

- the structure doesn't need too much treatments after placement, which means in time, cost savings.

- realizing the welds in a workshop, with a machine, reduces the erection costs and also, because of that, the final erection time is reduced and increases the productivity.

3.3 Present situation regarding FS welds evaluation in international standards

At this moment there are no public standards available for the calculus of strength of such a connection. Until now FSW applications were used on an industrial scale only after an important number of tests.

Until now, all applications of FSW were verified with a tandem between experimental evaluations and a finite element modelling, which seems to offers approximately the same results (it is known that the finite element modelling consider the material as ideal, without any imperfections).

Several research institutes [75] make demarches in the direction of realizing at least a guideline for several applications of FSW, for example pipelines for gas transportation or for oil transportation. But taking into account the multitude of the parameters number that influenced the quality of the weld, is hard to get a final answer to the questions about the endurance of a structure welded with FSW.

A solution in the direction of realizing a guideline for the calculation of an aluminium structure welded with FSW is to make, for the begin, a classification of the most used alloys on a industrial scale (for example in automotive industry, for aircraft industry – 2xxx and 7xxx alloys, for shipyards, for civil engineering - 5xxx and 6xxx alloys etc.). For the 2xxx and 7xxx alloys a very important number of papers were published and can serve as a start in putting together the information that can help to realize a base guideline to indicate the proper welding parameters, how to control the temperature dispersion, how to reduce the residual stresses etc., information about the best parameters that improve the quality of the weld seam.

It is known that for fusion welding procedures for aluminium (MIG and TIG) the weld seams achieve a maximum of 60% from the qualities of the base material and this happens in the best conditions, when the weld is ideal. Normally, for a welded connection in aluminium elements, only 40% (in some cases 60%, when is well known the seam quality) from the base material properties are taking in calculus [74].

In case of bridges, the joints have to present a higher resistance, especially to moving loads which may cause the structure failure by assigning of weakest section. This behaviour is known as ***fatigue***, term which will be presented in the following.

4. ALUMINIUM DESIGN

4. 1. Aluminium design according to British Standard

4.1. 1. Introduction

Aluminium is easily the second most important structural metal, yet few designers seem to know much about it. Since the 1940s, as aluminium rapidly became more important, engineers have been slow to investigate what it has to offer and how to design with it.

Structural aluminium, a strong ductile metal, has much similarity to steel and design procedures are not very different. Weight saving is more important in aluminium than in steel, because of the higher metal cost. More accurate design calculations are therefore called for. Critical areas in aluminium include buckling, deflection, weld strength and fatigue. Other aspects which do not arise at all in steel are the use of extruded sections, heat-affected zone (HAZ) softening at welds and adhesive bonding.

The physical properties of aluminium that present interest in design are:

- the density ρ of pure aluminium compares as follows with steel:

  Pure aluminium ρ = 2.70 g/cm^3

  Structural steel ρ = 7.9 g/cm^3

and the value for the alloys used for wrought products lies in the range 2.67-2.80 g/cm^3. A rounded value of 2.7 g/cm^3 is normally used in design, leading to the following practical formulae:

	Mass	Weigth
Sections	0,0027A kg/m	0,027A N/m
Plate, sheet	2,7t kg/m^2	27t N/m^2

where *A* is the section area (mm^2) and *t* the plate thickness (mm).

- e*lastic constants* (*E*)

  Pure aluminium E = 69 kN/mm^2

  Structural steel E = 205 kN/mm^2

while the value for wrought alloys lies in the range 69–72 kN/mm^2. For design purposes British Standard BS.8118 adopts a standard figure of *E =70* kN/mm^2

- shear modulus (G)

$$G = \frac{E}{2(1+v)} \approx 26 kN/mm^2 \qquad (4.1)$$

The melting point of aluminium is 660 °C, while for the mild steel is 1500 °C.

Comparison with steel

Wrought aluminium in its alloyed form is a strong ductile metal and has much similarity to structural steel. Its mechanical properties tend to be inferior to those of steel, the stronger alloys being comparable in strength but less ductile. The approach to structural design is much the same for the two metals and below we concentrate on the differences. Unlike steel, aluminium is, of course, non-magnetic.

The good points about aluminium
Lightness
Aluminium is light, one third the weight of steel.
Non-rusting
Aluminium does not rust and can normally be used unpainted. However, the strongest alloys will corrode in some hostile environments and may need protection.
Extrusion process
This technique, the standard way of producing aluminium sections, is vastly more versatile than the rolling procedures in steel. It is a major feature in aluminium design.
Weldability
Most of the alloys can be arc welded as readily as steel, using gas shielded processes. Welding speeds are faster.
Machinability
Milling can be an economic fabrication technique for aluminium, because of the high metal removal rates that are possible.
Glueing
The use of adhesive bonding is well established as a valid method for making structural joints in aluminium.
Low-temperature performance
Aluminium is eminently suitable for cryogenic applications, because it is not prone to brittle fracture at low temperature in the way that steel is. Its mechanical properties steadily improve as the temperature goes down.

The bad points
Cost
The metal cost for aluminium (sections, sheet, plate) is typically about 1.5 times that for structural steel volume for volume. For aircraft grade lower because of easier handling, use of clever extrusions, easier cutting or machining, no painting, simpler erection. Thus, in terms of total cost, the effect of switching to aluminium is usually much less than one would expect. An aluminium design can even be cheaper than a steel one. The other side of the cost picture is aluminium's relatively high scrap value, a significant factor in material selection for components designed to have a limited life. But high scrap value may not always be a good thing, as it encourages the unscrupulous to come on a dark night and remove an aluminium structure for sale as scrap. This has happened.
Buckling
Because of the lower modulus, the failure load for an aluminium component due to buckling is lower than for a steel one of the same slenderness.
Effect of temperature
Aluminium weakens more quickly than steel with increasing temperature. Some alloys begin to lose strength when operating above 100°C.
HAZ softening at welds

There tends to be a serious local drop in strength in the heat-affected zone (HAZ) at welded joints in some alloys.

Fatigue

Aluminium components are more prone to failure by fatigue than are steel ones.

Thermal expansion

Aluminium expands and contracts with temperature twice as much as steel. However, because of the lower modulus, temperature stresses in a restrained member are only two-thirds those in steel.

Electrolytic corrosion

Serious corrosion of the aluminium may occur at joints with other metals, unless correct precautions are taken. This can apply even when using alloys that are otherwise highly durable.

Deflection

Because of the lower modulus, elastic deflection becomes more of a factor than it is in steel. This is often a consideration in beam design.

4.1. 2. Limit state design and limiting stresses

British Standard BS.8118 follows steel practice in employing the limit state approach to structural design, in place of the former elastic ('allowable stress') method. Limit state design is now accepted practice in most countries, the notable exception being the USA.

LIMIT STATE DESIGN

In checking whether a component (i.e. a member or a joint) is structurally acceptable there are three possible limit states to consider:

- Limit state of static strength;
- Serviceability limits state;
- Limit state of fatigue.

Static strength is usually the governing requirement and must always be checked. Serviceability (elastic deflection) tends to be important in beam designs; the low modulus (E) of aluminium causes it to be more of a factor than in steel. Fatigue, which must be considered for all cases of repeated loading, is also more critical than for steel.

Some confusion exists because different codes employ different names for the various quantities that arise in limit state design. Here we consistently use the terminology adopted in BS.8118, as below.

- *Nominal loading.* Nominal loads are the same as 'working loads'. They are those which a structure may be reasonably expected to carry in normal service, and can comprise:
  - dead loads (self-weight of structure and permanently attached items);
  - imposed loads (other than wind);
  - wind loads;
  - forces due to thermal expansion and contraction;
  - forces due to dynamic effects.

It is beyond the scope of this book to provide specific data on loading. Realistic imposed loads may be found from particular codes covering buildings, bridges, cranes, etc. Wind is well covered. Often the designer must decide on a reasonable level of loading, in consultation with the client.

- *Factored loading* is the factored (up) loading on the structure. It is obtained by multiplying each of the individual nominal loads by a partial factor γ_f known as the *loading factor.* Different values of γ_f can be taken for different classes of nominal load.
- *Action-effect.* By this is meant the force or couple that a member or joint has to carry, as a result of a specific pattern of loading applied to the structure. Possible kinds of action-effect in a member are axial tension or compression, shear force, bending moment, and torque. In a joint, the possible action-effects are the force and/or couple that have to be transmitted.
- *Calculated resistance* denotes the ability of a member or joint to resist a specific kind of action-effect, and is the predicted magnitude thereof needed to cause static failure of the component. It may be found by means of rules and formulae given in codes or textbooks, in applying which it is normal to assume minimum specified tensile properties for the material and nominal dimensions for the cross-section.
- *Factored resistance* is the factored (down) resistance of a member or joint. It is the calculated resistance divided by a partial factor γ_m known as the *material factor.*

In discussing limit state design, we use the following abbreviations to indicate quantities defined above:

NA =action-effect arising under nominal loading;
FA =action-effect arising under factored loading;
CR =calculated resistance;
FR =factored resistance *(=CR/*γ_m*)*.

Table 4. 1. Suggested γ-values for checking the limit state of static strength

Loading factor γ_f			**Material factor γ_m**		
Sub-factor γ_{f1}			***Members***	γ_m =	1.2
Dead load, direct effect	γ_{f1} =	1.2			
Dead load, counterign effect		0.8	Connections:		
Imposed load, exclundig wind		1.33	Mechanical joints	γ_m =	1.2
Wind load		1.2	Welded joints		1.3-1.6
Force due to temperature effect		1.0	Bonded joints		1.6 min
Estimated force under impact		1.33			
Sub-factor γ_{f1}					
Dead load	γ_{f2} =	1.2	***Serviceability factor γ_s***		
Imposed, wind or impact load, producing an action-effect on the component that is:			HSFG bolted joints	γ_s =	1.1-1.2
(i) the most severe	γ_{f2} =	1.0			
(ii) second most severe		0.8			
(iii) third most severe		0.6			
(iv) fourth most severe		0.4			
Force due to temperature		1.0			

Limit state of static strength

The reason for checking this limit state is to ensure that the structure has adequate strength, i.e. it is able to resist a reasonable static overload, over and above the specified nominal loading, before catastrophic failure occurs in any of its components (members, joints). The check consists of calculating *FR* and *FA* for any critical component and ensuring that:

$$FR \geq FA \tag{4. 2}$$

In order to obtain FR and FA it is necessary to specify values for the partial factors γ_f and γ_m. These are for the designer to decide, probably in consultation with the client. The BS.8118 recommendations are as follows:

1. *Loading factor* (γ_f). This factor, which takes account of the unpredictability of different kinds of load, is taken as the product of two sub-factors as follows:

$$\gamma_f = \gamma_{f1} \cdot \gamma_{f2} \tag{4. 3}$$

γ_{f1} depends on the kind of load being considered, while γ_{f2} is a factor that allows some relaxation when a combination of imposed loads acts on the structure. For initial design of simple components one may safely put $\gamma_{f2}=1.0$.

2. *Material factor (γ_m)*. In the checking of *members,* BS.8118 adopts a constant value for this factor, namely $\gamma_m=1.2$. For *connections,* the recommended value lies in the range 1.2–1.6, depending on the joint type and the standard of workmanship. The lower value 1.3 given for welded joints should only be used if it can be ensured that the standard of fabrication will satisfy BS.8118: Part 2. Failing this, a higher value must be taken, possibly up to 1.6. If a particular imposed load is known to be very unpredictable, the designer would take γ_f higher than the normal value, or if there is concern that the quality of fabrication might not be held to the highest standard, γ_m ought to be increased.

Often a component is subjected to more than one type of action-effect at the same time, as when a critical cross-section of a beam has to carry simultaneous moment and shear force. Possible interaction between the different effects must then be allowed for. For some situations, the best procedure is to check the main action-effect (say, the moment in a beam) using a modified value for the resistance to allow for the presence of the other effect (the shear force). In other cases, it is more convenient to employ interaction equations. Obviously, a component must be checked for all the possible combinations of action-effect that may arise, corresponding to alternative patterns of service loading on the structure.

After checking a component for static strength, a designer will be interested in the actual degree of safety achieved. This can be measured in terms of a quantity LFC (load factor against collapse) defined as follows:

$$LFC = \frac{CR}{NA} \tag{4. 4}$$

where *CR* = calculated resistance and *NA* = action-effect arising under nominal loading. For a component which is just acceptable in terms of static strength *(FR=FA),* the LFC would be given by:

$$LFC = \gamma_f \cdot \gamma_m \tag{4. 5}$$

where γ_f is the ratio of the action-effect under factored loading to that arising under nominal loading (i.e. a weighted average of γ_f for the various loads on the structure). Thus for example a typical member might have and gm equal to 1.3 and 1.2 respectively, giving a minimum LFC of 1.56. This implies that the member could just withstand a static overload of 56% before collapsing. The aim of limit state design is to produce designs having a consistent value of LFC.

Different results are obtained in checking static strength, depending on whether the Elastic or Limit State method is used. The two procedures may be summarized as follows:

1. *Elastic design.* The structure is analysed under working load, and stress levels are determined. These must not exceed an allowable stress, which is obtained by dividing the material strength (usually the yield or proof stress) by *a factor of safety* (FS). For slender members, the allowable stress is reduced to allow for buckling.
2. *Limit state design.* The structure is assumed to be acted on by factored (up) loading, equal to working loads each multiplied by a *loading factor.* It is analysed in this condition and a value obtained for the resulting 'action-effect' (i.e. axial force, moment, shear force, etc.) arising in its various components. In any component, the action effect, thus found, must not exceed the factored (down) resistance for that component, equal to its calculated resistance divided by the *material factor.* By 'calculated resistance' is meant the estimated magnitude of the relevant action-effect necessary to cause failure of that component.

What really matters to the user of a structure is its actual safety against collapse. How much overload can it take above the working load before it fails? Safety may be expressed in terms of the quantity LFC. A sensible code is one providing a consistent value of LFC. Too high an LFC is oversafe, and means loss of economy. Too low an LFC is undersafe. By the very way it is formulated limit state design produces a consistent LFC. Elastic design does not, because stress at working load is not necessarily an indication of how near a component is to actual failure.

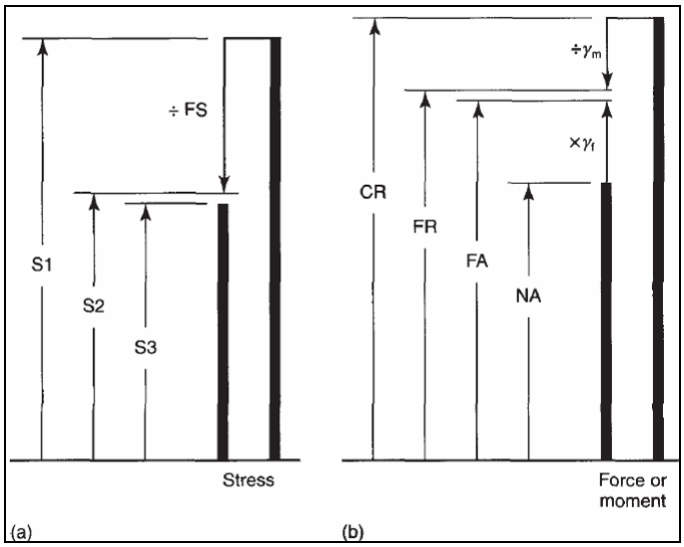

Fig. 4. 1. Static strength: (a) elastic design (S1=material strength, S2=allowable stress, S3=stress arising at nominal working load); (b) limit state design.

Serviceability limit state

The reason for considering this limit state is to ensure that the structure has adequate stiffness, the requisite calculations being usually performed with the structure subjected to unfactored nominal loading. It is usually concerned with the performance of members rather than joints.

When a member is first taken up to its nominal working load, its deformation comprises two components: an irrecoverable plastic deflection and a recoverable elastic one. The main causes for the plastic deflection are the presence of softened zones next to welds and the rounded stress-strain curve. Further factors are local stress concentrations and locked-in stresses, which also lead to premature yielding (as in steel). The serviceability check for a member simply consists of ensuring that its elastic deflection does not exceed an acceptable value:

$$\Delta_E \leq \Delta_L \tag{4. 6}$$

where Δ_E=predicted elastic deflection under nominal loading, and Δ_L=limiting or permitted deflection.

A specific design calculation for the plastic deflection (under the initial loading) is never made. This is because it is usually small, and disappears on subsequent applications of the load. However, with materials having a very rounded stress-strain curve, the initial plastic deformation tends to be more pronounced, and there is a danger that it may be unacceptable.

We cover this possibility in design by arbitrarily decreasing the limiting stress for such materials, when checking the ultimate limit state.

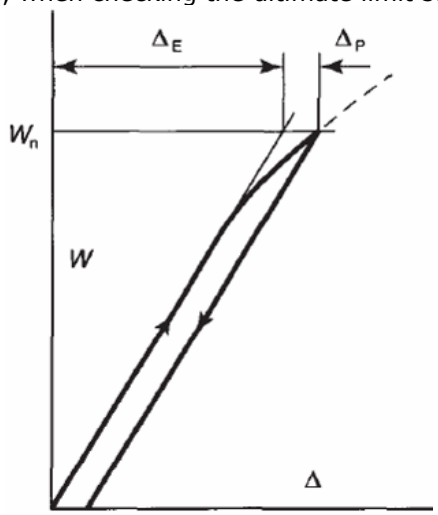

Fig. 4. 2. Elastic (Δ_E) and plastic (Δ_P) components of deflection at nominal working load

The type of member for which the serviceability limit state is most likely to be critical is a beam, especially if simply supported, for which Δ_E can be calculated employing conventional deflection. It is rarely necessary to check the stiffness of truss type structures.

The designer must decide on a suitable value for Δ_L, preferably in consultation with the client. The important thing is not to insist on an unduly small deflection, when a larger one can be reasonably tolerated.

This is especially important in aluminium with its relatively low modulus. A general idea of the deflection that can be tolerated is given by the value suggested in BS.8118, namely Δ_L=span/100 (under dead+snow+wind).

For a component that has to carry a combination of loads, the strict application of equation (4.6) may be thought too severe. A more lenient approach is to base Δ_E on a reduced loading, in which the less severe imposed loads are factored by γ_{f2} as given in Table 4.1.

Turning to joints, it is never necessary to check the deformation of welded ones, and even for mechanical joints an actual calculation is seldom required. With the latter, if stiffness is important, a simple solution is to specify close-fitting bolts or rivets, rather than clearance bolts.

Alternatively, for maximum joint stiffness, a designer can call for Friction grip (HSFG) bolts, in which case a check must be made to ensure that gross slip does not occur before the nominal working load is reached. In so doing the calculated friction capacity is divided by a serviceability factor (γ_s).

Limit state of fatigue

For a structure or component subjected to repeated loading, thousands or millions of times, it is possible for premature collapse to occur at a low load due to fatigue. This can be a dangerous form of failure without prior warning, unless the growth of cracks has been monitored during service.

The usual checking procedure is to identify potential fatigue sites and determine the number of loading cycles to cause failure at any of these, the design being acceptable if the predicted life at each site is not less than that required. The number of cycles to failure is normally obtained from an *endurance curve,* selected according to the local geometry and entered at a stress level (actually stress range) based on the nominal unfactored loading. Alternatively, for a mass-produced component, the fatigue life can be found by testing [76].

4. 2. Aluminium design according to Eurocode

In all modern codes of practice structural safety is established by the application of the partial safety coefficients to the loads (or 'actions') and to the strength (or 'resistance') of components of the structure. The new Eurocodes for the design and execution of buildings and civil engineering structures use a limit state design philosophy defined in Eurocode 1. (Common unified rules for different types of construction and material) [77].

The new Eurocode 9 [80] for aluminium design presents a broad range of wrought and cast alloys for structural components, along with characteristic values for the material properties, and for connecting devices (bolts, rivets) in both aluminium and steel. Respective information is included, in detail especially for welded joints, and adhesively bonded joints. This alloy list may have to be adapted for applications in shipbuilding and specific alloys should be controlled in respect to durability requirements or when in contact with other materials recommendations in EN 1999-1-1 Annex D and EN 1090-3 should be observed. Rules for fatigue design in EN 1999-1-3 cover all the above options [78].

In summary, the objectives of the design procedure are:

- to produce design documents (drawings, descriptions, specifications etc.) suitable as a basis for fabrication of the structure,

- to verify that the documents are in agreement with the purchaser's requirements according to the given design conditions and valid regulations, and
- to ensure, as far as possible, that the documents specify a structure satisfactory from an economical point of view.

Requirements on the Load Carrying Structure

⇒ Specification of requirements
⇒ Requirements on safety against failure
⇒ Requirements on the serviceability of structures in normal use
⇒ Limit state
⇒ Safety classes
⇒ Economic considerations on the formulation of requirements

Specification of Requirements

Requirements here and in the following sections denote expressions of expectations defined by the purchaser, future proprietor, utilizers, authorities, etc. concerning the function of the structure. The requirements may to some extent be varied with respect to the balance between quality level and cost.
The requirements on a load carrying structure may be specified as follows:

❖ requirements on safety against failure,
❖ requirements on serviceability in normal use,
❖ requirements on durability.

Requirements on Safety Against Failure

The concept of failure may imply anything from destruction of a structural element to collapse of the entire structural system. The cause of a failure may be of various kinds and can be classified in three categories:

1. Unfavourable combinations of factors affecting the resistance.

An unfavourable combination of critical parameters has occurred. These parameters may be interpreted as loads, strength of the material, dimensions, imperfections and minor damages. They possess values which may be extreme, but do not deviate significantly from normal conditions.

2. Unforeseen loads.

An event (explosion, fire, ship impact etc.) not considered in the design has appeared as a single occurrence with such a magnitude that the consequence was failure of the structure. The load may either be of a character entirely different from those considered in the design, or it may be of the same character but of a magnitude not foreseen.

3. Gross errors.

A gross error has been committed in the design work, material production, or construction. A gross error implies that the structure has received some material or geometrical property of a character entirely different from what was intended.

Requirements on the Serviceability of Structures in Normal Use

If a load carrying structural member is, in normal use, subjected to damage or causes damage to other members and, if the damage is unacceptable, the function or serviceability of the structural member can be considered to be unsatisfactory. The damage may be permanent or occasional. The word damage is used here in a wider sense and can be the cause of, for instance, some kind of inconvenience.

Examples of *permanent damages* may be open cracks in the structural member, cracks in other building components, e.g. partition walls, and disturbing permanent deflections of beams. If such damage has occurred and involves inconvenience, it will continue to bring the same or about the same inconvenience until repaired. In this case the requirements given and the measures taken to avoid the inconveniences should be aimed at reducing the *risk of generation* of the damage. In principle, the problem is equivalent to that concerning safety against failure. Even if no well-defined limit exists between these cases, the risk which can be accepted for a minor damage to occur to the structure in normal use, is normally higher, however, than the acceptable risk of failure.

Examples of *occasional damages* are occasional large deflections of beams and occasional vibrations. The inconvenience of such damages will only appear during those periods when the load or other actions occur which cause the damage. The requirements and measures to reduce the inconveniences should, in this case, be concentrated to the *duration of the damage*. Vibrations of a certain intensity may be acceptable from a comfort point of view if they appear infrequently and only during short periods of time.

On the other hand vibrations of the same intensity may be entirely unacceptable if they are effective during longer periods.

The requirements on the serviceability of a structure in normal use apply, in most cases, to deformations including oscillations and vibrations (considered as time dependent deformations). The inconveniences resulting from large deformations can be the following: they

- can cause damage to other building components,
- may convey a feeling of discomfort to people in the building,
- can disturb and impair the function of machines, instruments and similar objects supported by the structure,
- may be disturbing from an aesthetic point of view.

Limit States

The requirements on the load carrying function of a structure apply to both safety against failure and to serviceability in normal use. These two requirements are, at least in some cases, quite different in nature and should thus be separated in their formulation. This can be achieved by performing the design analysis at two limit states with regard to the function of the structure:

- ***ultimate limit state***, which is a state where the structure is at the limit of failure,
- ***serviceability limit state***, which is a state where the structure is at the limit of not satisfying the requirements for normal use.

The implication of the limit states is illustrated in Fig. 4. 3, which shows the deflection versus load for a simply supported beam. The serviceability limit state and the ultimate limit state are indicated by their upper limits.

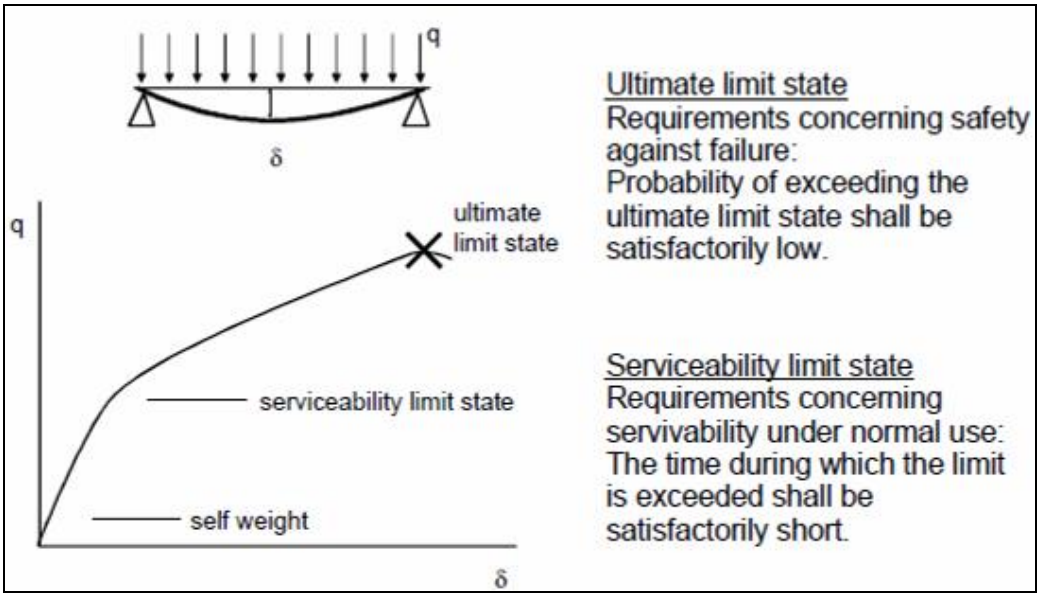

Fig. 4. 3. Limit states

4.2. 1. The Design Analysis Process

- Introduction
- Methods of verification
- The load and resistance factor method
- Method of allowable stresses

4.2.1. 1. Introduction

After the formulation of requirements follows the selection of systems and materials. At this point the design analysis begins, which involves a detailed determination of dimensions and strength of structural components. The methods of analysis can often be decided by the designer himself. It is essential that the verification of the structure, with the chosen dimensions and the properties of the materials selected, satisfies the requirements established. The procedure can be described according to Fig. 4. 4 for a simple case. With the assumptions stated concerning loads, dimensions and material properties, calculation models are applied which provide the load effect *S* (Solicitation, in ENV 1999-1-1, called E) and carrying capacity *R* (Resistance). The load effect may be expressed as a section quantity (e.g. a bending moment in a beam) caused by the load. The resistance is the capacity of the structure to resist a load effect of the same kind (the capacity of the beam to transfer a moment). The verification implies that the resistance R has to be higher than the load effect *S*.

The case described concerns safety against failure, but the procedure of verification that the requirements on the serviceability of the structure in normal use are satisfied will, in principle, be the same. In many cases the procedure is more complicated. Several different kinds of load effects and resistance (e.g. normal

forces and bending moment) may act at the same time. The verification analysis provides an answer, yes or no. In case the answer is no, the procedure has to be repeated with updated dimensions and material properties.

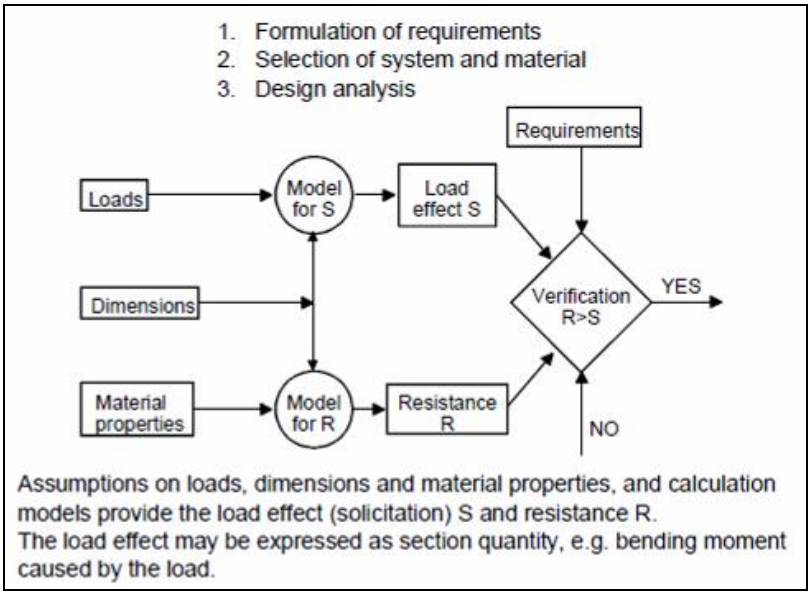

Fig. 4. 4 Schematic description of the design analysis process

4.2.1. 2. Methods of Verification

The quantities which describe the load effect *S* and the resistance *R* (e.g. load values *F*, strength values *f* and dimensions *l*) are stochastic variables which can be represented in a simplified manner by frequency curves according to Fig. 4. 5. The verification consists of demonstrating that the resistance *R* is greater than the load effect *S*. This can be done by use of a number of methods, listed in historical order:

- The safety factor method (method of allowable stresses)
- The load factor method with one single load factor (often used in plastic design)
- The load and resistance factor design method (method of partial coefficients),
- Probabilistic methods

The first method has been used earlier, and is still being used in design codes in many countries but it is being replaced by the third method.
Probabilistic methods have to be based on statistical data for loads, strength properties etc. which, so far, are available only on a very limited scale. The methods are, therefore, only used in very special cases.

The load and resistance factor method and the method of allowable stresses are briefly described below.

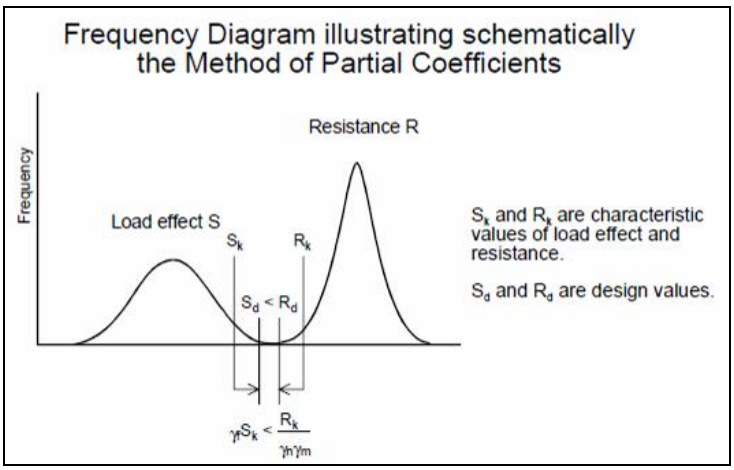

Fig. 4. 5 Frequency diagram illustrating schematically the method of partial coefficients

4.2.1. 3. The Load and Resistance Design Factor Method

The load and resistance factor method (often called the method of partial coefficients) is a verification method which is accepted in many countries. In the following, the method is described as it is applied in the Eurocodes. The formulation is very similar to that used in the different national codes and standards.

The basis is formed by the so called characteristic values:

F_k - for loads (called «actions» in Eurocodes)

f_k - for strength

l_k - for dimensions where, in most cases, l_k is equal to the nominal value, i.e. the value given in drawings and descriptions.

From the characteristic values the design values are deduced:

$$F_d = \gamma_F \cdot F_k \qquad \text{for loads} \qquad (4.\ 7)$$

$$f_d = \frac{f_k}{\gamma_M} \qquad \text{for strength} \qquad (4.\ 8)$$

$$l_d = l_k + \Delta l \qquad \text{for dimensions} \qquad (4.\ 9)$$

γ_F and γ_M are called partial coefficients. The partial coefficient γ_F for load is in the following referred to as the load factor, and the partial coefficient γ_M is named resistance factors. Δl is an additive quantity by which deviations from the ideal dimensions are considered. In most cases Δl can be set to zero.

The design values are used in the calculation models for load effect and resistance and provide the design criteria.

$$R(f_d, l_d) \geq S(F_d, l_d) \qquad (4.\ 10)$$

The load and resistance factor method is illustrated in Fig. 4. 4. Since the load factor can be given different values for different kinds of loads a more consistent design for a low risk of failure can be attained. For example, $\gamma_F = 1.1$ is adopted for gravity loads and 1.5 for environmental loads.

4.2.1. 4. Method of Allowable Stresses

In some design codes the scatter in loads, resistance etc. is covered by one single safety factor *s*. The verification consists of demonstrating that:

$$\sigma \leq \sigma_{all} \tag{4. 11}$$

where σ is the stress determined from the loads and, for instance when designing against yield failure (plastic deformations),

$$\sigma_{all} = \frac{\sigma_y}{s} \tag{4. 12}$$

The safety factor *s* may vary within rather wide limits (1.3 - 3.5) depending on what elements of uncertainity have to be considered. In design against buckling, safety factors to the order of magnitude 10 are found in older codes. It should be noted, however, that the analysis in this course provides lower limit values of the carrying capacity, for instance with respect to buckling and a safety factor of the order of 1.5 to 2 would be appropriate.

4.2. 2. Loads and Load Factors

• Introduction
• Classification of loads
• Characteristic loads, normal loads and long-term loads
• Load combinations, design value of the load
– Examples
• Loads on buildings, bridges and hydraulic structures

4.2.2 1. Introduction

The following discussion on loads is, primarily, applicable to the construction sector, i.e. for buildings, bridge and hydraulic constructions, and for scaffoldings in installation and erection, cranes, masts, power-line pylons, lighting posts and similar load carrying structures.

The discussion will, however, be of interest also to design engineers working with other types of structures such as cisterns, pressure vessels, tanks, transportation vehicles etc.

4.2.2 2. Classification of Loads

Loads are in the present publication used as a common name for effects due to forces and deformations. A force effect is primarily caused by external forces on a structure, while the deformation effect is primarily caused by a forced displacement, e.g. a support settlement, change of temperature or humidity.

Loads may be classified with respect to their variation with time as:

- permanent load approximately constant in time;

- variable load
  - static load
  - dynamic load which causes additional forces due to acceleration including resonance
  - fatigue load - load with so many load cycles that fatigue failure can occur
- accidental load e.g. impact, explosion;

Loads can also be classified with respect to variation in space:

- fixed load - the load distribution over the structure is uniquely defined;
- free load - has an arbitrary distribution over the structure within possible limits.

The duration t_q of variable loads (Fig. 4. 6) is the time during which the magnitude of the load amounts to at least the value q within the service life t_{tot} of the structure. The relative duration is defined as:

$$\eta_q = \frac{t_q}{t_{tot}} \qquad (4.\ 13)$$

It is assumed that the variations of the load are similar during the entire service life t_{tot}.

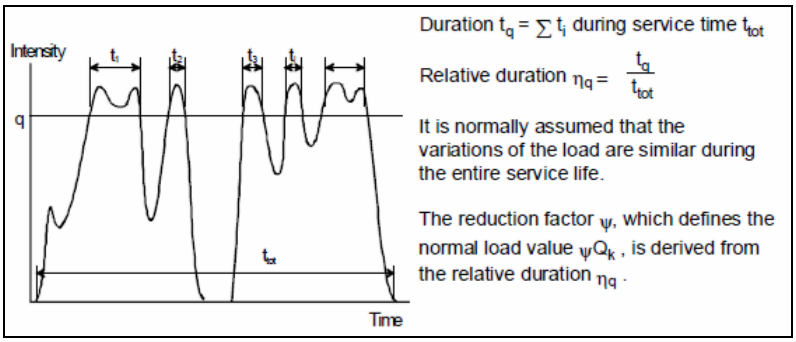

Fig. 4. 6. Variation of load with time

The reduction factor Ψ, which defines a normal load value of Ψ_{Qk}, is derived from the relative duration η_q.

In ENV 1991-1 the Ψ - factor (combination value) is divided into 3 factors:

Ψ_0 = coefficient for combination value of a variable load
Ψ_1 = coefficient for frequent value of a variable load
Ψ_2 = coefficient for quasi-permanent value of a variable load

The combination values (Ψ_0) are associated with the use of combinations of loads, to take account of a reduced probability of simultaneous occurrence of the most unfavourable values of several independent loads.

The frequent value (Ψ1) is determined such that the total time, within a chosen period of time, during which it is exceeded for a specified part, or the frequency with which it is exceeded, is limited to a given value. The part of the chosen period of time or the frequency should be chosen with due regard to the

type of construction works considered and the purpose of the calculations. Unless other values are specified the part may be chosen to be 0,05 or the frequency to be 300 per year for ordinary buildings.

The quasi-permanent value (Ψ_2) is so determined that the total time, within a chosen period of time, during which it is exceeded is a considerable part of the chosen period of time. The part of the chosen period of time may be chosen to be 0,5. The quasi-permanent value may also be determined as the value averaged over the chosen period of time.

These representative values and the characteristic value are used to define the design values of the loads and the combination of loads. The combination values are used for the verification of ultimate limit states and irreversible serviceability limit states. The frequent values and quasi-permanent values are used for the verification of ultimate limit states involving accidental loads and for the verification of reversible serviceability limit states. The quasi-permanent values are also used for the calculation of long term effects of serviceability limit states.

4.2.2 3. Characteristic Loads, Normal Loads and Long-Term Loads

According to most national codes, loads are defined as follows:

- the characteristic value G_k of a permanent load shall be assumed to be the mean value.
- the characteristic value Q_k of a variable load shall be a value with the probability 0.02 of being exceeded at least once during one year.
- the normal value $\Psi_i Q_k$ of a variable load shall be determined considering the relative duration $\eta_q = t_q/t_{tot}$,
- characteristic value Q_{ak} of an accidental load shall be determined with respect to the nature of the load.

Further below it is indicated where G_k, Q_k, Ψ_i and Q_{ak} for normal loads on buildings, bridges and hydraulic structures are defined. If the characteristic value is not available in a load standard, the value of Q_k may in principle be estimated by use of the following procedure (determination of G_k usually does not present a problem).

1. Several observations, about 50, of the yearly maximum load are available. Fit a reasonable distribution function F_Q to measured values and determine Q_k from the condition $F_Q = 0.98$.

2. A smaller number of observations are available. The problem consists of finding a conservative distribution. A lognormal distribution function complies with this requirement in most cases, and for such a distribution, Q_k can be determined by computing:

a) the mean value μ of log χ

b) the standard deviation σ of log χ_i

c) log $Q_k = \mu + 2.05\sigma$, or $Q_k = \exp(\mu + 2.05\ \sigma)$, where $2.05 = \Theta^{-1}(0.98)$ and Θ is the distribution function of the standardized normal distribution.

3) No observations of the yearly maximum load are available. In this case it is in principle not possible to determine Q_k. The situation is not unusual, however, and it is thus often necessary to make an estimate of Q_k.

a) Compare with other similar loads for which Q_k is known.

b) Guess the mean m and the standard deviation s. Adopt $Q_k = \exp(\log m + 2.05\sigma)$ (where δ= s/m, compare 2) above. It is normally easier to make a reasonable guess of *m* and *s* than to guess directly the 98 % fractile.

c) Assume Q_k to be equal to the physical upper limit of the load. It is sometimes possible to indicate an upper limit. For instance, a reservoir or a tank can only be filled to its capacity.

4.2.2 4. Load Combinations, Design Value of the Load

For each critical load case, the design values of the effects of loads should be determined by combining the values of loads which occur simultaneously, as follows:
a) Persistent and transient situations: Design values of the dominant variable loads and the combination design values of other loads.
b) Accidental situations: Design values of permanent loads together with the frequent value of the dominant variable load and the quasi-permanent values of other variable loads and the design value of one accidental load.

Seismic situations: Characteristic values of the permanent loads together with the quasi-permanent values of the other variable loads and the design value of the seismic loads.

When the dominant load is not obvious, each variable load should be considered in turn as the dominant load.

Table 4. 2. Design values of the loads

Design situation	Permanent actions G_d	Single variable actions Q_d		Accidental actions or seismic actions A_d
		Dominant	Others	
Persistent and transient	$\gamma_G G_k$ ($\gamma_P P_k$)	$\gamma_{Q1} Q_{k1}$	$\gamma_{Qi} \Psi_{0i} Q_{ki}$	
Accidental	$\gamma_{GA} G_k$ ($\gamma_{PA} P_k$)	$\Psi_{11} Q_{k1}$	$\Psi_{2i} Q_{ki}$	$\gamma_A A_k$ or A_d
Seismic	G_k		$\Psi_{2i} Q_{ki}$	$\gamma_I A_{Ed}$

In general, the design value of the loads is a load combination as follows:

$$\sum_{j\geq 1} \gamma_{Gj} \cdot G_{kj} + \gamma_{Q1} \cdot Q_{k1} + \sum_{i>1} \gamma_{Qi} \cdot \psi_{01} \cdot Q_{ki} \qquad (4.\ 14)$$

where γ_{Gj} = partial factor for permanent load j
G_{kj} = characteristic value of a permanent loads
γ_{Qi} = partial factor for variable load i
Q_{k1} = characteristic value of the variable load 1
Q_{ki} = characteristic value of the variable load i
Ψ_{0i} = combination coefficients
γ_P = partial factor for pre-stressing loads
P_k = characteristic value of pre-stressing load

In the relevant load cases, those permanent actions that increase the effect of the variable actions (i.e. produce unfavorable effects) shall be represented by their upper design values, those that decrease the effect of the variable actions (i.e. produce favorable effects) by their lower design values.

Where the results of verification may be very sensitive to variations of the magnitude of a permanent action from place to place in the structure, the

unfavorable and the favorable parts of this action shall be considered as individual actions. This applies in particular to the verification of static equilibrium.

For building structures, the partial factors according to ENV 1991-1 for ultimate limit states in the persistent, transient and accidental design situations are given in table below. The values have been based on theoretical considerations, experience and back calculations on existing designs.

In the relevant load cases, those permanent actions that increase the effect of the variable actions (i.e. produce unfavorable effects) shall be represented by their upper design values, those that decrease the effect of the variable actions (i.e. produce favorable effects) by their lower design values.

Where the results of verification may be very sensitive to variations of the magnitude of a permanent action from place to place in the structure, the unfavorable and the favorable parts of this action shall be considered as individual actions. This applies in particular to the verification of static equilibrium.

For building structures, the partial factors according to ENV 1991-1 for ultimate limit states in the persistent, transient and accidental design situations are given in table below. The values have been based on theoretical considerations, experience and back calculations on existing designs.

Table 4. 3. Partial factors

Case[1)]	Action	Symbol	Situations P/T	Situations A
Case A Loss of static equilibrium; strength of structural material or ground insignificant	Permanent actions: self weight of structural and non-structural compo-nents, permanent actions caused by ground, ground-water and free water			
	- unfavourable	γ_{Gsup}	1,10	1,00
	- favourable	γ_{Ginf}	0,90	1,00
	Variable actions			
	- unfavourable	γ_Q	1,50	1,00
	Accidental actions	γ_A		1,00
Case B Failure of structure or struc tural elements, including those of the footing, piles, basement walls etc., governed by strength of structural material	Permanent actions (see above)			
	- unfavourable	γ_{Gsup}	1,35	1,00
	- favourable	γ_{Ginf}	1,00	1,00
	Variable actions			
	- unfavourable	γ_Q	1,50	1,00
	Accidental actions	γ_A		1,00
Case C Failure in the ground	Permanent actions (see above)			
	- unfavourable	γ_{Gsup}	1,00	1,00
	- favourable	γ_{Ginf}	1,00	1,00
	Variable actions			
	- unfavourable	γ_Q	1,00	1,00
	Accidental actions	γ_A		1,00

P: Persistent situation T: Transient situation A: Accidental situation

1) The design should be verified for each case A, B and C separately as relevant

Recommended Ψ factors for buildings according to ENV 1991-1 are given in the table below. In ENV 1991-1 the values are boxed. For other applications see relevant parts of ENV 1991.

Table 4. 4. Ψ factors for buildings

Action	Ψ_0	Ψ_1	Ψ_2
Imposed loads in buildings [1]			
category A: domestic, residential	0,7	0,5	0,3
category B: offices	0,7	0,5	0,3
category C: congregation areas	0,7	0,7	0,6
category D: shopping	0,7	0,7	0,6
category E: storage	1,0	0,9	0,8
Traffic loads in buildings			
category F: vehicle weight: ≤ 30kN	0,7	0,7	0,6
category G : 30kN < vehicle weight ≤ 160kN	0,7	0,5	0,3
category H: roofs	0	0	0
Snow loads on buildings	0,6	0,2	0
Wind loads on buildings	0,6	0,5	0
Temperature (non-fire) in buildings [3]	0,6	0,5	0)

[1] For combination of imposed loads in multistorey buildings, see ENV 1991-2-1.
[2] Modification for snow loads for different geogaphical regions may be required.
[3] See ENV 1991-2-5.

The combination of actions to be considered for serviceability limit states depends on the nature of the effect of actions being checked, e.g. irreversible, reversible or long term. Three combinations designated by the representative value of the dominant action are given in the following table.

Table 4. 5. Combinations of dominant action

Combination	Permanent actions G_d	Variable actions Q_d	
		Dominant	Others
Characteristic (rare)	G_k (P_k)	Q_{k1}	Ψ_{0i} Q_{ki}
Frequent	G_k (P_k)	Ψ_{11} Q_{k1}	Ψ_{1i} Q_{ki}
Quasi-permanent	G_k (P_k)	Ψ_{21} Q_{k1}	Ψ_{2i} Q_{ki}
For serviceability limit states, the partial factors (serviceability) γ_G and γ_Q are taken as 1,0 except where specified otherwise.			

4.2.2 5. Loads on Buildings, Bridges and Hydraulic Structures

Frequently occurring loads on buildings, bridges and hydraulic structures are given in national or international specifications. Loads on overhead cranes are stated by the suppliers. Loads on power-line pylons are chosen according to special standards, etc.

4.2. 3. Resistance and Resistance Factors

- Assumptions concerning strength properties
- Models of analysis

4.2.3. 1. Assumptions Concerning Strength Properties

The material strength properties are the yield and ultimate strength limits in compression and tension, the modulus of elasticity and the shear modulus. Other material properties related to strength are Poisson's ratio, fatigue strength, fracture toughness, creep properties and thermal expansion.

The requirements for design analysis of a structure indicate the strength class of the material to be used. In the analysis, then, various kinds of strength values are introduced which apply to the strength class selected. The strength values introduced in the design analysis are sometimes based on results from tests performed in advance. The producer of the material certifies that the strength properties are according to the requirements specified. Alternatively, the strength properties are checked at the delivery.

The procedure used to verify that the strength of the material meets the given requirements normally includes tests with special test specimens and a specified procedure. In certain cases the results of these tests cannot be considered to be directly representative for the strength of the material in the actual structure and, thus, have to be corrected. This may be performed by dividing the strength values obtained in the tests by a number η, normally greater than 1, such that:

$$f_{structure} = \frac{1}{\eta} f_{test\ specimen} \qquad (4.\ 15)$$

The factor η should not be mistaken for the reduction factor with respect to buckling. *For metals*, the value of η should be *close to one*.

The characteristic value of strength f_k should be interpreted as a condition for the analysis which refers to the expected results of actual or imagined tests. It thus applies to the strength of the test specimen and not to that of the actual construction. The characteristic value is defined somewhat differently for different materials.

The design value for strength should, naturally, be valid for the material of the structure. The formula for computation of the design value f_d from the characteristic value f_k becomes:

$$f_d = \frac{f_k}{\eta \cdot \gamma_M} \qquad (4.\ 16)$$

The value of η depends on factors quite different for different materials, and no generally valid figures can be given. For metals, η= 1.0 may be used and η may, therefore, be omitted in the above equation.

By introducing the partial coefficient γ_M, uncertainties in the strength of the material are taken into consideration as caused by:

- the normal scatter of the material strength,
- the variability of the factor or function η which translates the strength of test specimens into strength of the structure.

For practical reasons other factors not directly related to the strength of the material are taken into consideration by γ_M. Such factors are:

- deviations of dimensions and geometry from the nominal values assumed in the design analysis, if such deviations are not considered elsewhere,
- unreliability of the model of analysis, if kept within reasonable limits.

The partial coefficients used in ENV 1999-1-1 is different for resistance of members and connections. They are, however, boxed values.

Resistance of class 1 cross sections: $\gamma_{M1} = 1,10$
Resistance of class 2 or 3 cross sections: $\gamma_{M1} = 1,10$
Resistance of class 4 cross sections: $\gamma_{M1} = 1,10$
Resistance of member to buckling: $\gamma_{M1} = 1,10$
Resistance of net section at bolts holes: $\gamma_{M2} = 1,25$
Resistance of bolted connections: $\gamma_{Mb} = 1,25$
Resistance of riveted connections: $\gamma_{Mr} = 1,25$
Resistance of pin connections: $\gamma_{Mp} = 1,25$
Resistance of welded connections: $\gamma_{Mw} = 1,25$
Slip resistance connections:
- ultimate limit state: $\gamma_{Ms,ult} = 1,25$
- serviceability limit state: $\gamma_{Ms,ser} = 1,10$

Adhesive bonded connections: $\gamma_{Ma} \geq 3,0$.

Four classes of cross sections are defined, as follows:
- **Class 1** cross sections are those which can form a plastic hinge with the rotation capacity required for plastic analysis.
- **Class 2** cross sections are those which can develop their plastic moment resistance, but have limited rotation capacity.
- **Class 3** cross sections are those in which the calculated stress in the extreme compression fiber of the member can reach its proof strength, but local buckling is liable to prevent development of the full plastic moment resistance.
- **Class 4** cross sections are those in which it is necessary to make explicit allowances for the effects of local buckling when determining their moment resistance or compression resistance.

The classification of a section depends on the proportions of each of its compression elements. The compression elements include every element of a cross section that is either totally or partially in compression.

The various compression elements in a cross section (such as a web or a flange) can, in general, be in different classes. The cross section should be classified by quoting the least favorable class of its compression elements.

4.2.3. 2. Models of analysis

The calculations used in the design are based on models by means of which the behavior of the structure is described. The models of analysis may be more or less complicated and provide a more or less accurate description of the function of the structure. Often a model giving a higher accuracy turns out to be more complicated. In certain cases the nature of the problem demands a more sophisticated model, e.g. for stress analysis in structures subjected to fatigue. Usually, there is an option, however, between different models and the choice has to be made on an economic basis, which applies to the cost of material/construction in relation to the cost of the design analysis.

Models of analysis should be considered as approximate descriptions of the function of a structure. Even the most advanced models are thus subject to some uncertainties. With regard to this fact numerical values of coefficients etc. should be chosen in such a way that the model gives results on the safe side. But it is often not feasible to enter such values of the coefficients that the results are conservative in all conceivable cases.

Probabilistic aspects may be introduced, choosing the strength coefficients in such a way that the model gives results on the unsafe side only in a small fraction of the cases. This fraction should not exceed 5 %. The resulting resistance may thus be interpreted as a characteristic value.

4.2. 4. Design Criteria

4.2.4. 1. The load and resistance factor method

The method is applied in many design specifications and is sometimes referred to as the method of partial coefficients. According to this method the characteristic values of loads and resistance are first determined. Then the design values are obtained by:

– multiplying the characteristic values of the loads by the load factor γ_F,
– dividing the characteristic values of the resistance by the resistance factors γ_M.

The design analysis should verify that the stresses caused by design loads σ_{Sd} (or section forces M_{Sd}) are smaller than the design value of the resistance expressed in terms of the same quantity (σ_{Rd}, or M_{Rd}), i.e.

$$\sigma_{Sd} < \sigma_{Rd} \qquad (4.\ 17)$$

where: $\sigma_{Sd} = \sum \gamma_G G_k + \sum \gamma_{Qi}\psi_{0i}Q_{ki}$ - stress caused by load

$$\sigma_{Rd} = \frac{f_k}{\gamma_M} \qquad (4.\ 18)$$

f_k = characteristic strength, referring to a limit state
γ_M = resistance factor considering uncertainties in the material parameters and tolerances for dimensions.

4.2.4. 2. Method of allowable stresses

A safety factor should consider the unreliability of load assumptions as well as the unreliability of resistance values. Since uncertainties of the methods of analysis are included in the estimation of the resistance, a moderately low safety factor may be chosen, normally 1.5 for normal types of loading.

The allowable stress σ_{all} is thus determined as:

$$\sigma_{all} = \frac{f_k}{s} \qquad (4.\ 19)$$

where f_k = the resistance according to this course.
s = safety factor, normally 1.5.

The allowable stress shall be higher than the stress determined from loads without load factors i.e.

$$\sigma < \sigma_{all} \qquad (4.\ 20)$$

4.2. 5. Aluminium Alloys as a Structural Material

Most of the structural aluminium alloys have relatively high strength compared to the modulus of elasticity. A comparison between different aluminium alloys and tempers and some other materials is presented in Table 4. 6.

Table 4. 6. Strength ($R_{p0,2}$) and modulus of elasticity (E) for some materials

Material	$R_{p0.2}$	E	$E/R_{p0.2}$
AA 5083-0	125	70000	560
AA 5083-H321	220	70000	318
AA 6082-T6	270	70000	259
AA 7108-T6	360	70000	194
St 42	260	210000	808
St 52	360	210000	583
Concrete C45	28	28000	994
Timber	20	9000	450

- Aluminium has high strength compared to modulus of elasticity, especially strain hardened and heat treated alloys
- Steel structures are often designed in the ultimate limit state
- Aluminium structures are mostly designed in the serviceability state (deflections)

This effect is especially clear when the aluminium alloy is strain-hardened or heat treated. Structural aluminium alloys have roughly twice the strength of steel compared to the modulus of elasticity.

When designing an aluminium alloy structure, it will often be the deflection criteria which are governing. The design procedure will for that reason be designing according to the deflection criteria or stability and than check the stress or the bearing capacity of the structure.

Comparing steel and aluminium alloy members in tension with the same elastic strain, the steel member will have 3 times the stress of the aluminium alloy member, see Fig. 4.7.

The stress in an aluminium alloy structure designed according to the deflection criteria is very often low. A structure or member in tension designed according to the deflection criteria will usually be in this situation. The safety against yielding and fracture will in this comparison be:

Table 4. 7. Factors for steel and aluminium alloy

	AA 6082 - T6	St 52
Factor against yielding	3,1	1,3
Factor against fracture	3,6	2,0 - 2,4

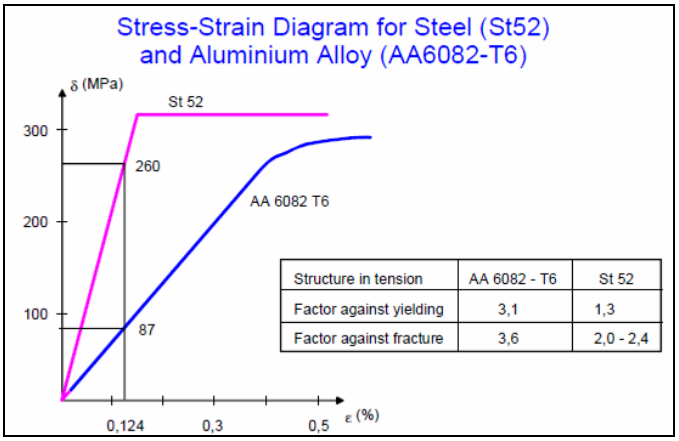

Fig. 4. 7. Stress-strain diagram for steel (St52) and aluminium alloy (AA6082-T6)

Because of the relatively low modulus of elasticity of aluminium alloys compared to their strength, the safety of designing an aluminium alloy structure to the deflection criteria is very high and usually higher than a steel structure.

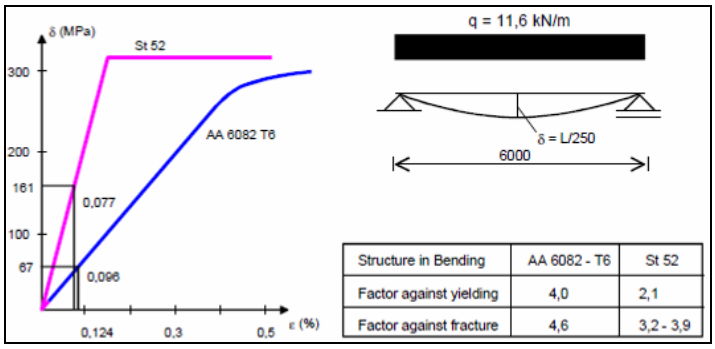

Fig. 4. 8. The stress and strain for beams made of St52 and AA6082-T6

The deflection of members in bending is dependent on the modulus of elasticity (E) and on the moment of inertia (I) together with the load and the span. With the same span and load, it will be the product E • I which will determine the deflection.

To get the same deflection of steel and aluminium alloy beams in bending, the moment of inertia of the aluminium alloy beam must be three times that of steel. If the increase in the moment of inertia is to be done only by increasing the thicknesses of the web and flanges the aluminium alloy beam will have the same weight as the steel beam. To save weight the aluminium alloy beams in bending have to be higher [79].

4. 3. Design of members

In all modern codes of practice structural safety is established by the application of the partial safety coefficients to the loads (or 'actions') and to the

strength (or 'resistance') of components of the structure. The new Eurocodes for the design and execution of buildings and civil engineering structures use a limit state design philosophy defined in Eurocode 1. (Common unified rules for different types of construction and material).

The partial safety coefficients for actions (γ_F) depend on an accepted degree of reliability, which is recognized as a national responsibility within the European Community. The probability of severe loading actions occurring simultaneously can be found analytically, if enough statistical information exists, and this is taken into account by the introduction of a second coefficient ψ. The design value of the action effects (when the effects are unfavorable) is then found by taking values of γ_F dependent on the type of loading and values for ψ that take account of the chances of simultaneous loading. A value of γ_F of 1,15 is suggested for permanent loads, such as the dead load of bridge girders, and 1,5 for variable loads such as traffic loads or wind loading. The loading actions on members are found by an elastic analysis of the structure, using the full cross-sectional properties of the members.

The partial safety coefficients for actions takes account of the possibility of unforeseen deviations of the actions from their representative values, of uncertainty in the calculation model for describing physical phenomena, and uncertainty in the stochastic model for deriving characteristic codes.

The partial safety coefficient for material properties (γ_M) reflects a common understanding of the characteristic values of material properties, the provision of recognized standards of workmanship and control, and resistance formulae based on minimal accepted values. The value given to γ_M accounts for the possibility of unfavorable deviations of material properties from their characteristic values, uncertainties in the relation between material properties in the structure and in test specimens, and uncertainties associated with the mechanical model for the assessment of the resistance capacity.

A further coefficient, γ_n, is specified in some codes, and this can be introduced to take account of the consequences of failure in the equation linking factored actions with factored resistance. It is often incorporated in γ_M. It recognizes that there is a choice of reliability for classes of structures and events that take account of the risk to human life, the economic loss in the event of failure, and the cost and effort required to reduce the risk. Typical values in recent European codes of practice for aluminium are $\gamma_M \cdot \gamma_n$ = 1,2 and 1,3, on the assumption that properties of materials are represented by their characteristic values.

The ultimate limit states defined by the use of the above factors refer to failure of members or connections by rupture or excessive deformation, transformation of the structure into a mechanism, failure under repeated loading (fatigue) and the loss of equilibrium of the structure as a rigid body.

Serviceability limit states, according to most definitions, correspond to a loss of utility beyond which service conditions are no longer met. They may correspond to unacceptable deformations or deflections, unacceptable vibrations, the loss of the ability to support load retaining structures, and unacceptable cracking or corrosion. Because certain aluminium alloys in the non-heat-treated condition, or in the work-hardened condition, do not have a sharply defined 'knee' to the stress/strain curve, it is sometimes possible for unacceptable permanent deformation to occur under nominal or working loads. The same may be true for alloys that have a substantial amount of welding during fabrication.

Design with regards to instability. Extruded and welded members are never totally perfect. They possess a number of imperfections. It is of great importance to take the influence of imperfections into consideration, especially for different types

of instability phenomena, e.g. flexural buckling, lateral-torsional buckling and plate buckling. In the past, the compressive force capacity was calculated with Euler's buckling formula. This formula is valid for a perfectly straight, elastic bar without imperfections. However, in reality, such a bar contains a number of imperfections that reduce the strength. In Fig. 4. 9 the behaviour of an idealized Euler column is compared to that of a real column.

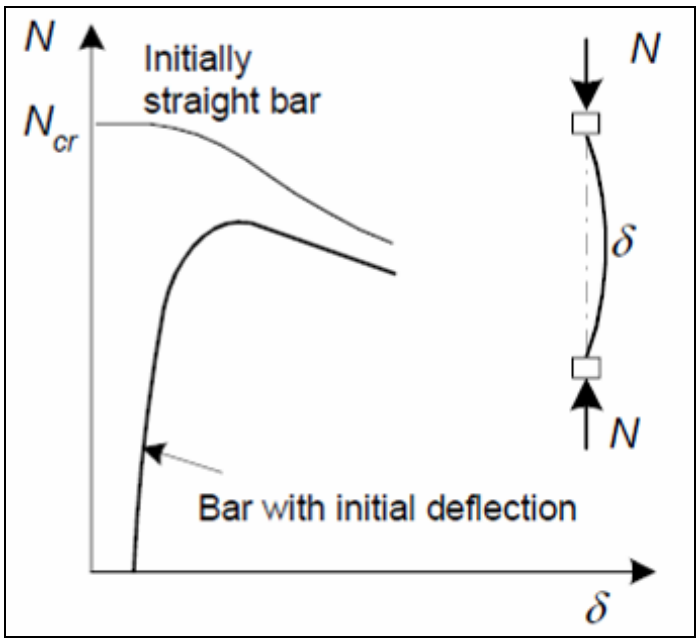

Fig. 4. 9. Comparison between buckling behavior of an idealized Euler bar and of a real bar with imperfections

It is possible, in the age of computers, to create calculation models that can, with great detail, simulate the actual behaviour, but under one condition. Every imperfection of the beam must be known and correctly modeled and taken into consideration. Residual stresses and variation in material properties have little influence on the behaviour of extruded members. On the other hand, the first two of these imperfections can have great effect on welded members.

Welding effects the member by creating residual stresses and reduction in strength of the material in the heat affected zones.

4.3. 1. Geometrical imperfections

4.3.1. 1. Initial curvature

The deviation of cross section dimensions and member length is often very small for extruded members. The effect is however not negligible if there is risk for instability, e.g. flexural buckling and lateral-torsional buckling.

A systematic analysis carried out on extrusions from several European countries showed that the initial curvature was approximately *L*/2000. In national specifications, initial curvature is usually presumed to lie between *L*/500 and

L/1000. It is common to use the same value as for rolled steel sections. The ECCS (European Convention for Constructional Steelwork) recommends that v_0 is taken as *L*/1000 when calculating buckling curves for extruded profiles, cf. Fig. 4. 10. This value may seem to be far on the safe side. However, another geometrical imperfection is considered within this value; deviation of sectional dimensions.

4.3.1. 2. Deviation of cross sectional dimensions

The effect of this imperfection is that a centric compressive load actually has a certain eccentricity. The point of load introduction, in this case, does not coincide with the centre of gravity for the cross section.

For extruded profiles and welded profiles, measurements show that the eccentricity, *e*, is less than *L*/1600. Together with the initial curvature of *L*/2000, this explains why initial curvature in national regulations is considered to be less than *L*/1000.

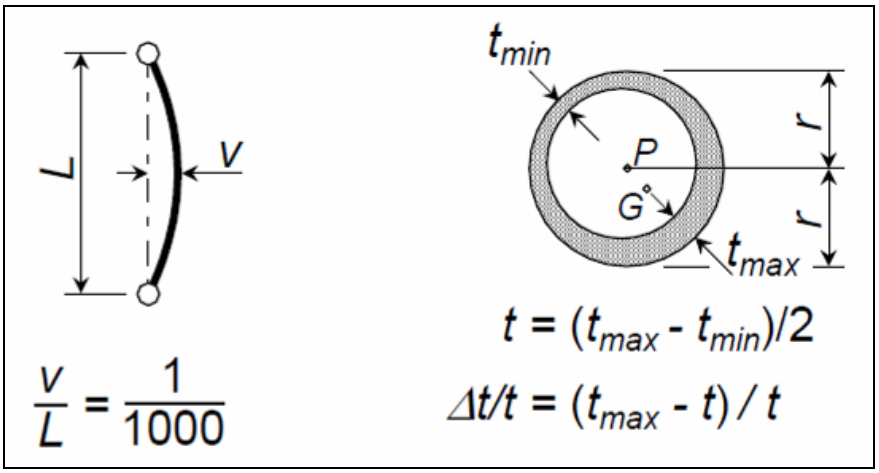

Fig. 4. 10. Definition of initial curvature and eccentricity

4.3.1. 3. Initial buckles

Flat parts in extruded profiles show very small initial buckles. This is of two reasons; the first is that it is difficult to produce extrusions with sectional parts so slender that initial buckles can develop. The second reason is that the traction process that follows extrusion reduces any initial buckles. Measurement of welded T-sections and box sections show that the initial curvature is always less than L/1300, i.e. always greater than for extruded profiles.

Initial buckles in welded beams (flanges and webs) cannot be avoided. The following tolerances are recommended, if smaller tolerances are not necessary for aesthetic or other reasons. Tolerated buckles in the web are given in the following expressions. The limit is applied to each panels of the web with horizontal stiffeners.

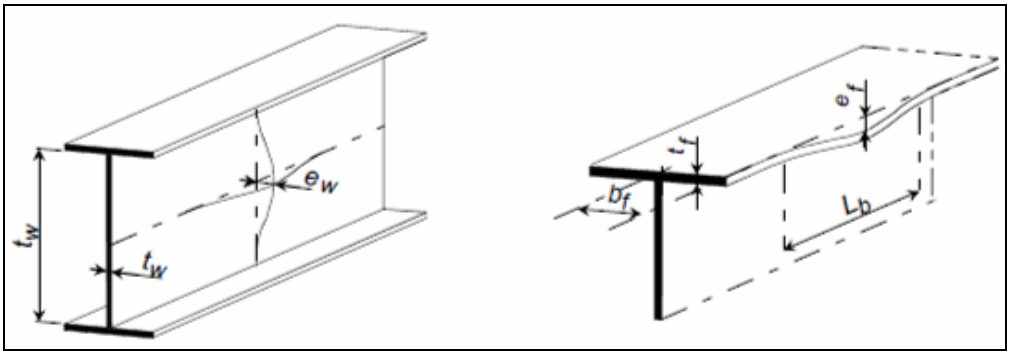

Fig. 4. 11. Tolerated divergence from flatness of web and flanges

$$e_w < \frac{b_w}{200} \text{ when } \frac{b_w}{t_w} \le 50$$
$$e_w < \frac{b_w^2}{10000 t_w} \text{ when } 50 < \frac{b_w}{t_w} < 125 \qquad (4.\ 21)$$
$$e_w < \frac{b_w}{200} \text{ when } \frac{b_w}{t_w} \ge 125$$

The largest tolerable deflections for an outstand element in compression, i.e. the compression flange for an I- ,U- or Z- cross section, are given in the following expressions.

$$e_f < \frac{L_b}{250} \text{ when } \frac{b_f}{t_f} \le 10$$
$$e_f < \frac{L_b \cdot b_w}{2500 \cdot t_f} \text{ when } \frac{b_f}{t_f} > 10 \qquad (4.\ 22)$$

4.3.1. 4. Residual stress in extruded profiles

Experiments conducted on I-profiles consisting of different alloys show that the residual stresses are randomly distributed over a cross section. It seems there is no simple rule for stress distribution as there is for rolled steel sections. Residual stresses are low, the compressive stresses almost never exceed 20 MPa and tensile stresses are much lower. These values are measured on the surface of the profiles. At the centre of the material the values are probably lower since residual stresses usually change sign from one side to the other. Different alloys do not affect the intensity and distribution of residual stresses. The residual stresses have a negligible effect on the load-bearing capacity.

4.3.1. 5. Bauschinger effect

If a specimen is loaded in tension and after that loaded in compression, the elastic limit is lower than for a specimen only loaded in compression. Normally the Bauschinger effect is neglected in national regulations. The reason is that the Bauschinger effect is more or less counterbalanced by the effect of the loss of residual stress when straightening extruded profiles. Furthermore the design

methods (buckling curves etc.) have been calibrated with tests on specimens including the Bauschinger effect.

4.3.1. 6. Heat affected zones

Two groups of welded profiles are distinguished: those consisting of heat-treated alloys and those consisting of non heat-treated alloys. The non heat-treated group is hardly affected by welding. The heat-treated group loses quiet an amount of strength in the heated affected zone close to the weld. The proof stress decreases up to 40-50 %. The reason for the phenomenon is that the heat-treated alloy is heated at the weld. The crystal structure is changed and the material loses its strength. The elastic limit, the strength at rupture and the elongation at rupture are influenced by welding when joining flat plates to an I-profile. The moment capacity is greatly reduced for such a beam. One solution is to place the weld in an area where the effect of welding is small on the bending strength.

4.3.1. 7. Influence of heat-affected zones

In ultimate limit state design the factored characteristic loads must be shown to be less than or equal to the calculated resistance of the structure or component divided by the material factor. In calculating the resistance of welded aluminium components, however, a problem occurs with the strong heat-treated alloys. The effect of the temperature generated by the welding process is to disrupt the heat treatment and produce softened zones in the vicinity of welds. This softening is a significant factor in 6xxx and 7xxx series alloys and in 5xxx series alloys in a work-hardened temper. It can have a noticeable effect on the ultimate strength of the welded component and must be allowed for in design.

The extent of the HAZ is affected by the metal temperature when welding begins and by the build-up of temperature in multi-passes. When neighbouring parallel welds are laid simultaneously the extent of their combined HAZ increases. For thicker material the extent of the HAZ measured radial from all points along the edge of a weld was found to be proportional to $\sqrt{A_w / N}$, where A_w is the total section area of the weld deposit per pass and N is the number of heat flow paths adjacent to the weld. The extent was increased if temperature build-up was allowed to take place between passes.

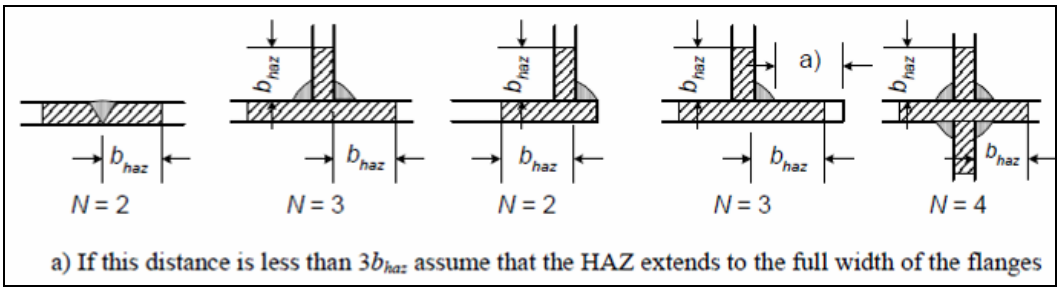

Fig. 4. 12. The extent of heat affected zones

The HAZ is assumed to extend a distance b_{haz} in any direction from a weld, measured as follows (see Fig. 4. 12).
a) transversely from the centre line of an in-line butt weld

b) transversely from the point of intersection of the welded surfaces at fillet welds
c) transversely from the point of intersection of the welded surfaces at butt welds used in corner, tee or cruciform joints.
d) in any radial direction from the end of a weld.

For thickness > 12 mm there may be a temperature effect, because interpass cooling may exceed 60°C unless there is strict quality control. This will increase the width of the heat affected zone (see Fig. 4. 13).

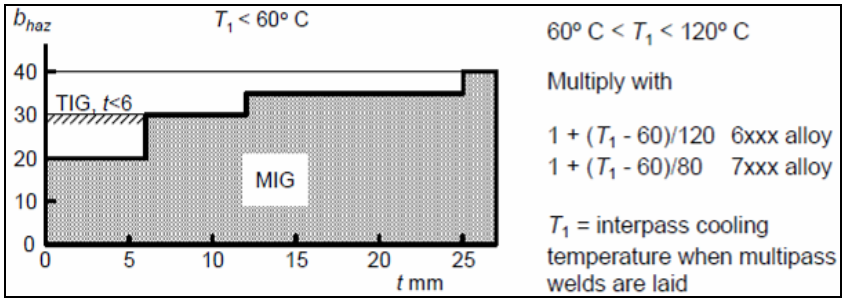

Fig. 4. 13. Width of heat affected zone (b_{haz})

Table 4. 8. HAZ softening factor (ρ_{HAZ})

For all alloys supplied as extrusions, sheet, plate, drawn tubes and forging in the O and F condition, ρ_{haz} = 1,0.			
Extrusions, sheet, plate, drawn tube and forging in the T4, T5 and T6 condition			
Alloy Series	Condition	ρ_{haz} (MIG)	ρ_{haz} (TIG)
6xxx	T4	1,0	--
	T5	0,65	0,60
	T6	0,65	0,50
7xxx	T6	0,80[a)] 1,0[b)]	0,60[a)] 0,80[b)]
Sheet, plate or forging in the work hardened (H) condition			
Alloy Series	Condition	ρ_{haz} (MIG)	ρ_{haz} (TIG)
5xxx	H22	0,86	0,86
	H24	0,80	0,80
3xxx	H14, 16, 18	0,60	0,60
1xxx	H14	0,60	0,60

a) apply when a tensile stress acts transversely to the axis on a butt or fillet weld;
b) apply for all other conditions, i. e. longitudinal stress, a transverse compressive stress or a shear stress.

The values of b_{haz} from Table 4. 8 apply to in-line butt welds (two valid heat paths = two plates welded together) or to fillet welds at T-junctions (three valid

heat paths). If the junctions between elements are fillet welded, but have different numbers of heat paths (N) from the three, multiply the value of b_{haz} by 3/N.

4.3.1. 8. Stress-strain relationship

One of the first difficulties, when dealing with aluminium alloys is the problem with defining its stress-strain relationship. The elastic limit, often defined as the $f_{0,2}$ - limit for aluminium, is not enough for defining the stress-strain relationship for the material. It is also necessary to include the variations in Young's modulus and the strain hardening of the material. These factors are the reason why the stress-strain curve is different for each alloy. These factors are also the main reasons why analysis of structural elements cannot be based upon simplified stress-strain relationships as for steel. Analysis must be based upon generalized inelastic stress-strain relationships. The most commonly used is the Ramberg- Osgood law, shortly presented in the following.

4.3.1. 9. The Ramberg-Osgood law

A generalized law $\varepsilon = \varepsilon(\sigma)$ has been proposed by Ramberg and Osgood for aluminium alloys as:

$$\varepsilon = \frac{\sigma}{E} + \left(\frac{\sigma}{B}\right)^n \qquad (4.\ 23)$$

where E is the Young's modulus at the origin. Parameters B and n have to be determined by experiment. Often $B = f_{0,2} / 0{,}002^{1/n}$ is used. Then:

$$\varepsilon = \frac{\sigma}{E} + 0{,}002\left(\frac{\sigma}{f_{0,2}}\right)^n \qquad (4.\ 24)$$

Aluminium has been classified according to n as follows:

n < 10 - 20 non heat-treated alloys

n > 20 - 40 heat-treated alloys

4.3.2. Basic values of strength

Design values of strength at the ultimate limit state, for the next subchapters, are defined as following:

- for the design 0,2 proof strength = $f_{0,d}$

$$f_{0,d} = \frac{f_0}{\gamma_{M1}} = \frac{f_{0,2p}}{\gamma_{M1}} \qquad (4.\ 25)$$

- for the design ultimate strength = $f_{a,d}$

$$f_{a,d} = \frac{f_a}{\gamma_{M2}} = \frac{f_u}{\gamma_{M2}} \qquad (4.\ 26)$$

- for the design ultimate strength in the heat affected zone = $f_{haz,d}$

$$f_{haz,d} = \rho_{haz} \cdot \frac{f_a}{\gamma_{M2}} = \rho_{haz} \cdot \frac{f_u}{\gamma_{M2}} \qquad (4.\ 27)$$

where $f_{0,d}$ and $f_{a,d}$ are the design yield stress and the design ultimate strength for both tensile stress and compression stress. Table 4. 9 presents minimum characteristic values of yield strength f_0, ultimate strength f_a and strength f_{haz} in the heat-affected zone for some wrought aluminium alloys, used in the field of civil engineering. The design value of strength in the heat affected zone is given in Table 4. 10.

Table 4. 9. Minimum characteristic values of yield strength f_0, ultimate strength f_a and strength f_{haz} in the heat-affected zone for some wrought aluminium alloys

Alloy EN-AW	Temper	Sheet/ Extrusion	Thickness		F_o	f_a	f_{haz}	A_{50}	
			over	up to	N/mm²	N/mm²	N/mm²	%	
5083	O/H111	Sheet	2	80	115	270	270	14	
	F/H112	Extrusion		200	110	270	270	12	
	H24/H34	Sheet	2	25	250	340	272	4	
	H24/H34	Extrusion		5	235	300	240	4	
6005A	T6	Extrusion		25	200	250	163	8	
6063	T6	Extrusion		20	170	215	140	8	
6082	T4	Sheet	4	12	110	205	205	12	
		Extrusion		25	110	205	205	14	
	T6	Sheet	4	125	255	300	195	6	
		Extrusion	5	150	250	290	190	8	

$f_{haz} = \rho_{haz}\ f_a$ (MIG welding)
Sheet = Sheet, strip and plate
Extrusion = Extruded profile, extruded tube and extruded rod (not drawn tube)

The partial safety factors γ_{M1} and γ_{M2} may be explained as:

- γ_{M1} = 1,1 is the partial safety factor for bending and overall yielding in tension and compression, for all cross section classes; it refers to the yield strength f_o and the effective cross section allowing for local buckling and HAZ softening but with no allowance for holes.
- γ_{M2} = 1,25 is the partial safety factor used for *the local capacity in net section* in tension or compression. It refers to the ultimate strength f_a and the net cross section with allowance for holes and HAZ softening but no allowance for local buckling.

Table 4. 10. Design values of yield strength $f_{0,d}$, ultimate strength $f_{a,d}$ and strength $f_{haz,d}$ in the heat-affected zone for some wrought aluminium alloys

Alloy EN-AW	Temper	Sheet/ Extrusion	Thickness over	Thickness up to	$f_{o,d}$ N/mm^2	$F_{a,d}$ N/mm^2	$f_{haz,d}$ N/mm^2	a)	b)
5083	O/H111	Sheet	2	80	105	216	216	2,07	2,07
	F/H112	Extrusion		200	100	216	216	2,16	2,16
	H24/H34	Sheet	2	25	227	272	218	1,20	0,96
	H24/H34	Extrusion		5	214	240	192	1,12	0,90
6005A	T6	Extrusion		25	182	200	130	1,10	0,72
6063	T6	Extrusion		20	155	172	112	1,11	0,72
6082	T4	Sheet	4	12	100	164	164	1,64	1,64
		Extrusion		25	100	164	164	1,64	1,64
	T6	Sheet	4	125	232	240	156	1,03	0,67
		Extrusion	5	150	227	232	150	1,02	0,66

$f_{o,d} = f_o / \gamma_{M1}$ $\quad f_{a,d} = f_a / \gamma_{M2}$ $\quad f_{haz,d} = \rho_{haz} f_a / \gamma_{M2}$

a) $f_{a,d} / f_{o,d} = (f_a / \gamma_{M2}) / (f_o / \gamma_{M1})$

b) $f_{haz} / f_{o,d} = (\rho_{haz} f_a / \gamma_{M2}) / (f_o / \gamma_{M1})$ (MIG welding)

4.3.3. Local buckling

The resistance of a cross-section part in compression is generally limited by local buckling. The buckling load depends on the slenderness of the cross-section part. The slenderness ratio of the cross section part is normally determined by the ratio of the width divided by the thickness ($\beta = b/t$). In many cases the more general parameter for slenderness, λ, is used:

$$\lambda = \sqrt{\frac{f_0}{f_{cr}}} \qquad (4.\ 28)$$

where f_0 is the 0,2-limit and f_{cr} is the elastic buckling stress for a perfect plate without initial buckles or residual stresses. λ is proportional to b/t and $\sqrt{f_0 / E}$ and depends on the loading and the boundary conditions, e.g. the connection to other cross sectional elements.

The behaviour of an element in **compression** depends on the slenderness ratio.

a. If the slenderness ratio of the element is small ($\beta < \beta_1 = 3$) no buckling occurs. The average stress is equal to or even larger than the ultimate strength of the material intension.

b. If the slenderness ratio is somewhat larger ($\beta_1 < \beta < \beta_2$) buckling occurs after the compressed element has been plastically deformed to a strain, which is more than about twice the strain corresponding to the $f_{0,2}$ (ε. 1%).

c. If the slenderness ratio is further increased ($\beta_2 < \beta < \beta_3$), buckling occurs once the 0,2 proof strength has been reached and plastic deformation has started.
d. If the slenderness ratio is large ($\beta > \beta_3$), then buckling occurs before the average stress in the compressed part of the section has reached the 0,2 proof strength.

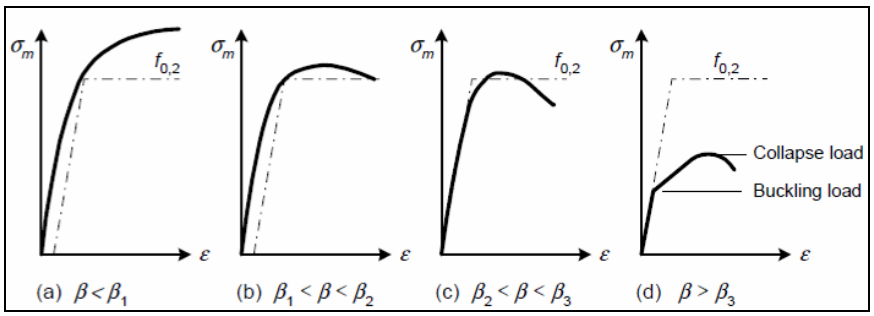

Fig. 4. 14. Principle relationship between mean stress σ_m and compression ε for different slenderness β

Failure normally does not occur when some cross sectional element starts to buckle, but after redistribution of stresses and yielding. The division of cross-sections into four classes for members in bending corresponds to the different behaviour as above. Class 1 and 2 cross sections have compact cross-section parts that behave according to a and b (Fig. 4. 14). Class 3 cross sections have semi-slender cross section parts and behave according to c. Class 4 cross sections have one or more slender section parts that behave according to d (Fig. 4. 14).

For a member in axial compression, actually only two classes are of interest: non-slender sections with class 1 - 3 cross section parts and slender sections with one or more slender section parts that behave according to d (**Fig. 4. 14**).

The effective area in case of plates in compression can be determined, according to Eurocode 9, by multiplying an effective thickness with the gross width.

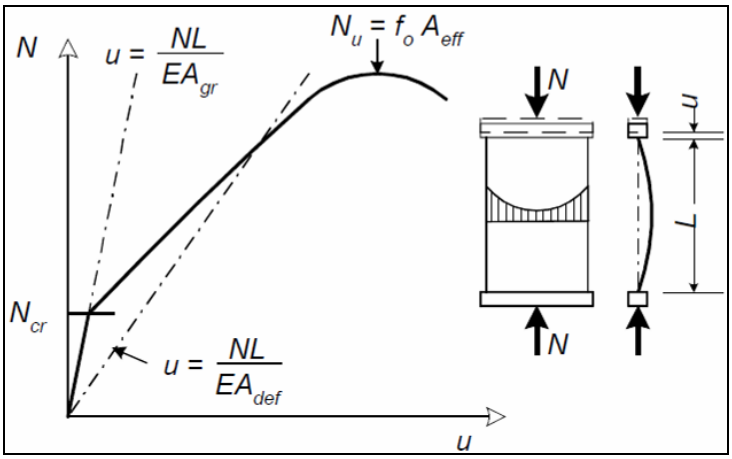

Fig. 4. 15. Principle relationships between compression *u* and axial load *N*

A_{gr}: area of gross cross section, used for calculation of deformation prior to buckling
A_{def}: area of effective cross section used for calculation of deformation. A_{def} depends on the load level
A_{eff}: area of effective cross section used for calculation of resistance.

Effective cross section for calculation of resistance is defined as:

$$N_u = A_{eff} \cdot f_0 \tag{4. 29}$$

where N_u is the rupture load for the cross section part.
The axial deformations can be calculated from the relationship:

$$u = \frac{N \cdot L}{E \cdot A_{def}} \tag{4. 30}$$

where A_{def} depends on the load level.

The definition of A_{def} is different from that for A_{eff}, and, in principle, $A_{def} \approx A_{eff}$ even just before failure.

4.3.4. Bending moment

The ultimate limit state of a beam can occur in different circumstances depending upon the geometry of the beam (the span *L*, the *b/t* ratio of the individual parts etc.), the loading and support conditions and the type of connection. Failure is most often accompanied by local buckling of compressed cross section part. Exceptions are compact cross sections, such as solid rectangular and circular sections and beams made by material with small ductility.

Class 1 cross section

In the case of a beam with compact cross-section, in which local buckling or flexural torsional buckling are not likely to occur, the beam experiences the inelastic range after reaching the limiting elastic moment $M_{el} = W_{el} \cdot f_o$ until the ultimate moment M_u is reached.

This moment cannot be defined (as it is for steel structures) as the full plastic moment $M_{pl} = W_{pl} \cdot f_0$. In fact, due to the hardening behaviour of the σ – ε law of aluminium, a limiting curvature has to be defined corresponding to the limit of strain in the outermost fibre of the cross section. The increase in strength, M_u - M_{el}, obtained in this phase can be quantified through a relation:

$$M_u = \alpha \cdot M_{el} \tag{4. 31}$$

which defines in a general form a shape factor $\alpha = \alpha_1$ which is not solely dependent upon the cross-sectional geometry, as is usual, but also depends upon the parameters in the σ – ε law and on the definition of the limiting curvature.

Fig. 4. 16 shows that $M_u > M_{pl}$ if ε is larger than about 1%. Then $\alpha_1 > M_{pl} / M_{el}$. In this case the rotational capacity of the cross-section, which characterizes the flexural ductility of the beam, allows redistribution of the internal forces, and it is therefore possible to carry out a limit analysis of the whole structure.

Class 2 cross-section

In the case of open profiles, local buckling phenomena are most likely to occur in the compressed region of the cross-section and cause a decrease in the M−ε curve of the beam. This unstable behaviour is dependent upon the β = *b/t* ratio. If the decreasing portion of the curve occurs after the ultimate moment M_u is reached, the beam keeps the same maximum load-carrying capacity, but the rotational capacity of the cross-section is reduced why redistribution of the internal forces is limited. Note that using M_{pl} as the ultimate resistance corresponds to a strain at the extreme fibres of about 1% for rectangular cross sections as well as for mayor and minor axis bending of H cross-sections.

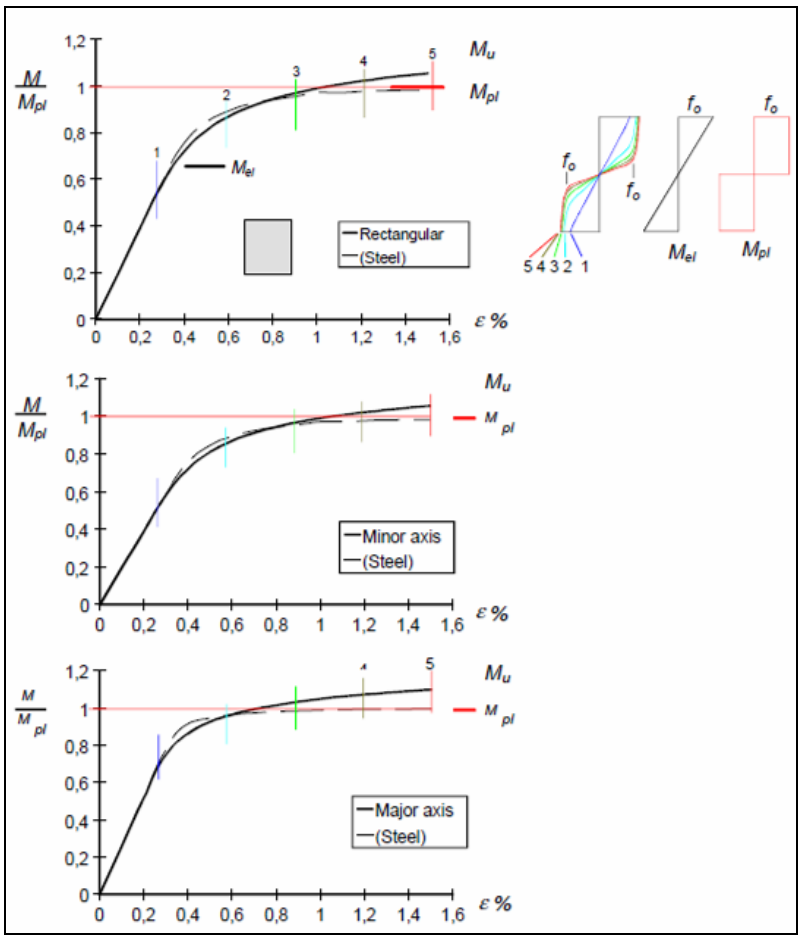

Fig. 4. 16. Moment-strain curves

Class 3 and 4 cross-section

If the decreasing portion of the curve occurs before the ultimate moment M_u is reached (class 3 cross-section, see

Fig. 4. **17**), or even before the elastic moment M_{el} (class 4 cross-section, see Fig. 4.17), the load-carrying capacity of the beam is affected by local buckling phenomena to a higher degree if the b/t ratio is large (e.g. thin walled profiles). Also ductility decreases to the extent that redistribution of internal forces cannot be considered.

The classification of elements in cross sections is linked to the values of the maximum slenderness parameter β. For elements in beams:

$\beta \leq \beta_1$: class 1

$\beta_1 < \beta \leq \beta_2$: class 2

$\beta_2 < \beta \leq \beta_3$: class 3

$\beta_3 < \beta$: class 4

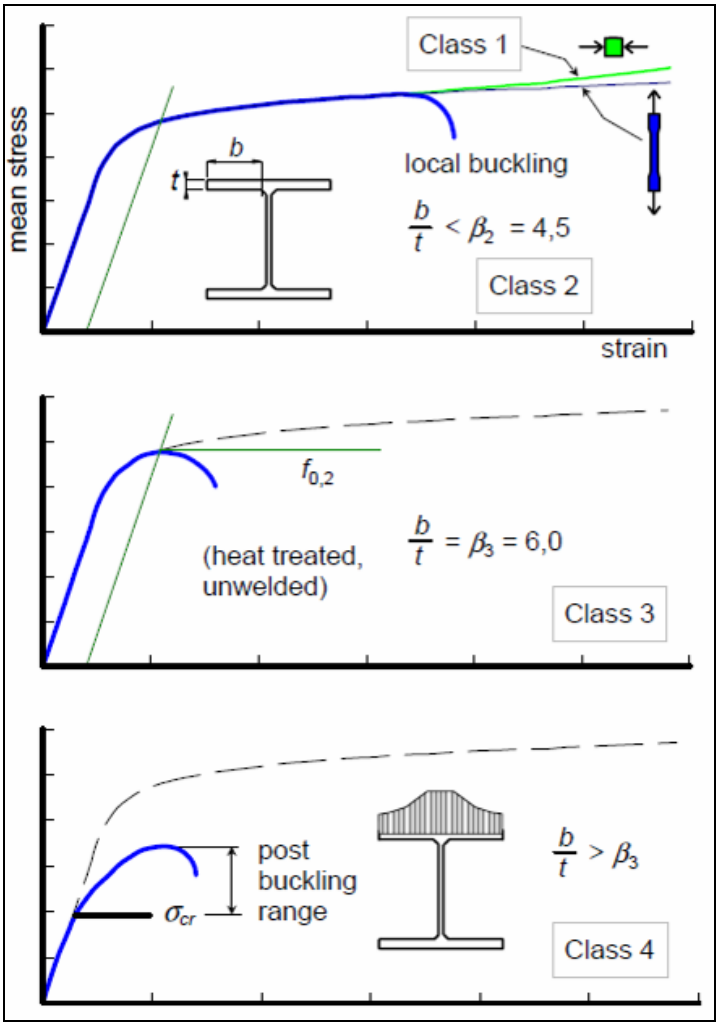

Fig. 4. 17. Stress-strain curves for compression flange in different cross section class

Table 4. 11. Slenderness parameters

	Heat treated, unwelded			Heat treated, welded or non heat treated, un-welded			Non heat treated, welded		
Elements	β_1/ε	β_2/ε	β_3/ε	β_1/ε	β_2/ε	β_3/ε	β_1/ε	β_2/ε	β_3/ε
Outstand	3	4,5	6	2,5	4	5	2	3	4
Internal	11	16	22	9	13	18	7	11	15

$\varepsilon = \sqrt{250/f_o}$ where f_o is in N/mm^2

By the welded sections the effective thickness is obtained using a reduced thickness $t_{eff} = \rho_{haz} \cdot t$ for the HAZ material or the reduced thickness $t_{eff} = \rho_c \cdot t$ for class 4 elements, whichever is the smaller (but $t_{eff} \leq t$). An example of effective section is shown in Fig. 4.18. $\rho_{c,1}$ is based on b_1/t_f for the outstand parts of the compression flange and $\rho_{c,2}$ is based on b_2/t_f for the internal part of the compression flange.

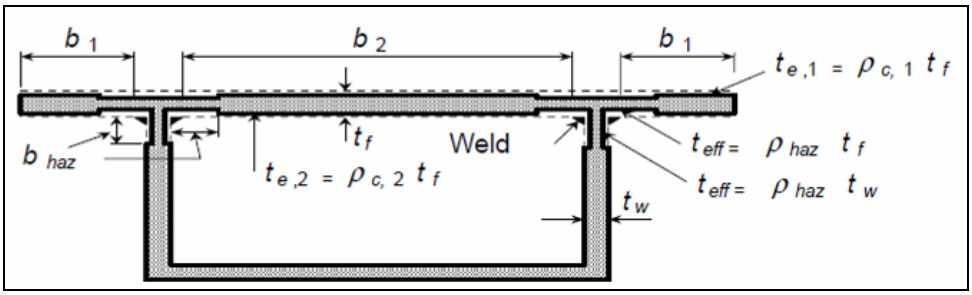

Fig. 4. 18. Effective section of a welded hollow section

In a section with holes the design value of the bending moment resistance M_{Rd} is the lesser of $M_{a,Rd}$ and $M_{c,Rd}$, where $M_{a,Rd}$ is based on the design value of the ultimate strength f_u/γ_{M2} in the net section and $M_{c,Rd}$ is based on the design value of the yield strength f_o/γ_{M1} with no allowance for holes. For both $M_{a,Rd}$ and $M_{c,Rd}$, allowance should be made for HAZ-softening, if:

$$M_{a,Rd} = W_{net} \cdot \frac{f_u}{\gamma_{M2}} \quad \text{- in the net section} \qquad (4.\ 32)$$

$$M_{0,Rd} = \alpha \cdot W_{el} \cdot \frac{f_0}{\gamma_{M1}} \quad \text{- at each cross-section} \qquad (4.\ 33)$$

where W_{net} is the elastic modulus of the net section allowing for holes and HAZ softening, if welded.

The elastic critical moment for lateral-torsional buckling of a beam of uniform symmetrical cross-section with equal flanges, under standard conditions of restraint at each end, loaded through its shear centre and subject to uniform moment is given by:

$$M_{cr} = \frac{\pi^2 E I_z}{L^2} \cdot \sqrt{\frac{I_w}{I_z} + \frac{L^2 G I_t}{\pi^2 E I_z}} \qquad (4.\ 34)$$

where: G - shear modulus
I_t – the torsion constant (see Annex J-EC9)
I_w – the warping constant (see Annex J-EC9)
I_z – the second moment of area about the minor axis
L – the length of the beam between points, which have lateral restraint.

The standard conditions of restraint at each end are:
- restrained against lateral movement
- restrained against rotation about the longitudinal axis
- free to rotate in plan

The elastic critical moment for lateral-torsional buckling of a beam of doubly symmetrical cross-section or mono-symmetric cross-section, under different conditions of restraint at the ends is found in Annex H of Eurocode 9.

4.3.5. Axial force

The resistance of a bar *in tension* is defined as the load where the mean stress is equal to the yield stress f_o/γ_{M1}. Failure in the structure will usually occur at a higher stress but then the deformation is so large that the structure no longer is of use. In certain cases of local weakening, such as bolt holes, small cut outs and welds, local yielding will occur without large deformations. Soon the stresses will reach the strain hardening range, and the resistance is governed by the ultimate stress f_a/γ_{M2}.

The term *local* as used above means a hole or a cut-out where the length parallel to the direction of the load is at the most 25% of the width of that part of the cross section.

In the case of a member subjected to tensile force only, the resistance is given by smallest of the following two expressions (see **Fig. 4. 19**):

$$N_{0,Rd} = A_g \cdot \frac{f_0}{\gamma_{M1}} \qquad (4.\ 35)$$

$$N_{a,Rd} = A_{net} \cdot \frac{f_a}{\gamma_{M2}} \qquad (4.\ 36)$$

A_{gr} = area of the gross cross section
A_{net} = net section area with deduction for holes and HAZ softening when required
f_o = characteristic value strength
f_a = characteristic ultimate strength
γ_{M1} = 1,1 = partial safety factor for yielding
γ_{M2} = 1,25 = partial safety factor for ultimate strength.

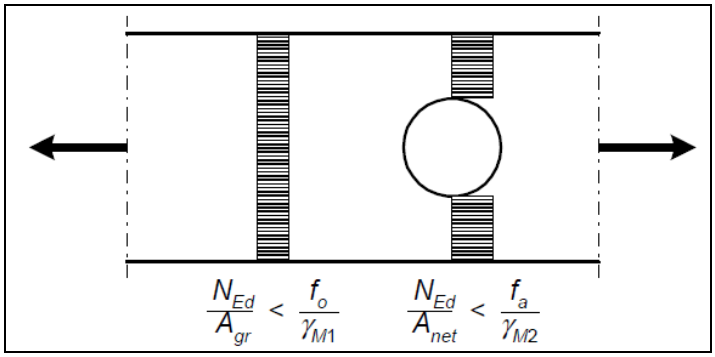

Fig. 4. 19. Stress in gross and net section

Expression 4.36 is valid for a local weakened section defined in 4.35. If the weakening is not to be considered as local, then A_{gr} is to be substituted with A_{net} in expression 4.35.

For the compressive force, Buckling will occur only for a centrally loaded, perfectly straight column. The strength of practical columns, however, depends upon whether there are imperfections such as initial out-of-straightness, eccentricity of load, transverse load, end fixity, local buckling, nonlinear σ−ε -curve, residual stresses or heat affected zones, HAZ. Most tests on columns did not isolate these various effects, and so a scatter band for column curves resulted because the maximum or ultimate load was observed, not the buckling load. The usual procedure for defining a column curve was much the same eighty years ago as now; the column curve was taken as the line of best fit through the test points, although modern calculation methods can explain, in many cases, the detailed behaviour if the imperfections are known.

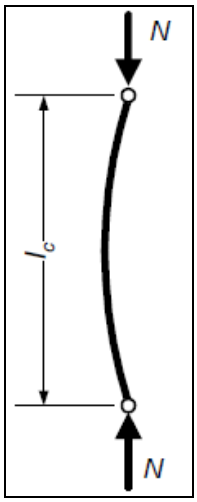

Fig. 4. 20. Compressive force on a column

To take into account the transition in the column curve from the Euler curve to the yield line, more or less complicated correction factors were involved, using estimated eccentricities, initial deflections or non-linear material curve. It has been shown that, for the hypothetical case of straight, centrally loaded, pin-end columns, the transition curve is due to, first of all, to the presence of residual stresses in the cross section. However, as residual stresses are small in extruded profiles, other imperfections such as non-linear σ–ε –curve and heat affected zones are of importance for aluminium columns.

4.3.6. Shear force

For webs in shear there is a substantial post-buckling strength provided that, after buckling, tension membrane stresses, anchored in surrounding flanges and transverse stiffeners, can develop. In a pure shear state of stress the magnitude of the principal membrane stresses σ1 and −σ2 are the same as long as no buckling has occurred ($\tau < \tau_{cr}$, see Fig. 4. 21). After reaching the buckling load ($V_{cr} = \tau_{cr} \cdot h_w \cdot t_w$) the web will buckle and redistribution of stresses start. Increased load results in increased tensile stress σ_1 but only slight, if any, increase in the compressive stress σ_2 [79].

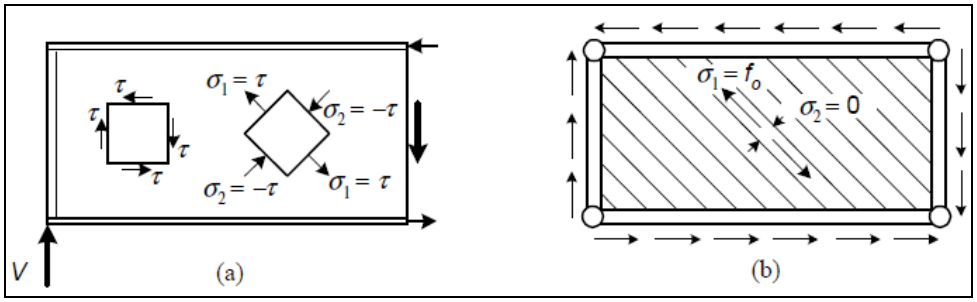

Fig. 4. 21. a) Pure shear state of stress; b) Ideal tension field

For a slender web, the shear force resistance is then given by:

$$V_w = \frac{\sqrt{3}}{2} f_v h_w t_w \qquad (4.\ 37)$$

where:

- $f_v = f_o / \sqrt{3}$ is the yield stress in shear. This is only 13% less than the resistance of a web that does not buckle.
- h_w - web depth inclusive fillets
- t_w – web thickness.

For a web panel with large aspect ratio a/h_w the shear buckling stress is:

$$\tau_{cr} = k_\tau \cdot \frac{\pi^2 \cdot E}{12 \cdot (1 - \upsilon^2)} \cdot \frac{t_w^2}{b_w^2} \qquad (4.\ 38)$$

where:

- $k_\tau = 5{,}34$
- a – stiffeners distance
- b_w – depth of flat part of web

The shear resistance of a web of a girder is the lesser of V_{wd} allowing for local buckling and V_{ad} allowing for failure in a net section where:

$$V_{wd} = \rho_v \cdot h_w \cdot t_w \cdot \frac{f_0}{\gamma_{M1}} \quad (4.\ 39)$$

$$V_{ad} = 0{,}58 \cdot A_{w,net} \cdot \frac{f_a}{\gamma_{M2}} \quad (4.\ 40)$$

where:

- ρ_v - reduction factor
- b_w – depth of flat part of web
- h_w - web depth inclusive fillets
- t_w – web thickness
- $A_{w,net}$ – the net area of a cross section through bolt holes in the web.

Table 4. 12. Reduction factor ρ_v for shear buckling

λ_w	Rigid end post	Non-rigid end post
$\lambda_w \geq 0{,}48/\eta$	η	η
$0{,}48/\eta < \lambda_w < 0{,}949$	$0{,}48/\lambda_w$	$0{,}48/\lambda_w$
$0{,}949 \leq \lambda_w$	$1{,}32/(\lambda_w+1{,}66)$	$0{,}48/\lambda_w$

where: $\eta = 0{,}4 + 0{,}2 \cdot \frac{f_{uw}}{f_{0w}} < 0{,}7$

f_{0w} – the characteristic strength for overall yielding

f_{uw} - the characteristic ultimate strength of the web material

λ_w – slenderness parameter; $\lambda_w = 0{,}35 \cdot \frac{b_w}{t_w} \cdot \sqrt{\frac{f_0}{E}}$.

A more detailed calculation for a structure will be presented in the Chapter six – Case study.

5. EXPERIMENTAL PROCEDURE

To establish parameters set in order to obtain an aluminium friction stir welded footbridge deck it was necessary to perform a series of weld tests on plates realised from the two selected aluminium alloys (6082-T651 and 5083-H111). This procedure has been chosen based on the easy of test specimens cut and also considering the clamping system, welding of 2 extruded profiles may cause some difficulties at this moment. According to the literature reports, there would be no differences between the results of welded plates test specimens and the results of welded extrusions test specimens. In this case, the welded zone will be also a plane zone, with a simple form, where only a butt weld seam is used.

In the first stage, an experimental program on simple elements was realised. Here, by simple elements we understand simple plates, joint by a butt weld seam. The program steps and also details and results are presented in the next subchapters.

5.1. Methodology

Fig. 5. 1 presents a flow chart that describes the steps of the experimental procedure that will be done.

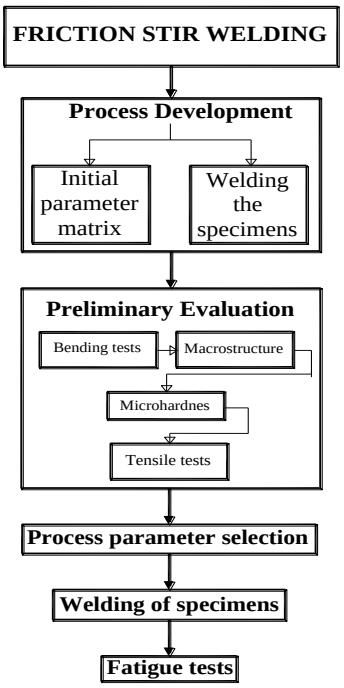

Fig. 5. 1. Experimental procedure flow chart

This flow chart was made in order to make a short abstract of the experimental procedure. The steps of this flow chart are detailed, by presenting the highlighted parts and actions of the program. This chart may be interpreted by considering 5 special parts:

1. the initial FSW process, using the given parameters sets;
2. investigation of the welded samples and cutting the tests specimens;
3. evaluation of the results and chosen of an proper parameters set for the welding of the fatigue samples;
4. welding of the new samples, testing the new samples for the mechanical characterization;
5. fatigue tests for the new samples and results evaluation.

5.2. Base materials (6082-T651 and 5083-H111)

These two materials were chosen for this experimental procedures on the basis of the good properties related in the literature concerning corrosion – the biggest enemy of steel bridges.

5.2.1. Aluminium alloy 6082 – $AlSi_1MgMn$

The 6XXX aluminium series alloys are very frequently used for many fatigue-critical parts of structures, mainly due to the fact of allying a relatively high strength, good corrosion resistance and high toughness to a good formability and weldability.

Names, according to different norms:

- EN-AW-6082 (EU Numerical)
- $AlSi_1MgMn$ (EU Chemical)
- AA6082
- SS-EN-AW-6082 (Sweden)

Aluminium alloy 6082 is a medium strength alloy with excellent corrosion resistance. It has the highest strength of the 6XXX series alloys. Alloy 6082 is known as a structural alloy. As a relatively new alloy, the higher strength of 6082 has seen it replace 6061 in many applications. The addition of a large amount of manganese controls the grain structure which in return results in a stronger alloy.

According to the Eurocode 9 [80] the 6082 alloy belongs to the B stability class. Table 5. 1 presents the chemical composition of the AA 6082.

Table 5. 1. Typical chemical composition for aluminium alloy 6082

Element	Si	Fe	Cu	Mn	Mg	Zn	Ti	Cr	Al
% Present	0.7 - 0.13	0.5	0.1	0.4 – 1.0	0.6 - 1.2	0.2	0.1	0.25	Balance

The most common tempers for 6082 aluminium are:

- **O** – annealed wrought alloy
- **T4** – Solution heat-treated and naturally aged to a substantially stable condition. This designation applies to products which are not cold worked after solution heat-treatment, or in which the effect of cold work in flattening or straightening does not affect mechanical properties.
- **T6** – Solution heat-treated and then artificially aged. This designation applies to products which are not cold worked after solution heat-treatment, or in

- which the effect of cold work in flattening or straightening does not affect mechanical properties.
- **T651** - Solution heat treated, stress relieved by stretching and then artificially aged

Here the **6082-T651** alloy was selected, because of the artificially aged and taking in account the good extrudabilty of the material.

5.2.2. Aluminium alloy 5083 – $AlMg_{4,5}Mn_{0,7}$

Aluminium 5083 is known for exceptional performance in extreme environments. 5083 is highly resistant to attack by both seawater and industrial chemical environments.

Alloy 5083 also retains exceptional strength after welding. It has the highest strength of the non-heat treatable alloys but is not recommended for use in temperatures in excess of 65°C. According to the Eurocode 9 the 5083 alloy belongs to the A stability class. The recommendations that are given in Eurocode 1999-1-3 do not apply for this alloy in all tempers from the temperature of 65°C, unless an efficient corrosion preventing coating is provided [80]. The chemical composition of this alloy is presented in Table 5. 2.

Table 5. 2 Typical chemical composition for aluminium alloy 5083

Element	Si	Fe	Cu	Mn	Mg	Zn	Ti	Cr	Al
% Present	0.4	0.4	0.1	0.4 – 1.0	4.0 - 4.9	0.25	0.15	0.05 - 0.25	Balance

The most common tempers for 5083 aluminium are:

- **0** – Annealed wrought alloy
- **H111** – Some work hardening imparted by shaping processes but less than required for a H11 temper.
- **H32** – Work hardened and stabilised with a quarter hard temper

Here **5083-H111** was selected based on the previous experimental works that reported a very good weldability of this temper.

5.3. FSW process

5.3. 1. Machines

The process was realised in two steps (first set of welds needed for pre-tests and the second set of welds needed for the fatigue tests), using two welding machines or comparison.

1. The welds for the pre-tests were realised with the **TRICEPT 805 robot**, specially equipped to perform FSW, presented in Fig. 5. 2

Fig. 5. 2. TRICEPT 805 Robot

Combined with superior stiffness the Tricept® 805 can apply forces up to 45.000N (vertical axis) and 10.000N in the horizontal axis (welding direction). Due to its accuracy, high velocity, strength and rigidity this system is predominantly employed in the field of high-speed machining. The Tricept® 805 and its derivatives have opened new horizons for robotic FSW. The force and stiffness available allow positional welding of high strength Aluminium alloys in the thickness range between 0,5 mm and 10 mm.

The FSW unit assembled to the robot end-effectors is based on a 45kW hydraulic spindle. Welds can be produced under force or positional control associated to an on-line control of the rotational speed. State-of-the-art sensing and control systems are employed to produce on-line records of force, welding speed, rotational speed and torque.

2. The welds for the fatigue tests were realised with the Guttering machine presented in Fig. 5. 3.

Fig. 5. 3. Guttering machine

5.3. 2. Tools

a) The welds from A to G were realised with a tool configured from a flat shoulder with machined spiral flute, 15 mm diameter and a conical pin, 5 mm diameter, thread M8L at the socket (Fig. 5. 4). The pin was broken and for the next welds a new pin was used.

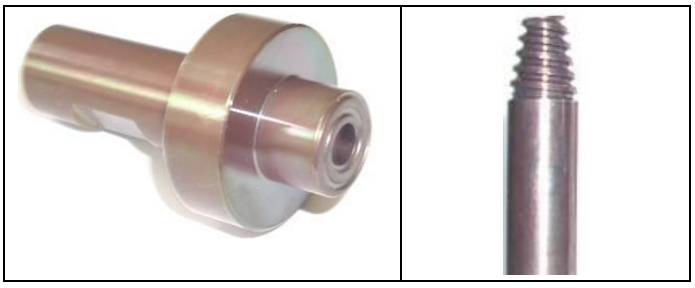

Fig. 5. 4 Tool for welds A to G

b) The welds from H to W were realised with a tool configured from a flat shoulder with machined spiral flute, 15 mm diameter; threaded pin with thread M6L, conical tapered with three milled flats, 5 mm diameter (Fig. 5. 5).

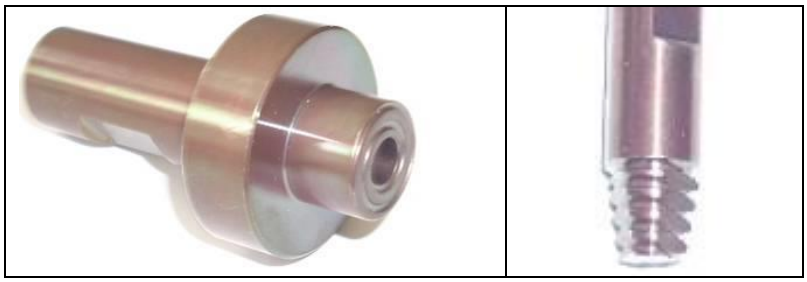

Fig. 5. 5 Tool for welds from H to W

5.4. Initial parameters matrix

There were welded a number of 22 samples, 12 for the 5083-H111 alloy and 10 for the 6082-T651 alloy. During the weld process were measured the forces in all 3 directions and also was measured the temperature during the welding process, in the plates and in backing bar.
The initial welding parameters are presented in Table 5. 3 and Table 5. 4.

Table 5. 3 The parameters for 5083-H111 alloy

5083-H111			
Probe Name	**ω [RPM]**	**v [mm/min]**	**F [kN]**
A	1200	300	13
B	1200	300	13
C	600	200	13
D	600	400	13
E	800	267	13
F	800	400	13
G*	1200	400	13
H	1200	300	13
I	800	400	13
J	800	600	13
K	600	150	13
W	1200	180	10

*Pin was broken.

Table 5. 4 The parameters for 6082-T651 alloy

6082-T651			
Probe Name	**ω [RPM]**	**v [mm/min]**	**F [kN]**
L	1200	180	10
M	1200	300	13
N	1200	400	13
O	1200	600	13
P	1200	600	13
R	1200	800	13
S	800	400	13
T	800	600	13
U	600	400	13
V	600	200	13

All the samples were welded on a vacuum table which assure stability of the clamping system.

In the following will be presented only the characteristics of that samples that had good results to the bending tests – the first test that were realised. These samples are presented in Table 5. 5.

Table 5. 5. Investigated elements

Material	**Sample**	**Parameters**		
		ω [RPM]	**v [mm/min]**	**F [kN]**
5083-H111	C	600	200	13
	E	800	267	13
	K	600	150	13
6082-T6	L	1200	180	10
	M	1200	300	13

5.5. Temperature measurements

During the welding process were measured temperatures in the plates but also in the backing bar. These measurements were realised with a thermocouples system. Fig. 5. 6 a) and b) and illustrate thermocouples position in plates and backing bar; the thermocouples from the plates are set out symmetrically to the weld middle line (8, 9, 10 are on the advancing side and 11, 12, 13 are on the retracting side).

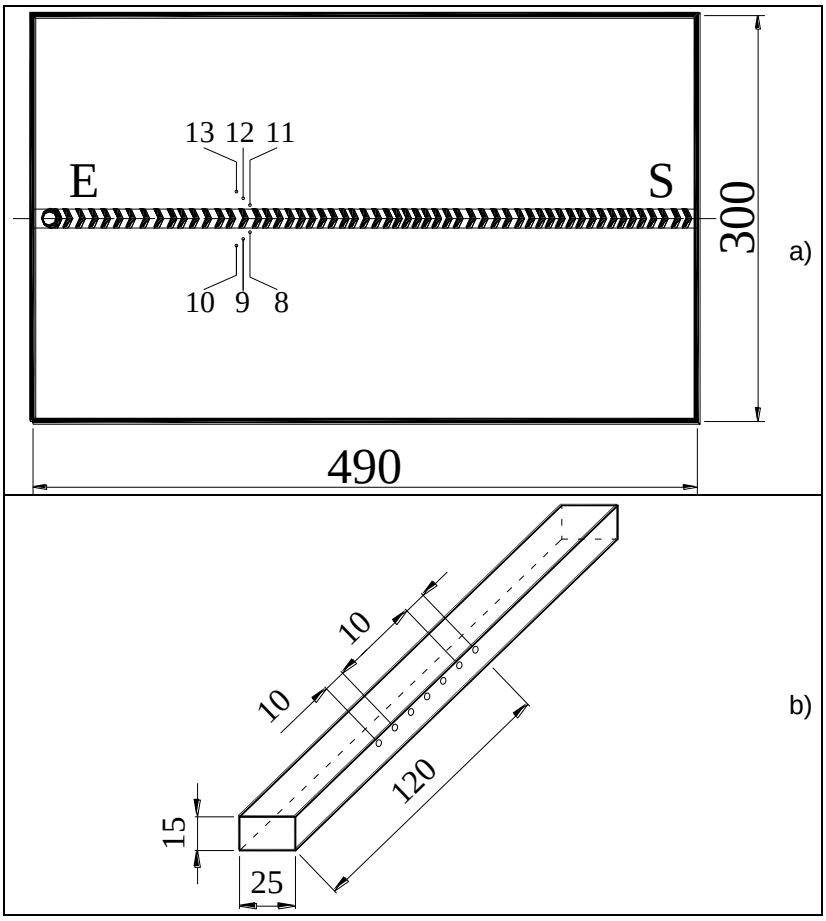

Fig. 5. 6. Thermocouples positions. a) In plates; b) In backing bar

The maximum temperature values achieved in plates, respectively in backing bar, are plotted in the next pictures (Fig. 5. 7, Fig. 5. 8).

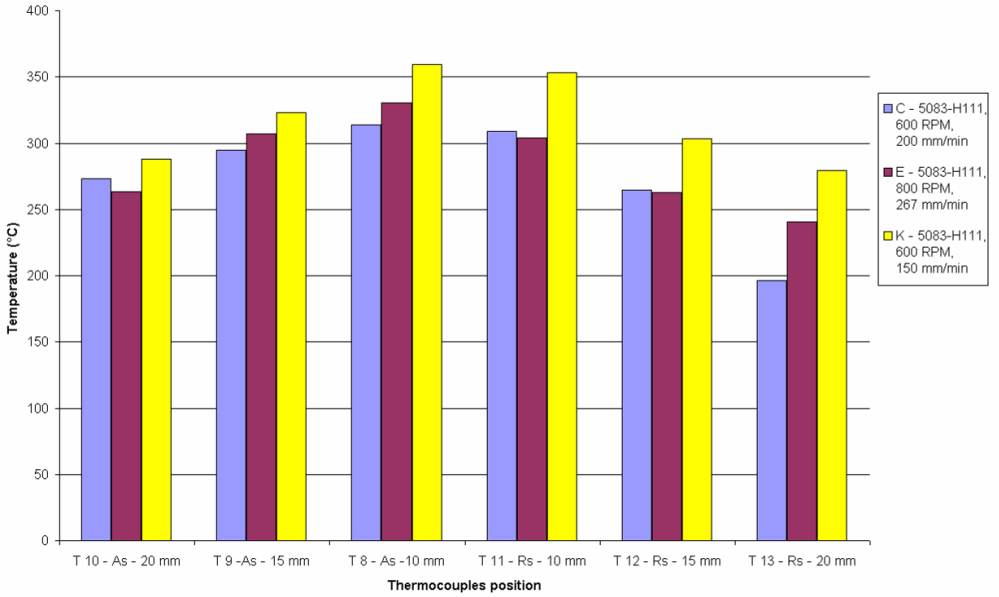

Fig. 5. 7. Temperature measurements for FS welded 5083-H111 alloy

It can be concluded that the temperatures depend on the rate between rotational speed and welding speed. It is necessary to use a proper welding speed that gives the necessary time to bring the material to that condition that allows for the welding tool to move the material from one side to another of the welding line. For samples C and K was used the same rotational speed – 600 RPM – and different welding speeds, so that for sample C the rate rotational speed/welding speed is 3 and for sample K is 4. For sample E was kept the rate to 3, as for sample C and the temperatures measured in sample C and E are roughly the same (Fig. 5. 7).

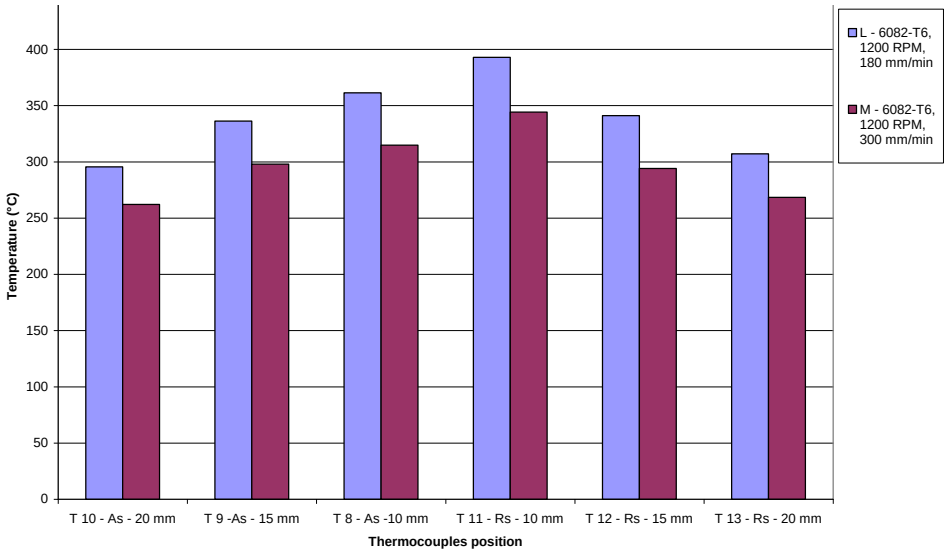

Fig. 5. 8. Temperature measurements for FS welded 6082-T651 alloy

These two samples were welded with the same rotational speed but a different welding speed. Also in this case the increase of welding speed leaded to lower temperatures measured in the plates (Fig. 5. 8).

5.6. Force measurements

The robot used for the production of the joints was instrumented with a Kistler three channel load cell in order to record forces along the tool axis – F_z, along the welding direction – F_x and perpendicular on the welding direction – F_y.

For the welding process was used an input force of 13 kN for samples C, E, K and M, respectively 10 kN for L.

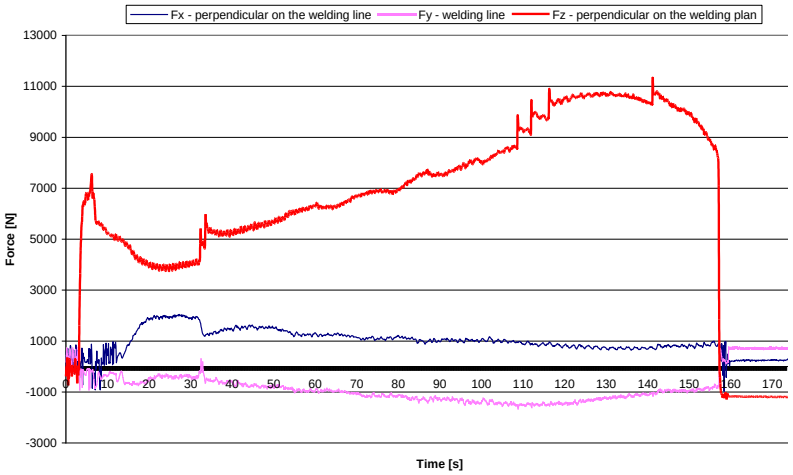

Fig. 5. 9. Forces measured during joining with butt joint the 6 mm thickness plates for C sample (AA 5083-H111, 600 RPM, 200mm/min)

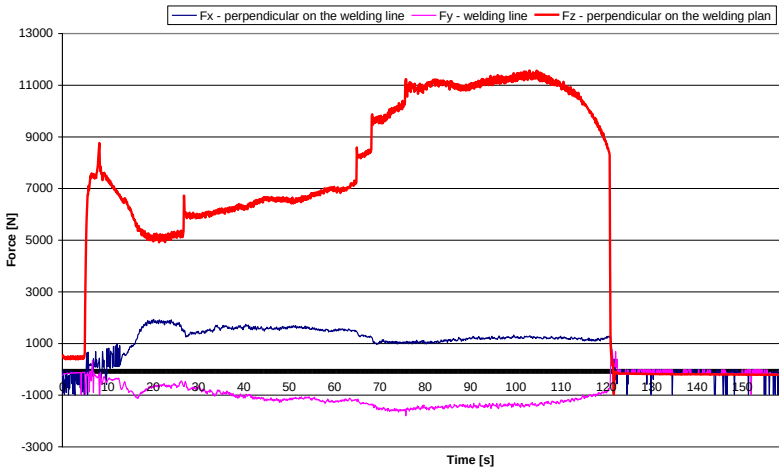

Fig. 5. 10. Forces measured during joining with butt joint the 6 mm thickness plates for E sample (AA 5083-H111, 800 RPM, 267mm/min)

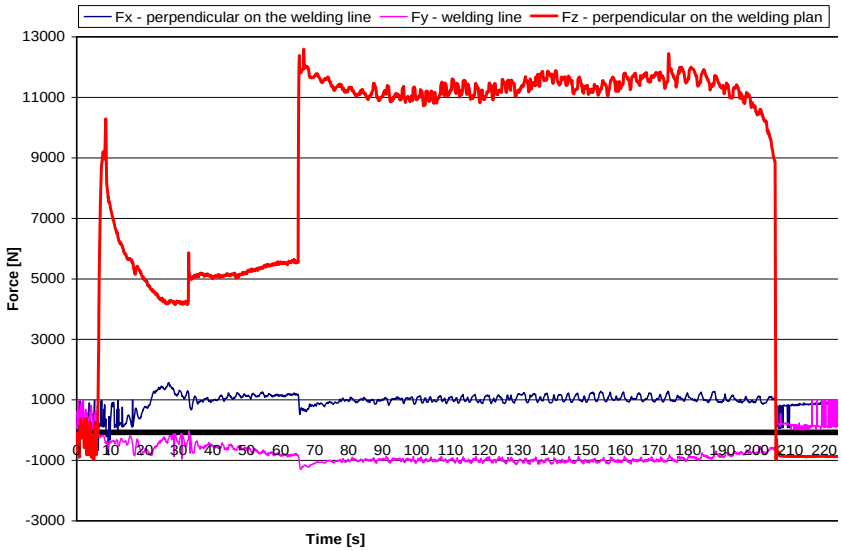

Fig. 5. 11. Forces measured during joining with butt joint the 6 mm thickness plates for K sample (AA 5083-H111, 600 RPM, 100mm/min)

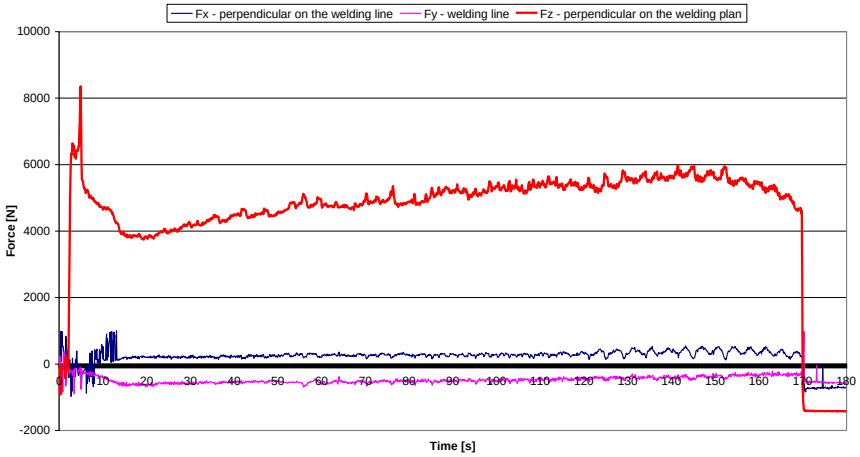

Fig. 5. 12. Forces measured during joining with butt joint the 6 mm thickness plates for L sample (AA 6082-T651, 1200 RPM, 180mm/min)

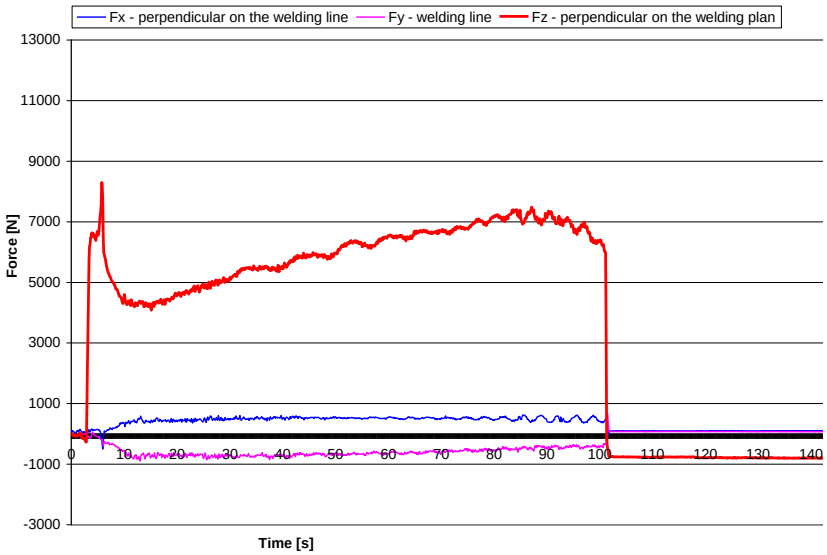

Fig. 5. 13. Forces measured during joining with butt joint the 6 mm thickness plates for M sample (AA 6082-T651, 1200 RPM, 300mm/min)

From the pictures presented above (Fig. 5. 9-Fig. 5. 13) it can be observed that the robot could not reach the input force (initial data) which leaded to instability of the process, especially at begin of weld seam. Also the robot welding head vibration were enough big to influence the weld quality.

5.7. Mechanical Characterization. Bending tests

To determine the quality of welds connections several testing methods have been used to study the mechanical features of the joints, such as bending, hardness and tensile tests. These are presented in detail below.

For bending test have been assayed three samples from all welded plates (one from the begin of the weld – tested on the joint root, one from the middle of the weld – tested on the joint surface, one from the end of the weld – tested on the joint root). From these, two were used to examine the joint root because the welding process was not very stable (the robot could not build the input force, of 13 kN). The bending tests have been realised according to the EN 910:1996 D [81]. The removed specimens have been grinded coplanar and at the edges have been milled. In
Fig. 5. **14** - Fig. 5. 18 the first two samples were used to identify root joint ductility, and the third was used to identify surface joint ductility and also to identify possible macro-defects that may cause sagging of welded elements.

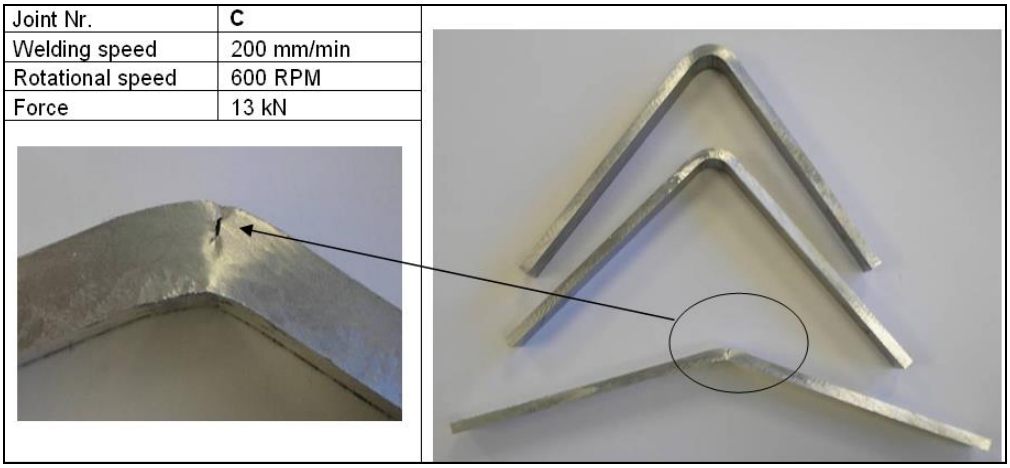

Fig. 5. 14. Bending specimens for 5083-H111 joint root (up) and joint surface (down). Surface rupture

The test specimens for joint root from C (
Fig. 5. **14**) welded plates present no defect – the specimens' bend angle is α ≥ 90°. On the other hand the test specimen for joint surface had failure; the specimens' bend angle is much under 90°. The failure was caused of a defect presence, situated near the weld surface. A better inspection will be provided by macrostructure tests specimens.

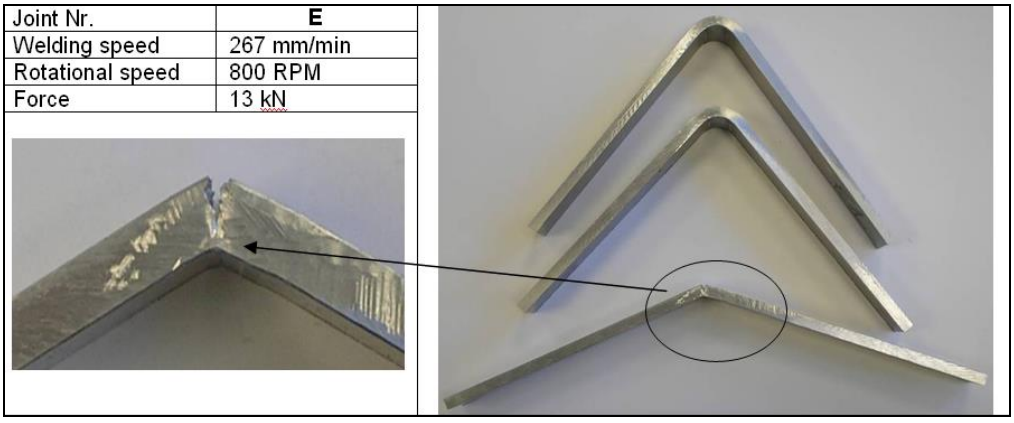

Fig. 5. 15. Bending specimens joint for 5083-H111 root (up) and joint surface (down). Surface rupture

The same situation, as to above presented specimens, can be observed for the test specimens from E sample (Fig. 5. 15). In this case, the surface joint failure was brittle, following through most of specimen thickness.

Joint Nr.	K
Welding speed	150 mm/min
Rotational speed	600 RPM
Force	13 kN

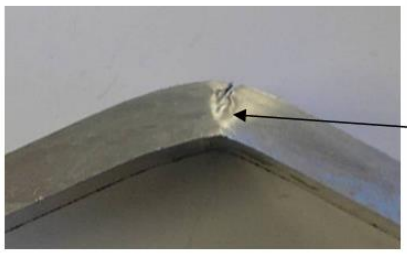

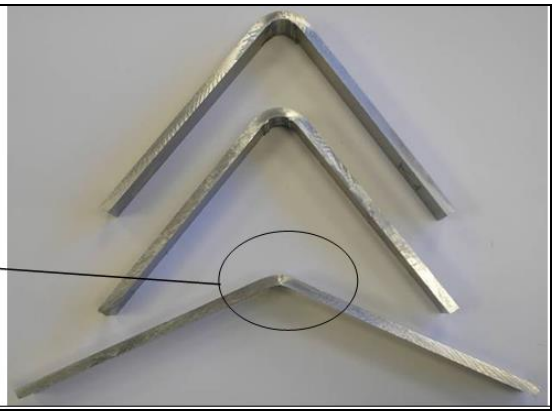

Fig. 5. 16. Bending specimens' joint for 5083-H111 root (up) and joint surface (down). Surface rupture

The root joint test specimens cut off from welded sample K (Fig. 5. 16) presented good behaviour; the joint surface failed, probably in the presence of a defect situated near joint surface.

Joint Nr.	L
Welding speed	180 mm/min
Rotational speed	1200 RPM
Force	10 kN

Obs: Both root and surface of the joint present very good behaviour to bending test

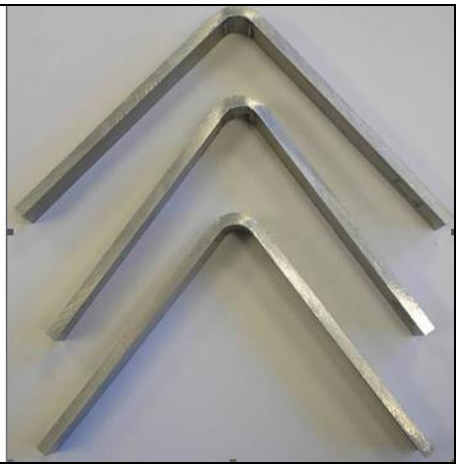

Fig. 5. 17. Bending specimens for 6082-T651 joint root (up) and joint surface (down)

Joint Nr.	M
Welding speed	300 mm/min
Rotational speed	1200 RPM
Force	13 kN

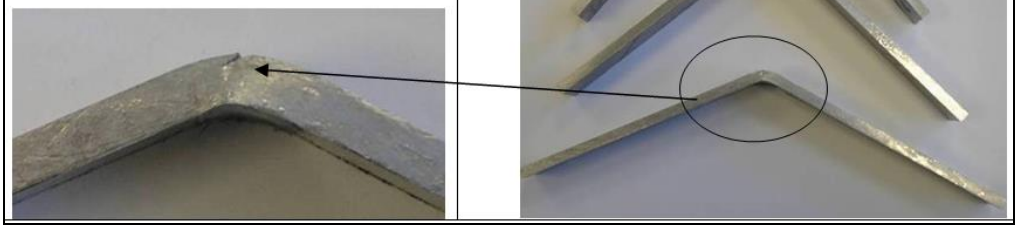

Fig. 5. 18. Bending specimens for 6082-T651 joint root (up) and joint surface (down). Surface rupture

Joint root of weld sample M (Fig. 5. 18) presented no defect (no failure during bending test); joint surface, on the other hand, had reached failure on a bend angle < 90°, probably caused by a defect or some impurities on the plates surface.

Obs: There were realised bending tests for all other welding parameter sets, but no other set provided specimens with good joint root (most of specimens presented the „tunnel defect").

5.8. Macrostructures

After being friction stir welded, from each welded sample have been cut 3 specimens in order to perform macrostructure analysis which can provide informations concerning the weld seam quality. These specimens have been cut from different places along the weld seam perpendicular on the welding direction.

Positions from where have been cut the specimens:

- weld start - named **MACRO 1** – here must be mentioned that „weld start" was considered the point where no surface defects were visible; most of welded samples present to weld real start some major defects, like plates separation;
- near thermocouples position – named **MACRO 2** – to see if the holes for thermocouples have some influence on the weld quality;
- weld end - named **MACRO 3** – very close of end hole of weld seam.

These specimens have been embedded in an epoxy resin (DEMOTEC 30), subjected to mechanical grinding and then polish according to ASTM E3 [82]. After that, the specimens were etched; qualitative analyses have been performed photographing the specimens in the vicinity of weld seams.

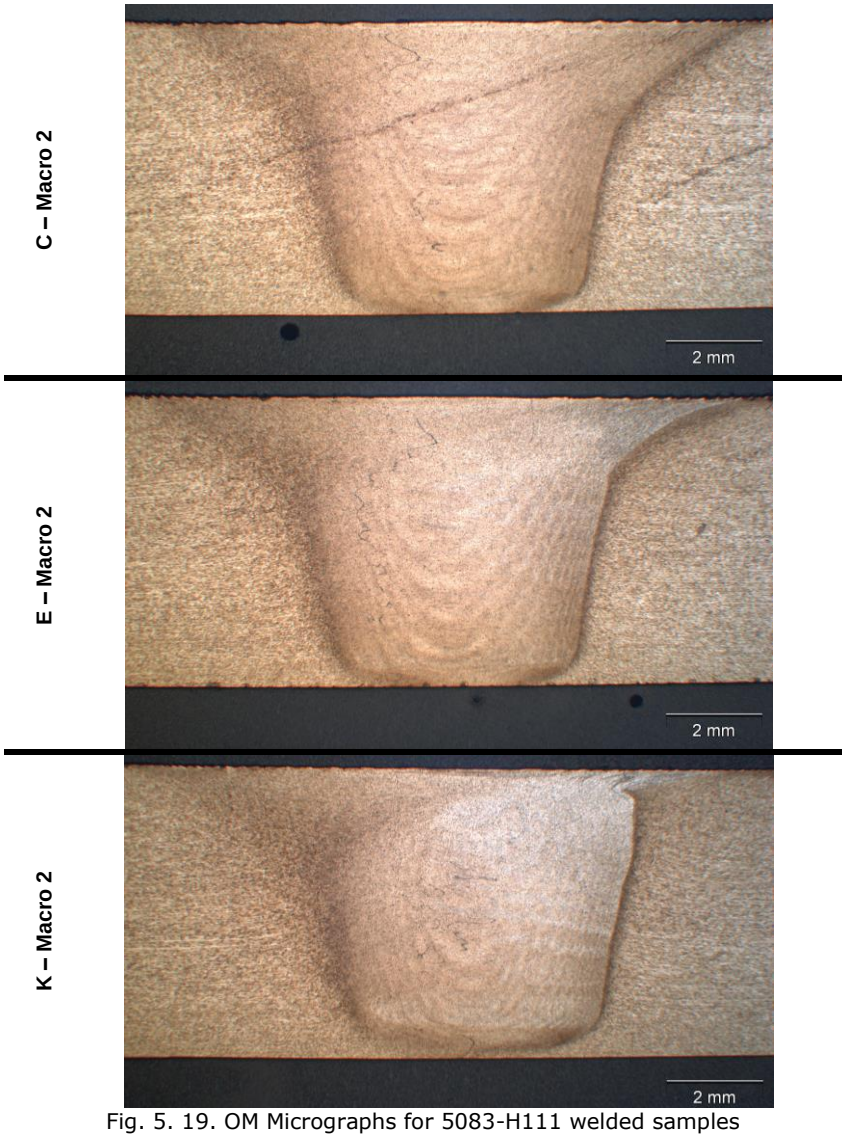

Fig. 5. 19. OM Micrographs for 5083-H111 welded samples

Fig. 5. 19 presents the macrostructure analyse of weld seams of AA 5083-H111 alloy. In these specimens assayed from the very close vicinity of end hole of weld seam, are visible volumetric defects, situated close to the weld surfaces, on the retracting side. These defects may be related with the presence of some impurities on plates surface or may be caused by some process factors. Probably a microstructure analyse will be able to offer an accurate explanation regarding the defects generators.

These defects have not been observed to the other macro specimens assayed from the same sample.

Fig. 5. 20 presents the test specimens for macrostructure analyse of weld seams of AA 6082-T651 alloy. To this alloy, none of the macro specimens presented

any defect/imperfection. Here it can be observed a brighter processed zone in the weld cross-section, as a result of a higher rotational speed (1200 RPM) that helped to reach an enough high temperature for a good material flow and movement during the process.

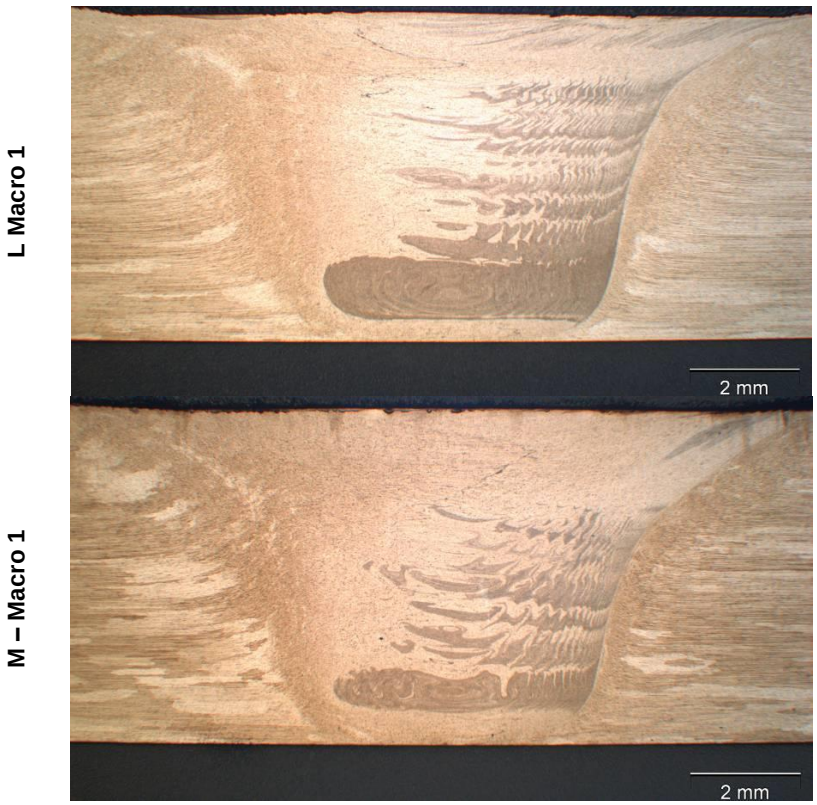

Fig. 5. 20. OM Macrographs for 6082-T651 welded samples

5.9. Hardness measurements

For these tests have been used the same specimens as for the macro structure analyses of the welds seams. For the hardness measuring a Zwick machine was used. There have been realised measurements on three different levels, first at 1 mm from the upper side of the specimen, second line at 3 mm from the surface and the last at 5 mm from the surface. Fig. 5. 21 indicates the positions of these virtual lines.

Fig. 5. 21. Specimens for hardness measurements

5.10. Tensile Test

There have been realised tensile test for both base material - to establish the base material resistance, and welded plates. The base material tensile tests were necessary to identify if there are any differences between resistances of base material when the axial load is applied in the rolling direction and when the axial load is applied perpendicular on the rolling direction. From the welded plates, the tensile specimens have been cut perpendicular on the rolling direction – in this case the axial load during the tensile test is applied in the rolling direction. The specimens have been machined according to the ASTM E8 [83]. In the welded specimens the weld nugget was placed in the middle of the coupon. The general dimensions of the specimens are shown in Fig. 5.22. For brevity purpose, here is illustrated only the welded specimen while the base material specimen has the same dimensions.

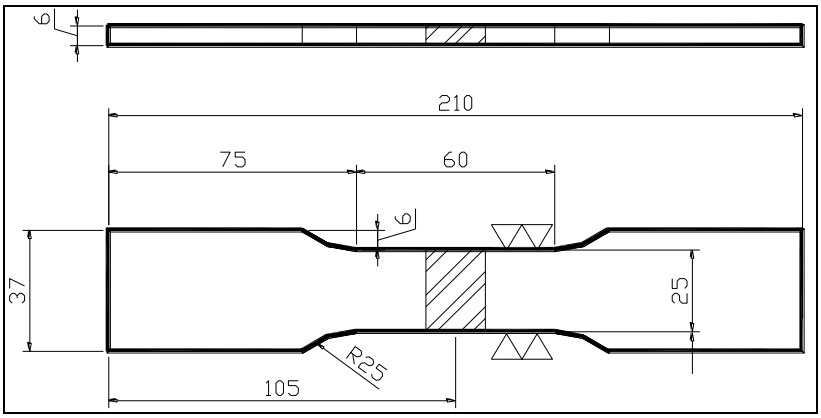

Fig. 5. 22. Dimensions of the FSW tensile test specimens

Table 5. 6 and Table 5. 7 present the resistances of base material, identified on direction of rolling specimens and the results of present tensile tests on specimens cut of perpendicular on direction of rolling.

Table 5. 6. Base material resistance – AA 5083-H111 alloy

	R_m [MPa]	**$R_{p0.2}$ [MPa]**	**A [%]**
Base Material II to rolling direction	326	190,2	47,21
Base Material $\perp$ to rolling direction	328,1	166,9	46,63

Average of minimum 3 Specimens

As it can be seen in this table, the 5083-H111 base material yield strength $R_{p0,2}$ is influenced by the rolling direction; the value of $R_{p0,2}^{\perp}$ represents only 88%

from the value $R_{p0,2}^{II}$. Regarding the 5083-H111 base material ultimate strength it can be observed that the rolling direction does not influence negative the R_m value.

Table 5. 7. Base material resistance – AA 6082-T6 alloy

	R_m [MPa]	**$R_{p0.2}$ [MPa]**	**A [%]**
Base Material II to rolling direction	317	255	38,12
Base Material $\perp$ to rolling direction	316,2	237,2	37,54

Average of minimum 3 Specimens

For 6082-T661 base material $R_{p0,2}^{\perp}$ represents 93% from $R_{p0,2}^{II}$. Also for this alloy the rolling direction does not has a significant influence on R_m value.

There have been assayed and tested 4 specimens from each welded sample for tensile tests. In case of 5083-H111 alloy the results of tensile tests were very good; all C specimens brooked in base material, by the E specimens 2 specimens brooked in base material and 2 specimens brooked in the middle of weld seam; the K specimens presented also a relative good behaviour. Table 5. 8 present the performances of the 5083-H111 welded samples. It is clearly that these values are much improved than the values for usual welding (here, as usual welding, MIG welding)

Table 5. 8. Welded samples performances – 5083-H111

	BM $\perp$ to rolling direction	Sample C	Perfor. C	Sample E	Perfor. E	Sample K	Perfor. K
R_m [MPa]	328,1	301,93	92%	240,91	83%	300,76	92%
$R_{p0.2}$ [MPa]	166,9	135,08	81%	139,1	73%	131,30	79%
A [%]	43,63	44,88	-	25,28	-	42,83	-

Fig. 5. 23 illustrated the comparison with the base material resistances. Also it may be observed the elongation capacity of the welded elements, which is quite nearly from the base material elongation capacity.

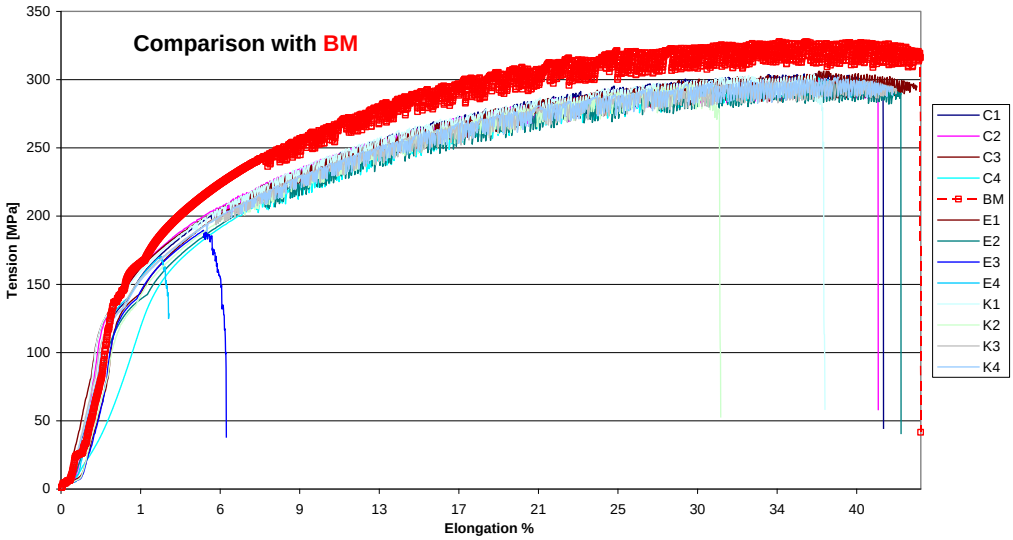

Fig. 5. 23. Comparison weld-BM for 5083-H111 alloy

Regarding the tensile test results for specimens assayed from 6082-T651 welded samples, it may be mentioned that in all specimens the rupture produced close to the weld seam, in the advancing side.

Table 5. 9. Performance of the welded samples – 6082-T651

	Base Material ⊥ to rolling direction	Sample L	Performance L	Sample M	Performance M
R_m [MPa]	316,2	213,85	73%	226,07	72%
$R_{p0.2}$ [MPa]	237,2	128,45	54%	140,75	59%
A [%]	37,54	10,84	-	10,56	-

Average of 4 Specimens

Table 5. 9 presents the performances of the 6082-T651 FS welded plates. Also here the values are much better than for the usual welding procedure for aluminium alloys.

For a better explanation Fig. 5. 24 present the tensile variation of the 6082-T651 FS welded samples. In this case, the resistance did not achieve the similar values as the base material. The most affected was the elastic capacity. This phenomenon can be observed by the hardness drop, in the heat affected zone.

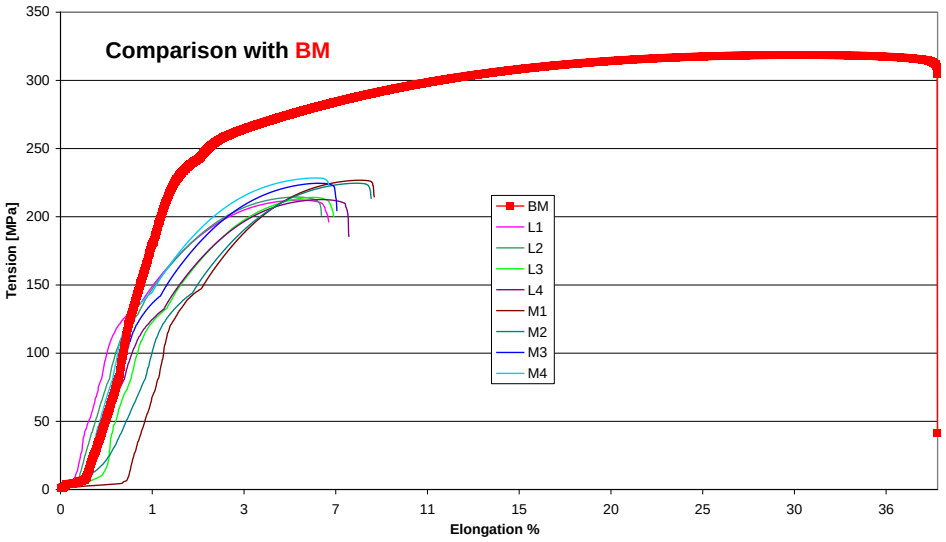

Fig. 5. 24. Comparison weld-BM for 6082-T651 alloy

5.11. Results and discussions of the preliminary welds

The formation of friction stir welded zone is affected by the material flow behaviour under the action of the rotating tool. On the other hand, the material flow behaviour is direct influenced by the material properties such as yield strength, ductility, hardness of the base material, tool design and FSW parameters.

Usually, the friction stir welded joints are defect free joints since no melting takes place during the welding process and the metals are joined in the solid state due to the heat generated by the friction between the tool shoulder and components surfaces and flow of metal by the stirring process. The generated heat has to be high enough to ensure a proper material flow in order to produce defect free joints. Therefore the process parameters have to be in such manner combined to produce the proper heat amount for a good joint. Until now in literature are reported only the optimum combinations between travel speed and rotating speed that may assure a defect free weld seam. These two parameters are also used as welding „pitch" (defined as ratio between travel speed and rotating speed). From many data available in literature, the optimum welding pitch value is around 0,1 [84]. However these reports did not mentioned the downward force, also an important input parameter of this process.

It is well know that under a higher downward force (named as vertical force or as axial force, corresponding to the tool axe) a higher friction force between tool shoulder and components surfaces takes place. A higher friction force will provide an increased heat amount. Tool advancing action (inclined at a certain angle) is extremely similar to an extrusion process which requires optimal temperature conditions for the better quality of the material, in terms of microstructure [6]. To reach the necessary temperature (heat amount) to ensure adequate plasticization of the alloy during the welding process, fine, stable microstructure of the processed

zone, without any defects that may cause the failure of the weld seam, two different combinations may be used:

1. high rotational speed and low travel speed, taking in account 0,1 value for welding pitch (no mention about the downward force);
2. a higher value for the welding pitch and a downward force high enough to produce the necessary temperature for a good weld seam (thru the increased friction force between tool shoulder and the surfaces).

In this experimental program, the preliminary welds have been realised taken in account the 2. Point above presented. As a start point was used a previous work realised to GKSS-Forschungszentrum, Germany. The welding parameters used in this work were combined with a higher downward force, and also new sets of parameters were adopted (especially the travel speed was increased, to increase the productivity of the process, by using the TRICEPT 800 robot).

From the first visual inspection could be observed defects situated, to most of samples, at the weld seam start. These defects have been, firstly, interpreted as a lack of clamping system (which permitted plates separations under tool action). But when was made the evaluation of forces during the welding process it could be seen that the robot couldn't built the input forces. This phenomenon may be explained thru a robot pressure loss or as instability during welding process, caused by the instability of the Kistler table for force measurements combined with the high downward force. In spite of these defects, the length of good weld seam (based on the visual inspection) was enough to cut bending specimens, macrostructure specimens and specimens for tensile test. In order to save time, the first tests realised were the bending tests. Specimens from all welded samples were investigated to bending tests, but only 5 samples proved good welding root. For good results to bending test in the rot area is essential a correct adjustment of the pin within a tolerance field. A too short pin length and therefore a too large distance of the pin toe to the backing plates leads to bonding defects in the root area. Under tensile and bending loads the root opens and in the worst case initiates the failure of the joint. This may be the explanation for the failure in the root area of some specimens' assayed form welded samples, welded with the same parameters as another sample with good root bending test results (sample A and B were welded with the same parameters as sample C, but no good bending tests results).

The next test have been carried out only on the specimens machined from the samples with good bending test results (here, the welded plate is represented as sample). These samples were:

- for 5083-H111 alloy: C, E and K;
- for 6082-T651 alloy: L and M.

The macrographs of the specimens cut off from the weld seam end indicate the presence of some internal defects, which may be the explanation for the surfaces collapse to a reduced angle during the bending tests. The specific zones for FSW are visible and also the different granulations in these zones. These defects do not appear in the other zones of the weld seams.

The hardness measurements for both materials show a usual variation of the diagram. It can be seen that for the 5083-H111 (Fig. 5. 25) the variations are not significant; also there is not a drop down of hardness values in the HAZ or in the nugget zone.

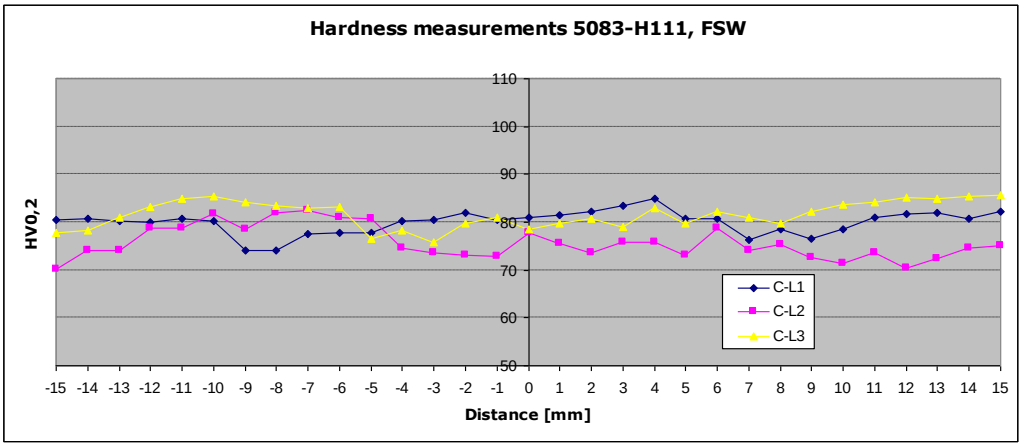

Fig. 5. 25. Hardness measurements for 5083-H111, welded with FSW

It can be observed the almost stability of the hardness of this alloy, welded with FSW. This may be translated that the 5083-H111 does not get softer under FSW.

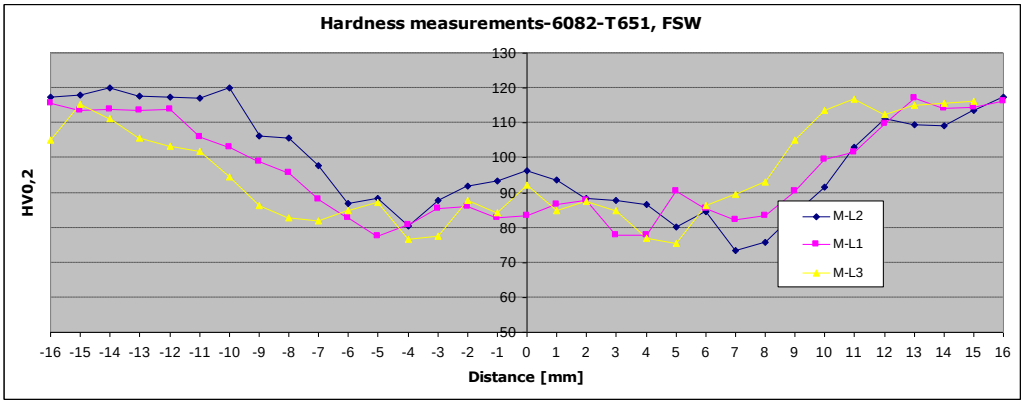

Fig. 5. 26. Hardness measurements for 6082-T651, welded with FSW

Fig. 5. 26 presents the hardness measurements to the FS welded 6082-T651 alloy. It may be observed the material softening in the region of the HAZ – Nugget zones. This softening causes the collapse in the HAZ zone.

5.12. Parameters for the fatigue welded samples

Based on the previous results, combined with previous experiences performed to GKSS, a serious of parameters has been used, in order to realise the final weldings for the fatigue tests.

Table 5. 10. Final welding parameters

5083-H111	**Ω [RPM]**	800
	v [mm/min]	400
	F_z [kN]	10
6082-T651	**Ω [RPM]**	800
	v [mm/min]	350
	F_z [kN]	10

Table 5. 10 presents the parameters used to produce the welded plates for the fatigue tests. The process has been executed with the guttering machine, using a shoulder withmachined spiral flute, 15 mm diameter; threaded pin with thread M6L, conical tapered with three milled flats, 5 mm diameter (Fig. 5. 5)

From the new welded plates there have been cut off samples for:

- bending tests;
- macro-analysis;
- hardness measurements;
- tensile tests;
- fatigue tests.

For the AA 6082-T651 the results of these tests were good, with a performance of $R_{p0,2}$ of 50 % from the base material and R_m of 78 %. The results may be seen in the next pictures (Fig. 5. 27-Fig. 5. 29).

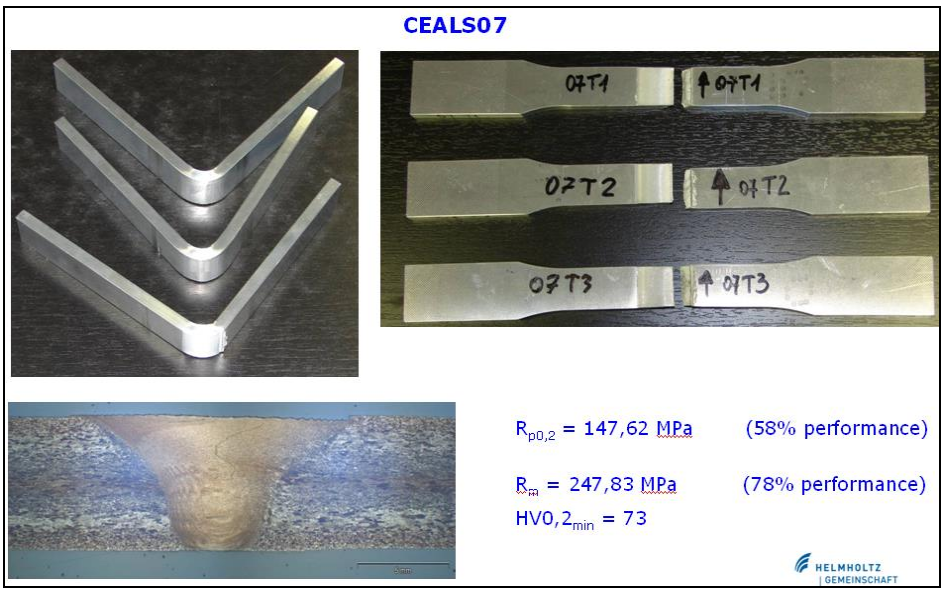

Fig. 5. 27. Tests results CEALS07

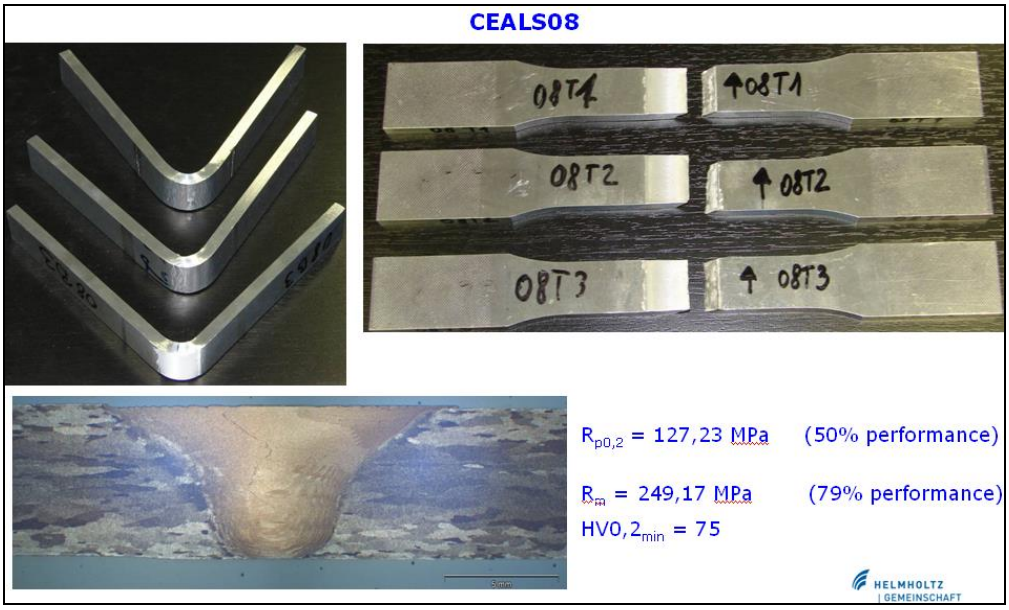

Fig. 5. 28. Tests results CEALS08

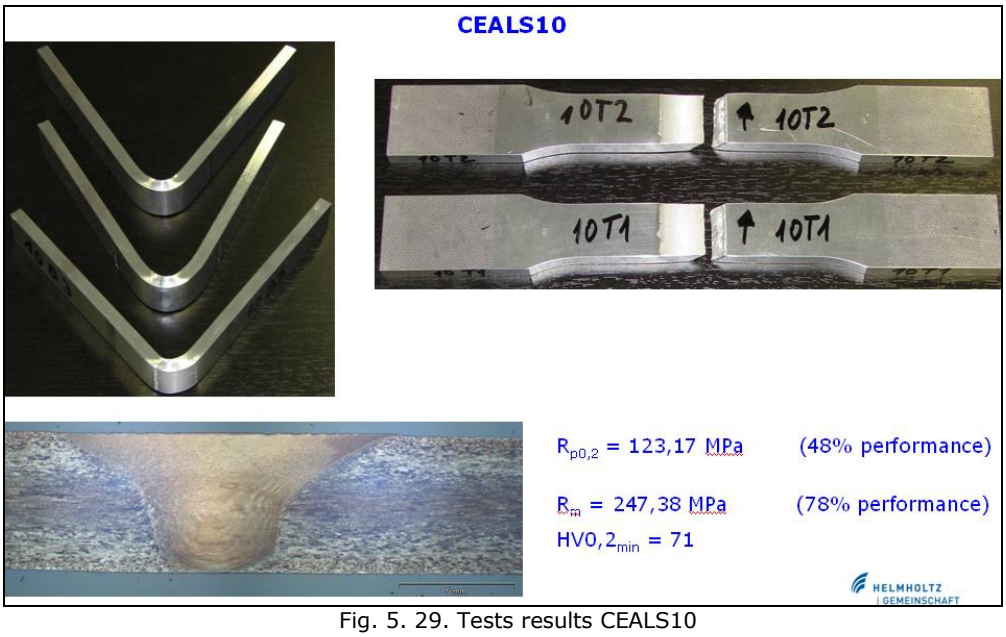

Fig. 5. 29. Tests results CEALS10

In the case of AA 5083-H111 the results of these tests were very good, with a performance of $R_{p0,2}$ of 97 % from the base material and R_m of 90 %.

In the diagram for hardness measurements (Fig. 5. 30) of CEALS07, CEALS08 and CEALS10, there is a drop of hardness in the welded region, with the

lowest values in the limit between the HAZ and BM. This drop of hardness draw in a drop of resistance in this area. This may be the explanation of the most samples breackege to the limit between HAZ and BM zone. Also in this area is situated the end of the shoulder contact zone with the elements, and it may be considered as a defects concentration area. It was found that hardness drastically decreases in the thermomechanically affected zone and the yield stress and rupture stress of friction stir welded specimens presented lower values than un-welded specimens.

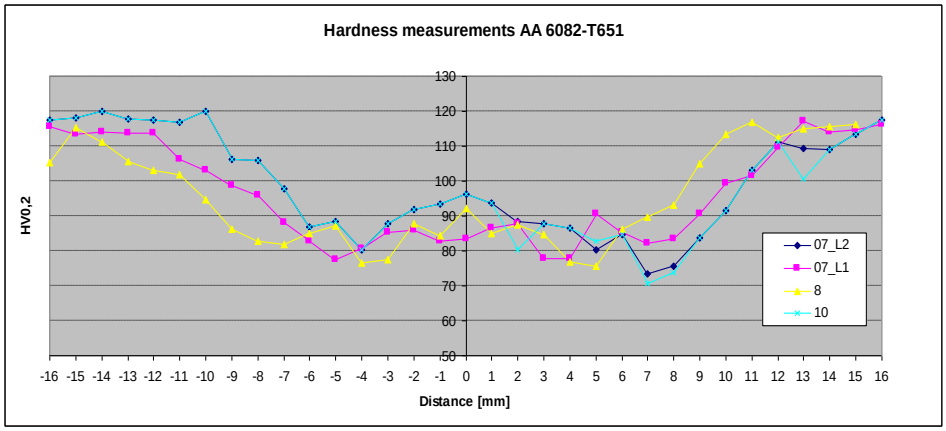

Fig. 5. 30. Hardness measurements CEALS07, CEALS08, CEALS10

5.13. Fatigue tests

Here is presented the last step of the experimental chart illustrated at the beging of this chapter (Fig. 5. 31). After the statically characterizations of the welded plates, to complete the experimental program, a number of fatigue tests have been carried out.

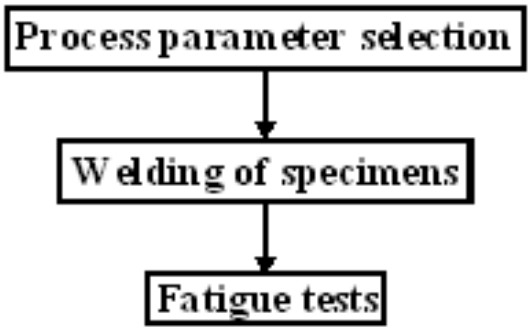

Fig. 5. 31. Experimental flow chart – step 3

These tests have been realizd on the AA 6082-651 FS welded samples. The reason that only these material was tested is because the AA 6082-T651 is the material used for the design of the bidge deck. These alloy is indicated for the

bridge deck elements because of his good extrudability and good resistance. Also, in case of this alloy, the intergranular corrosion does not appeare as a problem.

The fatigue samples have been cut-off according to the American Standards ASTM E 466-96 (2004) and AECMA – prEN6072 (2006) [86]. The dimensions of these samples are presented in Fig. 5. 32.

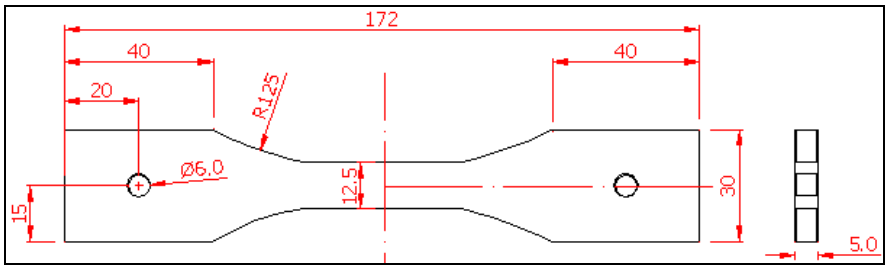

Fig. 5. 32. Fatigue samples dimensions

The fatigue tests were carried out in a servo-hydraulic testing machine equipped with an actuator of 50 kN load capacity. The weld was transverse to the stress axis in the *S–N* specimen (cross-weld). A sinusoidal load–time function was used, with the stress ratio *R* set to 0.5. Average stresses in the interval of 89–133 MPa were tested (60% to 90% from the yield resistance resulted from the tensile tests). The oscillation frequency was in the interval of 1–20 Hz. A short overview of this machine is presented in

Fig. 5. **33**.

Fig. 5. 33. Fatigue testing machine

For comparison of the experimental results, there have been realized an analysis based on the EC 9- Part 2 – Structures susceptible to fatigue [78]. Equation

6.1. represents the fatigue design relationship for endurances in range between 10^5 to $5x10^6$ cycles.

$$N_i = 2 \times 10^6 \left(\frac{\Delta\sigma_c}{\Delta\sigma_i} \cdot \frac{1}{\gamma_{Ff} \cdot \gamma_{Mf}} \right)^{m_1} \quad (6.\ 1)$$

where: N_i - is the predicted number of cycles to failure of a stress range σ_i;

$\Delta\sigma_c$ - is the reference value of fatigue strength at 2 x 106 cycles, depending on the detail category;

$\Delta\sigma_i$ - is the stress range for the principal stresses at the constructional detail and is constant for all cycles;

m_1 -is the inverse slope of the $\Delta\sigma$-N curve, depending on the detail category;

γ_{Ff} - is the partial factor allowing for uncertainties in the loading spectrum and analysis of response;

γ_{Mf} - is the partial factor for uncertainties in materials and execution.

Here:

$\gamma_{Ff} = 1$

$\gamma_{Mf} = 1$

$m_1 =$ (4; 4.3; 7) (according to EC9, Part 2, Annex J, Tab. J.7)

$\Delta\sigma_c$ – see Table 5. 11

Table 5. 11. Standardized $\Delta\sigma_c$ values (N/mm^2)

140, 125, 112, 100, 90, 80, 71, 63, 56, 50, 45, 40, 36, 32, 28, 25, 23, 20, 18, 16, 14, 12

Based on the above presented informations, the life of the welded elements is presented in the next diagram. Fig. 5. 34 presents also the test results on the CEALS07-element series.

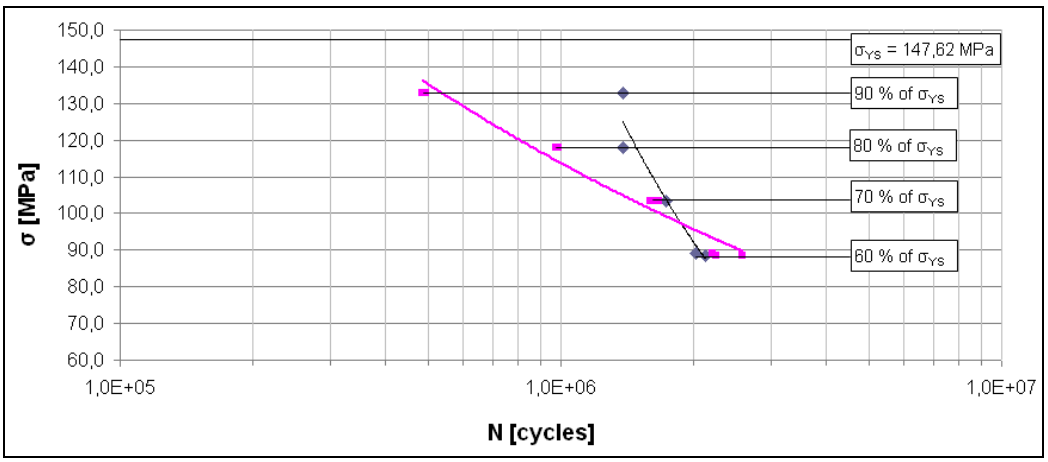

Fig. 5. 34. Comparison between predicted fatigue strength curve logΔσ-logN-CEALS07 FS welded plate and the test results

The average values of the other two element series tested to fatigue tets are presented in the next Tables.

Table 5. 12. Average results of fatigue life for FS welded specimens – CEALS08 series

Stress [%]	Max stress [MPa]	Fatigue life [cycles]
60	76,3	1666500
70	89,02	895300
80	101,78	625250
90	117,45	485100

Table 5. 13. Average results of fatigue life for FS welded specimens – CEALS10 series

Stress [%]	Max stress [MPa]	Fatigue life [cycles]
60	73,9	1765600
70	86,22	1015300
80	98,54	595200
90	110,85	453300

The fracture propagated in the center of the welding seam. The location of the fracture is presented in Fig. 5. 35.

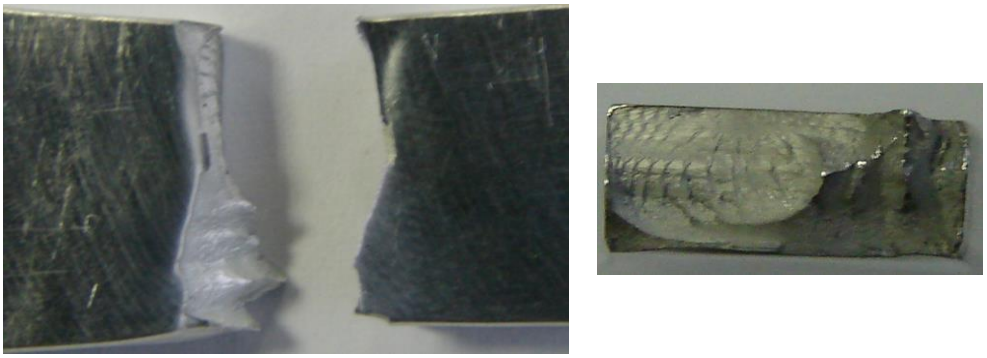

a. b.

Fig. 5. 35. a) AA6082-T6 FS welded fatigue tested specimen, fracture location; b) AA6082-T6 FS welded specimen, fracture surface

Compared with the results values for the base material, from the Phd Thesis of Moreira [9], it was found that FSW specimens display longer fatigue lives than similar unwelded specimens tested under the same loading conditions.

5.14. Conclusions

Both studied materials (AA 5083-H111 and AA 6082-T651) are good weldable with FSW. In the case of the AA 5083-H111 it may be observed:

- the decrease of the hardness profile in the heat affected zone;
- in the welded zone the re-crystallization that takes place during the welding process produces very fine alloy grains;
- the insignificant decrease of the tensile resistance (the welded elements reached cca. 95% from the ultimate stress of the base material).

In the case of AA 6082-T651 may be observed:

- the hardness profile knows a insignificant drop in the heat affected zone;
- the tensile resistance of the welded elements represents cca 75% from the base material tensile resistance;
- the fatigue life is increased that in case of the MIG and TIG welding process to this alloy.

6. CASE STUDY – DESIGN OF AN ALUMINIUM ALLOYS BRIDGE SUPERSTRUCTURE

In the last decade aluminium alloys have been more and more used in the field of bridge construction. The main applications are: pedestrian bridges, movable bridges and replacing the old concrete or steel bridge decks. The aluminium alloys present an increasing interest for these applications based on the good characteristics presented in Chapter 3, but also because of the new alloys with resistance properties comparable with the steel characteristic.

An important issue to discuss by using aluminium alloys is represented by the joining technology. It is known that during the welding of aluminium alloys with MIG or TIG process the main characteristics of the alloys are significant reduced. Also, by using the steel screws, it may form the galvanic corrosion by the contact of these two materials, so a special protection of the hole or of the screw is needed.

During the last years an important number of experimental works have been developed in order to analyze the behaviour of aluminium alloys bridge decks. Thomasz Siwowski realized the analytical and experimental evaluation of an aluminium bridge deck. Several service load and ultimate load tests have been carried out on the prefabricated 2,10 X 3,20 m MIG welded deck panels, in order to examine and evaluate the panel behaviour under standard truck load. The results of the service load study indicated adequate strength and stiffness of the deck panel. Two ultimate-load tests were conducted to further investigate the failure mechanism. The study clearly demonstrates that an aluminium bridge deck panel is a feasible alternative to reinforced concrete decks from the standpoint of stiffness, strength and load carrying capacity [87].

Netherlands is one country with an important number of applications of aluminium bridge decks. Based on the interest of the industry and government, a group of researchers from Technical University of Eindhoven conducted the fatigue tests on aluminium bridge. The structural design of the bridge consists of a deck that is supported by webs with a distance of 1.5 m in between. The construction is closed on the lower side with a bottom flange. Aluminium plates of alloy 5083-H321 with a thickness of 12 mm are applied for the webs and bottom flange. Aluminium extrusions made of alloy 6063 T6 are welded together to form the deck (Fig. 6. 1).

They have been developed the structural design of an aluminium bridge loaded by heavy traffic. The S-N curves of a welded detail that is often applied in the deck of aluminium bridges were determined by testing and the test results were compared to the standard SN curve prescribed by standard pr EN 1999-1-3. Additional tests were carried out in which the passage of vehicles was simulated on a model of the entire bridge, in order to obtain a better approximation of the real fatigue load on the bridge. The fatigue lifetimes resulting from these tests are compared to the arithmetical lifetimes, determined by using the S-N curve and Miner's summation. In the end they have been concluded that aluminium is suitable as structural material for heavily loaded bridges [88].

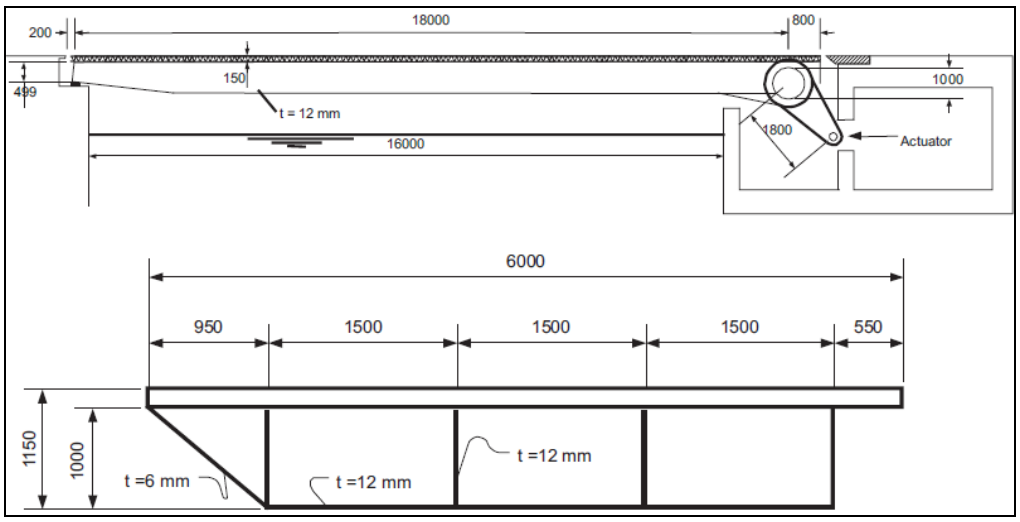

Fig. 6. 1. Longitudinal (top) and transverse (bottom) cross-section of the bridge [2]

Based on the change of design vehicle load from 196 kN to 245 kN, a group of researchers from Osaka University, Japan, realized a study regarding the fatigue analysis for a aluminium deck fabricated by friction stir welding This solution have been introduced in order to reduce the weight of the slab by existing bridges, by replacing the concrete slabs with aluminium decks. To complete this research, the team realized also a static and fatigue behaviour of the connections of aluminium deck to steel girders (Fig. 6. 2). The conclusions regarding fatigue behaviour of the aluminium deck fabricated by FSW have been:

- in the aluminium deck, the stress in the bridge-longitudinal direction alternates positive and negative for the move of a load, but the stress in the bridge-transverse direction does not;
- The aluminium deck is a structure in which a load is supported in the limited area around the load [89].

Regarding the connection:

- The proposed connection of aluminum decks to steel girders is a rigid one. The compressive force is developed at the edge on the loading side of the supporting mortar, and the tensile force is induced in the central stud and the one far from the loading side. These two forces develop a moment, which makes the connection rigid.
- The static strength of the connection is governed by crush of the supporting mortar.
- The fatigue strength of the connection is governed by that of the studs. The fatigue strength of the studs is the grade E in the Japanese Fatigue Guideline. Even if the stud far from the loading side has fatigue failure, the durability of the connection does not decrease, since the tensile force shifts to other studs.
- In the fatigue test of the overhang type specimen, fatigue cracks are initiated at the air-release hole on the top flange of the aluminum beam. It is required to move the location of the hole or to change the shape of the hole to an ellipse [90].

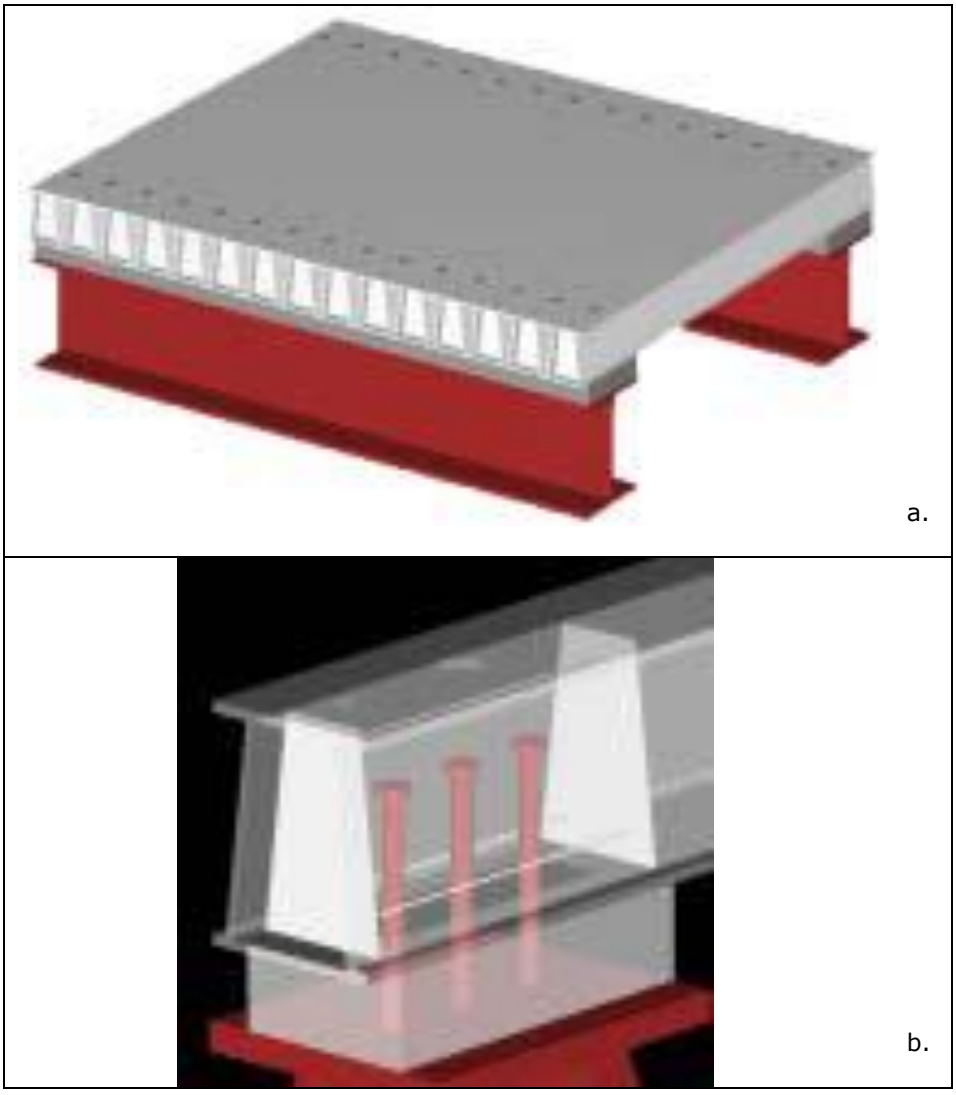

Fig. 6. 2. a. Aluminum deck on steel girders;
b. Connection of aluminum deck to steel girder [90]

Having as a start point the presented studies, in this chapter will develop the analyses of the superstructure of a bridge realized using aluminium alloys. The two aluminium alloys are: AA 5083-H111 for the main girders and AA 6082-T651 for the bridge deck. The present structure is designed to be used as an "emergency bridge".

Bridges are one of the most important elements of any country's surface transportation system. Closing a bridge always causes inconvenience to the public. Thus, a critical need exists for a "bypass" bridge that can be assembled quickly, economically, and easily at the original site or close to the bridge that is being repaired or replaced. [91]

Aluminum is an ideal material to add width without increasing weight to the substructure and decks of load-restricted bridges, historic bridges, movable bridges, and bridges with narrow roadways. Because seismic forces are directly proportional to weight, aluminum is also excellent for seismic retrofitting of bridges.

New aluminum deck systems are shop-fabricated, welded, and have multivoid extruded bridge deck panels with a shop-applied wearing surface to speed construction. Prefabricated aluminum deck panels can be installed faster than other systems and require no field welding. Advances by using aluminium bridges:

- Aluminum bridge decks are 80 percent lighter than concrete, offering increased bridge width and capacity without the need to strengthen the supporting bridge elements.
- Corrosion-resistant aluminum bridge decks require no painting and minimal maintenance, and are better suited than steel or concrete where de-icing chemicals are used.
- Aluminum allows for rapid, cost-effective construction. In comparison, concrete typically requires extensive formwork and cure time.
- Downtime for a bridge receiving an aluminum deck is a fraction of the time needed for concrete.
- Low-temperature toughness makes aluminum ideal for bridges and other highway structures in colder climates.

6.1. Structure general description

Present analysis refers to a bridge superstructure realized from main girders from aluminium alloy AA 5083-H111 and bridge deck panel realized from extruded elements from AA 6082-T651. The idea is to design and analyze a few spans, starting with a minimum span of 5,0 m. The cross-section consists of one traffic lane. The entire width of the bridge is 4,0 m.

The span of the bridge is 5,128 m. A structure preview is presented in Fig. 6. 3.

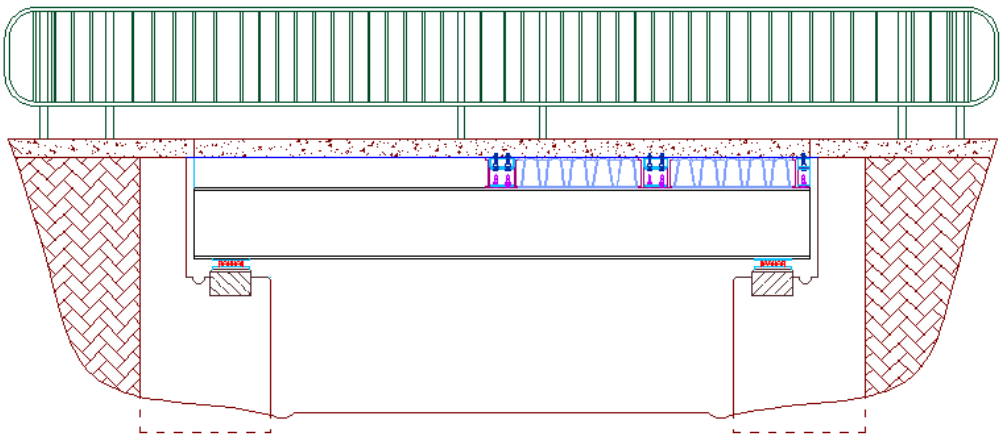

Fig. 6. 3. Bridge structure

The cross-sections of the main girders and bridge deck extruded profile are presented in Fig. 6. 4.

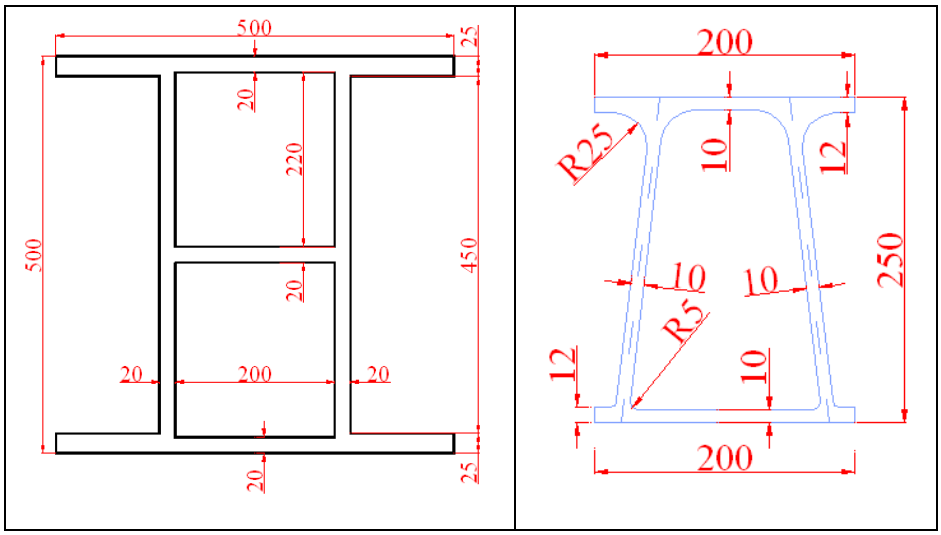

a. b.

Fig. 6. 4. Cross-sections. a. Main girder; b. Extruded profile

This structure is designed to be fully demountable, in order to re-use the components. The main components are: two main girders, four deck elements welded with FSW, protection profiles for the connections between main girders and deck elements. The connection between main girders and the deck profiles will be realized with the help of a number of aluminium studs, friction welded on the top flange of the main girders. Every deck element has in component a number of five extruded elements as presented in Fig. 6. 4 b., and two connection extrusions.

6.2. Loads on the structure

The structure is designed to serve as a road bridge for emergency cases. The reduced width of 4,0 m allows just one lane for heavy traffic. The components of the structure are: main girders, bridge deck elements which are covered on the upper side with one layer polymer foil to protect the aluminium alloys elements from the direct contact with the asphalt layer, and a 15 cm asphalt layer.

The alloys used are listed in Table 6. 1.

Table 6. 1. Mechanical properties of alloys employed in the structure

	Denomination	f_0 [MPa]	f_u [Mpa]	$f_{0,w}$ [MPa]	$f_{u,w}$ [Mpa]
The deck extrusions	EN AW-6082 - T651	255	317	147	226
The main girders	EN AW-5083 - H111	190	326	135	302

The design values of the basic properties assumed for all alloys are shown in Table 6. 2.

Table 6. 2. Design values of material

Design values of material coefficients			
Modulus of elasticity	**E**	70000	[N/mm^2]
Shear modulus	**G**	27000	[N/mm^2]
Density	**ρ**	2800	[daN/m^3]
Poisson's ratio	**υ**	0,3	
Coefficient of linear thermal expansion	**α**	23 x 10^{-6}	1/°C

6.2.1. Permanent loads

Nominal values of permanent loads consist of structure selfweight and the asphalt layer. They are summarized in Table 6. 3.

Table 6. 3. Permanent loads

Support structure	160 daN/m
Deck extrusion	150 daN/m
Asphalt layer - 15 cm	750 daN/m

6.2.2. Variable loads

The variable load is represented by the weight of an A30 truck, as represented in
Fig. 6. **5**.

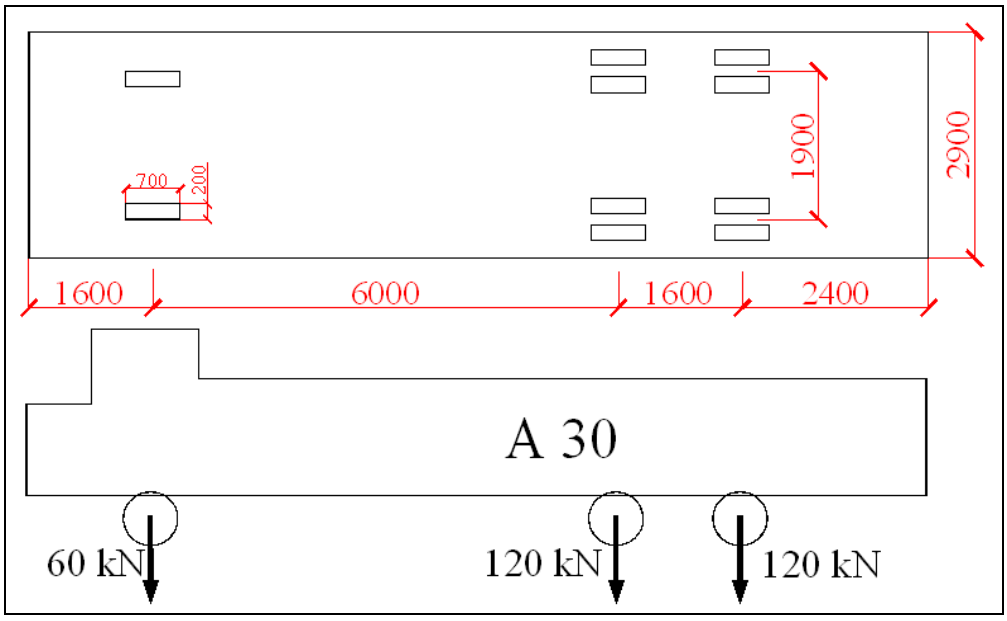

Fig. 6. 5. Variable load A 30

6.2.3. Load combinations

Rules provided in EC 1 have been followed for evaluating the partial safety factors γ_G for statically loads and γ_Q for movable loads (see Table 6. 5). The safety factors for material are presented in Table 6. 5.

Table 6. 4. Partial safety factors for applied loads

	Ultimate limit state		Serviceability limit state	
	γ_G	γ_Q	γ_G	γ_Q
Support structure	1,35	1,50	1,00	1,00
Deck extrusion	1,00	1,50	1,00	1,00

Table 6. 5. Partial safety material factors

The partial safety factor for the members	γ_{M1}	1,10
The partial safety factor for bolted connections	γ_{M2}	1,25
The partial safety factor for welded connections	γ_W	1,25

6.2.4. Buckling evaluation

In order to check the ultimate limit state the cross section has to be classified. According to EC9 part 1-1, Chapter 6.1.4.3, the slenderness parameter β must be evaluated. In the case of bending β is calculated with equation 6.1; for compressed elements equation 6.2 determines the β parameter.

$$\beta = 0{,}4 \cdot \frac{b}{t} \tag{6.1}$$

$$\beta = \frac{b}{t} \tag{6.2}$$

where: b – the width of the section element
t – the thickness of the section element

As it can be seen in Table 6. 6 both main girder and deck plate sections are situated in the class 1 to 2 for cross sections. For a better understanding, the definitions of these classes are presented:
Class 1 cross-sections are those that can form a plastic hinge with the rotation capacity required for plastic analysis without reduction of the resistance. These sections are named also "ductile sections".

Class 2 cross-sections are those that can develop their plastic moment resistance, but have limited rotation capacity because of the local buckling. These sections are also named as "compact sections".
Class 3 cross sections are those in which the calculated stress in the extreme compression fiber of the aluminium member can reach its proof strength, but local buckling is liable to prevent development of the full plastic moment resistance. They are also named as "semi-compact sections".
Class 4 cross-section are those in which local buckling will occur before the attainment of proof stress in one or more parts of the cross-section. They are also named as "slender sections".

Table 6. 6. Slenderness factor calculation

Material	Internal part			Outstand part		
	β_1	β_2	β_3	β_1	β_2	β_3
6082-T651 - class A, without welds	14,3	20,8	28,6	3,9	5,85	7,8
6082-T651 - class A, with welds	11,7	16,9	23,4	3,25	5,2	6,5
ε = 1,30						
5083-H111 - class B, without welds	14,95	18,98	20,70	4,03	5,2	5,75
5083-H111 - class B, with welds	11,50	15,53	17,25	3,45	4,03	4,60
ε = 1,15						

For the deck profile:

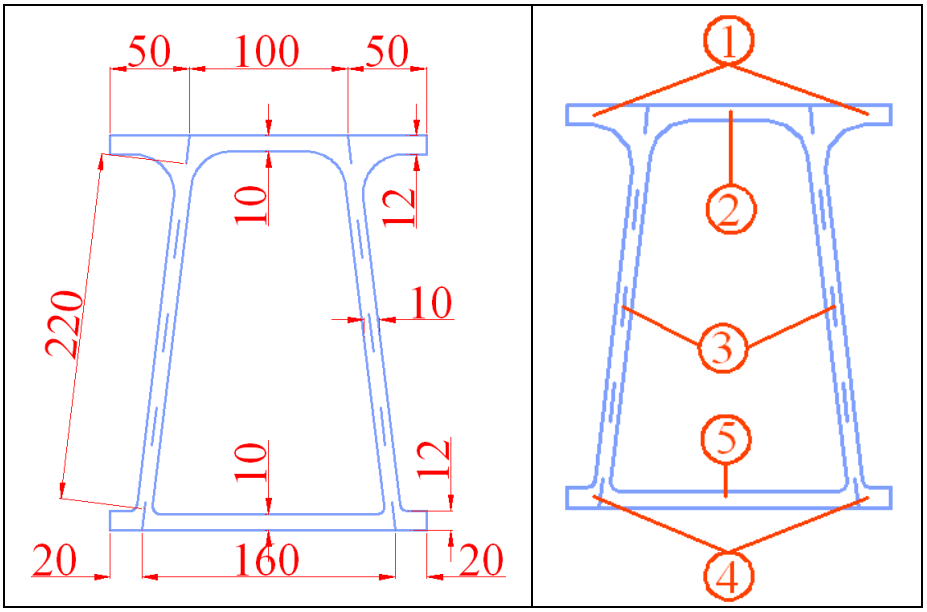

a. b.

Fig. 6. 6. Deck profile elements

t_1 = 12 mm b_1 = 50 mm	t_2 = 10 mm b_2 = 100 mm	t_3 = 10 mm b_3 = 220 mm	t_4 = 12 mm b_4 = 20 mm	t_5 = 10 mm b_5 = 160 mm

$$\varepsilon = \sqrt{\frac{250}{f_{02}}} = \sqrt{\frac{250}{147}} = 1.3$$

$$\beta^1 = \frac{b_1}{t_1} = \frac{50}{12} = 4.17 \rightarrow \text{outpart, with weld} < \beta_2 = 5.2$$

$$\beta^2 = \frac{b_2}{t_2} = \frac{100}{10} = 10 \rightarrow \text{intpart, without weld} < \beta_1 = 14.3$$

$$\beta^3 = 0.4 \cdot \frac{b_3}{t_3} = 0.4 \cdot \frac{220}{10} = 8.8 \rightarrow \text{intpart, without weld} < \beta_1 = 14.3$$

$$\beta^4 = \frac{b_4}{t_4} = \frac{20}{12} = 1.67 \rightarrow \text{outpart, with weld} < \beta_1 = 3.25$$

$$\beta^5 = \frac{b_5}{t_5} = \frac{160}{10} = 16 \rightarrow \text{intpart, without weld} < \beta_2 = 20.8$$

Section of the deck profile is categorized as a **Class 2 section** - "compact sections".

For the main girder:

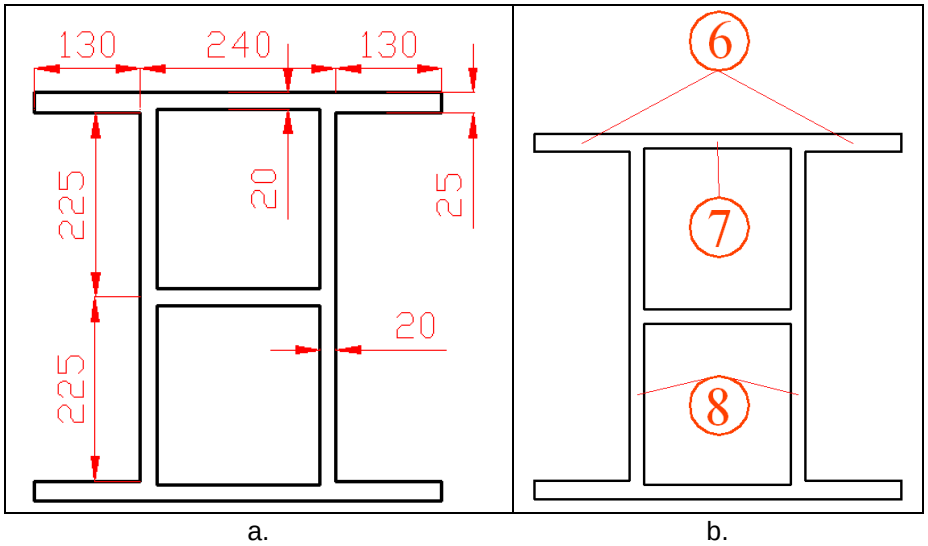

a. b.

Fig. 6. 7. Main girder elements

t_6 = 25 mm b_6 = 130 mm	t_7 = 20 mm b_7 = 240 mm	t_8 = 20 mm b_8 = 225 mm

$$\beta^6 = \frac{b_1}{t_1} = \frac{130}{25} = 5.2 \rightarrow \text{outpart, without weld} \leq \beta_2 = 5.2$$

$$\beta^7 = \frac{b_2}{t_2} = \frac{240}{20} = 12 \rightarrow \text{intpart, without weld} < \beta_1 = 14.95$$

$$\beta^8 = 0.4 \cdot \frac{b_3}{t_3} = 0.4 \cdot \frac{225}{20} = 4.5 \rightarrow \text{intpart, without weld} < \beta_1 = 14.95$$

$$\varepsilon = \sqrt{\frac{250}{f_{02}}} = \sqrt{\frac{250}{190}} = 1.15$$

Section of the main girder is categorized as a **Class 2 section** - "compact sections".

6.3. Structure analysis

A structure shall be designed and constructed in such a way that:

- with acceptable probability, it will remain fit for the use for which it is required, having due regard to its intended life and its costs;
- with appropriate degrees of reliability, it will sustain all actions and other influences likely to occur during execution and use and have adequate durability in relation to maintenance costs.

Also, a structure shell be designed in such way that it will not be damaged by events like explosions, impact or consequences of human errors, to an extent disproportionate to the original cause.

The potential damage shall be limited or avoided by appropriate choice of one or more of the following:

- avoiding, eliminating or reducing the hazards which the structure is to sustain;
- selecting a structural form which has low sensibility to the hazards considered;
- tying the structure together;
- selecting a structural form and design that can survive adequately the accidental removal of an individual element.

The above requirements shall be met by the choice of suitable materials, by appropriate design and detailing using the indications from the available norms and standards regarding the limit states and design situations.

6.3.1. Limit states and design situation

A. Limit states

Limit states are states beyond which the structure no longer satisfies the design performance requirements. Limit states are classified into:

- ultimate limit states (**ULS**);
- serviceability limit states (**SLS**).

Ultimate limit states are those associated with collapse, or with other forms of structural failure which may endanger the safety of people. States prior to structural collapse which, for simplicity, are considered in place of the collapse itself are also classified and treated as ultimate limit states. Ultimate limit states which shall require consideration include:

- loss of equilibrium of the structure or any part of it, considered as a rigid body;
- failure by excessive deformation, rupture, or loss of stability of the structure or any part of it, including supports and foundations.

Serviceability limit states correspond to states beyond which specified service criteria are no longer met. SLS which may require consideration include:

- deformations or deflections which adversely affect the appearance of effective use of the structure (including the proper functioning of machines or services) or cause damage to finishes or non-structural elements;
- vibrations which causes discomfort to people, damage to the building or its contents, or which limits its functional effectiveness.

B. Design situations

- persistent situations corresponding to normal conditions of use of the structure;
- transient situations, for example during construction or repair;
- accidental situations (include exceptional situations that may not be the result of an accident).

6.3.2. Ultimate limit states (ULS)

The limit states that concern:

- the safety of people, and/or
- the safety of the structure

shall be classified as ultimate limit states.

Design for limit states shall be based on the use of structural and load models for relevant limit states. It shall be verified that no limit state is exceeded when relevant design values for:

- actions,
- material properties, or
- product properties, and
- geometrical data

are used in these models.

When considering a limit state of static equilibrium of the structure (EQU), it shall be verified that:

$$E_{d,dst} \leq E_{d,stb} \tag{6.4}$$

where :

$E_{d,dst}$ - is the design value of the effect of destabilizing actions ;

$E_{d,stb}$ - is the design value of the effect of stabilizing actions.

When considering a limit state of rupture or excessive deformation of a section, member or connection (STR and/or GEO), it shall be verified that:

$$E_d \leq R_d \tag{6.5}$$

where:

E_d - is the design value of the effect of actions such as internal force, moment or a vector representing several internal forces or moments;

R_d - is the design value of the corresponding resistance.

For the elements solicited for **tension**:

$$\frac{N_{Ed}}{N_{t,Rd}} \leq 1{,}0 \tag{6.6}$$

where:
N_{Ed} – the design value of the tensile force;
$N_{t,Rd}$ – the design tension resistance of the cross-section; this value represents the minimum value between $N_{0,Rd}$ and $N_{u,Rd}$.

$$N_{0,Rd} = \frac{A_g \cdot f_0}{\gamma_{M1}} \tag{6.7}$$

$$N_{u,Rd} = \frac{0.9 \cdot A_{net} \cdot f_u}{\gamma_{M2}} \tag{6.8}$$

where:
A_g – is the gross section or the reduced cross-section (HAZ softening)
A_{net} – is the net section area, with deduction for the holes and a deduction for HAZ softening.

In the case of the discussed section, no tension or compression appears.

The design of the **bending moment** M_{Ed} at each cross section shall satisfy:

$$\frac{M_{Ed}}{M_{Rd}} \leq 1{,}0 \tag{6.9}$$

where:
M_{Rd} – the design resistance for bending about one principal axis of a cross-section; this value represents the minimum value between $M_{0,Rd}$ and $M_{u,Rd}$.

$$M_{0,Rd} = \frac{\alpha \cdot W_{el} \cdot f_0}{\gamma_{M1}} \quad (6.10)$$

$$M_{u,Rd} = \frac{W_{net} \cdot f_u}{\gamma_{M2}} \quad (6.11)$$

Where:
W_{el} – is the elastic modulus of the gross section;
W_{net} – is the elastic modulus of the net section allowing for holes and HAZ softening;
α – is the shape factor (See Table 6. 7)

Table 6. 7. Values of shape factor α

Class	Unwelded	Welded
1	W_{pl}/W_{el}, but see Annex G	W_{ple}/W_{el}, but see Annex G
2	W_{pl}/W_{el}	W_{ple}/W_{el}
3	$\alpha_{3,u}$	$\alpha_{3,w}$
4	W_{eff}/W_{el}	W_{effe}/W_{el}

W_{pl} – plastic modulus for gross section
W_{eff} – effective elastic section modulus
W_{ele} – effective elastic modulus of the gross section, obtained using a reduces thickness $\rho_{haz}t$ for the HAZ material
W_{ple} - effective plastic modulus of the gross section, obtained using a reduces thickness $\rho_{haz}t$ for the HAZ material
W_{effe} – effective elastic section modulus, obtained using a reduced thickness t_{eff} for tha class 4 elements
$\alpha_{3,u} = 1$
In this case, both sections are classified as class 2 of cross-section and α = 1.

For the main girder the permanent loads on the main girders are:

- self weight of the girder
- self weight of the deck
- self weight of the asphalt layer

The variable loads are:
- A30 heavy truck with F_1 = 60kN and $F_2 = F_3$ = 120 kN.
The permanent loads introduce to the main girders a bending moment:

$$M_{Ed} = \frac{\gamma_G \cdot q \cdot L^2}{8} = \frac{1.35 \cdot (160 + 150 + 750) \cdot 5.128^2}{8} = 4704 daN \cdot m$$

For the analysis of the structure there has been used Axis program. The next pictures present the values of the design bending moment, by applying also the movable loads from the truck A30.

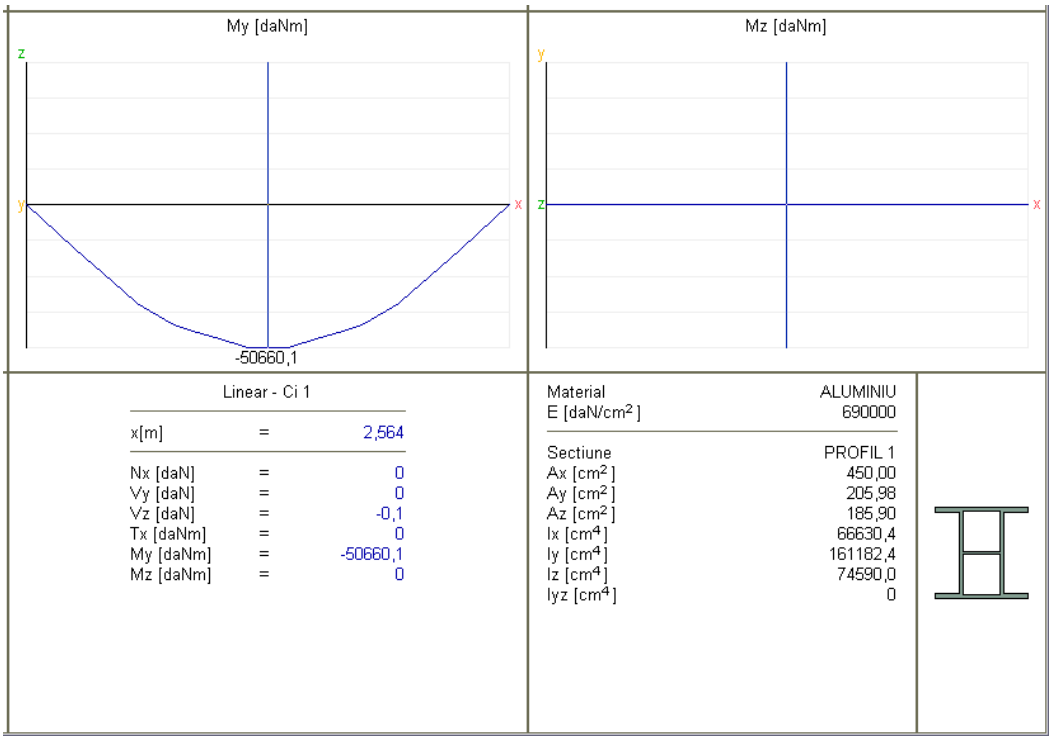

Fig. 6. 8. Maximum bending moment – main girder

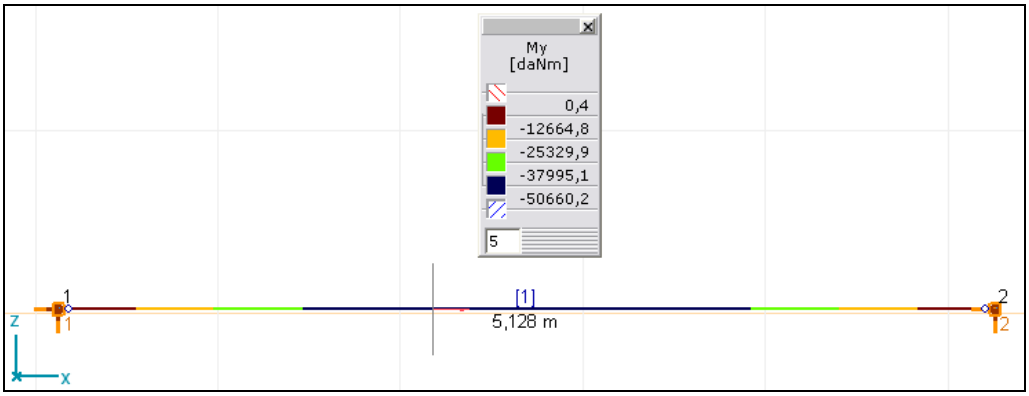

Fig. 6. 9. Bending moment on the main girder under the permanent and movable loads

$\Rightarrow M_{Ed} = 50660.1 \text{ daN} \cdot \text{m}$

Here, for the main girder section:

$$W_{y,pl} = 7527.5 \text{ cm}^3$$

$$W_{y,el} = 6447.2 \text{ cm}^3$$

$$\alpha = \frac{W_{pl}}{W_{el}} = 1.17$$

$$M_{0,Rd} = \frac{\alpha \cdot W_{y,el} \cdot f_0}{\gamma_{M1}} = \frac{1.17 \cdot 6447.2 \cdot 10^3 \cdot 190}{1.1} = 1302920509 \text{ N} \cdot \text{mm} = 130292 \text{daN} \cdot \text{m}$$

$$M_{u,Rd} = \frac{W_{net} \cdot f_u}{\gamma_{M2}} = \frac{7164 \cdot 10^3 \cdot 326}{1.25} = 1868371200 \text{ N} \cdot \text{mm} = 186837 \text{daN} \cdot \text{m}$$

$$\frac{M_{Ed}}{M_{0,Rd}} = \frac{50660}{130292} = 0.4 < 1$$

For the **deck section**, composed from 5 extruded elements and 2 connection elements:

$$W_{z,pl} = 20115.8 \text{ cm}^3$$

$$W_{z,el} = 13205.6 \text{ cm}^3$$

$$\alpha = \frac{W_{pl}}{W_{el}} = 1.52$$

$$M_{0,Rd} = \frac{\alpha \cdot W_{z,el} \cdot f_{0,w}}{\gamma_W} = \frac{1.52 \cdot 13205.6 \cdot 10^3 \cdot 147}{1.25} = 2360527411 \text{ N} \cdot \text{mm} = 236053 \text{daN} \cdot \text{m}$$

$$M_{u,Rd} = \frac{W_{net} \cdot f_{u,w}}{\gamma_{M2}} = \frac{13185 \cdot 10^3 \cdot 226}{1.25} = 2383848000 \text{ N} \cdot \text{mm} = 238385 \text{daN} \cdot \text{m}$$

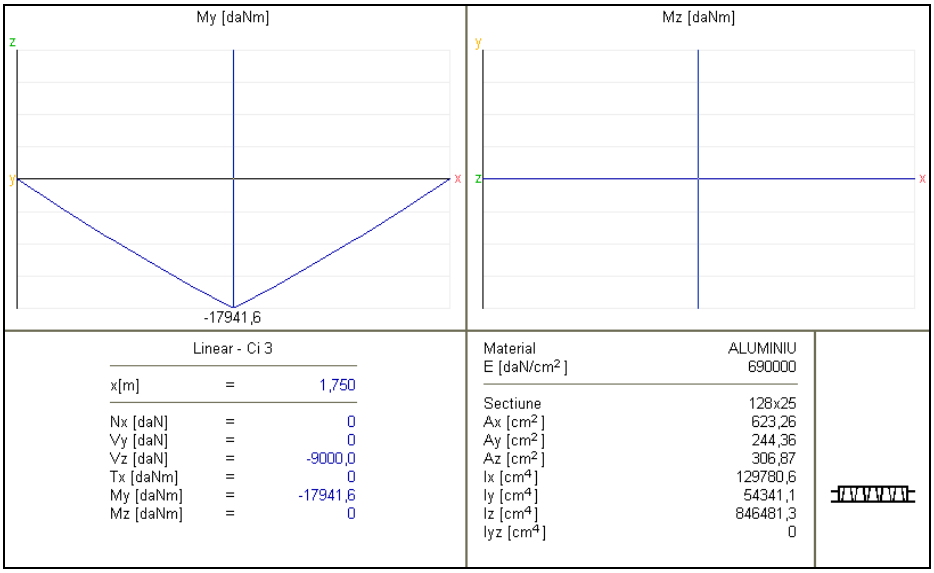

Fig. 6. 10. Maximum bending moment – deck section

$M_{Ed} = 179416\ daN \cdot m$

$$\frac{M_{Ed}}{M_{0,Rd}} = \frac{179416}{236053} = 0.08 < 1$$

For the design value of the **shear force** V_{Ed} at each cross-section shall satisfy:

$$\frac{V_{Ed}}{V_{Rd}} \leq 1 \qquad (6.12)$$

where: V_{Rd} is the design shear resistance of the cross-section.

$$V_{Rd} = A_v \cdot \frac{f_0}{\sqrt{3} \cdot \gamma_{M1}} \qquad (6.13)$$

A_v is the shear area.

$$A_v = \sum \left[\left(h_w - \sum d \right) \cdot t_{wi} - (1 - \rho_{0,haz}) \cdot b_{haz} \cdot t_{wi} \right] \qquad (6.14)$$

where:

h_w – is the depth of the web between flanges.
b_{haz} – is the total depth of HAZ material
t_w – is the web thickness
d – is the diameter of hole along the shear plane
n – is the number of webs.

For the **main girders**:

$$A_v = 2 \cdot 45 \cdot 2 = 180\ cm^2$$

$$V_{Rd} = A_v \cdot \frac{f_0}{\sqrt{3} \cdot \gamma_{M1}} = 180 \cdot \frac{1900}{\sqrt{3} \cdot 1.1} = 179503\ daN$$

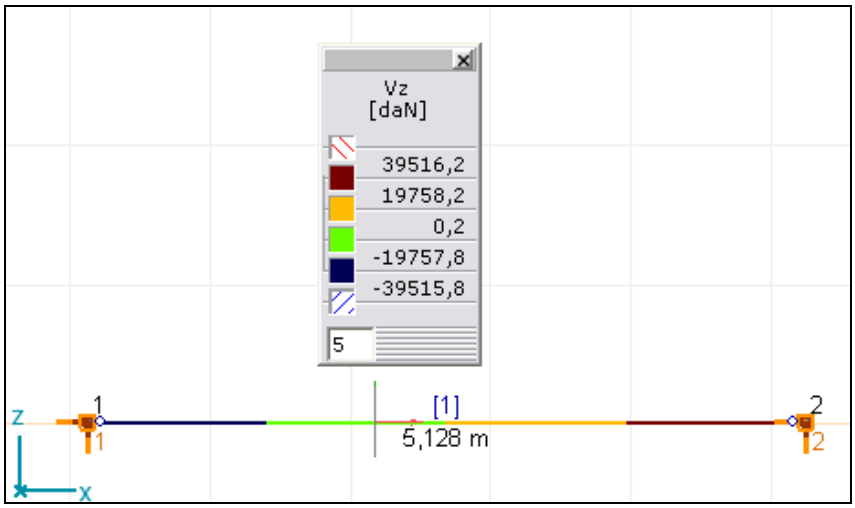

Fig. 6. 11. Shear forces on the main girder

$$\Rightarrow V_{Ed} = 39516.2\ daN$$

$$\frac{V_{Ed}}{V_{Rd}} = \frac{39516.2}{179503} = 0.22 \leq 1$$

For the **deck section**

$$A_v = 10 \cdot 20 \cdot 1 - (1 - 0.58) \cdot 5 \cdot 10 + 21.5 \cdot 1.2 \cdot 2 = 230.6\ cm^2$$

$$V_{Rd} = A_v \cdot \frac{f_0}{\sqrt{3} \cdot \gamma_{M1}} = 230.6 \cdot \frac{2550}{\sqrt{3} \cdot 1.1} = 308636\ daN$$

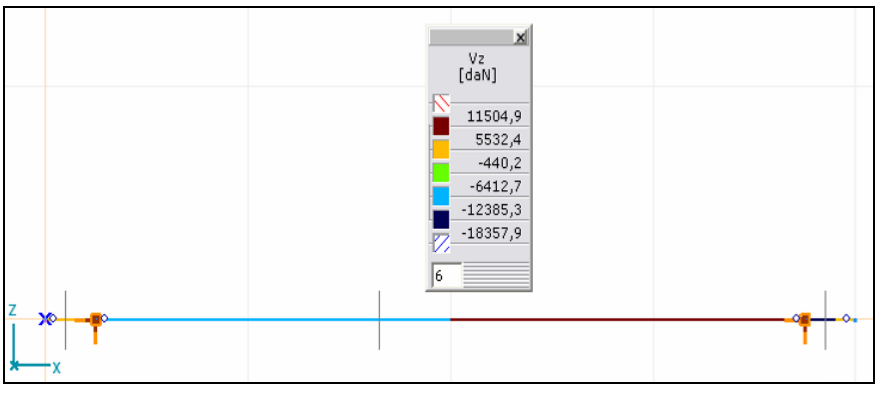

Fig. 6. 12. Shear forces on the deck section

$\Rightarrow V_{Ed} = 18357.9$ daN

$$\frac{V_{Ed}}{V_{Rd}} = \frac{18357.9}{308636} = 0.06 \leq 1$$

As it can be observed, all the design forces have values much lower than the admissible values. The next subchapters, referring to the serviceability limit state, will presents the reason for working, in the case of aluminium alloys structures, with such values.

6.3.3. Serviceability limit state (SLS)

As presented above, the SLS for aluminium is represented by the deformations and vibration. In the case of the discussed structure, only the deformations are considered. The limiting values for vertical deflections are:

$$\delta_{max} = \delta_1 + \delta_2 - \delta_0 \tag{6.15}$$

where:

δ_{max} – is the sagging in the final state relative to the straight line joining the support;

δ_1 – is the pre-camber (hogging) of the beam in the unloaded state (state 0)

δ_2 – is the variations of the deflection of the beam due to the permanent loads immediately after loading (state 1)

δ_0 – is the variation of the deflection of the beam to the variable loading plus any time dependent deformations due t the permanent load (state 2).

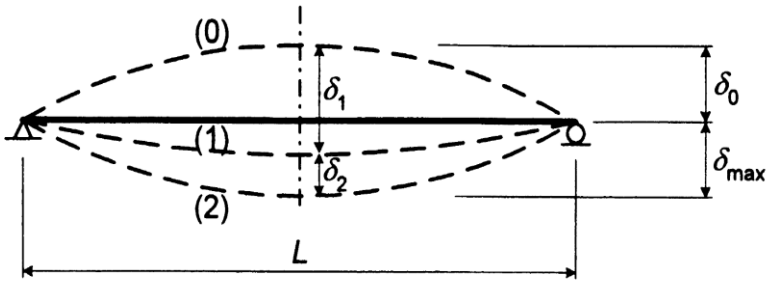

Fig. 6. 13. Vertical deflections to be considered

In the case of the discussed structure, the maximal admissible deflection is given by the next relation:

$$\delta_{max} = \frac{L}{360} \tag{6.3}$$

where: L – is the total length between the support systems.

Here, total length of the main girder is L = 5,128 m $\Rightarrow \delta_{max} = 14.24$ mm.

Main length of the deck section is l = 3,500 m $\Rightarrow \delta_{max} = 9.72$ mm.

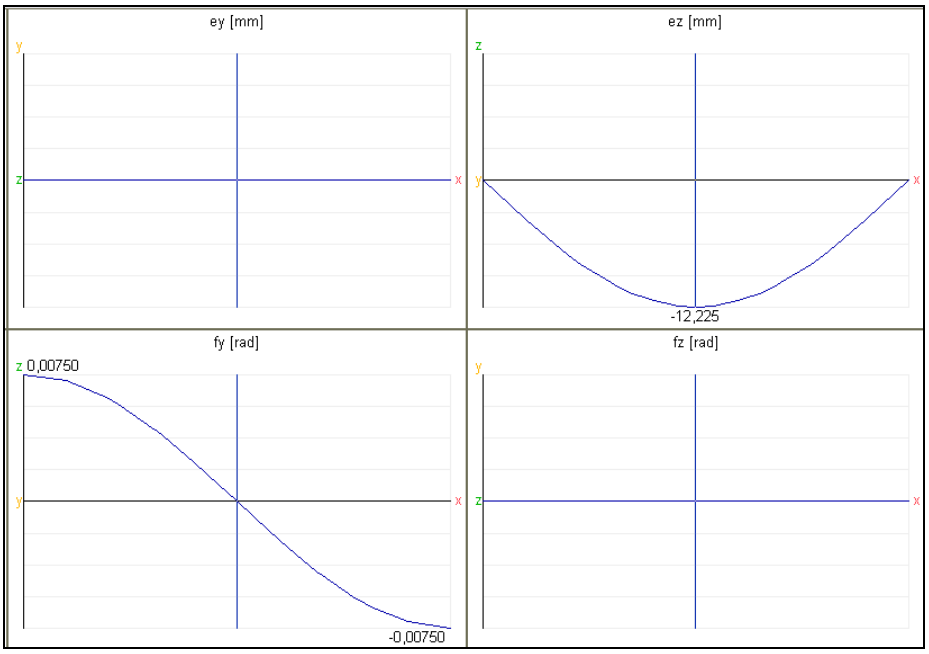

Fig. 6. 14. Maximum deformation of the main girder, under loadings

Here, the maximum value of the deformation is: $\delta = 12.225\,\text{mm} < \delta_{max} = 14.24\ \text{mm}$

For the deck section:

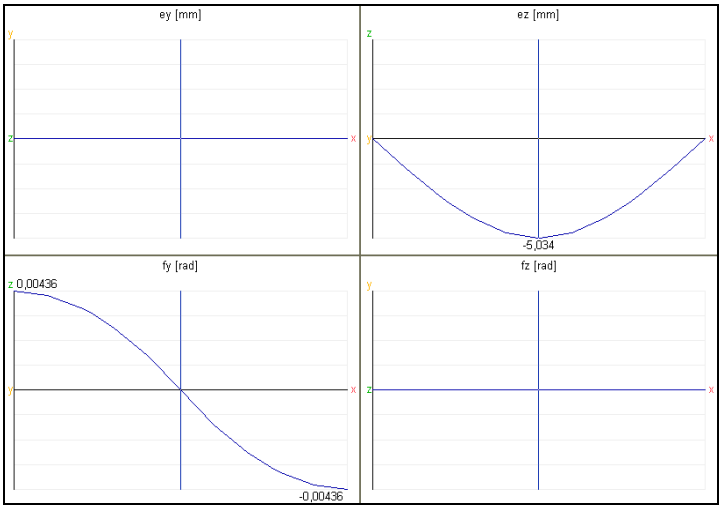

Fig. 6. 15. Maximum deformation of the deck girder, under loadings

Here, the maximum value of the deformation is $\delta = 5.034\,\text{mm} < \delta_{max} = 9.72\,\text{mm}$

6.4. Conclusions

This chapter presented a calculus for a simple bridge structure, but completely demountable, indicated to be used as an emergency bridge or temporary bridge, for short spans.

The results of this calculus indicated the used profiles as proper for the bridge construction.

7. CONCLUSIONS AND CONTRIBUTIONS

7.1. Conclusions

Aluminium was relatively new when it was first introduced as a structural material. The selection of alloys was limited and the fabrication techniques very primitive compared with the situation today. Despite these facts, structural aluminium applications were successfully introduced into many areas. The most important applications of aluminium alloys are in:

- ship and off-shore building industry;
- land and air transport industry;
- civil engineering.

Aluminium came into use in **marine** applications interestingly soon after steel. During the 1890s aluminium components were added to reduce the weight of ships and boats. But the alloys and the fabricating techniques then available were unsatisfactory and aluminium felt into disuse. Aluminium construction received great impulse with the development of high-speed welding techniques on one hand and other weldable alloys on the other hand, particularly the Al-Mg 5000 series. Since the early 1950's the majority of naval and merchant ships with aluminium structure have been welded. In addition to commercial ships and warships, aluminium is now used for tankers, fishing vessels, personnel boats, ferries and hydrofoils.

In **air transport** the development and use of aluminium alloys is directly linked to the development of that industry; 70% of the airframes of civil aircraft are realized with aluminium alloy.

Around the turn of century the **railway industry** took immediate interest in using aluminium when it became available on an industrial scale. During the twenties and thirties the design philosophy changed to increase passenger safety and to reduce weight. The approach was to consider the whole superstructure as a load bearing entity. Steel panels riveted to a steel framework were used initially followed shortly by aluminum sheet fastened to aluminium extrusions.

The full application of the aluminium extrusion technology for the **vehicle body design** resulted in cost reductions to such an extent, that light-weight aluminium coaches were and are being built at equal or lower costs than conventional steel coaches. The all-extrusion design has consequently been applied in numerous modern railcar projects all over the world.

Since the beginning of the century aluminium alloys always have been used for **automotive** components including engine parts, wheels, body panels and the structure frame since the beginning of the century. In most cases the technical performance was satisfactory with significant weight savings. However these increased costs were not at that times justified; today with the demand for reduced fuel consumption and the need to add safety and antipollution devices is accepted.

During the 1930's a gradual introduction of aluminium applications into the **civil engineering industries** took place. Special attention was directed towards various kinds of roof structures, building systems, stairs, stair towers, gangways, masts, silos, cranes, pylons, towers, pedestrian bridges etc. In addition more

recently a large number of structural military applications were developed, e.g. transportable bridges.

Due to the lack of informational and educational materials about the properties and advantages for the aluminium alloys, concerning the design criteria, the present use of these alloys is still limited. To create an informational support for the designers, the European officials introduced a new code only of aluminium structures: Eurocode 9. This standard, together with TALAT [7,8,77,79] publications and the vast work of prof. Mazzolani [15], materialized in a number of books, and the research programs of prof. Kosteas [92] – offers today the only informational materials about the importance of aluminium alloys and the large scale of possibilities for the practical use of these alloys.

To expand the applications possibilities of the aluminium alloys, in 1991 Friction Stir Welding process has been invented. This process, invented practically for the aluminium alloys. Since than the procedure has been developed, especially for the aeronautic industry. Based on the very good properties of the weld seams realized with FSW, the domains using this process have been enlarged. Even today this procedure is considered as a "young process" and is not entirely developed and discussed, to be applied for the civil engineering field. Finally, based on the good experimental testing results and the high resistance under the cycling loading, this new welding procedure is recommendable as suitable to be used in the field civil engineering and bridge construction, bringing a serious of important advantages.

7.2. Contributions

The thesis presents the importance of aluminium and aluminium alloys in different industries, including the domain of Civil Engineering.

It represents a part of a large research program realized together with National R&D Institute for Welding and Material Testing Timisoara and the continuous support of GKSS (Geesthacht) Hamburg.

The main contributions are:

- at the beginning of the thesis a briefly presentation of the aluminium production and the present method for aluminium alloys production is given
- state of the art about the applications of aluminium and its alloys in different interest fields as marine industry, transport industry and especially in civil engineering;
- short history and the development of different conceptions in aluminium bridges;
- detailed description of Friction Stir Welding technology;
- practical application of the new Friction Stir Welding procedure, realizing the first welded elements together with National R&D Institute for Welding and Material Testing (ISIM) Timisoara,
- over 50 tests specimens were realized and tested.
- for two the most used alloys in civil engineering the optimum welding parameters were studied.
- the complex characteristic of the friction stir welds in order to optimize the procedure were studied;
- experimental fatigue tests on friction stir welded elements were also performed;

- the initiation of an program for the design of emergency bridges with short spans, entirely realized from aluminium alloys, with low costs and short erection time.
-

The subject of this work was valorized through a number of publications:

1. Friction Stir Welding – an innovative solution for civil engineering, Ramona Gabor, Anca Gido and Radu Bancila, Proceedings "Highway and Bridge Engineering 2007", International Symposium, Iaşi, România, December 7, 2007, ISBN: 978-973-8955-29-5-158-169, pg. 158-169

2. Friction Stir Welding – a new connection concept; possible application in the field of civil engineering; Ramona GABOR, Radu BĂNCILĂ, Dorin DEHELEAN, Anca GIDO; Buletinul Ştiinţific **al Universităţii "Politehnica" din Timişoara,**

3. **Friction stir welding of Al 6082 alloy;** Radu Cojocaru, Dorin Dehelean, Ramona Gabor, Cristian Ciuca, Uros Zupanc; Proceedings of The 13th International Conference Modern Tehnologies, Quality and Innovation, 21-23 Mai 2009, Iaşi, ISSN: 2066-3919, pg. 195-198

4. **Friction stir welding of AA 5083-H111 alloy**, R.Gabor, A. Roos, J.dos Santos, L. Bergmann, Proceedings The 3rd International Conference Innovative technologies for joining advanced materials, 11-12.06.2009, Timişoara, România.

The results of this work have been used during the research project CEEX 66/2006, under the leading of prof. dr. ing. Radu Bancila.

8. ANNEXE

8.1. SOFiSTiK – Modeling

There have been realized a finite element model using SOFiSTiK. Four quadrilateral thin shell elements, so called QUAD, have been defined, to describe the deck element system.

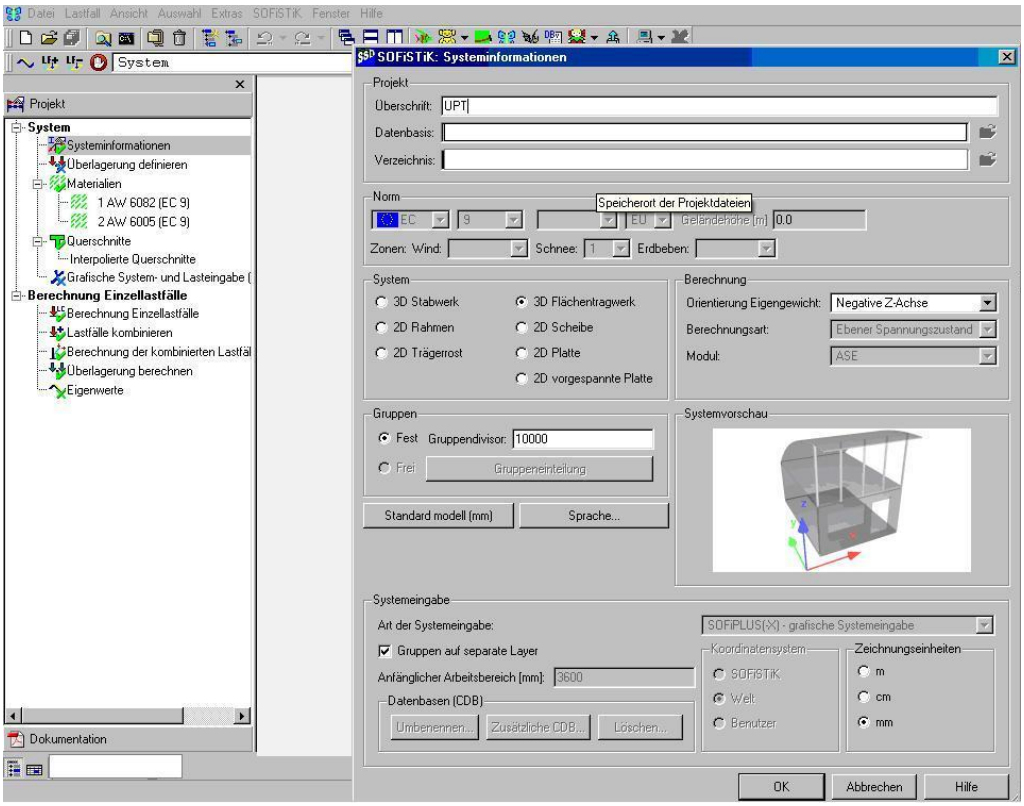

Fig. 8. 1. Main window of Sofistik structural desktop

As it can be seen in Fig. 8.1. there have been defined a 3D model for the support structure. The analisys has been performed according to Eurocode 9.

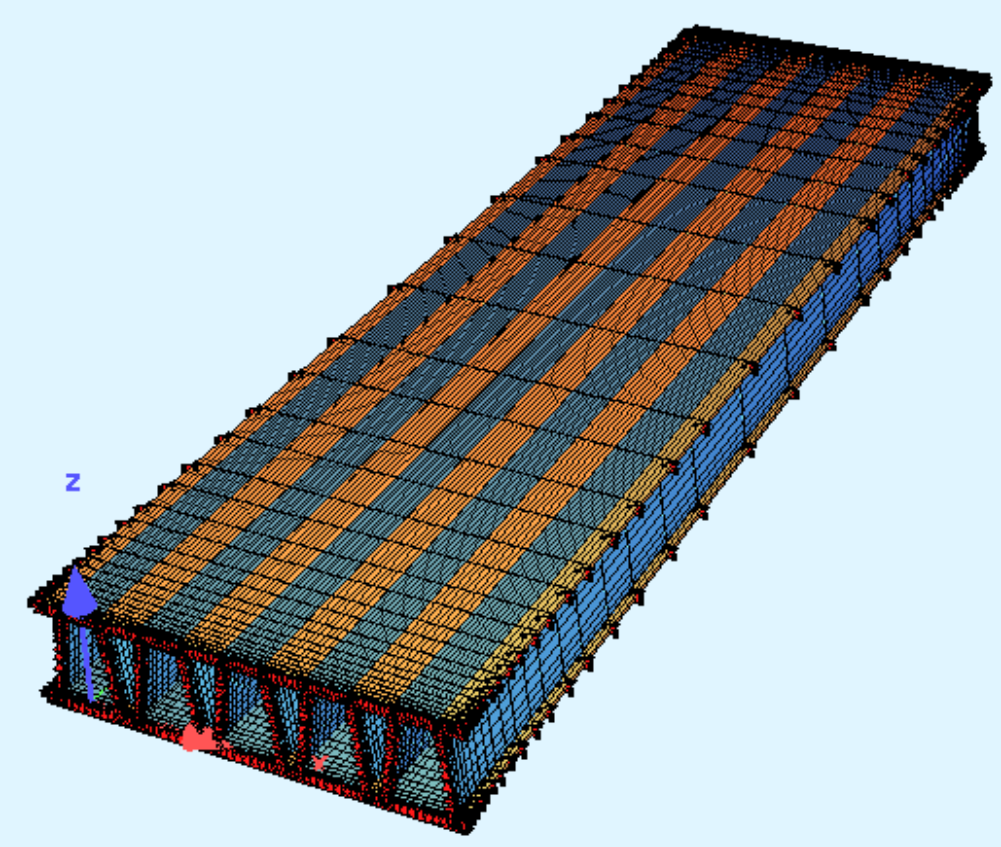

Fig. 8. 2. Mash definition

Fig. 8.2. presents the mash definition. As it can be seen, there have been defined different properties for the base material and the weld affected zone – the blue mash elements define the base material and the yellow mash elements define the weld affected zone.

The analized structure has 3,6 m length and 1,00 m width. This represents one deck element.

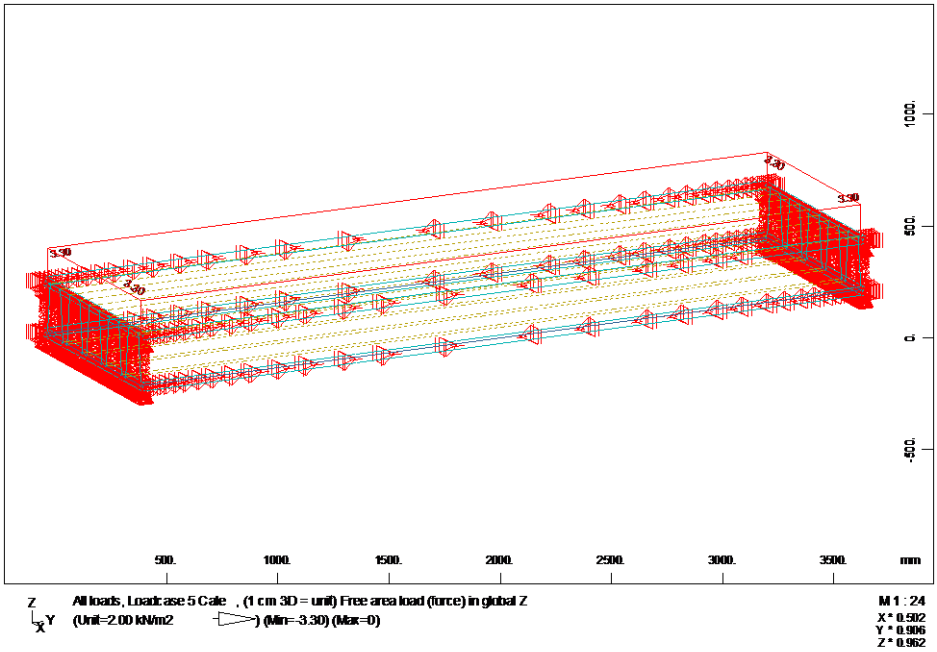

Fig. 8. 3. Load definition – permanent load

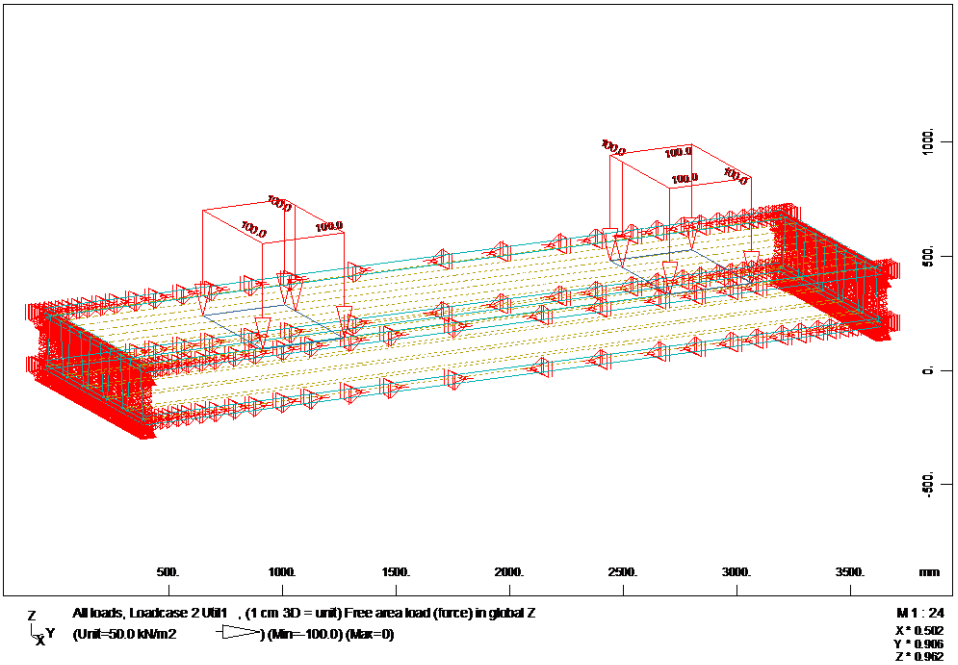

Fig. 8. 4. Load definition – payload 1 – mode 1 A30 truck position

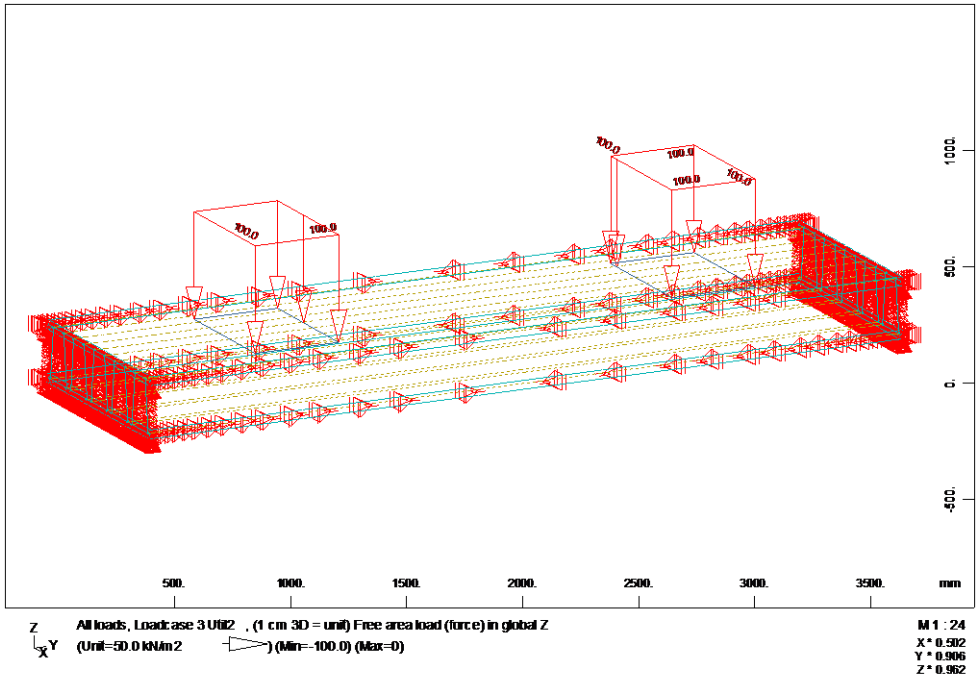

Fig. 8. 5. Load definition – payload 2 – mode 2 A30 truck position

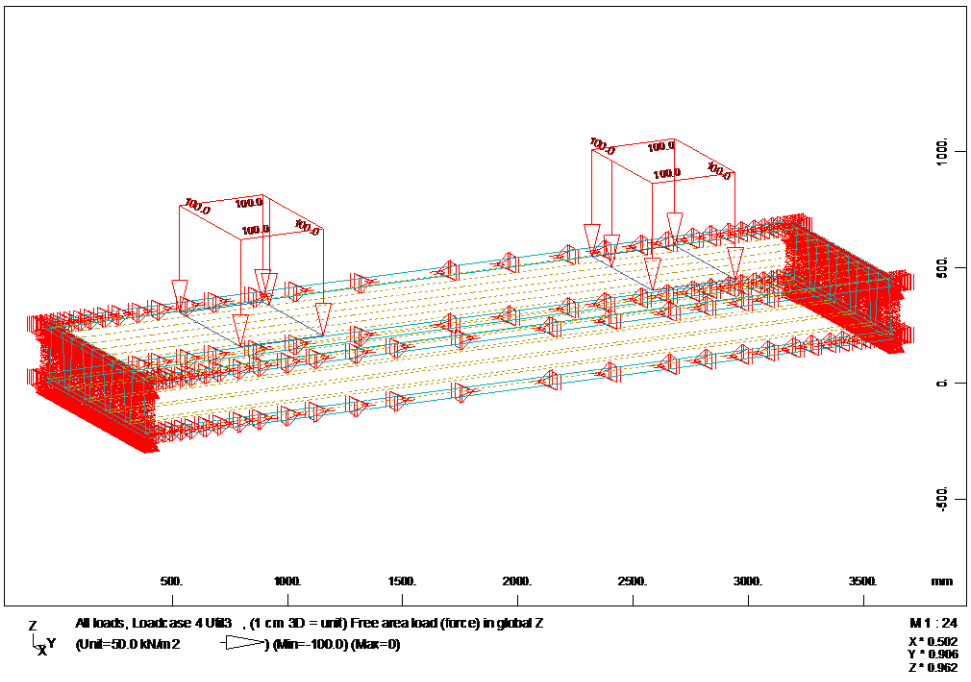

Fig. 8. 6. Load definition – payload 3 – mode 3 A30 truck position

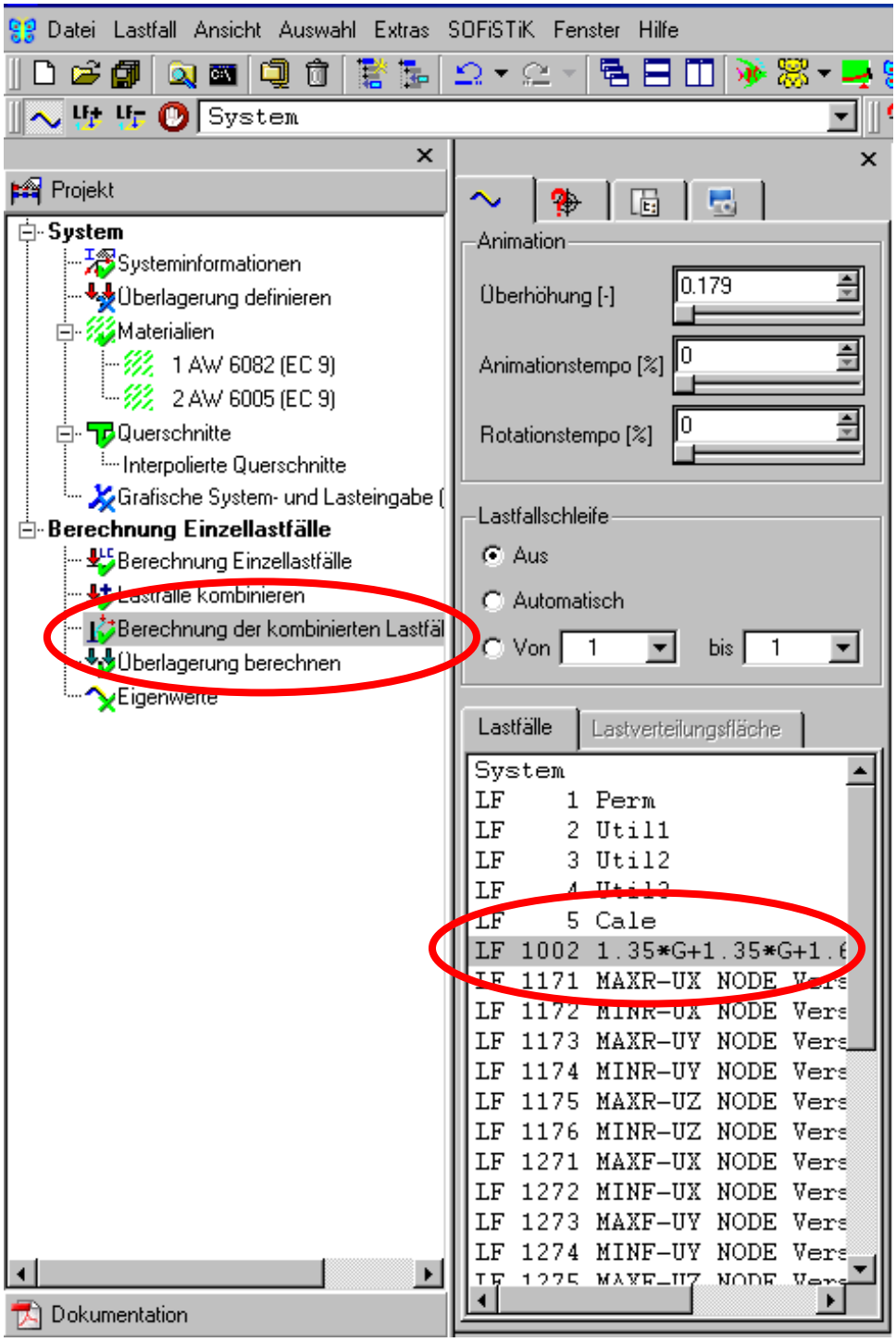

Fig. 8. 7. Load combination

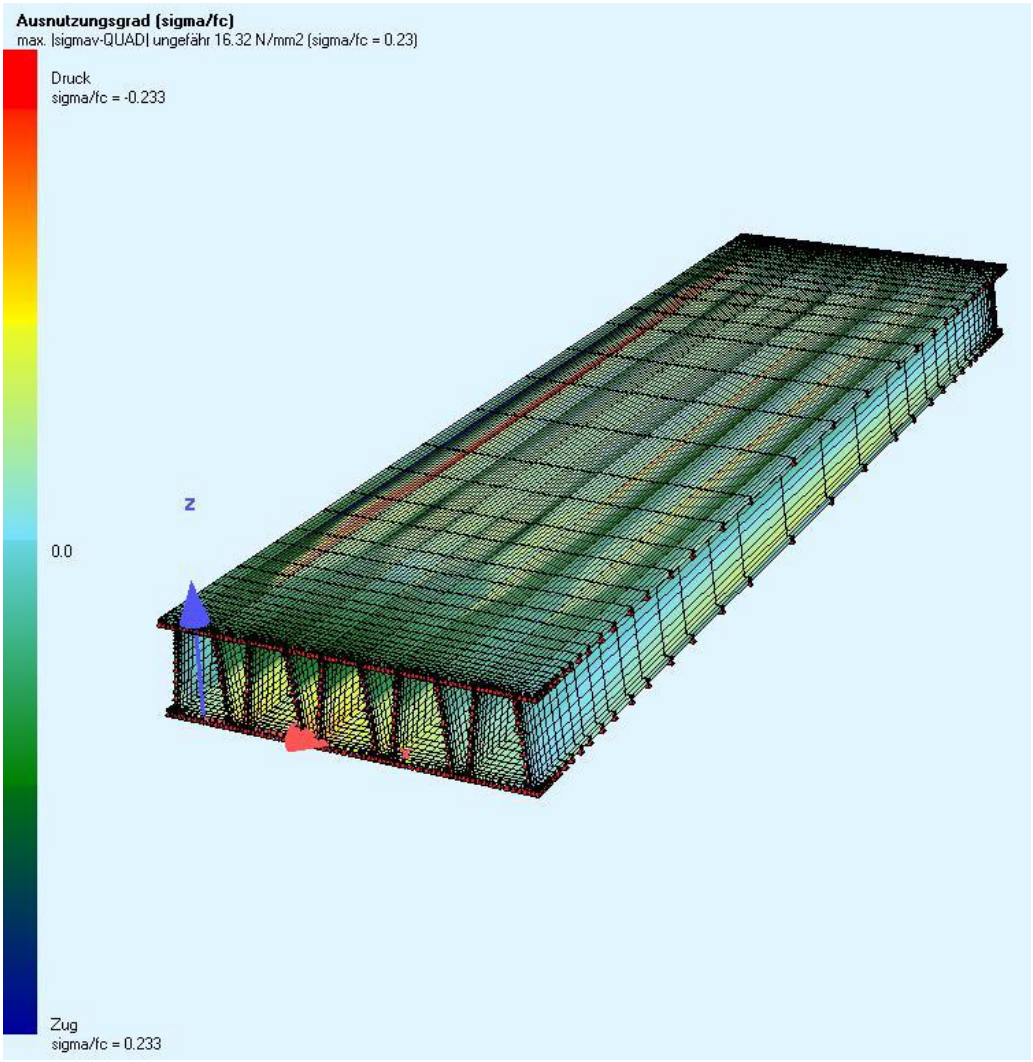

Fig. 8. 8. Usage grade of the deck element under the considered load combination

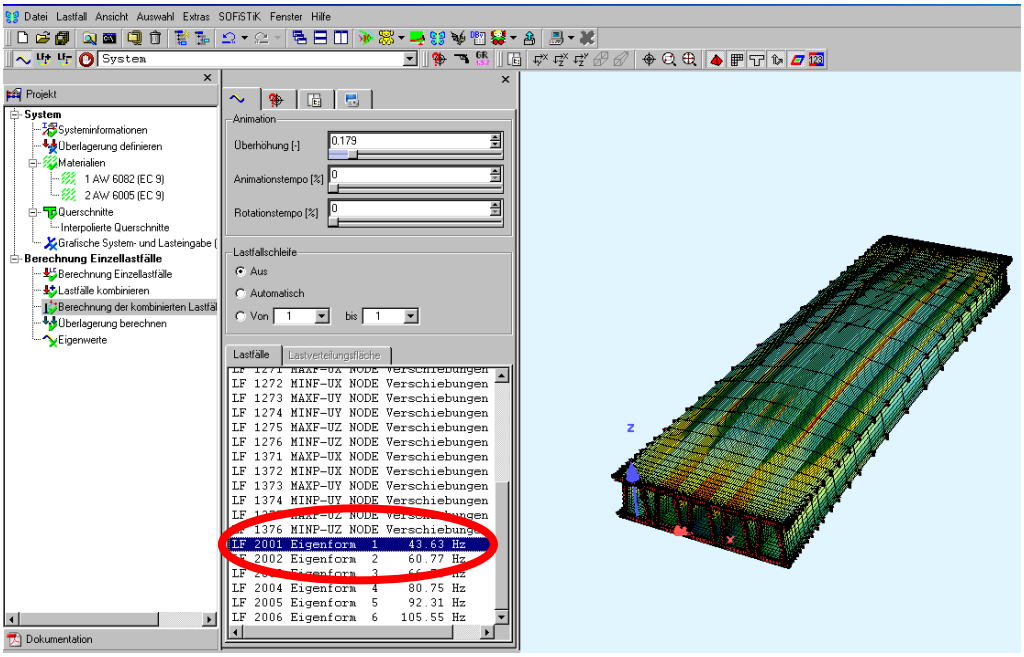

Fig. 8. 9. Frequenz eigenvalue

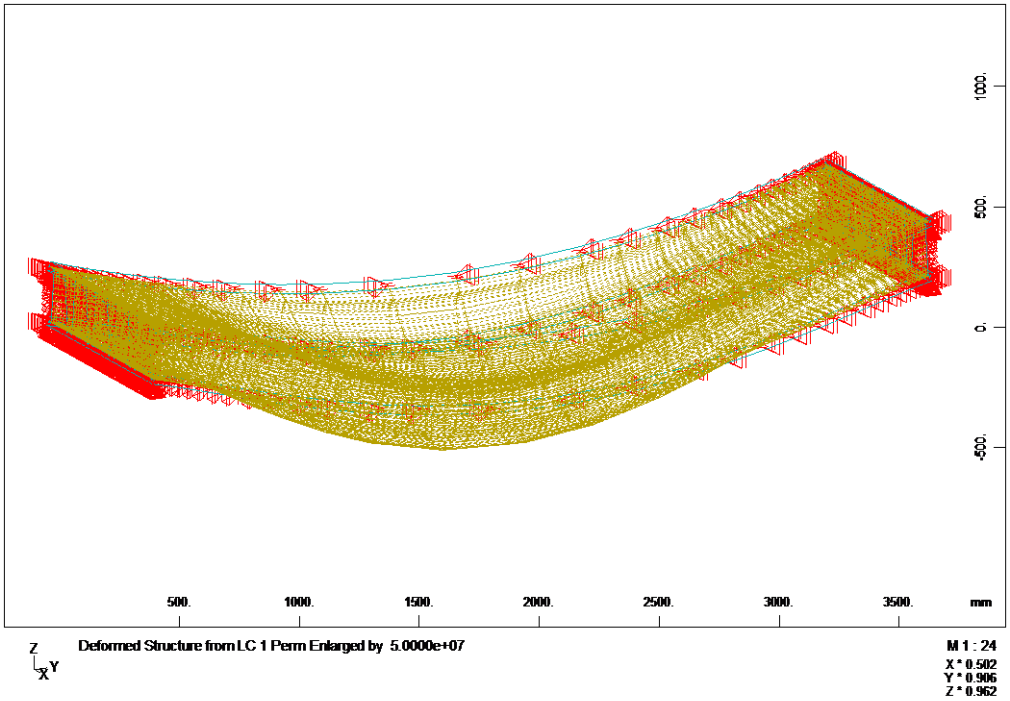

Fig. 8. 10. Structure deformation under the consideren load combination

REFERENCES

[1] Altenpohl DG. *Aluminum: technology, applications and environment Sixth edition*. The Aluminum Association, Inc. 1998.

[2] *The properties of Aluminium and its Alloys*, Aluminium Federation, Birmingham, UK, regularly updated, 2004

[3] *ALUSELECT - The European Engineering Properity Database for Wrought, Aluminium and Aluminium Alloys, KTH 1992*

[4] Dwightv J., *Aluminium Design and Construction*, 1999, E & FN Spons, London

[5] E.Hatch: Aluminium - Properties and Physical Metallurgy, American Society for Metals, Metals Park, Ohio, 1984, ISBN 0-87179-176-6

[6] *The Properties of Aluminum and ist Alloys*. Aluminum Federation Ltd., Birmingham 1993

[7] Helge Grine Johansen, *Structural Aluminium Materials, Hydro Aluminium Structures*, Karmoy, TALAT Lecture 2202, 1994

[8] Asmond Broli, TALAT Lecture 2201.01, *State of the Art*, Hydro Aluminium Structures, Karmoy

[9] *Aluminium-Taschenbuch*, Edited by Aluminium Zentrale. XXVI/1094, 14. Edition, 1983/1988, ISBN 3-87017-169-3

[10] Robert Dean, Abstracted from Materials World, vol. 3, pp. 65-67, 1995

[11] Koewius, A., Gross, G. and Angehrn, G.: *Aluminium-Konstruktionen des Nutzfahrzeugbaus.* 358 S., Aluminium-Verlag Düsseldorf, 1990

[12] Wright W., *Building the Bridge to the 21st Century with – aluminium?*

[13] Dobmeier J. M., Barton F.W., et co., *Analytical and experimental evaluation of an aluminium bridge deck panel, Part II: Failure Analysis*, 1999

[14] Subodh K. Das, J.G. Kaufman, *Aluminum alloys for bridges and bridge decks, aluminium alloys for Transportation, Packing*. Aerospace and other Applications, 2007, pg. 61-67

[15] F.M. Mazzolani, *Aluminium Structural Design*, ISBN 3-211-00456-4

[16] F.M. Mazzolani, *Structural Applications of Aluminium in Civil Engineering*, Structural Engineering International, 4/2006

[17] Woodward, A.R.**:** *Development in Aluminium - a Review. Metals and Materials*, Feb.1991

[18] http://aluminium.matter.org.uk/content/html/ENG/default.asp?catid=227&pageid=2144417161

[19] Thomas W M, *Friction Stir Welding and Related Friction process Characteristics*, Inalco 98, 7th International Conference, joints in Aluminium, Cambridge, UK. April 1998.

[20] Zettler R., Konstruktion, *Fertigung and Erprobung von innovativen Leichtbau Strukturen*, GKSS-Forschungszentrum Intern Publication, 2004

[21] L.E. Murr, Y. Li, R.D. Flores, E.A. Trillo, Mater. Res. Innovat. 2 (1998) 150.
[22] Y. Li, E.A. Trillo, L.E. Murr, J. Mater. Sci. Lett. 19 (2000) 1047
[23] Y. Li, L.E. Murr, J.C. McClure, Mater. Sci. Eng. A 271 (1999) 213
[24] C.G. Rhodes, M.W. Mahoney, W.H. Bingel, R.A. Spurling, C.C. Bampton, Scripta Mater. 36 (1997) 69.
[25] G. Liu, L.E. Murr, C.S. Niou, J.C. McClure, F.R. Vega, Scripta Mater. 37 (1997) 355.
[26] Y.S. Sato, H. Kokawa, M. Enmoto, S. Jogan, Metall. Mater. Trans. A 30 (1999) 2429.
[27] B. Heinz, B. Skrotzki, Metall. Mater. Trans. B 33 (6) (2002) 489.
[28] K.V. Jata, K.K. Sankaran, J.J. Ruschau, Metall. Mater. Trans. A 31 (2000) 2181.
[29] M. James, M. Mahoney, in: Proceedings of the First International Symposium on Friction Stir Welding, Thousand Oaks, CA, USA, June 14–16, 1999.
[30] Z.Y. Ma, R.S. Mishra, M.W. Mahoney, in: K.V. Jata, M.W. Mahoney, R.S. Mishra, S.L. Semiatin, T. Lienert (Eds.), *Friction Stir Welding and Processing II,* TMS, 2003, pp. 221–230.
[31] A.P. Reynolds, Sci. Technol. Weld. Joining 5 (2000) 120.
[32] Z.Y. Ma, R.S. Mishra, M.W. Mahoney, Acta Mater. 50 (2002) 4419
[33] M.W. Mahoney, C.G. Rhodes, J.G. Flintoff, R.A. Spurling, W.H. Bingel, Metall. Mater. Trans. A 29 (1998) 1955.
[34] H.N.B. Schmidt, T.L. Dickerson, J.H. Hattel, *Material flow in butt friction stir welds in AA2024-T3*, Acta Materialia 54 (2006) pg. 1199–1209
[35] Lombard H et al., *Optimizing FSW process parameters to minimize defects and maximize fatigue life in 5083-H321 aluminium alloy*, Eng Fract Mech (2007), doi: 10.1016/j.engfracmech.2007.01.026
[36] Ericsson M., Sandström R., *Influence of the welding speed on the fatigue of friction stir welds, and comparison with MIG and TIG*, Intern. Jorn. O Fatigue 25, 2003, pg 1379-1387
[37] Z.Y. Ma, S.R. Sharma, R.S. Mishra, M.W. Manohey, Mater. Sci. Forum 426–432 (2003) 2891.
[38] Krishnan, K.N., *On the Formation of Onion Rings in Friction stir Welds*. Mater. Sci.Eng., 2002, A327: p. 246-251
[39] T. Haelker, *Thermische Einflüsse beim Rührreibschweißen und die daraus folgenden Defekte*, Diplomarbeit, 2008
[40] Frigaard G, Midling OT. Met Mater Trans 2001; 32A(5): 1189-2000
[41] W. Tang, X. Guo, J.C. McClure, L.E. Murr, J. Mater. Process. Manufact. Sci. 7 (1998) 163
[42] Y.J. Kwon, N. Saito, I. Shigematsu, J. Mater. Sci. Lett. 21 (2002) 1473.
[43] Y.S. Sato, M. Urata, H. Kokawa, Metall. Mater. Trans. A 33 (2002) 625.
[44] T. Hashimoto, S. Jyogan, K. Nakata, Y.G. Kim, M. Ushio, in: Proceedings of the First International Symposium on Friction Stir Welding, Thousand Oaks, CA, USA, June 14–16, 1999

[45] W.J. Arbegast, P.J. Hartley, in: Proceedings of the Fifth International Conference on Trends inWelding Research, Pine Mountain, GA, USA, June 1–5, 1998, p. 541
[46] H. Schmidt, J. Hattel, J. Wert, Model. Simul. Mater. Sci. Eng. 12 (2004) 143
[47] S.R. Sharma, R.S. Mishra, Unpublished research, 2005.
[48] M. Guerra, J.C. McClure, L.E. Murr, A.C. Nunes, in: K.V. Jata, M.W. Mahoney, R.S. Mishra, S.L. Semiatin, D.P. Filed (Eds.), Friction Stir Welding and Processing, TMS, Warrendale, PA, USA, 2001, p. 25.
[49] W.M.Thomas, D. .Staines, E.R.Watts and I.M.Norris, The simultaneous use of two or more friction stir welding tools
[50] Thomas W M, Nicholas E D, Needham J C, Murch M G, Temple-Smith P and Dawes C J: Improvements relating to friction welding. European Patent Specification 0 615 480 B1.
[51] R., S., Mishra, Z., Y., Ma. Friction stir welding and processing. Materials Science Engineering, R50, (2005), pg. 1-78
[52] R. Nandan, G.G. Roy, T.J. Lienert, T. DebRoy, Sci. Technol.Weld. Joining 11 (5) (2006).
[53] Judy Schneider, Ronald Beshears, Arthur C. Nunes Jr., Mater. Sci. Eng. A435-436 (2006) 297–304.
[54] Ying Chun Chen, Liu Huijie, Feng Jicai, Mater. Sci. Eng. A 420 (2006) 21–25.
[55] Y.H. Zhao, S.B. Lin, Z.Q. He, L. Wu, Sci. Technol. Weld. Joining 11 (2) (2000) 178–182.
[56] A.P. Reynolds, W. Tang1, Z. Khandkar1, J.A. Khan1, K. Lindner, Sci. Technol. Weld. Joining 2 (2005) 190–199.
[57] H.J. Liu, H. Fuji, M. Maeda, K. Nogi, Sci. Technol.Weld. Joining 8 (2003) 450–454.
[58] K. Elangovan, V. Balasubramanian, J. Mater. Sci. Eng. A 459 (2007) 7–18.
[59] K. Elangovan,V. Balasubramanian, Effect of tool pin profile and axial force on the formation of friction stir processing zone in AA6061 aluminium alloy, Int. J. Adv. Manuf. Technol., in press.
[60] A. Barcellona, G. Buffa, L. Fratini, D. Palmeri, Mater. Process. Technol. 177 (2006) 340–343.
[61] Won Bae Lee, Mater. Trans. Vol.45 (5) (2004) 1700–1705.
[62] V. Balasubramanian, Relationship between base metal properties and friction stir welding process parameters, Mater. Sci. Eng. A (2007), doi:10.1016/j.msea.2007.07.048
[63] M. Peel, A. Steuwer, M. Preuss, P.J. Withers, Acta Mater. 51 (2003) 4791.
[64] C.D. Donne, E. Lima, J. Wegener, A. Pyzalla, T. Buslaps, in: Proceedings of the Third International Symposium on Friction Stir Welding, Kobe, Japan, September 27–28, 2001.
[65] X.L. Wang, Z. Feng, S. David, S. Spooner, C.S. Hubbard, in: Proceedings of the Sixth International Conference on Residual Stresses (ICRS-6), IOM Communications, Oxford, UK, 2000, pp. 1408–1420.

[66] Y.S. Sato, S.H.C. Park, H. Kokawa, Metall. Mater. Trans. A 32 (2001) 3023.
[67] G. Bussu, P.E. Irving, Int. J. Fatigue 25 (2003) 77.
[68] M. Kumagai, S. Tanaka, in: Proceedings of the First International Symposium on Friction Stir Welding, Thousand Oaks, CA, USA, June 14–16, 1999.
[69] G. Bussu, P.E. Irving, in: Proceedings of the First International Symposium on Friction StirWelding, Thousand Oaks, CA, USA, June 14–16, 1999.
[70] H. Hori, S. Makita, H. Hino, in: Proceedings of the First International Symposium on Friction StirWelding, Thousand Oaks, CA, USA, June 14–16, 1999.
[71] L. Magnusson, L. Kaellman, in: Proceedings of the Second International Symposium on Friction Stir Welding, Gothenburg, Sweden, June 26–28, 2000.
[72] G. Biallas, R. Braun, C.D. Donne, G. Staniek,W.A. Kaysser, in: Proceedings of the First International Symposium on Friction Stir Welding, Thousand Oaks, CA, USA, June 14–16, 1999.
[73] C.D. Donne, G. Biallas, T. Ghidini, G. Raimbeaux, in: Proceedings of the Second International Symposium on
Friction Stir Welding, Gothenburg, Sweden, June 26–28, 2000.
[73] Tommaso Ghidini, Fatigue Life predictions of Friction Stir Welded Joints by Using Fracture Mechanics Methods, TUM, Universitätbibliothek

[75] G., Buffa, L., Donati, L., Fratini, L., Tomesani. Solid state bonding in extrusion and FSW: Process mechanics and analogies. Journal of Materials Processing Technology, 177 (2006), Issues 344-347
[76] Dwightv J., *Aluminium Design and Construction*, 1999, E & FN Spons, London
[77] Höglund T., Talat Lecture 2301 - Design of members, Training in Aluminium Structural Design, TAS WP1, June 1998
[78] EUROCODE 9, Bemessung und Konstruktion von Aluminiumstragwerken - Teil 1-3: Ermüdungsbeanspruchte Tragwerke, prEN 1999-1-3: 2006
[79] S. Lundberg, Talat Lecture 2204 - Design Philosophy, EAA - European Aluminium Association, 1994
[80] EUROCODE 9, Bemessung und Konstruktion von Aluminiumstragwerken - Teil 1-1: Allgemeine Bemessungsregeln
[81] EN 910: 1996 – Zerstorende Prufung von Schweissnahten an metallischen Werkstoffen - Biegeprufungen
[82] ASTM E3 - ASTM E3-01 Standard Practice for Preparation of Metallographic Specimens (2002)
[83] ASTM E8 - Standard Test Methods for Tension Testing of Metallic Materials (2002)
[84] R., S., Mishra, Z., Y., Ma. Friction stir welding and processing. Materials Science Engineering, R50, (2005), pg. 1-78
[85] G., Buffa, L., Donati, L., Fratini, L., Tomesani. Solid state bonding in extrusion and FSW: Process mechanics and analogies. Journal of Materials Processing Technology, 177 (2006), Issues 344-347
[86] American Standards ASTM E 466-96 (2004)

[87] Siwowski, T., W., Structural behaviour of aluminium bridge deck panel, Engineering Structures 31, pg. 1349-1353, 2009
[88] Maljaars, J., Soetens, F., van Straalen,I., Fatigue tests on aluminium bridges, Heron, Vol. 50, No. 1, 2005
[89] Okura, I., et all, Fatigue of aluminum deck fabricated by friction stir welding, Technical Memorandum of Public Works Researhc Institute, vol no. 3843, 2002, pg. 153-166
[90] Okura, I., et all, Static and fatigue behavior of the connections of aluminum decks to steel griders, Journal of the Japan Welding Society 2003 72 (1), pg. 53–64;
[91] F Fanous, F Andrey, D Klaiber, F W, Analytical investigation for shell structures utilized as emergency bridges, Transportation Research Record Issue Number: 1180, ISSN: 0361-1981
[92] Kosteas, D., Aluminium in der Praxis, Ernst&Sohns, Verlag fur Architektur und technische Wissenschaften, 1998